Ph.D PROGRAM IN INFORMATION AND COMMUNICATION TECHNOLOGIES (ICT)

University of Granada
Departament of Electronics and Computer Technology

Development of instrumented insoles for biometric parameters monitoring

Thesis Dissertation

Candidate:
Fernando Martínez Martí

Supervisors:
Alberto J. Palma López
Miguel Ángel Carvajal Rodríguez

Editor: Universidad de Granada. Tesis Doctorales
Autor: Fernando Martínez Martí
ISBN: 978-84-9125-885-8
URI: http://hdl.handle.net/10481/43712

PROGRAMA DE DOCTORADO EN TECNOLOGÍAS DE LA INFORMACIÓN Y LA COMUNICACIÓN

Universidad de Granada
Departamento de Electrónica y Tecnología de Computadores

Desarrollo de plantillas instrumentadas para la monitorización de parámetros biométricos

Tesis Doctoral

Candidato:
Fernando Martínez Martí

Supervisores:
Alberto J. Palma López
Miguel Ángel Carvajal Rodríguez

Alberto J. Palma López, Catedrático de Universidad, y Miguel Ángel Carvajal Rodríguez, Profesor Titular de Universidad, ambos adscritos al Departamento de Electrónica y Tecnología de Computadores de la Universidad de Granada.

GARANTIZAMOS AL FIRMAR ESTA TESIS DOCTORAL

que el trabajo de investigación recogido en la presente memoria, titulada "Desarrollo de plantillas instrumentadas para la monitorización de parámetros biométricos", y presentada por Fernando Martínez Martí para optar al grado de Doctor por la Universidad de Granada, ha sido realizado en su totalidad bajo nuestra dirección en el Departamento de Electrónica y Tecnología de Computadores de la Universidad de Granada.

Granada, Enero de 2016

Directores de la Tesis

Dr. D. Alberto J. Palma López

Dr. D. Miguel A. Carvajal Rodríguez

II

El doctorando D. Fernando Martínez Martí y los directores de la tesis Alberto J. Palma López y Miguel Ángel Carvajal Rodríguez, garantizamos, al firmar esta tesis doctoral, que el trabajo ha sido realizado por el doctorando bajo la dirección de los directores de la tesis y hasta donde nuestro conocimiento alcanza, se han respetado los derechos de otros autores a ser citados, cuando se han utilizado sus resultados o publicaciones.

Granada, Enero de 2016

Directores de la Tesis

Dr. D. Alberto J. Palma López

Dr. D. Miguel A. Carvajal Rodríguez

Doctorando

D. Fernando Martínez Martí

II

Agradecimientos

Resulta bastante sencillo sentarse a escribir estos agradecimientos. Son muchas las personas que ha participado tanto de forma activa como pasiva, para ayudarme a conseguir este objetivo.

En primer lugar, quiero agradecer con todo mi corazón a los profesores Jesús Banqueri y Alberto Palma por apostar por mí. Aun no siendo durante mi época de estudiante un alumno de grandes marcas, es gracias a ellos por los que he vivido los que por ahora son los mejores años profesionales de mi vida. Me han dado la oportunidad de descubrir un mundo que me fascina y que no olvidaré nunca. Muchas gracias Jesús, siempre has estado ahí, para las malas, y para las buenas. Siempre has sabido cuando darme un abrazo. Tu preocupación por mí y por los míos es algo que nunca olvidaré.

A continuación quiero agradecer a todo el departamento, desde los directores Juan Antonio López y Juan Carceller, hasta Toñi, Encarni, Luis, Fran y Antonio Martínez. Mención muy especial para Pablo, que a pesar de lo poquito que lleva en el departamento, me ha sabido entender y en muchos casos calmar. También para Antonio García, porque es muy difícil encontrar a personas tan buenas como él. Y por supuesto para Diego, que desde hace mucho tiempo se convirtió en algo más que un compañero, un buenísimo amigo. No quiero tampoco olvidarme de aquellos amigos que dejaron el departamento buscando un futuro, muchas a gracias a Pepe, Nuria y Almudena. También quiero agradecer los ratos con todos mis compañeros de despacho.

Al profesor José Luis González Montesinos, porque gracias a él conseguí sentirme orgulloso por primera vez de los resultados obtenidos por nuestro trabajo en Cádiz.

A la profesora Olga Ocón, por aguantarme, por no mandarme bien lejos después de tantos correos y por ayudarme a estar preparado para cuando alguien en mi familia esté embarazado, casi me siento capaz de asistirlos. También quiero agradecer al profesor Jesús Florido, al que le dedico esta tesis doctoral, porque siempre tuvo unas palabras de ánimo para mi, y porque siempre aún desde su punto de vista, valoro mi trabajo incluso más que yo mismo.

A Víctor Soto y Alejandro Molina, por facilitarme el utilizar las instalaciones del IMUDS una y otra vez, y por querer seguir participando de forma activa en esta línea de investigación.

A Nicolás Rojas y Jesús López, por la motivación, la dedicación y el detalle con el que cuidáis vuestro trabajo. Por lo sencillo que me pusisteis las cosas desde un principio, por volver a darme el último empujón de motivación que necesitaba.

I would like to thank to professor Dr. Klaus Jahn and Dr. Roman Schniepp, for giving me the chance to do my short stay with their research group. I learnt how important and determinant gait analysis can be, and how many possibilities these types of studies have if we all work together with passion and interest. And of course, thanks to Cauchy, for putting up with me during those months trying to make things easier for me. Also I would like to thank to professor Dr. Kai Bötzel for letting me to participate in his work.

Dejo para el final a los más grandes, a mis directores. Muchisimas gracias Alberto, no tengo suficientes palabras para describir lo mucho que agradezco tu tiempo, siempre has intentado sacar un hueco no sólo para mí sino para todos tus doctorandos. Eres sin duda un ejemplo de lo que para mí es ser investigador. Muchísimas gracias por tu ayuda absolutamente desinteresada, por tu orientación, por tus consejos tanto en el ámbito profesional como personal, por tener siempre en la cabeza aquellas cuestiones personales que me preocupaban, en definitiva, por estar ahí. Muchísimas gracias a ti también Migue. Por intentar buscar siempre el lado bueno de las cosas, incluso cuando no lo había. Por tus consejos y orientación, por motivarme a aprender equivocándome, a probar lo que se me ocurriese, por no impedirme curiosear en lo que encontrase. A pesar de nuestras incompatibilidades horarias, siempre has estado ahí. Eres la persona más inteligente que conozco, y gracias a ti he aprendido multitud de cosas que no se enseñan en los libros. Muchas gracias.

Muchísimas gracias a mi familia. A mi madre, por su infinita paciencia y compresión. A mi hermano, por admirar mi trabajo aun cuando no es realmente importante. Y a mi padre, por transmitirme esa pasión, amor y dedicación a esta Universidad. También quiero dar las gracias a mi familia política: a Carolina, María Luisa, Juan y Pablo, vuestro apoyo y palabras de ánimo han sido siempre muy importantes. Mención especial tienes tú, Merluis, sabes que nunca podré estar suficientemente agradecido, aun cuando algunas cosas te pillaban un poco lejos, no te has rendido nunca y has seguido esforzándote al máximo hasta conseguir ayudarme. Esta tesis tiene un gran porcentaje tuyo.

Y finalmente quedas tú, mi Peta. Por no rendirte conmigo, por ayudarme, por consolarme, por cuidarme, por quererme. Muchísimas gracias por tu ayuda y participación en esta tesis, muchas gracias por opinar y aconsejarme después de saber de qué va mi trabajo. Eres mi motivación, tanto personal como profesionalmente. Porque sin ti, todavía estaría calculando momentos de fuerza. Muchas gracias mi vida.

VI

Preface

The document you have in your hands includes the dissertation entitle “Development of instrumented insoles for biometric parameters monitoring” written to apply for obtaining the Ph.D. graduation with the mention of international quality from the University of Granada.

Along this dissertation, an instrumented insoles with pressure and inertial sensors named ECnsole are described.

It has taken me almost 4 years to carry out this work. During these time, I have learnt uncountable things, both professionally and personally. This work has been very hard to accomplish due to problems experienced when working outside from the lab and the fact that suppose to experiment with real people, I have never thought it could be so difficult.

Finally, the results of my effort, my supervisors, and my colleagues department, as a team, are compiled in the document you have in your hands. We all hope you enjoy reading it as much as we did developing everything that is contained inside.

VIII

Abstract

The study of the plantar pressure distribution is becoming a very important tool to obtain information about any type of foot or gait disorders in many fields such as medicine, rehabilitation and sport.

This work describes the design and development of an instrumented insoles named ECnsole to measure not only the plantar pressure distribution, but also many others variables related to gait such as time support, centre of pressure, position of the foot in swing phase, etc. Four different version of the ECnsole are presented. Version 1.0 consist of two datalogger devices that sample and send the data to a MiWi™ receiver at a personal computer (PC) (or store it into μSD memory card) connected two a pair of insoles which contains four pressure sensors located at big toe, 1^{st} and 5^{th} metatarsal heads, and heel, and one analogue accelerometer placed in the arch of the foot. In the next version the two datalogger were joint into just one placed at the waist in order to reduce both complexity in communications and costs, this version was enumerated as 1.2. In ECnsole version 1.5 the analogue accelerometer was replaced by a digital inertial measurement unit (IMU), integrated by a 3D gyroscope, 3D accelerometer, and 3D magnetometer, placed in the arch of the foot. The location of the datalogger unit was also the waist. In the last prototype described, the whole electronic system is embedded inside the insole. μSD memory card socket is removed and MiWi™ is replaced by a Bluetooth transceiver. Moreover, a pair of additional pressure sensors are added to the 3^{rd} metatarsal and to the midfoot area. An android application have been designed also to plot the data obtained by the instrumented insoles. The prototypes have been validated both for the pressure sensors and for the IMU. To validate the pressure sensors a

commercial in-shoe system F-Scan was used together with ECnsole. In case of the IMU, an algorithm to obtain the foot orientation during the swing phase have been used, comparing the resulting euler's angles with the angles measured using an infrared video camera system, obtaining very good agreement in both cases.

A couple of experiments related to sports science and physical education have been carried out. At first, the instrumented insoles has been validated as a heigh measurement tool in vertical jump. 66 participants performed 3 different jump tests (squat jump, countermovement jump and Abalakov jump) twice with flight times determined using an instrumented insole composed of 4 pressure sensors (PreECnsole) and an accelerometer sensor (AccECnsole), a laser platform (Sport Jump System Pro), and a high-speed motion capture system (HSC); the latter 2 systems are considered as reference methods. One-way analysis of variance (ANOVA), simple linear regression, and the Bland-Altman method were used to assess validity. Regardless of the jump test performed, the ECnsole system showed a systematic bias close to 0 and a low random error (average random error: ± 2.8 cm; ± 3.1 cm PreECnsole and AccECnsole vs. HSC system respectively and ± 2.3 cm; ± 2.9 cm PreECnsole and AccECnsole vs. SJS system respectively). The associations between PreECnsole and AccECnsole with the HSC were very high (R^2 = 0.967 and 0.958 respectively). Furthermore, the associations between PreECnsole and AccECnsole with the SJS were very high (R^2 = 0.978 and 0.966 respectively) as well. Therefore, the ECnsole system can be considered an alternative method for measuring jump height during vertical jump performance. On the other hand, ECnsole has been also used to monitor the influence of the fatigue in gymnast. A set of 12 volunteers performed 5 different jump test (squat jump, countermovement jump, Abalakov jump, drop jump, and repeat jump) in three series. Once they finish first series (PreTest), they perform an specific training protocol consisting in 12 series of 6 forward tucked somersault, with 10 seconds between somersaults and 2 minutes between series. Once the training is done, they carried out the second series (PostTest). After that, they rested for 15 minutes and perform the last serie (ReTest). Several parameters have been recorded using the ECnsole like flight time, pressure at jumping and landing, and accelerometer value in Z-axis also at jumping and landing. The results obtained shows that there are significant

changes in the pressure at jumping in countermovement jump, Abalakov jump, and repeat jump, while in drop jump there are compelling changes in flight time and pressure at landing.

Related to medical applications, a couple of experiment were also done. An study to a group of 62 pregnant in their regular check-up weeks (12^{th}, 20^{th}, and 32^{nd} of pregnancy) to evaluate if there is any relationship between plantar pressure distribution and back pain have been carried out. On the one hand, a clinical study has been carried out, concluding that younger women and those who consumed hormonal contraceptives suffer more lumbar pain at the beginning of the pregnancy while those who were mother before suffered more in last weeks of gestation. The shoulder pain seems to be related to the sleeping hours in the two last check-ups. Finally, the inguinal pain correlated with those women who have high BMI, those whose work required a high physical load, and those who also consumed hormonal contraceptives. According to the plantar pressure distribution study. A Repeated Measures ANOVA test has been carried out to determine the variation and its influence on the centre of pressure in the Y-Axis, concluding that the centre of pressure of both feet displace towards the forefoot as continuing the pregnancy. Also an ANOVA test has been carried out to evaluate the differences between a painful group and a non painful, obtaining only significant differences in the pressure on the big toe of the right foot in week 32^{nd}. The final experiment in which the insoles have been used was done in Klinikum Großhadern. The objective of this study was to correlate the data from shank-mounted gyroscopes and three reference systems,namely accelerometers,pressure-sensitive soles and a motion capture system in a group of 14 young healthy men. It has been possible to confirmed that the heel strike corresponds to a trough in the gyroscope curve, as several previous reports have stated. However, the toe-off moment clearly did not coincide with another trough of the gyroscope trace,as had been assumed in the past. The heel-off moment was reliably at 51% of the step cycle, irrespective of gait velocity, in our data. These findings are crucial for gait recording systems which aim to assess the temporal as well as spatial descriptors of human gait.

Resumen

El estudio de la distribución de la presión plantar está convirtiéndose en una herramienta muy importante para obtener información acerca de cualquier tipo de desorden en la marcha o en el pie en muchos campos tales como la medicina, rehabilitación o el deporte.

Este trabajo describe el diseño y desarrollo de una plantilla instrumentada denominada ECnsole para medir no sólo la distribución de la presión plantar, si no también muchas otras variables relacionadas con la marcha tales como el tiempo de apoyo, el centro de presiones, la posición del pie durante la fase de vuelo, etc. Se han presentado cuatro versiones diferentes de ECnsole. La versión 1.0 consiste en dos dispositivos que adquieren y envían la información a un receptor MiWi™ en un ordenador personal (o la almacenan en una tarjeta de memoria μSD) conectados a un par de plantillas que contienen cuatro sensores de presión colocados en el dedo gordo, primer y quinta cabeza metatarsiana, y el talón, y un acelerómetro analógico situado en el arco del pie. En la siguiente versión, las dos unidades se fusionan en una única colocada en la cadera para reducir tanto complejidad en las comunicaciones como costes, está versión se enumeró como 1.2. En la version 1.5 el acelerómetro analógico se sustituye por una unidad de medida inercial (IMU) digital, integrada por un giroscopio 3D, un acelerómetro 3D y un magnetómetro también 3D, colocada en el arco del pie. Este dispositivo también se colocaba en la cadera. En el ultimo prototipo descrito, toda el sistema electrónico se embebió dentro de la plantilla. El lector de tarjetas μSD se eliminó y el transceptor MiWi™ se sustituyó por uno Bluetooth. Además, se colocaron un par de sensores de presión adicionales, situados en el tercer metatarso y en la zona media del pie. Una aplicación

android ha sido diseñada para representar los datos obtenidos por las plantillas instrumentadas. Los prototipos han sido validados tanto para los sensores de presión como para la IMU. Para validar los sensores de presión se utilizó el sistema de medida de presión comercial F-Scan junto con las plantillas ECnsole. En el caso de la IMU, se utilizo un algoritmo para obtener la posición del pie durante la fase de vuelo, comparando los ángulos de euler resultantes con los ángulos medidos por el sistema de video camera, obteniendo en ambos casos muy buena correlación.

Se han llevado a cabo un par de experimentos relacionados con las ciencias del deporte y la educación física. En primer lugar, las plantillas instrumentadas se han validado como herramienta para medir altura en salto vertical. 66 participantes realizaron tres diferentes tipos de salto vertical (squat jump, countermovement jump y Abalakov jump) dis veces determinando el tiempo de vuelo usando tanto los sensores de presión (PreECnsole) como el acelerómetro (AccECnsole), una plataforma láser (Sport Jump System Pro), y un sistema de captura del movimiento de alta velocidad (HSC); se consideran los dos últimos sistemas como sistemas de referencia. Análisis de la varianza (ANOVA), regresión lineal simple, y el método de Bland-Altman se utilizaron para asegurar la validez. A pesar del tipo de salto realizado, las plantillas ECnsole mostraron un error sistemático cercano a cero y un bajo error aleatorio (error aleatorio medio: ± 2.8 cm; ± 3.1 cm PreECnsole y AccECnsole vs. HSC respectivamente y ± 2.3 cm; ± 2.9 cm PreECnsole y AccECnsole vs. SJS respectivamente). La asociación entre PreECnsole y AccEnsole con HSC fueron muy altas (R^2 = 0.967 y 0.958 respectivamente). Además, la asociación entre PreECnsole y AccEnsole con SJS fueron también muy altas (R^2 = 0.978 y 0.966 respectively). Por lo tanto, el sistema ECnsole puede ser considerado como método alternativo para medir la altura del salto durante el desarrollo del salto vertical. Por otro lado, ECnsole ha sido utilizado para monitorizar la influencia de la fatiga en gimnastas. Un grupo de 12 voluntarios llevaron a cabo 5 tipos diferentes de saltos (squat jump, countermovement jump, Abalakov jump, drop jump y repeat jump) en tres series. Una vez que terminaron la primera serie (PreTest), ellos realizaron un protocolo de entrenamiento especifico que consistió en 12 series de 6 volteretas mortales hacia adelante, con diez segundos entre voltereta y dos minutos entre serie. Una vez se realizó el entrenamiento, ellos repitieron el test (PostTest).

Después de esto, descansaron durante 15 minutos y volvieron a repetir una vez más el entrenamiento (ReTest). Varios parámetros han sido grabados utilizando ECnsole como por ejemplo el tiempo de vuelo, la presión en el momento del salto y la recepción, la aceleración en en el eje Z en el momento del salto y la recepción. Los resultados obtenidos muestran que hay cambios significativos en la presión en el despegue en countermovement jump, Abalakov jump, y repeat jump, mientras que en drop jump existen también cambios importantes en el tiempo de vuelo y en la presión al caer.

Relacionado con las aplicaciones medicas se realizaron un par de experimentos. Un estudio a un grupo de 62 embarazadas en sus semanas habituales de revisión (semanas 12, 20 y 32 de embarazo) para evaluar si existe una relación en la distribución de la presión y el dolor de espalda a lo largo del embarazo. Por un lado, se llevó a cabo un estudio clínico, concluyendo que las mujeres jóvenes y aquellas que consumieron anticonceptivos sufría más dolor lumbar al principio del embarazo mientras que aquellas que había sido madres anteriormente tenían mayor dolor en las semanas finales de embarazo. El dolor de hombros parece estar relacionado a las horas de sueño en las dos últimas revisiones. Finalmente, el dolor pélvico relacionó con aquellas mujeres que tenían un alto indice de masa corporal, aquellas cuyos trabajos requerían una alta carga física, o aquellas que habían tomado anticonceptivos. Se llevó a cabo un test ANOVA de medidas repetidas para determinar la variación y su influencia en el eje Y del centro de presiones, concluyendo que el centro de presiones se desplazaba en ambos pies hacia la zona posterior del pie a medida que continuaba el embarazo. También se realizó un test ANOVA para evaluar las diferencias entre un grupo de dolor y otro sin dolor, obteniendo diferencias significativas en la presión del dedo gordo del pie derecho en la semana 32 de embarazo. El último experimento realizado con las plantillas instrumentadas se llevó a cabo en el hospital Klinikum Großhadern de Munich (Alemania). El objetivo de este estudio era correlacionar los datos de un giroscopio colocado en la pierna con tres sistemas de referencia: un acelerómetro, unas plantillas sensibles a la presión y un sistema de captura del movimiento a un grupo de 14 hombres jóvenes. Fue posible confirmar que el inicio de apoyo (Heel strike) corresponde a un mínimo en la curva del giroscopio, como varios informes habían declarado previamente. Sin embargo, el instante de fin de apoyo no coincidió con otro mínimo de la

curva del giroscopio, como había sido asumido en el pasado. El inicio de apoyo tenia una fiabilidad del 51% del ciclo del paso, independientemente de la velocidad, en nuestros datos. Estos descubrimientos son cruciales para los sistemas de grabación de la marcha los cuales tienen como objetivo evaluar los descriptores tanto temporales como espaciales de la marcha humana.

XVIII

Contents

Acronyms **XXXI**

1 Introduction **1**
1.1 Motivation . . . 2
1.2 Objectives . . . 3
1.3 Document structure . . . 4
1.4 The Foot . . . 5
1.5 Human Gait . . . 10
1.5.1 Ground Reaction Forces . . . 13
1.5.2 Centre of Gravity . . . 16
1.5.3 Common Gait Abnormalities . . . 17
1.6 Clinical Framework . . . 20
1.6.1 Pain and Plantar Ulcers . . . 21
1.6.2 Lumbar Pain and Pregnancy . . . 22
1.7 Physical and Sport Activity Framework . . . 24
1.8 State of the Art . . . 25
1.8.1 Instrumented Insoles in Industry . . . 30
1.8.2 Instrumented Insoles in Academics . . . 36
1.8.3 Previous work by the research group . . . 58

2 Instrumented insole prototypes **63**
2.1 ECnsole v1.0 . . . 64
2.1.1 Instrumented Insoles . . . 65
2.1.2 Datalogger Unit . . . 71

2.1.3 Software Processing . . . 89
2.2 ECnsole v1.2 . . . 92
2.2.1 Changes on Datalogger Unit . . . 92
2.3 ECnsole v1.5 . . . 98
2.3.1 Changes on Instrumented Insole . . . 98
2.3.2 Changes on Datalogger Unit . . . 103
2.3.3 Changes on Software Processing . . . 107
2.4 ECnsole v2.0 . . . 108
2.4.1 Changes on Instrumented Insoles . . . 110
2.4.2 Changes on Datalogger Unit . . . 116
2.4.3 Changes of Software Processing . . . 123

3 ECnsole validation and preliminary test 131
3.1 Validation of pressure sensor values . . . 132
3.1.1 Test definition . . . 132
3.1.2 Results . . . 133
3.2 Validation of foot position by means of inertial sensor values . . . 134
3.2.1 Test definition . . . 135
3.2.2 Results . . . 138
3.3 Preliminary test . . . 139
3.4 Conclusions . . . 147

I Sports and physical activity experiments 149

4 Height measurements in vertical jumps 151
4.1 Introduction . . . 152
4.2 Test Definition . . . 154
4.2.1 Participants . . . 154
4.2.2 Hardware equipment . . . 154
4.2.3 Procedure . . . 156
4.2.4 Experimental setup and data collection . . . 158
4.2.5 Statistical Analysis . . . 160
4.3 Results . . . 160

4.4 Discussion . . . 162
4.5 Limitations . . . 166
4.6 Conclusions . . . 166

5 Influence of fatigue on gymnasts in vertical jump performance 167
5.1 Introduction . . . 168
5.2 Test Definition . . . 169
5.2.1 Participants . . . 169
5.2.2 Hardware equipment . . . 169
5.2.3 Procedure . . . 169
5.3 Results . . . 171
5.4 Conclusions . . . 174

II Medical experiments 175

6 Plantar pressure alterations during pregnancy 177
6.1 Introduction . . . 178
6.2 Test Definition . . . 179
6.2.1 Participants . . . 179
6.2.2 Test description . . . 180
6.2.3 Materials and methods . . . 181
6.3 Results . . . 183
6.3.1 Clinical study . . . 185
6.3.2 Plantar pressure study . . . 192
6.4 Conclusions . . . 198

7 Gait analysis in neurological diseases 201
7.1 Introduction . . . 202
7.2 Test Definition . . . 203
7.3 Results . . . 204
7.3.1 Initial contact . . . 204
7.3.2 Heel-off . . . 206
7.3.3 Terminal contact . . . 206
7.3.4 Impact of velocity . . . 206

7.4 Discussion 208

III Conclusions **215**

8 Conclusions and Future Work **217**
8.1 Development of instrumented insoles 218
8.2 Applications in sport framework 221
8.3 Applications in medical framework 222
8.4 Future Work 223

9 Conclusiones y trabajo futuro **225**
9.1 Desarrollo de unas plantillas instrumentadas 226
9.2 Aplicaciones en el ámbito deportivo 230
9.3 Aplicaciones en el ámbito médico 230
9.4 Trabajo Futuro 232

Scientific Contributions **235**

IV Appendix **239**

I Pressure Calibration System **241**
I.a Design 242
I.b Fabrication process 243
I.c Calibration System 245

II Documentation related to pregnancy study **247**
II.a Hospital Ethics Committee 248
II.b Informed Consent 249
II.c Questionnaire Spanish 250
II.d Questionnaire English 254

Bibliography **259**

List of Figures

1.1 Lower leg and foot anatomy 5
1.2 Different division areas in foot. 6
1.3 Gait Cyclein one consecutive step. 10
1.4 Gait cycle components 12
1.5 Gait cycle timing 13
1.6 Component of ground reaction forces. 14
1.7 Centre of pressure of both feet during one step. 15
1.8 Plot of vertical ground reaction force against time. 15
1.9 Centre of Gravity path. 16
1.10 Static measurement instruments 26
1.11 SportJump System PRO. 26
1.12 GaitRide pressure sensitive carpet. 29
1.13 BTS GaitLab configuration. 29
1.14 Biofoot insole and use of the insole in research 30
1.15 The Parotec system. 32
1.16 F-Scan system in use. 33
1.17 F-Scan insoles. 33
1.18 Pedar-X System. 34
1.19 OpenGo insole. 35
1.20 OpenGo insole layout. 36
1.21 Hysteresis caused by loading and unloading a pressure sensor. . . 37
1.22 Effect of sensor sizing and placement. 39
1.23 Resistive pressure sensor. 40

1.24 Capacitive pressure sensor. 40
1.25 Piezoelectric pressure sensor. 41
1.26 Piezoresistive pressure sensor. 42
1.27 Shoes and transducers used in Cong and Zhang study. 43
1.28 Plantar pressure signal acquisition system. 44
1.29 Placement of WalkinSense and F-Scan. 45
1.30 Wearable sensor sock. 46
1.31 Schematic of the GaitShoe system. 47
1.32 Instrumented insole with FSR sensor. 48
1.33 Wireless insole with capacitive sensors. 49
1.34 Wireless sensor sock with capacitive sensors. 50
1.35 Pressure sensor and instrumented insole. 51
1.36 Instrumented insoles and application use. 52
1.37 Outline of the assisted measurement system. 53
1.38 In-shoe device developed to measure plantar pressure.. 54
1.39 StabilitySole design and real use. 55
1.40 Base sensitive element of the pressure sensitive insole. 56
1.41 Sensors used in the Smart Insole system. 57
1.42 The sensorized insole prototype. 58
1.43 Schematic of presented patent. 60
1.44 Previous work by the research group. 61

2.1 Measurement system ECnsole v1.0. 64
2.2 Top and side views of instrumented insoles v1.0. 65
2.3 Flexifore Force Sensor A201 66
2.4 Flexiforce A201 Sensor characteristic. 68
2.5 Response of the A201 sensor. 69
2.6 Functional block diagram of ADXL330 accelerometer. 71
2.7 Schematic diagram of ECnsole v1.0. 72
2.8 Typical Application circuit of LM2623 DC-DC converter. 73
2.9 Efficiency versus input voltage. 75
2.10 Recommended circuit for flexiforce sensor A201. 76
2.11 Non-inverter operation amplifier used in ECnsole v1.0. 77
2.12 Wireless Module MRF24J40MA. 79

2.13 Flowchart of slave datalogger unit in ECnsole v1.0. 82
2.14 Flowchart of master datalogger unit in ECnsole v1.0. 84
2.15 Sequence diagram of ECnsole v1.0. 88
2.16 Case of use of ECnsole v1.0. 89
2.17 ECnsole v.1.0 Software Application. 90
2.18 Configuration of MCP1700. 93
2.19 Second order low pass filter Sallen-Key. 95
2.20 Frequency response of Sallen-Key filter. 95
2.21 Layout of ECnsole v1.2. 97
2.22 ECnsole v1.2 Printed Circuit Board (PCB) with components. . . . 97
2.23 Instrumented insoles ECnsole v1.2. 98
2.24 Schematic diagram of ECnsole v1.5. 99
2.25 Top view and axis layout of L3GD20. 100
2.26 Top view of *LSM303DLHC* accelerometer and magnetometer. . . . 101
2.27 Instrumented insole ECnsole version 1.5. 102
2.28 Instrumented insole ECnsole version 1.5. 102
2.29 Inverter operation amplifier used in ECnsole v1.5. 103
2.30 Charge pump Direct Current (DC)-DC converter *TC1044S*. 104
2.31 Layout of ECnsole v1.5. 105
2.32 ECnsole v1.5 PCB with components. 106
2.33 Matlab®application on the PC side. 107
2.34 Prototype ECnsole v1.5. 108
2.35 Architecture of ECnsole version 2.0. 109
2.36 Flexiforce Sensor A401 110
2.37 Flexiforce A401 Sensor Response. 111
2.38 Calibration curves of A401 sensor of right foot. 112
2.39 Instrumented insole ECnsole version 1.5. 114
2.40 Instrumented insole ECnsole version 2.0. 115
2.41 Dimensions of LIR2450 battery. 116
2.42 Voltage divider used in ECnsole v2.0. 117
2.43 *RN-42* Bluetooth module. 118
2.44 Flowchart of firmware datalogger unit in ECnsole v2.0. 120
2.45 Sequence diagram of the protocol in ECnsole v2.0. 121
2.46 Layout of ECnsole v1.5. 122

2.47 ECnsole v2.0 PCB with components. 123
2.48 Main mobile operating systems. 124
2.49 Flowchart of android application ECnsole v2.0. 125
2.50 Icon of the ECnsole v2.0 android application. 126
2.51 Splash screen of the ECnsole v2.0 android application. 127
2.52 Patients list of the ECnsole v2.0 android application. 127
2.53 Patient selected in ECnsole v2.0 android application. 128
2.54 Pressure graphs available in android application ECnsole v2.0. . . 128
2.55 Graphs available ECnsole v2.0 for IMU data. 130

3.1 Validation of ECnsole v1.2 together with F-scan system. 134
3.2 Passive markers placed on the shoe. 137
3.3 Inertial frame with the corresponding Euler angles. 138
3.4 Comparison of Euler's angles. 140
3.5 Right plantar pressure and accelerations during walking. 142
3.6 ΔA_x of the right foot. 144
3.7 A_Y of the left foot of participant 4 over ten steps. 146

4.1 Participant in heigh jump measurement test. 155
4.2 Squat Jump and Countermovement Jump process. 157
4.3 ECnsole response of a vertical jump 159
4.4 Scatter plots of correlated data. 161

5.1 Novatrack One tumbling track. 170
5.2 Drop Jump Process. 171

6.1 Deviation of the mean value of the Centre of Pressure. 184
6.2 Distribution of women with pain over the weeks 12^{th},20^{th}, and 32^{nd}.186

7.1 Initial contact, right leg. 205
7.2 Heel-off, right leg. 207
7.3 Correspondence between "heel-off" and gyroscope trace. 208
7.4 Terminal contact, right leg. 209
7.5 Computation of TC (toe-off) in shank mounted gyroscope. 211
7.6 Timing of events in fractions of step cycle. 212

I.1 Pressure Calibration System designed. 243
I.2 Pressure Calibration System manufactured. 245
I.3 Real use of the calibration system manufactured. 246

List of Tables

2.1 Specification of Flexiforce A201 sensors 67
2.2 Specification of ADXL330 accelerometer. 71
2.3 Main characteristics of MRF24J40MA wireless module. 80
2.4 Memory usage of the Microchip file I/O library 81
2.5 Specifications of PIC24FJ256GB106 microcontroller. 81
2.6 Technical specifications of ECnsole v1.0. 91
2.7 Technical specifications of ECnsole v1.2. 96
2.8 Technical specifications of L3GD20. 100
2.9 Technical specifications of *LSM303DLHC*. 101
2.10 Specification of Flexiforce Sensor A401 111
2.11 Technical specifications of L3GD20H. 113
2.12 Technical specifications of *LSM303D*. 113
2.13 Technical specifications of ECnsole v2.0. 114
2.14 Specifications of *PIC18LF26K22* microcontroller. 120

3.1 Participant characteristics of the preliminary study. 132
3.2 Specification of Treadmill Woodway PRO XL. 135
3.3 $< |\Delta A_X| >$ of right and left feet of participants. 145
3.4 Temporal parameters in gait test for the ten participants. 146

4.1 Descriptive data from the variables of the study sample. 162
4.2 Summary of regression coefficients in vertical jumps. 163

5.1 Multivariate analysis of the jumps performed. 172

5.2 Repeated Measures ANOVA for Countermovement Jump (CMJ). . 172
5.3 Repeated Measures ANOVA for Abalakov Jump (ABK). 173
5.4 Repeated Measures ANOVA for Drop Jump (DJ). 173
5.5 Repeated Measures ANOVA for Repeat Jump (RJ). 174

6.1 Study group demographic characteristics (N=62). 180
6.2 Preliminary results of the evolution from week 12^{th} to week 32^{nd}. 183
6.3 Results of clinical study in week 12^{th}. 187
6.4 P-value of Chi-Square test of rest of variables in week 12^{th}. 188
6.5 Results of clinical study in week 20^{th}. 189
6.6 P-value of Chi-Square test of rest of variables in week 20^{th}. 190
6.7 Results of clinical study in week 32^{nd}. 191
6.8 P-value of Chi-Square test of rest of variables in week 32^{nd}. 192
6.9 Descriptive analysis of plantar pressure for each session. 193
6.10 Descriptive analysis of plantar pressure evolution. 194
6.11 Multivariate analysis of the Centre of Pressure $(CoP)_y^{\alpha}$. 195
6.12 Pairwise comparison CoP_y^L Mean value. 195
6.13 Pairwise comparison CoP_y^L Max value. 196
6.14 Pairwise comparison CoP_y^L Min value. 196
6.15 Pairwise comparison CoP_y^R Max value. 197
6.16 ANOVA test considering pain as a factor. 197

7.1 Computation of the terminal contact in gyroscope curves 210

I.1 Dimensions of calibration systems designed. 242
I.2 Real dimensions of calibration systems manufactured. 244
I.3 Configuration parameters of the 3D printer. 244

Acronyms

ABK Abalakov Jump

ACK Acknowledgement

ADC Analog-digital converter

A_X X-Axis Acceleration

A_Y Y-Axis Acceleration

A_Z Z-Axis Acceleration

BMI Body Mass Index

CI Confidence Interval

CMJ Countermovement Jump

CoP Centre of Pressure

CPU Central Processing Unit

CSV Comma Separated Values

dB Decibels

DC Direct Current

DJ Drop Jump

dps Degree Per Second

EDR Enhanced Data Rate

EMBC Engineering in Medicine and Biology Society

EMG Electromyography

EVA Ethylene-vinyl acetate

FAT File Allocation Table

fps Frame Per Second

GRF ground reaction force

HCI Host Controller Interface

HSC High-speed captured system

I^2C Inter-Integrated Circuit

IC Integrated Circuit

IMU Inertial Measurement Unit

IMUDS Instituto Mixto Universitario de Deporte y Salud

KB Kilo Bytes

kbps kilo bits per second

LR-WPAN Low-Rate Wireless Personal Area Network

m Meters

Mbps Mega bits per second

MIPS Millions of Instructions Per Second

OTG On-The-Go

PC Personal Computer

PCB Printed Circuit Board

re Random Error

RF Radio Frequency

RJ Repeat Jump

RTCC Real Time Calendar/Clock

SD Standard Deviation

SJ Squat Jump

SJS SportJump system

SSOP Shrink small outline package

SPI Serial Peripheral Interface

SPP Serial Port Profile

TQFP Thin Quad Flat Package

UART Universal Asynchronous Receiver-Transmitter

USB Universal Serial Bus

μSD Micro Secure Digital

V Volts

Chapter 1

Introduction

Contents

1.1 Motivation 2
1.2 Objectives 3
1.3 Document structure 4
1.4 The Foot 5
1.5 Human Gait 10
1.5.1 Ground Reaction Forces 13
1.5.2 Centre of Gravity 16
1.5.3 Common Gait Abnormalities 17
1.6 Clinical Framework 20
1.6.1 Pain and Plantar Ulcers 21
1.6.2 Lumbar Pain and Pregnancy 22
1.7 Physical and Sport Activity Framework 24
1.8 State of the Art 25
1.8.1 Instrumented Insoles in Industry 30
1.8.2 Instrumented Insoles in Academics 36
1.8.3 Previous work by the research group 58

Traditionally, the clinical diagnosis, evaluation, and treatment of foot pathologies as well as the sport studies of foot, are based on the examination and anamnesis of patient with the support of conventional techniques like radiography, podography, and in case of orthopaedics treatments, obtain the footprint of affected foot[1]. However, it is well-known that aetiology of most foot disorders are mechanical type. Because of this, the study of plantar pressure distribution patterns both in static and dynamic are a growing need for the experts in many fields not only in medicine but also in physical and sport activity (rehabilitation, sport medicine, gynaecology, sport training, etc.).

1.1 Motivation

The incursion of new technologies in medicine has been evident in last few years. They allows doctors from any speciality to carry out a better diagnosis which means better treatments. Foot and gait disorders can provided a very useful information related to many diseases[1], not only related to orthopaedic surgery that could be the obvious, but also to neurological diseases, which may manifest in modifications in gait parameters, such as plantar pressure distribution or temporal parameters, that will be explained in detail later.

Nowadays, several neurological diseases have been demonstrated that can modify human gait pattern. The best known is Parkinson[2, 3], but there are some other that also may provoke a gait disorder[4, 5], like cerebellar ataxia, vertigo, etc. In this way, a good evaluation of human gait can provided useful information as early diagnosis or how the patient is responding to a treatment. This information is not exclusive to neurology, it can help in rehabilitation processes after an orthopaedic surgery or an orthopaedic injury.

The measurement of human gait is not only important in medicine. In physical and sport activity the possibility of having a feedback about the training or practice of any sport can help to improve the training as well as to avoid possible injuries due to a bad practice. The information obtained from the plantar pressure distribution and the relative foot position during the exercise can contribute hugely to perform a better biomechanic study of the body, lower limbs and feet in many exercises such as running or jumping.

A precise and reliable measurement of human gait parameters like flight and contact times, force and pressure distribution, symmetries or asymmetries during contact time, double support time length, acceleration and orientation of the movements, etc., allow to distinguish regular gait patterns or pathological gait patterns.

All these measurements can be extrapolated also to running. By means of these data, others parameters like calorie consumption, power during running or vertical jumping can be obtained using computing techniques. The use of plantar pressure distribution evaluation systems in neurodegenerative patients, diabetes, rehabilitation processes, post-surgery, provide an additional, objective, and accurate information about patients with locomotion disorders. On the other hand, it permits to detect gait or running alterations that could be unnoticed using other control systems, making early diagnosis of many diseases possible.

Nowadays, there are many instrument to measure not only plantar pressure distribution, but also human gait temporal parameters. Depending on the type of device used, the information obtained might be more limited. Most of these devices are only available in biomechanical laboratories. Despite the large number of pressure and force measurement system, as it will be explained later, most efficient systems are instrumented insoles[1, 6].

1.2 Objectives

This Ph.D. thesis has been funded by an Excelence Research Project from Junta de Andalucía (Spain) called “Desarrollo de un sistema electrónico para la monitorización inalámbrica de parámetros biométricos mediante sensores plantares vestibles TIC-5997”, in the call for funds of 2010.

The main objective of this Ph.D. thesis is the design and development of an instrumented insoles to monitor several biomechanical and chemical qualities for different applications. This goal will be achieved by using the previous work developed by members of the research group [7, 8, 9, 10] as starting point. The final system will be embedded inside the insole, it will contains several pressure and kinetic sensors.

Therefore, in the final prototype, each insole will contain six pressure sensors, located at the big toe, first, third and fifth metatarsal heads, midfoot, and heel. In addition, a 9 degrees of freedom Inertial Measurement Unit (IMU), integrated by a triaxials gyroscope, accelerometer, and magnetometer, will be also placed at foot arc. Electronics will be supplied by a coin battery.

During the design, simulation, and development of the different versions of this instrumented insoles, several experimental test have been carried out. Resulting in a high quality publications in international journal and congress.

1.3 Document structure

This thesis document has been organised as follows:

- In chapter 1, a brief introduction of main concepts such as foot, gait, posture, and all those variable involved in their analysis have been explained. After that, the possible application in the main frameworks that study plantar pressure distribution and inertial information from those exercises are introduced. Finally, the state of the art both in industry and academics is presented.

- Along the chapter 2, there is a description of the evolution of the plantar pressure system designed, named ECnsole. This chapter is structured explained in temporal order the different prototypes developed by the candidate and the research group.

- The validation of the prototypes previously described is presented in chapter 3. Not only force or pressure sensor but also inertial measurement unit according to its possibility to obtain foot orientation during swing phase in gait.

- In chapters 4 and 5 the application of the ECnsole in vertical high jump is shown. Chapter 4 is focused on the validation of the instrumented insoles as a tool for vertical high jump measurement while chapter 5 presents the influence of performance trainings in vertical jumps for professional athletes.

- On the other hand, chapter 6 refers to the application of the instrumented insoles to monitor plantar pressure evolution and gait pattern evolution along pregnancy, while chapter 7 is related to the use of the ECnsole in the neurological diseases framework.

- To sum up, chapter 8 draws the main conclusions of this research.

- Additional information related to the research process is described in the appendices I and II. In appendix I a customised calibration system, manufactured using a 3D printer, is presented. On the other hand, all the documentation and the questionaire used in the study of chapter 6 are contained in appendix II.

1.4 The Foot

The foot, that is the terminal portion of a limb, sustains weight and permits movement and locomotion. In most of vertebrates, it is an anatomical structure. In many animals that have feet, the foot is a separate organ at then end of the leg composed of bones, and usually claws or nails.

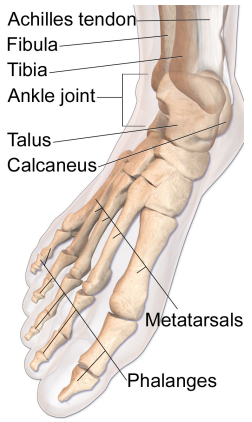

Figure 1.1: Lower leg and foot anatomy[11].

In humans, foot contains 26 bones, 33 joints (20 of which are actively articulated), and more than a hundred muscles, tendons, and ligaments[12]. It is a complex mechanical structure where joints of the foot are the ankle and subtalar joint and the interphalangeal articulations of the foot (see figure 1.1). An anthropometric study of 1997 North American adult Caucasian males (mean age 35.5 years) found that a man's foot length was 26.3 cm with a standard deviation of 1.2 cm[13].

As Shu et al.[14] mentioned, the sole of foot can be divided into 15 areas (see figure 1.2), these areas, which support most of the body weight and are adjusted by the body's balance, are grouped into: heel, midfoot, metatarsal, and toes, as is presented in figure 1.2. The foot can be subdivided into the hindfoot, the midfoot, and the forefoot.

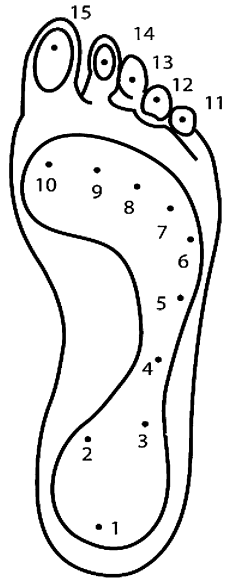

Figure 1.2: The sole of the foot can be divided into 15 areas: heel (area 1-3), midfoot (area 4-5), metatarsal (area 6-10), and toe (area 11-15). Picture of the anatomy of the foot[14].

The hindfoot is composed of the talus (or ankle bone) and the calcaneus (or heel bone). The two long bones of the lower leg, the tibia and fibula, are connected to the top of the talus to form the ankle. Connected to the talus at the subtalar joint, the calcaneus, the largest bone of the foot, is cushioned inferiorly by a layer of fat[12]. The five irregular bones of the midfoot, the cuboid, navicular, and three cuneiform bones, form the arches of the foot which serves as a shock absorber. The midfoot is connected to the hind- and fore-foot by muscles and the plantar fascia[12]. The forefoot is composed of five toes and the corresponding five proximal long bones forming the metatarsus. Similar to the fingers of the hand, the bones of the toes are called phalanges and the big toe has two phalanges while the other four toes have three phalanges. The joints between the phalanges are called interphalangeal and those between the metatarsus and phalanges are called metatarsophalangeal (MTP)[12]. Both the midfoot and forefoot constitute the dorsum (the area facing upwards while standing) and the planum (the area facing downwards while standing). The instep is the arched part of the top of the foot between the toes and the ankle. The foot has a fundamental responsibility in human support system, in addition, it is a great exponent of evolutionary biological changes development, and in turns an change examples that social situations can cause on organs and human structures. As a consequence, the study and understanding are essential to quarantine the foot health for every single person.

It is important to highlight that in order to make a complete morphological and biomechanic foot study different techniques are applied. Most known are:

- Kinetic
- Radiologic
- Photographic
- Hipodynamic. Shulzhenko Method.
- Tensometric. Strain Amplifier.
- Load Oscillographic.

- Computing.
- Baropodometry.

All these methods have permitted to study the foot to manage it classification and to determine the modifications and alterations that occur therein. The sole's foot suffers the application of important pressures influenced by many factors like locomotion, speed, etc., as in parameters related to the subjects, such as weight, age, and possible pathologies. Among them, the most significant factors are:

Weight: There is an important relationship between weight and plantar pressure. Some studies claim that the less heavy someone is, the less plantar pressure distribution are along the foot, except in toes, not only in gait, but also in race[15, 16]. Actually, it seems that overweight in people, with or without footwear, modify the plantar pressure distribution, increasing on a foot side, specially during contact time.

Age: Gait on children has some special characteristic that evolve within nervous system maturation and that stabilize when adult gait characteristic are obtained. This happens, according to most of authors, at the age of seven[17, 18, 19, 20]. Concerning to plantar pressure distribution in children, it is obviously lower than in adults due to the lower weight, and proportionally there is a higher pressure over the head of the first metatarsal due the genu valgum, commonly called "knock-knee", that cause foot pronation. In elderly people (since 60-70 years old) there are variations in gait indicators, regardless of alterations due to any pathology. Among them, foot is more horizontal in heel contact, due to a slightly smaller lower limb movement range, that make it conditional on a decrease of the vertical reaction force and the peak pressure during support.

Sex: Most of authors agree that many times sex does not determine plantar pressure distribution, but the use of different soles and anthropometrics characteristic, like a lower weight in women[17, 20]. On the other hand, articular mobility of women is higher and that might influence men with

stiffness and low pronation in support phase, that tends to locate most of pressure on lateral forefoot and toes.

Gait Speed and Cadence: Speed and cadence are interrelated, as higher speed with the same step length, more steps will be performed by minute, so cadence will be higher. It is shown that plantar pressure are directly proportional to those factors. As higher speed and cadence, pressure on heel, medium forefoot area and the first four toes increase linearly, while there are no differences in lateral forefoot or fifth toe.

During running practice most of speed increase the total of forces and pressures. However, most of pressure is not located in heel but forefoot, and in particular head of second metatarsal, following by first and third.

In any foot study, it is very important to know the pressure that any part of the foot support, among other variables. The heel and metatarsal heads present the highest pressures. During locomotion, forces that apply on the shoe come from body weight and forces applied by muscles, that are transmitted to the bones through the tendons. Reaction forces, that registered by force platforms, are identical to the those already mentioned, but in opposite direction. The reaction force vector can be split up into three orthogonal components (vertical, anteroposterior, transversal).

Usually, horizontal forces are studied (anteroposterior and transveral) to detect problems in the interaction between insole and ground surface since adhesion point of view. Vertical forces are tested specially for all those aspect related to the attenuation of footwear.

The path of the application point of resulting force of body weight starts just at the impact of the foot, in the central zone of the heel. After that, it moves quickly in a straight line till the head of the first and second metatarsals, it turns inside and moves slowly until the base of the first toe. It finishes at the end of the first or second toe, or between them.

1.5 Human Gait

Gait is commonly defined as a series of rhythmical, alternating movements of the trunk and limbs which result in the forward progression of the centre of gravity or a series of “controlled falls”[21].

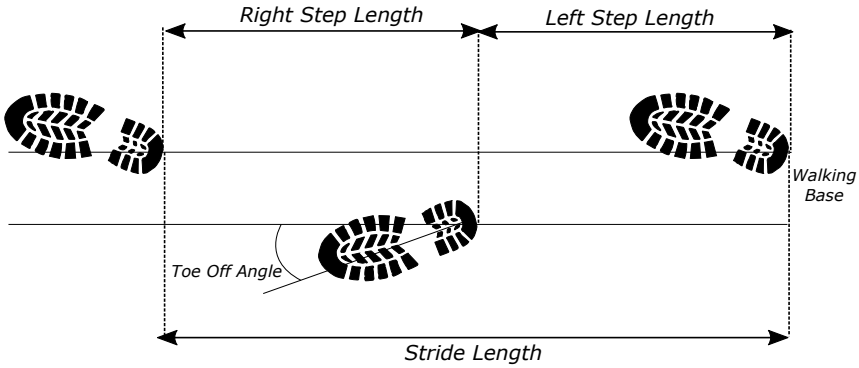

Figure 1.3: Gait Cycle in one consecutive step. It is important to highlight some definitions like step length, stride length and walking base. Alterations in these parameters might mean neurological or orthopaedic disorders.

There are some important definitions to understand gait, some of then are shown in figure 1.3:

Gait Cycle: Single sequence of functions by one limb. Begins when reference font contacts the ground. Ends with subsequent floor contact of the same foot.

Step Length: Distance between corresponding successive points of heel contact of the opposite feet. In normal gait, right step length must be equal to left step length.

Stride Length: Distance between successive points of heel contact of the same foot. It is the double of step length (in normal gait).

Walking Base: Side-to-side distance between the line of the two feet. It is also known as "stride with".

Cadence: Number of steps per unit time. Normal gait = 100-115 $^{steps}/_{min}$. It is modified by cultural/social variations.

Velocity: Distance covered by the body in unit time. It is usually measured in meters per second ($^{m}/_{s}$). Instantaneous velocity varies during gait cycle. The average velocity ($^{m}/_{min}$) is defined as the product of the step length (m) and the cadence ($^{steps}/_{min}$).

Confourtable Walking Speed (CWS) It is the speed per unit distance when the energy consumption is minimal. The average is $80^{m}/_{min}$ ($5^{km}/_{h}$, $3mph$).

Gait consist of two main phases. Stance phase, that refers when the reference limb is in contact with the floor; and the Swing phase, that encompasses when the reference limb is not in contact with the floor. During these two phases, there are single contact, when only one foot is in contact with floor, and double contact, when both feet are in contact with the floor simultaneously.

There are some subdivisions in each phase (see figure 1.4):

1. Stance Phase:
   (a) **Initial Contact (Heel Stike):** In initial contact, the heel is the first part of the reference foot to touch the ground.
   (b) **Loading Response (Foot Flat):** In the loading response phase, the weight is transferred onto the referenced leg. It is important for weight-bearing, shock-absorption and forward progression.
   (c) **Midstance:** It involves alignment and balancing of body weight on the reference foot.
   (d) **Heel Off:** It is the terminal stance. In this phase the heel of reference foot rises while the its toe is still in contact with the ground.
   (e) **Toe Off (Pre Swing):** In this phase, the toe of reference foot rises and swings in air. This is the beginning of the swing phase of the gait cycle.

2. Swing Phase:

   (a) **Acceleration (Initial Swing)**

   (b) **Mid Swing:** Swinging limb overtakes the limb in stance.

   (c) **Decceleration (Terminal Swing)**

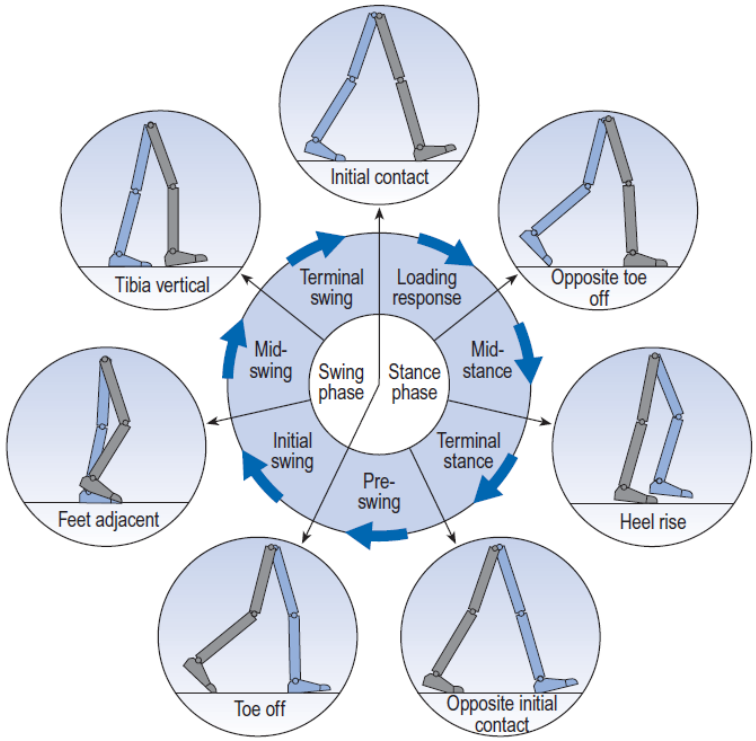

Figure 1.4: Gait cycle components[21]. Reference limb is in blue.

As figure 1.5 shows, in gait stance phase takes almost 60% of gait cycle while swing phase is 40%. In addition, single support means 40% of gait cycle per foot, while double support corresponds to 20%. If walking speed increases, the

stance phases decrease while swing phase increase, and besides, double support decrease. By default, running is defined like the walking speed that means no double support. In this case, ratio stance/swing phases is reversed. And depending on the speed, double swing time might appear.

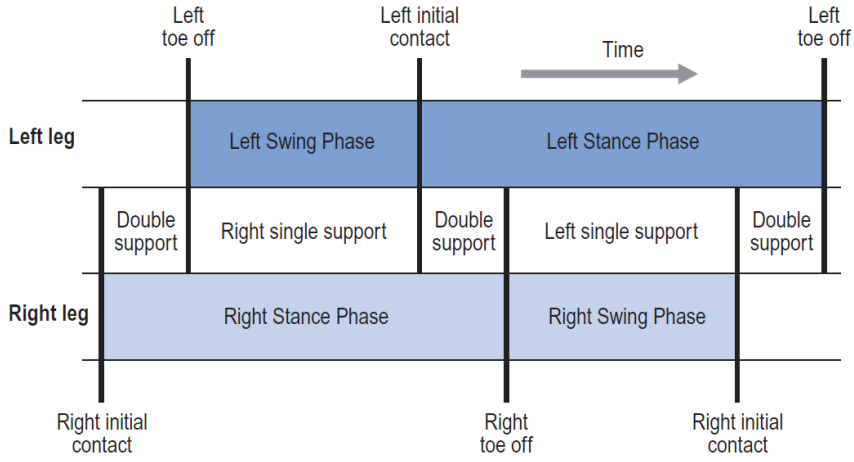

Figure 1.5: Gait cycle timing[21].

1.5.1 Ground Reaction Forces

The force platform is the most common instrument used in gait analysis. It provides the total forces applies by the foot to the ground, however, it does not give information about the distribution of this force on the walking surface. These type of system provide from one (usually vertical) to three dimensional description of the ground reaction force vector. These signal may be processed to obtain three components of force (vertical, lateral, and fore-aft) as well as the two coordinates of the centre of pressure and the moments about the vertical axis. *"The centre of pressure is the point on the ground through which a single resultant force appears to act, although in reality the total force is made up of innumerable small force vectors, spread out across a finite area on the surface of the platform"*[21].

In figure 1.6 a most common form of display the three-dimensional ground reaction force is shown. It represents a simple walk, where the gound reaction force is positive upwards, forwards and to the right.

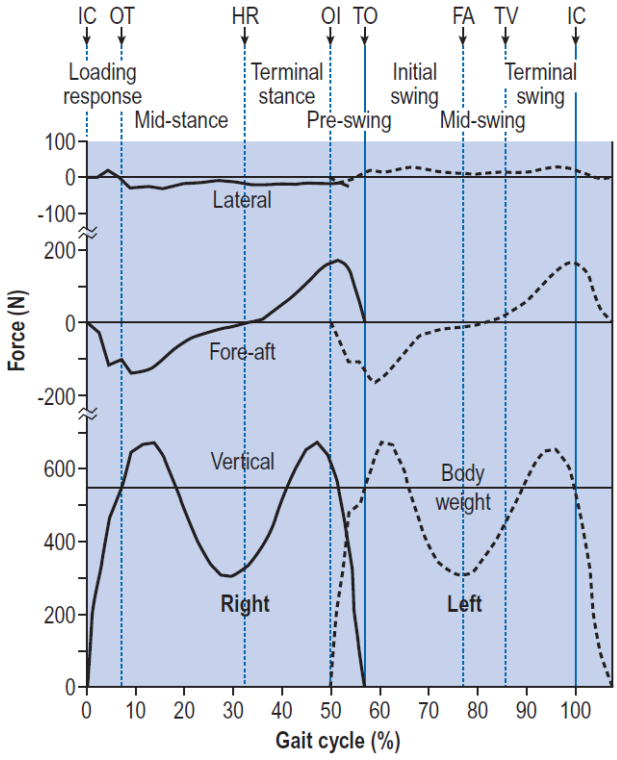

Figure 1.6: Lateral, fore-aft, and vertical components of the ground reaction force, in newtons, for right foot (solid line) and left foot (dashed line)[21].

In addition to the components of ground reaction force, a very useful information in order to detect or identify abnormal patterns of foot contact, including an abnormal toe out or toe in angle, is the position of the centre of pressure of the feet on the ground (see figure 1.7). The calculation of this parameter will be explained in next chapters.

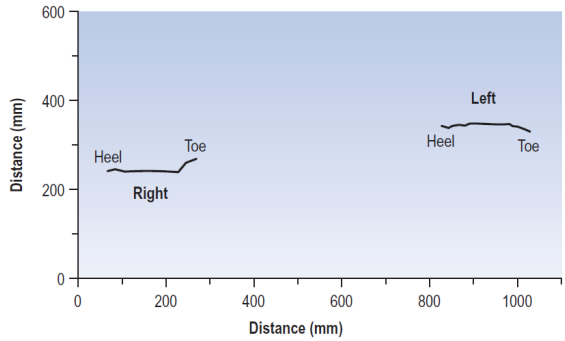

Figure 1.7: View of the walking surface from above, showing the center of pressure beneath the two feet, with the right heel contacting first and the subject walking towards the right of the diagram[21].

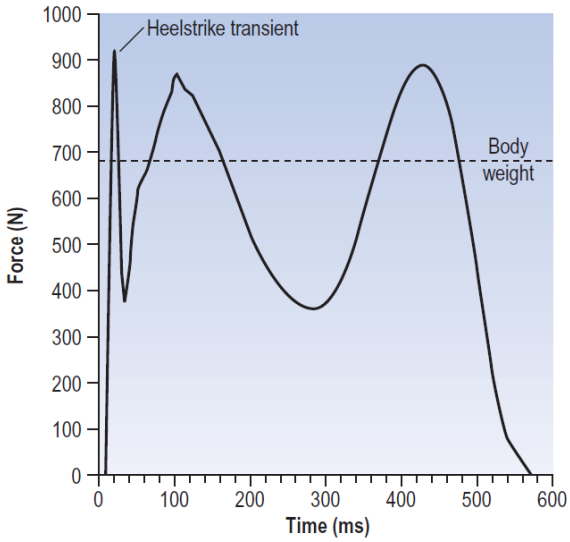

Figure 1.8: Plot of vertical ground reaction force against time, showing the heelstrike transient in a particularly 'vigorous' walker wearing hard-heeled shoes[21].

It is very important to notice, that vertical ground reaction force varies very much during a simple step. Figure 1.8 show a single step of a 'vigorous' walker, it is possible to observe that maximum of force is usually at heelstrike or initial contact, and is even higher than body mass weight.

1.5.2 Centre of Gravity

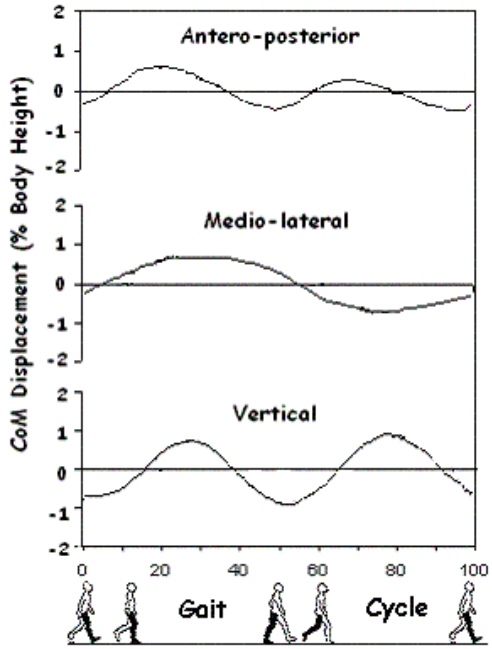

Figure 1.9: Centre of Gravity(or Mass) path. Antero-posterior, medio-lateral, and vertical displacement.

The centre of gravity is a geometric property of any object. The centre of gravity is the average location of the weight of an object. We can completely describe the motion of any object through space in terms of the translation of the centre of gravity of the object from one place to another, and the rotation

of the object about its centre of gravity if it is free to rotate. If the object is confined to rotate about some other point, like a hinge, we can still describe its motion. In flight, both airplanes and rockets rotate about their centres of gravity. A kite, on the other hand, rotates about the bridle point. But the trim of a kite still depends on the location of the centre of gravity relative to the bridle point, because for every object the weight always acts through the centre of gravity.

In normal gait, centre of gravity is located approximately in a midway between the hips. The least energy consumption occurs when centre of gravity travels in straight line. Centre of gravity has two different displacements: vertical and horizontal. Vertical displacement is based on a rhythmic up and down movement, the highest point occurs at the midstance and the lowest point when double support, the average displacement is about 5 cm and the path is extremely smooth sinusoidal curve. On the other hand, horizontal displacement is based on rhythmic side-to-side movement, the average displacement is also about 5 cm and the curve is the same type as vertical one as figure 1.9 shows.

The Centre of Gravity has a projection in the ground plane. It is possible to calculated by using the pressure points of both foots. The algorithm and calculation process will be described in detail in next chapters.

1.5.3 Common Gait Abnormalities

There are many gait abnormalities, but most important can be summarized in:

1. Antalgic Gait.
2. Lateral Trunk Bending.
3. Functional Leg-Length Discrepancy.
4. Increased Walking Base.
5. Inadequate Dorsiflexion Control.
6. Excessive Knee Extension.

An antalgic gait pattern is applied to a rhythmic disturbance, in which the painful limb support the weight during a time as short as possible. It reduces the amount of pain a person is experiencing. These types of patterns are asymmetrical between the two legs but is usually regular from one cycle to the next. It also happens when there is a difference in leg length[21].

Bending the trunk towards the side of the supporting limb during the stance phase is known as lateral trunk bending. The purpose of the manoeuvre is generally to reduce the forces in the abductor muscles and hip joint during single leg stance. Lateral trunk bending is best observed from the front or the back. During the double support phase, the trunk is generally upright but as soon as the swing leg leaves the ground, the trunk leans over towards the side of the stance phase leg, returning to the upright attitude again at the beginning of the next double support phase[21].

Four gait abnormalities (circumduction, hip hiking, steppage and vaulting) are closely related, in that they are designed to overcome the same problem - a functional discrepancy in leg length. An 'anatomical' leg length discrepancy occurs when the legs are actually different lengths, as measured with a tape measure or, more accurately, by long-leg x-rays. A 'functional' leg length discrepancy means that the legs are not necessarily different lengths (although they may be) but that one or both are unable to adjust to the appropriate length for a particular phase of the gait cycle. In order for natural walking to occur, the stance phase leg needs to be longer than the swing phase leg. If it is not, the swinging leg collides with the ground and is unable to pass the stance leg. This usually occurs as the result of a neurological problem. Other causes of functional leg length discrepancy include musculoskeletal problems such as sacroiliac joint dysfunction. An increase in functional leg length is particularly common following a 'stroke', where a foot drop (due to anterior tibial weakness or paralysis) may be accompanied by an increase in tone in the hip and knee extensor muscles. The gait modifications designed to overcome the problem may either lengthen the stance phase leg or shorten the swing phase leg, thus allowing a normal swing to occur. They are not mutually exclusive and a subject may use them in combination. The gait modification employed by a particular person may have been forced on them by the underlying pathology or it may have been a matter of chance, two people with apparently identical

clinical conditions having found different solutions to the problem[21].

If the walking base is abnormally wide, there is a problem with balance during single leg stance. Rather than tip the whole body to maintain balance, lateral bending of the trunk may be used to keep the centre of gravity of the body roughly over the supporting leg. In most cases, this will need to be done during the stance phase on both sides, leading to bilateral trunk bending and a waddling gait. A number of conditions, which will be described later, may cause a wide walking base[21].

The dorsiflexors are active at two different times during the gait cycle, so inadequate dorsiflexion control may give rise to two different gait abnormalities. During loading response, the dorsiflexors resist the external plantarflexion moment, thus permitting the foot to be lowered to the ground gently. The dorsiflexors are also active during the swing phase, when they are used to raise the foot and achieve ground clearance. Failure to raise the foot sufficiently during initial swing may cause toe drag. Both problems are best observed from the side of the subject and both make a distinctive noise. A subject with inadequate dorsiflexion control can often be diagnosed by ear, before they have come into view! Inadequate dorsiflexion control may result from weakness or paralysis of the anterior tibial muscles or from these muscles being overpowered by spasticity of the triceps surae[21].

In the gait abnormality of excessive knee extension, the normal stance phase flexion of the knee is lost, to be replaced by full extension or even hyperextension, in which the knee is angulated backwards. This is best seen from the side. Hyperextension of the knee, accompanied by anterior trunk bending, is seen quite frequently in people with paralysis of the quadriceps following poliomyelitis. The gait abnormality is clearly of great value to the subject, since without it he or she would be unable to walk. However, the external hyperextension moment is resisted by tension in the posterior joint capsule, which gradually stretches, allowing the knee to develop a hyperextension deformity ('genu recurvatum'). As a result of this deformity, the joint frequently develops osteoarthritis in later life[21].

1.6 Clinical Framework

In clinical framework there are many possibilities to classify gait disorders depending on pathology, aetiology, affected zone, gait phase altered, etc. Nevertheless, all pathological process end provoking alterations that diagnosable by means of study and analysis of gait[22]. However, in real medical applications there are a number of deficiencies or improvement needs in order to detect those alterations and consequently in diagnosis, valuation and foot treatment processes, which show that the inclusion of a new method is a vital need.

The clinical examination of the foot is essential for doctors working on locomotor system (orthopaedic surgeon, physical therapist, and rheumatologist), podiatrist, orthopaedic technician and for any other professional related to foot health. It is very important to have diagnostic methods able to register the plantar pressure distribution during gait in an objective and reliable way, as well as pressure values at any point on the foot, this information can assist to the specialist to issue a diagnostic and to apply a better treatment.

Those registered pressure values, may be grouped in characteristic load pattern in some pathologies that affect to the foot, even correlated them with clinical indicators like pain. Obtaining those patterns can help considerably the diagnostic task of clinical specialist.

The use of plantar pressure measurement system in daily clinical practice makes possible to evaluate the effects achieved by a patient after the application of a surgery or conservative treatment.

The relationship between all clinical specialist responsible of orthoses medical prescription to a patient and the orthoprosthetic technician responsible of manufacturing the insole or plantar orthoses is in many cases limited.

The work methods of orthopaedic industry are mainly home-made. It is very difficult to find identical work methodologies between two orthopaedic workshop. Designing details fixed by the specialist usually let some decisions like materials choice or layout of the elements to the orthopaedic technician. So, it exists a market where introduce new objective methodologies to replace classics techniques.

Therefore, using the information obtained by changes in plantar pressure pattern, both the distribution and the pressure, some clinical diagnosis may be

related to:

1. Pain at the plantar supporting surface, regardless of the pathology that causes.

2. Orthotist prescription and validation of the relation ankle-foot [6, 23, 24].

3. Pathology on plantar support, not related with pain, and among them, diabetic neuroangiopathy and sensivity neuropathy, motor or from nervous vegetative system, and that are able to develop ulcers in the plantar support surface[25]. In these cases it have a pre-emptive value, in order to introduce elements that might reduce excessive pressure in certain zones.

4. Central neurological pathology and orthopaedic, due to the reasons already highlighted[3, 26, 27].

Next, the utility of the plantar pressure detection will be presented against some concrete semiotics cases.

1.6.1 Pain and Plantar Ulcers

Foot clinical exploration by means of qualitative and traditional methods provides information about foot and ankle structure: anthropometric data, foot and/or articular balance, load feet and/or ankles radiography, both front-rear and lateral[28]. This information complements others data from clinical exploration, like callosity analysis, ulcer or any other type of injure in plantar support surface. Disorders are appreciated in the lining up of limbs, dysmetria, malformations, and naturally, the location of pain by the subject[6]. In addition, information about the patient's problem must be available, if that information about dynamic functionality of the foot is obtained, our knowledge about subject's problem and how to solve or improve it will be much more complete. If gait is no analgesic, it means, stands over painful zone, the coincidence of analgesic zone and the maximum pressure zones make easier the prescription of release orthotic. The fact that orthopaedic technician have plantar pressure record at his

disposal on scale facilitates the proper manufacturing of those orthotic. Knowledge of plantar pressure have shown a great utility in orthotic ankle-foot prescription, spastic diplegia children, hemiplegia adults[23]; in evaluation of release orthotic in healthy subjects[24]; and a better knowledge about modifications that footwear introduce on plantar pressure[29].

Regarding the ulcers presentation at plantar surface in diabetic patients or those affected by neuropathies or motor-sensitivity polyneuropathies, it has been appreciated the coincidence of ulcer zones with higher maximum pressures zones[30], such as changes in pressure distribution patterns[31], and time support length[32]. Structural charasteristics of diabetic feet are conditioned, principally, by the sensitivity of the disorder, derived from neuropathy, and determine hyperpressure plantar zones[33]. The neuropathy presence is, therefore, responsible in a small contribution for changes in plantar pressure distribution and increasing on stance time[32]. In those diabetics patients with sensitivity disorders, the determination of plantar pressure is a predictive valuable element[34, 35], regarding the possibilities of ulcers development on plantar support surface[36]. This allows to adopt preventive measures[37].

1.6.2 Lumbar Pain and Pregnancy

In the course of pregnancy, together with the progressive uterus and abdomen growth, as well as breasts, the gravity centre of women displaces forward significantly, appearing important changes in static corporal position. For this reason, in order to maintain the balance in erect position, pregnant woman must go to adapt to this new situation by means of exaggerate her lumbar lordosis, increasing her stress at the spine and muscles taking the projection of gravity centre behind the head and trunk. With the same objective, and trying to increase sustenance base, pregnant woman resort to legs abduction opening the feet outside modifying the extension level of the instep. As a consequence of these news static conditions pregnant have, specially at the end of pregnancy, a new walking way: leaning backward and swinging from one side to the other (goose or duck walk). The modifications described require on the other hand that muscles and ligaments that hold the spine to carry out a higher strength, tightening more than usual, being able even to become insufficient because of

exhaustion. Due to this overstrain pains in cervical and specially in lumbosacral region may appear[38, 39].

Changes in locomotor system of pregnant are divided into:

- Osteoarticular system, which occurs:

  1. Ligamentous laxity: relaxing of the last pregnacy stage of sacroiliac, sacrococcygeal, and pubic articulations provoking duck gait.
  2. Elastic ligamentous as a consequence of its relaxation.
  3. Reduction of the cartilage resistance, because it absorbs the water increased at the expense of progesterone.

  These three points will give as a result next disorders:

  1. Increase of lumbar lordosis.
  2. Increase of dorsal kyphosis.
  3. Pelvic anteversion.
  4. Sacral horizontalization.
  5. Horizontalization ribs.
  6. Retraction of the hamstrings.

- Muscular system, which occurs:

  1. Decrease of muscle tone.
  2. Activation of muscular growth.
  3. Muscles change their biomechanics, since bones modify their regular organization, specially rachis and ribs.
  4. Affectation of abdominal muscles.

More than a third part of women suffer back pain in any time of pregnancy. Symptoms are related with physical changes. It intensity, variability and length can vary during pregnancy. Thus, symptomatology are rigidity, numbness, mechanic pain, neuralgic pain or total handicap. Back pain more often occurs in

those women that already have back pain before pregnancy, and those who carry out intense physical work[38].

Pelvic lumbar pain includes:

1. Pelvic pain (PPP).

2. Lumbar pain.

3. Combination of both.

Regarding to the foot there are some studies already published that analyse the changes that happen on feet during pregnancy. There are many changes in ligaments due to the mechanical stress, hormonal changes and physiological changes such as the accumulation of interstitial fluid and fat[40]. This can lead to a bad foot position that can cause lumbar and lower limbs pains[41]. During pregnancy hindfoot and midfoot present more pronation and forefoot in valgus. The head of the talus ascends around 1 cm due to the pronation of middle part. In addition, there is an increase of the amplitude of the movement of the first metatarsophalangeal joint. It attributes this increase on joint mobility to the relaxin secretion[40]. The group of Niska et al.[42] have observed that it exists a deviation of the force and gravity centre toward forefoot, and with the goal to restore to its regular location, tendency is to increase plantar pressure on hindfoot.

1.7 Physical and Sport Activity Framework

En high-level competition and sport research, the calculus of jump power is carried out on biomechanicals laboratories where the main tests performed are Wingate test using cycle ergometer, Margaria steps test[43], and the most used, force and contact platforms[44]. The integrated package widely spread in jumping ability evaluation, consist in a conductive platform connected to a electronic timekeeping system that is activated by the subject thought the jump and the reception, so flight time and stance time are obtained. The system is connected to a pocket computer. It also exists a system that use a infrared

or laser barrier to calculate those variables. However, using both contact platforms and infrared/laser barriers in calculation on explosive forces and lower limbs power, some failures and problems have been observed in test performing. The imbalance in anteroposterior and mid-lateral areas produced during jumping over limited dimension platforms, the excessive distance and low sensitivity of conductive plate of contact platform, and the high cost of laser barriers, are some of these deficiencies[45].

Others studies based on pressure data allow to diagnose the evolution of plantar fasciitis[46], just like in the improvement of sport performance in high-level competition, the study of football players movement[47, 48], the adhesion of tennis player to different competition surfaces[49] or the differences in run patterns using different sport shoes[50].

1.8 State of the Art

Measurement techniques that allow to measure plantar pressure inside the footwear contribute to a better patient treatment. Feet problems related to pressure manifest mainly in pain, callosity, neuropathic and decubitus ulcers. Some of the methods used so far to perform studies that require measurement and detection of support during, gait, jump, and race, precise of a high technology and complex instrumentation, while others used simple method with few instrumentation and provided just qualitative results. Next, most common methods will be cited according to the classification provided by Biomechanical Institute of Valencia[1]:

- **Statics**:

  Pedigraphy: Footprint obtained after impregnate the plantar surface with a fatty and colour substance and print that footprint on a regular paper sheet(see figure 1.10a).

  Photopodogram: Same technique, but printing on photographic paper.

  Podoscope: Optical system based on a transparent surface onto which subject's feet are placed. The image of footprint can be studied through

the other side of transparent surface or using illuminated mirror system(figure 1.10b).

(a) Pedigraph (b) Podoscope

Figure 1.10: Static measurement instruments to measure plantar pressure distribution.

Figure 1.11: SportJump System PRO[51].

- **Kinetics**:
  - Load measurement system between footwear and ground:
    1. Instrumented shoes, that employs transducers and load cells inside or over the shoes' sole.
    2. Shoes with metallic plate instrumented with gauge attached to the sole.
  - Load measurement system between foot and ground:
    1. Ink printing techniques. Based on the deformation of flexible elements that are modified as subject walks.
    2. Optical techniques, using barograph. The material on which the foot rests is deformable, and once is exposed to pressure, it produces an images due to the liquid between the deformable material and the crystal that underlies to photoelastic material.
    3. Electromechanical transducers matrix. They are pedometer or transducer included platforms.
  - Load measurement system between foot and footwear:
    1. Discrete sensors that use:
       (a) Capacitive transducers.
       (b) Transducers based on strain gage.
       (c) Piezoelectric transducers.
       (d) Resistive transducers.
       (e) Magnetoresistive transducers.
    2. Instrumented insoles. Insoles that add several types of sensors.

Others combination of techniques to dynamic gait study are:

1. Video recording of the subject while he/she performs any physical activity (walking, running or jumping), to carry out the movement using a computer afterwards. This method results quite expensive, uncomfortable to the researcher and not too accurate since video cameras offers a resolution of about 20 ms. In addition, the results are not immediate because a hard work is needed after recording.

2. Video recording using high-speed video camera. This video cameras are very accurate, but totally unreachable for medium trainer or for a researcher with a low budget. They are able to record in high-speed frame rate, that means a precision of milliseconds, avoiding accuracy problem of last method, but still needing a post-processing of recorded data.

3. Infrared or laser platforms(figure 1.11). The working principle consist in the use of two infrared or lasers barriers separated one each other with the subject of the study in the middle. This method allows to quantify the length of support of the subject by measuring the times that subject interfere the infrared/laser lines created by the barrier. The main problem is again the precision, that depends of the number of sensors, and the location of them that force the subject to stay in a concrete space.

4. Support detectors in conductive corridors(figure 1.12). They consist in an instrumented insoles with metallic components that once they reach the conductive corridor, the contact and non-contact time of the subject is quantified. Its main problem lies in the movement of the subject that is limited to the platform or metallic carpet, so that means that it is not applicable in real sport cases.

5. Support detectors using accelerometers. They consist in an instrumented insoles with accelerometers that allow to quantify distances, speed and high jumps. Accelerometers are placed on the sole of one of the sport shoes and send the data using a radiofrequency transmitter to a receiver usually located at the wrist to make the appropriate calculations. Its main limitation lies in no discrimination the time support length of the different parts of the foot because it is located just in one of the shoes.

Most of the systems described are shown in figure 1.13.

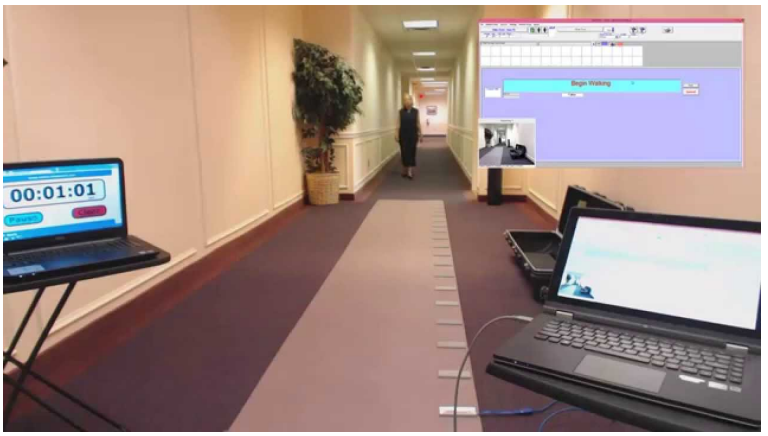

Figure 1.12: GaitRide pressure sensitive carpet[52].

Figure 1.13: Example of non wearable system: BTS GaitLab configuration. (1) infrared videocameras; (2) inertial sensor; (3) GRF measurement walkway; (4) wireless EMG; (5) workstation; (6) video recording system; (7) TV screen; (8) control station. Reproduced with permission from BTS Bioingenieering[53, 54].

1.8.1 Instrumented Insoles in Industry

Biofoot/IBV

Biofoot/IBV[55](Valencia, Spain) is an advanced instrumented insoles system designed to measure and analyse foot plantar pressure in regular conditions (walking and with footwear). It means a great progress, against traditional optical plantar analysis systems, and it is very often used in next application areas:

- Design and evaluation of footwear.
- Biomechanics: gait analysis, human gait characterization.
- Sport: study, selection, and adjustment of sport footwear. Analysis of sport gestures (jumping, running, gait, cycling).

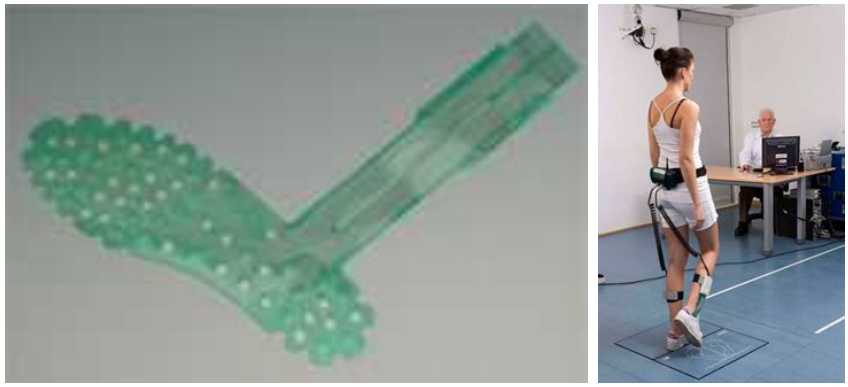

(a) (b)

Figure 1.14: Biofoot insole (a) and subject using biofoot (b). It is possible to observ that insoles are connected to an amplifier and them to the datalogger placed on the waist.

In order to keep a organized subject history record, Biofoot/IBV manages data of each subject arranged in studies, sesions and measurements. It performs an analysis of pressures during measurement session, and shows data in several formats:

- Numeric pressure and maximum pressure map.
- Total force versus time plot.
- Three dimensional map with colour or grey scale.
- Support surface versus time plot.
- Isobars plot.
- Pressure versus time plot.
- Position and trajectory of the barycentre.
- Real time monitoring of pressure.
- Calculated parameters table by zones (defined by the user).

Each insole is formed by a maximum of 64 pressure points (depending on the size), figure 1.14a shows the Biofoot/IBV insole. The useful life of the insoles is about 3000 steps. Each insole have its own calibration file. The insoles are connected to an amplifier that is also connected to a datalogger placed at the waist (see figure 1.14b) that sends the information from sensors through WiFi. Sampling frequency goes from 50 to 250 Hz as it has been shown in the the several research works which have been developed using this system[56, 6, 1].

Parotec

Parotec[57] is a high-performance measurement system for pressure analysis during the natural movement cycle. It is manufactured by Paromed (Neubeuern, Germany). The paroTec®-system measures actual foot pressure while standing or moving. Pressure distribution is precisely recorded using measurement soles worn in the shoes of the patient.

In figure 1.15 The parotec system is shown. Parotec's insoles contains from 24 to 36 measurement points, based on hydrocell technology. The frequency sample is up to 300 Hz. After the measurement process is complete, the data

are transmitted to the PC where they can be individually visualised and also digitally combined. For example with the shape measurement data in the paroContour® modelling software, where the data can be integrated into the insole design[34, 58, 41].

Figure 1.15: The Parotec system.

F-Scan

The F-Scan[59] In-Shoe analysis system is designed by Tekscan (Boston, USA), that is a manufacturer that also sells force and pressure sensors. As well as in others commercial systems, it is composed by two insoles with pressure or force sensors, connected to amplifiers (see figure 1.16) and these one again to a datalogger unit placed at the waist. There is two different versions of this product. The one that sends data via wirelessly, achieving up to 100 Hz frequency sample, and the one that record data into a internal memory, that reach up to 750 Hz, but only 30 seconds of recording at that frequency sample.

F-Scan insoles provided a huge number of sensors. As figure 1.17 shows, they consist in a force sensor matrix, in one of the sides, sensors are located in horizontal, and in the other side in vertical orientation. Total number of sensing point is up to 954. Due to the fragility of the insoles, it can be used from 5 to 15 trials according to the manufacturer datasheet[59]. There are many works in literature that have used F-Scan insoles to carry out gait analysis[60, 61, 50, 62, 36, 63, 64, 65].

Figure 1.16: F-Scan system in use.

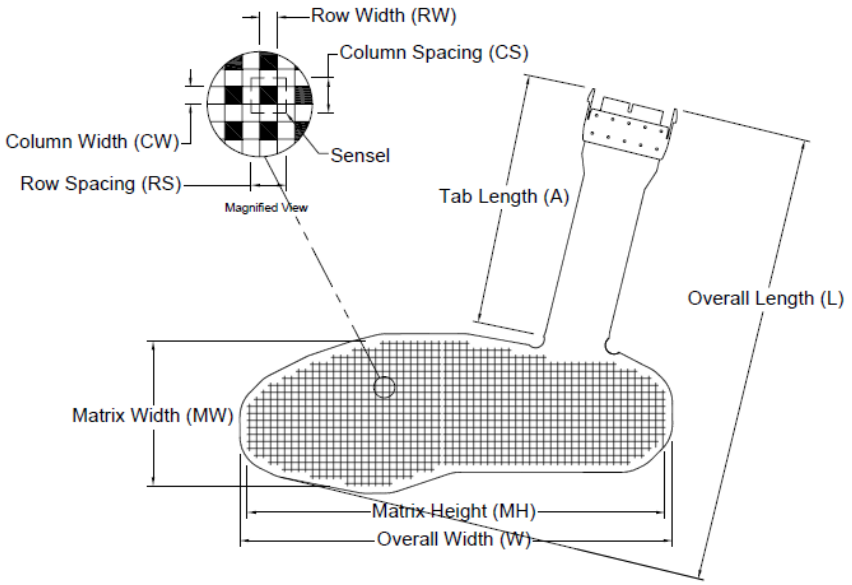

Figure 1.17: F-Scan insoles.

Pedar-X

Pedar-X is manufacture by Novel Gmbd[66] (Munich, Germany). It includes optionally the trublu® calibration system, that help to calibrate individually all sensors of Pedar-X using constant air pressure. This procedure is computer assisted and can be performed in a short time. Calibration guarantees accurate and reproducible data. The calibration curves, one for each sensor, can be checked by the user at any time.

Figure 1.18: Pedar-X System.

The pedar-x is an accurate and reliable measurement system for monitoring local loads between the foot and the shoe(see figure 1.18). The system operates with a straight connection to the PC, but also via radio signal with its built-in Bluetooth telemetry system. In addition, measurement data can be stored in built-in flash memory, to be downloaded to the computer at a later stage. The pedar-x is also suitable to monitor loading through the ground reaction forces.

Insoles contains 85 to 99 sensors, and the datalogger unit is able to measure up to 120 Hz. The software provided by manufacturer allows user to get information about individual sensors or group of them, make 2D, 3D, and iso-

bars plots. And many more options related to study of feet parameters. It is a very common device in gait analysis[49, 67, 68].

OpenGo Science

OpenGo Science is the most mobile and flexible way to analyse the plantar pressure distribution, contact forces and dynamics of the human foot. It is developed by Moticon[69](Munich, Germany). It is used in clinical research as well as for sports science and analysis in daily life. It is based on wireless sensor insoles.

Figure 1.19: OpenGo insole.

Each insole (see figure 1.19) contains 14 capacitive pressure sensing pads and a three axis accelerometer for measuring motion. The sensor data is processed in the embedded microsystem. From this raw data, a variety of essential gait and motion parameters are computed.

In figure 1.20 the location of the pressure sensors and the accelerometer are shown. These sensor have an output resolution of 7 bits and a sensitivity of $0.25^{N}/_{cm^2}$. The sensitivity of three axial accelerometer is configurable to ±2, 4, and 8 g, it also has 7 bits as output resolution. The sample frequency of OpenGo Insoles is up to 100 Hz, but using the maximum frequency is only able to obtain 8 sensors value.

This system has been validated in research in 2015[70].

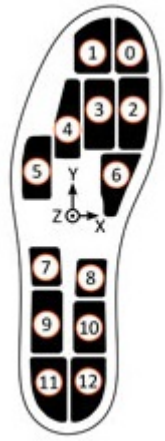

Figure 1.20: OpenGo insole layout.

1.8.2 Instrumented Insoles in Academics

According to literature research, there are some requirements when a instrumented insoles or a plantar pressure measurement system is going to be designed [71]:

1. Mobile. In order to achieve this goal, the system must be light and of small overall size[72, 73]. The weight of the device should be 300g or less.

2. Limited cabling. Wireless is ideal, but in case that wires are use and to ensure comfortable, safe and natural gait, the wire must be as reduced as possible[73].

3. Shoe and Sensor Placement. It is important to avoid modifications in gait due to sensors' size, because of this, sensors must be chosen thin, flexible[74] and light[72]. It has been already reported that a shoe attachment of mass 300 g or less does not affect gait significantly[72].

4. Low cost. The main idea is to be able to combine these sensors for general application[73] with any other novel sensor solution.

5. Low Power Consumption. It is directly related to mobility and size of the device. The lowest the power consumption is, the smallest the battery can be, reducing therefore the size of the complete device.

When choosing plantar pressure sensors, there are many key specifications that must be taken into account: linearity, hysteresis, sensing size, pressure range and temperature sensitivity[72, 74, 75]. It is very important a brief discussion of these requirements or specifications as a basic for the selection of a sensor for specific applications.

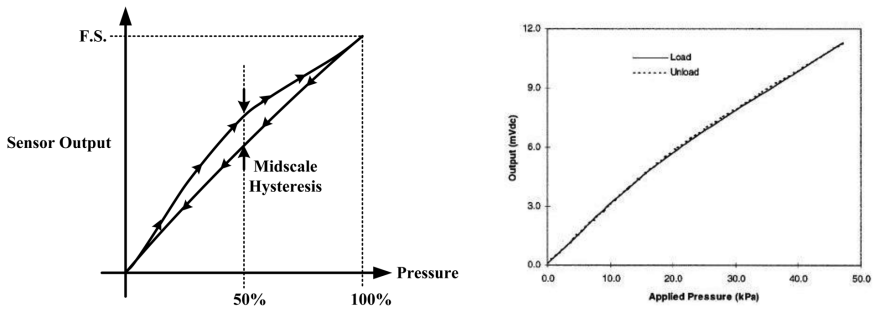

(a) Adopted from *Beeby et al.*[76] (b) Adopted from *Lee et al.*[74]

Figure 1.21: Hysteresis caused by loading and unloading a pressure sensor.

1. Hysteresis. It can be determined by observing the output signal during a loading cycle and unloading one. When the applied pressure is increased by loading or decreased by unloading, two different responses are observed (see figure 1.21).

2. Linearity. It is defined by how straight is the response of the sensor once a pressure is applied. Linearity indicates how simple or complicated the calibration and signal processing will be. As highly linear the circuit is, much simpler the signal processing circuit will be and vice versa.

3. Temperature Sensitivity. Depending on the temperature changes in the ambient, sensor readings may be different. This is mainly due to the ma-

terials that are part of the sensor body as they respond differently to temperature changes. A sensor with low temperature sensitivity is preferred [74].

4. Pressure Range. This parameter is the key specification for a pressure sensor. Different applications would required different pressure ranges. Foot plantar pressure values of up to 1900 kPa are typically reported in the literature but an extreme pressure of up to MPa has been documented by Urry[75].

5. Sensing Area of the Sensor. Others critical factors are the size and placement of the sensor, as shown in figure 1.22. Large sensors may underestimate the peak pressure and it is suggested that minimum sensor area of $5mmx5mm$ should be used, whereas sensors smaller than this must be designed as array sensors.

6. Operating Frequency. For running activities the minimum sampling frequency recommended is 200 Hz[75]. This value is generally considered sufficient for sampling most everyday activities.

7. Creep and Repeatability. Creep is the deformation of material under elevated temperature and static stress. It depends directly on the time that material is under a deformation due to a constant load or stress[77]. Low creep sensors are one the key requirements in foot pressure measurements, due that insoles can suffer lot of deformations and temperature might be elevated. Repeatability is the ability to produce reliable results even after long period of time[74]. Deformation or fatigue may occur when there are high cyclic loads[77]. Repeatability problems may be discarded if the sensors exhibits no creep or deformation after several or high cyclic loads.

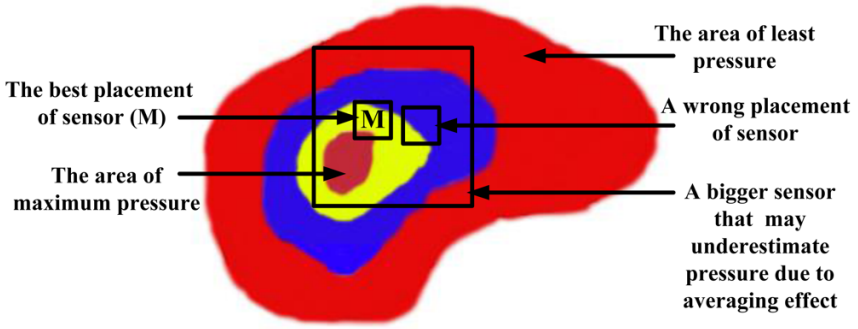

Figure 1.22: Effect of sensor sizing and placement.

Commercial Foot Plantar Pressure Sensor

There are several pressure sensors available on the market. The signal output provided by these sensors is some kind proportional to the measured pressure value. As it has been already explained, there are several required key specification that must be fulfilled by the sensors. Next, most common pressure sensors are described:

Resistive Strain gauges are the most common kind of sensors that use resistance change as a the method of transduction. In last few years, new techniques based on conductive rubber, conductive ink or conductive polymers have also been developed[75].

When pressure is applied on the sensor, the resistance of the conductive foam between two electrodes changes. The current through the resistive sensor varies as the conductive layer changes. In figure 1.23 a resistive sensor is shown.

Some commercial systems use this type of sensors, like MatScan®platform system (Tekscan, USA)[http://www.tekscan.com] and F-Scan®in-shoe system (Tekscan, USA)[79] or commercial sensors like Force Sensing Resistor®(FSR, Interlink Electronics, USA)[80]

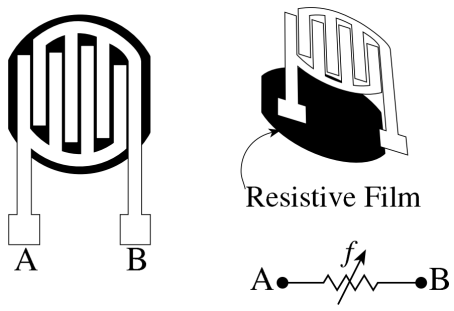

Figure 1.23: Resistive pressure sensor. The resistance between electrodes A and B is modified once a pressure is applied on the sensor due to physical changes on the conductivity of the foam between the electrodes[78].

Capacitive As well as any capacitor, this type of sensor consist of two conductive electrically charged plated separated by a dielectric, but in this case, the dielectric is an elastic layer. Once a pressure is applied, the elastic dielectric layer bends, reducing the distance between the two electrodes resulting in a voltage change proportional to the applied pressure[75]. Figure 1.24 shows the capacitive sensor construction. Commercial products based on this system are the Emed®platform system (Novel, Germany) and Pedar®in-shoe systems (Novel, Germany)[66].

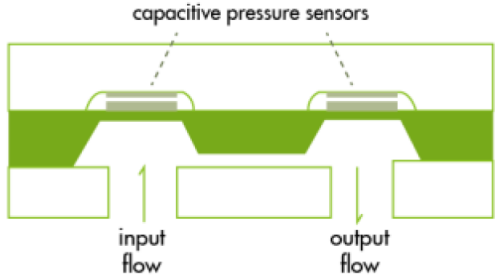

Figure 1.24: Capacitive pressure sensor. A pressure once applied to the sensor results in a voltage change proportional to the applied pressure[81].

Piezoelectric The sensor produces an electric field (voltage) in response to pressure. Piezoelectric devices have high impedance and therefore susceptible to excessive electrical interference that leads to an unacceptable signal-to-noise ratio. Figure 1.25 shows the piezoelectric sensor construction.

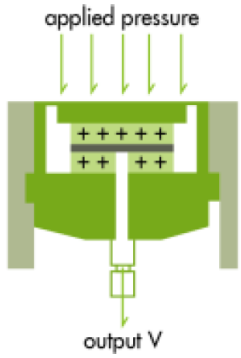

Figure 1.25: Piezoelectric pressure sensor. When pressure is applied, the displacement of the piezoelectric element produces an electric field[81].

The most suitable material for clinically oriented body pressure measurement is polyvinylidene fluoride (PVDF) because it is flexible, thin and deformable[82, 75]. There are some commercial products that are based on this technology, most important are Measurement Specialties (USA)[83] and PCB Piezotronics, Inc., (USA)[84].

Piezoresistive This sensor is made of semiconductor material(see figure 1.26). The bulk is usually the element whose resistivity is influenced by the force or pressure applied in piezoresistive materials, when the sensor is unloaded resistivity is high and when force is applied resistance decreases[82].

Most important commercial product is ParoTec (Paromed, Germany)[57] and commercial sensor is Flexiforce®(Tekscan, USA)[79]. As it has been already defined, main requirements of pressure sensors for the specific application are low hysteresis, linearity of output, and pressure range[74, 72, 75]. Normally, the recommended pressure gait for general purpose gait analysis (walking) is

approximately 1000 kPa[75] but for sports larger range must be considered due to the nature of the movements.

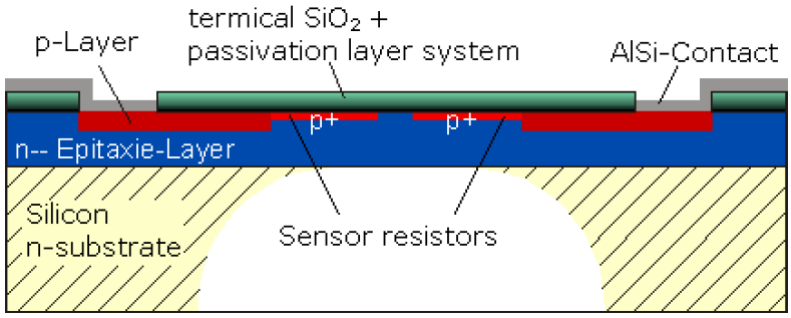

Figure 1.26: Piezoresistive pressure sensor. When there is a pressure on the piezoelectric element it produces electric charges from its surface. These charges create voltage proportional to the applied force[71].

Wired Instrumented Insoles

One of the first plantar measurement system was designed by *Zhu et al.*[85, 86] in 1990, its goal was to measure the pressure distribution beneath the foot to distinguish pressure during walking and shuffling. This system uses seven force sensitive resistor FSR (Interlink, USA) located at big toe, the five metatarsal heads, and under the centre of the heel. Sensors were sampled at 20 Hz. In 1995, Hausdorff et al.[87] built a footswicht system to detect timing parameters related to gait using two FSR resistive sensors, located one in the anterior part of the foot and the other one in the heel. It was compared to a platform forces and temporal parameters were calculated from rising and falling edges from sensor's signals.

Many years later, the group of *Gafurov et al.* developed a system to authenticate gait using an acelerometer was performed[88]. This system contains a ADXL202 accelerometer manufactured by Analog Devices(Norwood, Massachusetts, USA)[89] Its goal was to perform gait recognition from the data of an accelerometer placed at lower leg. For that purpose, it uses the sensor to obtain

the gait patterns of the subjects. It shows that not only pressure or force sensor provide a useful information about gait, but also kinetic sensors. The equal error rates (EER) obtained were of 5% and 9% for histogram similarity and cycle length methods respectively.

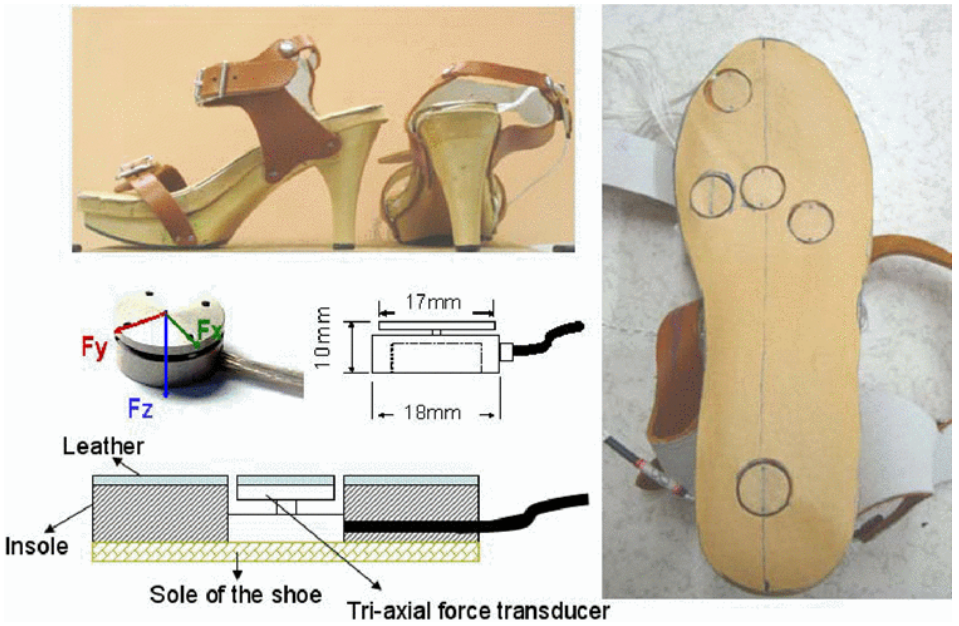

Figure 1.27: Shoes and transducers used in Cong and Zhang study and the locations of the transducers[90].

There are research works that have developed instrumented insoles using sensors different from the one described previously. For instance, a system that use five in-shoe triaxial force transducer[90], designed by Anhui June Sport product Co. Ltd, China, were mounted under the hallux, the first, second and fourth metatarsal heads as well as the heel (see figure 1.27). It measured the distribution of contact pressure and shear stress simultaneously in high-heeled shoes in any of the three directions of the space, providing a very interesting information at any sensor key point. The results showed that both the peak pres-

sure and peak shear stress occurred at the 2nd metatarsal head. The sampling frequency achieved by this system was up to 300 Hz.

Other studies have carried out an study to achieve a method for identifying humans based on their dynamic plantar pressure distribution[91]. Each foot contains 32 pressure sensors. System in used is shown in figure 1.28. The sensor used is the piezoresistive A201 from Flexiforce (Tekscan, USA[79]). Experiments were sample at 100 Hz. The goal of this study was to compare the pressure at different position of key points and then identified and classified them using a support vector machine (SVM). Using a sample of 35 people the recognition rate reached was around 96%.

Figure 1.28: Plantar pressure signal acquisition system designed by *Feng et al.*[91].

The work developed by *Healy et al.*[92] consist of a self-design of their own in-shoe system, named WalkinSense®. It has 8 pressure sensors per insole located on the big toe, midfoot, medial heel and lateral heel, and four on the forefoot (in the metatarsal heads) as figure 1.29 shows. Its frequency sample is 100 Hz. The results were compare to F-Scan (Tekscan, USA[79]) to show that the results from WalkinSense had better repeatability compared to other commer-

cial devices. F-Scan insole was placed under WalkinSense insole mapping the sensors from both systems to compare the results.

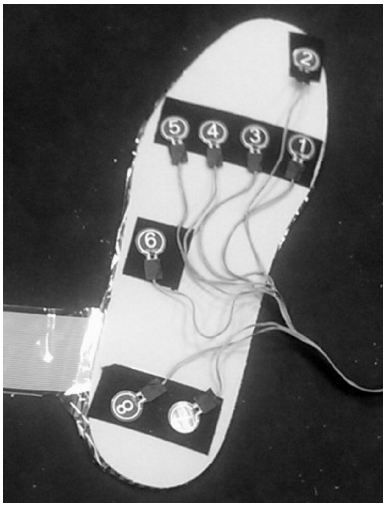

Figure 1.29: Placement of WalkinSense sensors and F-Scan sensor beneath the flat insole[92].

There have been other research groups that have chosen to use a different way to measure the plantar pressure distribution. In case of group of *Tirosh et al.*[93], they have developed an instrumented sock using mainly neoprene. Sensors used are non commercial, they are manufactured inside the sock and placed on big toe, first and fifth metatarsal heads, midfoot, and medial and lateral heel. The sensor consist of an outer shell of a non-conductive fabric (neoprene), with a conductive thread stitched into the neoprene so the stitches of the two layers form a criss-cross. In between these two layers is the exstatic layer providing to the sensor a surface resistivity of 105 Ohms per square. As well as previous cases, the purpose of this study was compare temporal parameters with a commercial system F-Scan (TekScan, USA[79]). Figure 1.30 shows the sock developed by *Tirosh et al.*.

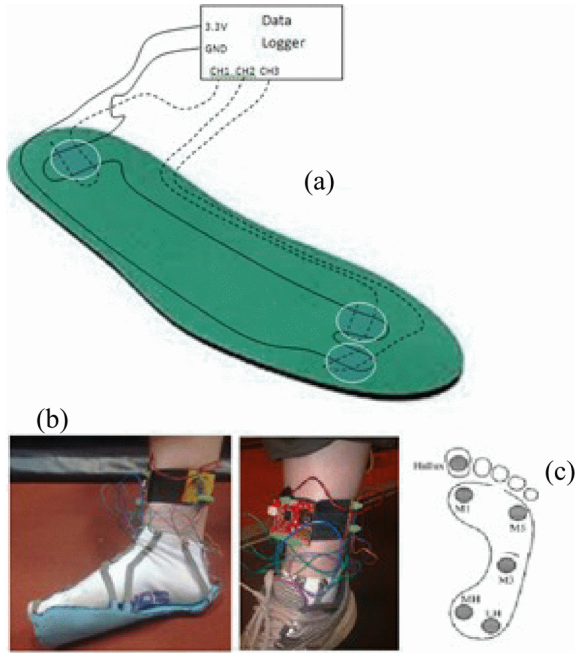

Figure 1.30: The wearable sensor sock illustrating: a) the sensors placement on the neoprene cut to a shape of a foot, b) the neoprene stitched to the bottom of a sock with the wires fixed to the data logger strapped to the shank, and c) the position of the 6 textile sensors under the foot[93].

Wireless Instrumented Insoles

One of the first works related to wireless instrumented insoles that appeared on the literature is the work of *Lawrence and Schmidth*[94] in 1997, called WIFS (Wireless Instrumented Force System). It measures times of foot contact contact occurrence, the approximate weight on each foot, and the centre of pressure (COP) on each foot (as a function of time). The sensors are resistive type, and are located on the first and fifth metatarsals, heel (divided into medial and lateral portion), and optionally under the big toe and second metatarsal. The data are transmitted to a PC at 902-928 MHz.

One of the most completed in-shoe systems is the developed by *Morris and Paradiso*[95, 96, 72], named GaitShoe. They propose a shoe with several sensors (see figure 1.31): four pressure sensor (FSR) located at medial and lateral heel, first metatatarsal, and fifth metatarsal; two piezelectric sensors (PVDF) located at big toe and heel to detect timing of toe-off and heel strike; two pairs of resistive bend sensor placed at the ankle and insole, one three axis accelerometer and one tree axis gyroscope located at the ankle, and sensors to measure the distance above ground. The frequency sample of GaitShoe is 75 Hz and it sends the data through RF link at 916.5 MHz.

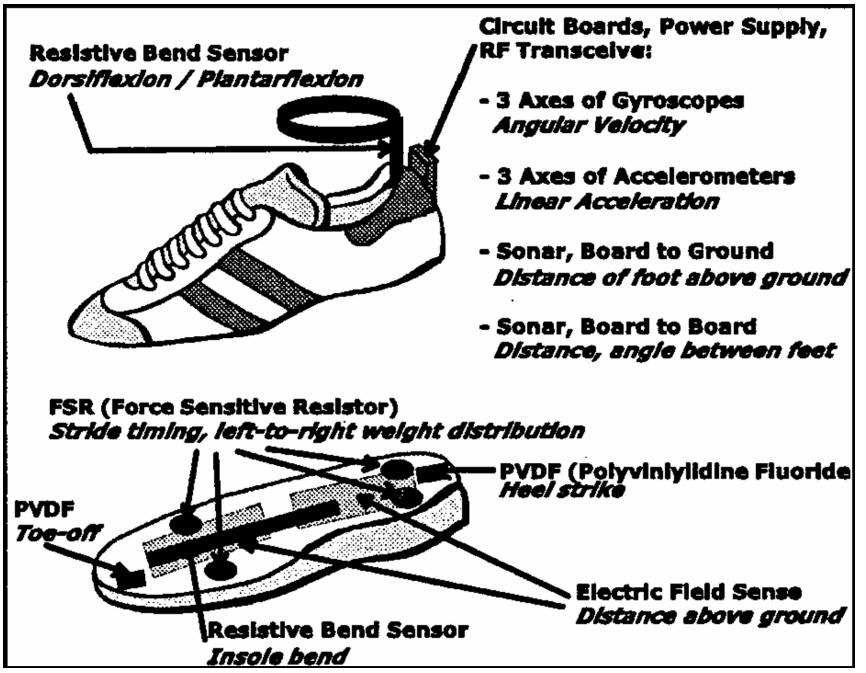

Figure 1.31: Schematic of the GaitShoe system[95, 96, 72]. It consist in four pressure sensor, two piezelectric sensors, two pairs of resistive bend sensor, one three axis accelerometer, one tree axis gyroscope, and one sensor to measure the distance above ground.

The Work from *Chen et al.*[97] presents an instrumented insole to detect abnormal gait. It is composed of four FSR pressure sensor (Interlink Electronics, USA[80]) and one bend sensor (Bend Sensor Images SI, Inc., USA[98]) placed on a plastic insole as figure . FSR sensors are located at the first metatarsal and the position between the forth and fifth metatarsal heads, and the other two are placed under the heel. While bend sensor is located at the center of the insole to provide information about the flexion of the foot. in addition, it contains one three axis accelerometer and one three axis gyroscope, both located in the ankle. It send the information using a low power radio frequency (RF) communication module, GW100B.

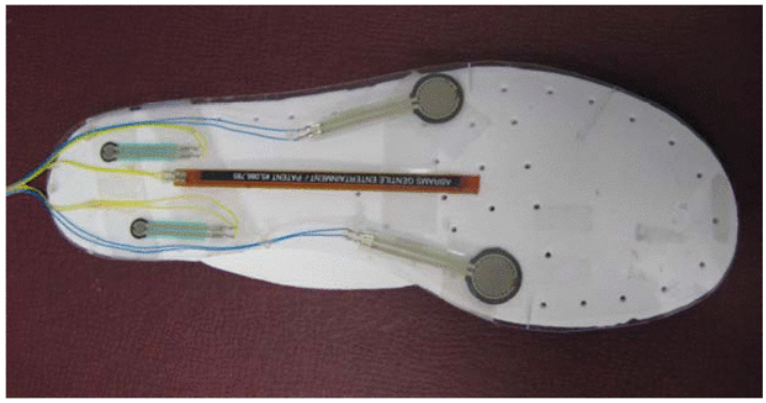

Figure 1.32: Insole developed by *Chen et al.*[97]. It contains four FSR pressure sensors and one bend sensor.

Salpavaara et al.[26] designed a wireless insole to measure plantar force during sport events, specifically, the goal is to monitor the timing and movement of the athletes' legs during throwing, jumping and running in several sport disciplines. Figure 1.33 shows the insoles developed by *Salpavaara et al.*, it is based on custom capacitive technology, frequency sample is 100 Hz and the wireless link technology used is ZigBee. The study proposed was related to javelin throwing, and they concluded that the timing of the steps has a great importance in the performance of the exercise.

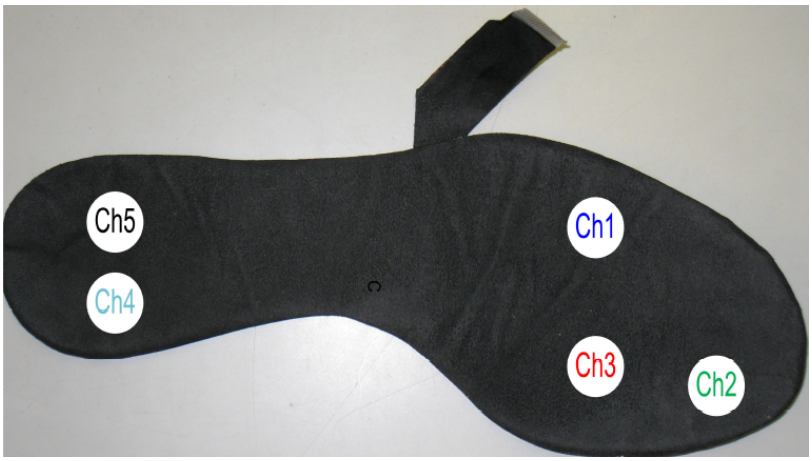

Figure 1.33: The insoles developed by *Salpavaara et al.* were custom-made to fit the track shoes. There are five measurement areas in the insole. The place and the size of the capacitive sensor elements inside the insole are illustrated with white colour[26].

The research group of *Benocci et al.*[99] from University of Bologna (Italy) developed a wireless system for gait and posture analysis. The system includes 24 hydrocells (manufactured by Paromed) to measure plantar pressure and a inertial measurement system that contains a three axis accelerometer and three axis gyroscope in each insole. To control the system it uses a microcontroller MPS430 from Texas Instrument(Texas Instrument, USA[100]) and Bluetooth transceiver in each foot. It allows to distinguish gait parameters such as swing and stance phases, step and stride duration, double and single support. It allows sampling at a frequency up to 250 Hz.

In 2009, *Yang et al.*[101] designed a instrumented sock that uses four dome shaped sensors. The system permits to record spatio temporal plantar pressure patterns which were used to calculated the centre of pressure (COP) of both feet. In addition, it contains five clip type sensors to record lower limb movement. The microcontroller unit (Texas Instrument MPS430) and the bluetooth link were attached to waist. The frequency sample of this system is 100 Hz.

Another example related to sports and physical activity research, is the proposed system by *Holleczek et al.*[102], it is a wearable sensing sock, designed for snowboarders, with an objective to improve the technique in this sport. It is able to analyse the dynamics of the weight distribution inside the boots, that seems to be directly related to painful crashes in snowboarding sport. It provide feedback of this position in real time through a bluetooth protocol. The sock is designed using custom capacitive sensors, but it has only three sensors, on located under the heel and the rest on the lateral and medial forefoot (See figure 1.34)

(a) Integrated textile pressure sensors with connecting measurement lines.

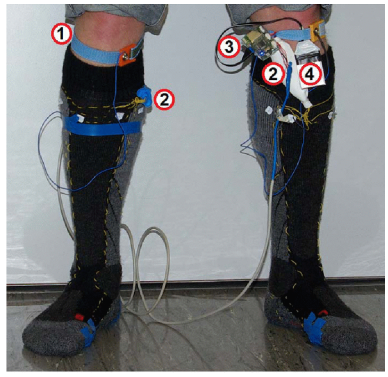

(b) Test subject wearing the sensor socks: strap (1), capacitance measurement unit (2), Bluetooth transmitter (3) and battery (4).

Figure 1.34: Wireless sensor sock with capacitive sensors by *Holleczek et al.*[102].

In last decade, many instrumented insole systems have been published. *Shu et al.*[14] developed an in-shoe plantar pressure measurement and analysis system based on fabric pressure sensing array. The pressure sensors was fabricated using a conductive sensing fabric with conductive yarns and a top-and-bottom conversion layer. Measurement ranges of this sensors are from 10 Pa to 800 kPa. Figure 1.35a shows an schematic of the pressure sensor. As figure 1.35b, the insole has six sensing points. Insole is connected a to a PIC18F452 (Microchip, USA[103]) and a bluetooth link located at the ankle of the patient. It provide information about mean a peak pressure, CoP and shift speed of CoP.

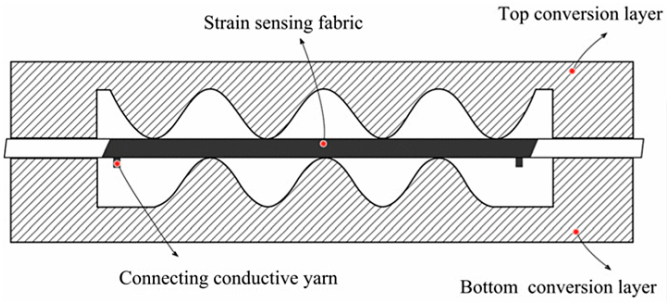

(a) Schematic diagram of the structure of the pressure sensor (side view).

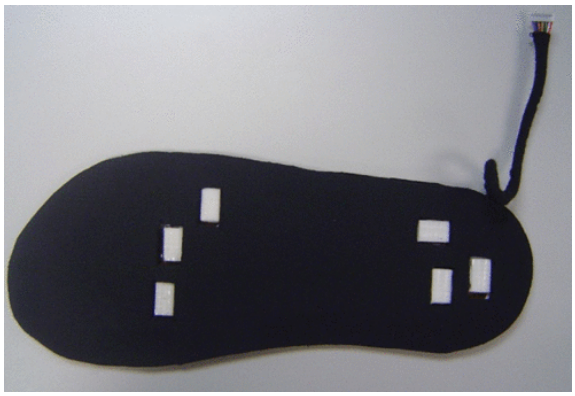

(b) Insole and its package. Textile sensors with bottom layer.

Figure 1.35: Pressure sensor and instrumented insole by *Shu et al.*[14].

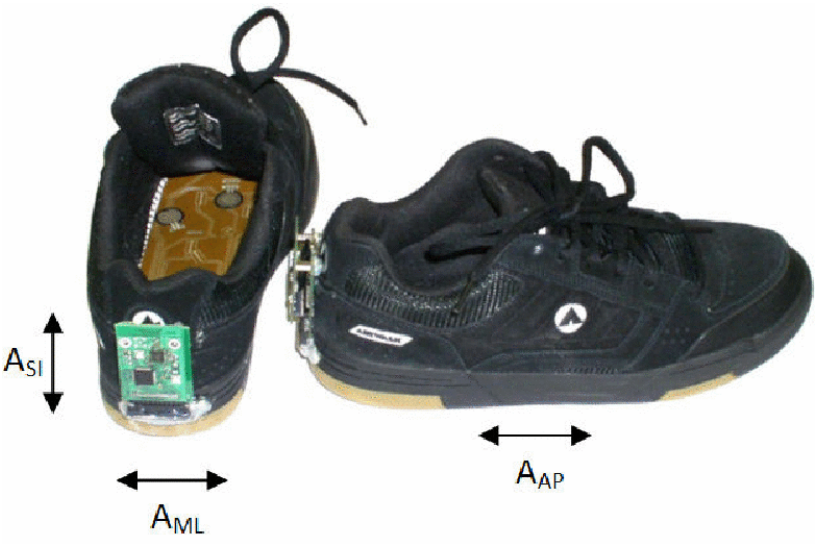

(a)

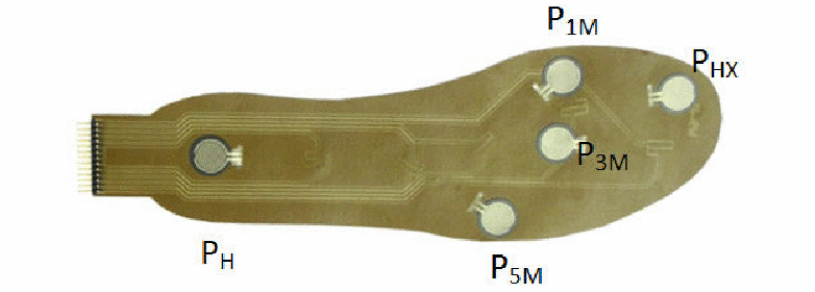

(b)

Figure 1.36: A pair of shoes equipped with sensors, wireless transmitter, and batteries. Arrows show anterior-posterior (AAP), medial-lateral (AML), and superior-inferior (ASI) axes of accelerometer. (b) A pressure sensitive insole with FSRs. PH is heel pressure sensor, PMO , PMM , and PMI are the fifth, third, and first metatarsal head sensors, respectively, and PHX is the big toe sensor[104].

There have been many works about gait disorders due to neurological diseases using instrumented insoles[105]. The group of *Sazonov et al.*[104, 106, 107, 108] designed an instrumented insoles with five force resistive sensors (FSR, Interlink Electronics, Inc.[80]) located at big toe, heads of metatarsal bones, and the heel. In addition it contains a three axis accelerometer LIS3L02AS4 (STMicroelectronics, Switzerland[109]). Frequency sample of this system is 25 Hz. It has been used to monitor posture during gait, in rehabilitation of stroke patients, and to measure energy expenditure to predict bodyweight. Figure 1.36 shows the insole manufactured at how it fits into a shoe.

The group of *Wada et al.*[110] used an instrumented insoles with 8 pressure points and low sampling frequency (30 Hz), but it also contains accelerometer, gyroscope and ultrasonic sensor. In figure 1.37 a outline of the experiment is shown. The purpose is to provide a feedback to the patient during rehabilitation processes in walking. So it have an screen where a kind path must be follow by the patient.

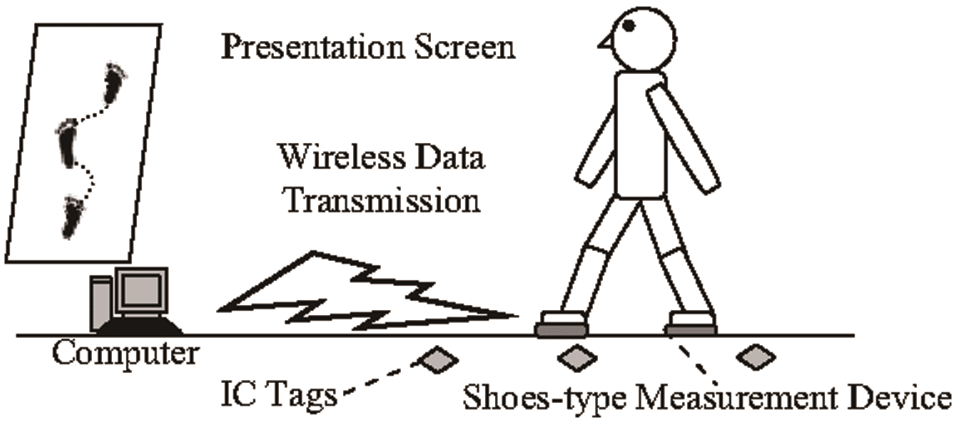

Figure 1.37: Outline of the assisted measurement system by *Wada et al.* [110].

Saito et al.[111] proposed a system that contains seven pressure sensitive conductive rubber (PSCR) sensors manufactured by Yokohama Image System (Japan). Sensors are located at heel, lateral midfoot, big toe, head of the first metatarsal, centre midfoot and centre forefoot as figure 1.38. Sensors are quite

limited due to maximum pressure that are able to measure, that is 250 kPa. That means that this system is not useful for every type of study. Sampling rate is 50 Hz. Data obtained from sensors were compared to a F-scan[59] system to validate the system.

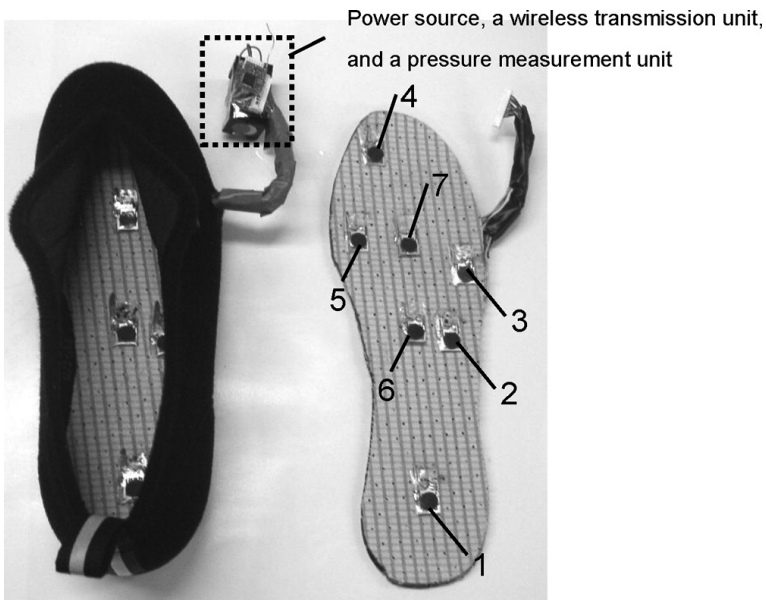

Figure 1.38: In-shoe device developed to measure plantar pressure. Sensors were placed at seven locations: heel (sensor 1), lateral midfoot (2), lateral forefoot (3), big toe (4), head of first metatarsal (5), centre midfoot (6), and centre forefoot (7)[111].

The group of *Paulick et al.*[112] have designed a embedded sensor insole for balance and gait monitoring, named StabilitySole. The insole is conformed by four flexiforce pressure sensors (Tekscan, USA[79]) and three axis accelerometer by Freescale Semiconductor[113] (see figure 1.39a). Pressure sensors are located at big toe, the heads of 1^{st} and 5^{th} metatarsals, and the heel. The system is controlled by a PICAXE®microcontroller, and then information is transmitted to an XBee®wireless module. Real use of the insole is presented in figure

1.39b. It was used together with a sandal.

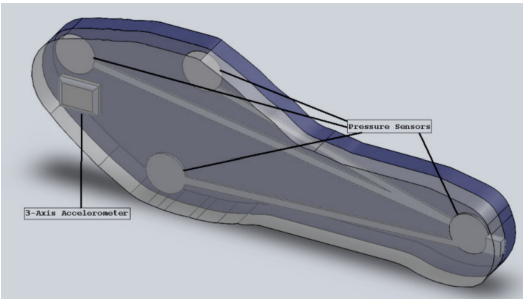

(a)

(b)

Figure 1.39: (a) Computer aided conceptual design of StabilitySole demonstrating both the MEMS accelerometer and pressure sensors. (b) StabilitySole integrated into a standard athletic sandal demonstrating versatility of technology[112].

A novelty instrumented insole is presented at *De Rossi et al.*[114, 115] work. This insole is made of 64 silicone covered opto-electronic pressure sensors, in figure 1.40a the sensor size can be observed, while figure 1.40b shows its transduction principle. System is able to measure pressure in all important areas of foot, and also it calculates from pressure values the CoP and the GRF of each foot. The Sensors are directly connected to a four 16-channel 14-bit analog to

digital converters, and then data are sent using a bluetooth module. Frequency sample of this system is up to 1.2 kHz, while data y sent by means of a Bluetooth connection to remote receivers at 100 Hz. At the Personal Computer (PC) side, they developed a Labview environment to plot the data from sensors in real time.

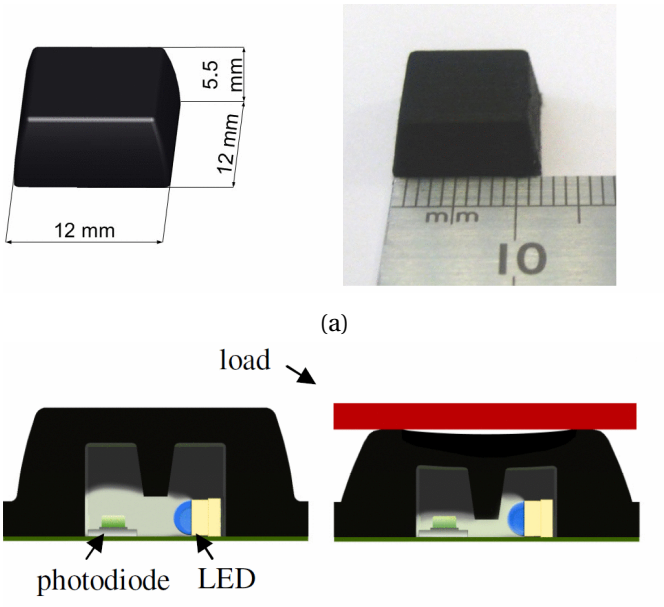

Figure 1.40: Base sensitive element of the pressure sensitive insole. (a) Silicone cover of the sensitive element. (b) Representation of the transduction principle. When a load is applied (on the right), the consequent deformation of the structure occludes the light path, and results in a diminished output from the photodiode[114].

The research group of *Xu et Al.*[116] have designed a very completed embedded insole called "Smart Insole". It contains 48 pressure sensors and an inertial measurement unit that provides 9 degrees of freedom. It is integrated

by a gyroscope, accelerometer, and compass. Frequency sample of the system is up to 100 samples per second (Hz), and communications is performed using bluetooth directly to a smartphone. The mobile application obtains several gait parameters like pitch, roll and yaw angular velocity. Figure 1.41 shows an example of the embedded insole.

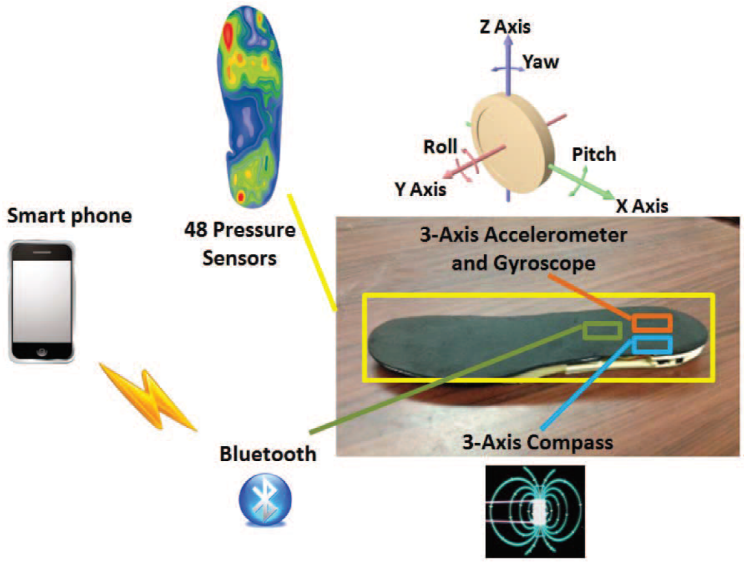

Figure 1.41: Sensors used in the Smart Insole system[116].

In last year others work like *Cristiani et al.*[117] have appeared. They proposed an instrumented insole for long term monitoring. The insole contains four pressure sensors which are made of a very thin conductive plastic material whose electrical resistance decrease when it is pressed. In addition, insole contains a accelerometer LIS302DL (by STMicroelectronics[109]), and a temperature and humidity sensor SHT11 (Sensirion AG[118]). Figure 1.42 presents the insole designed by *Cristiani et al.*.

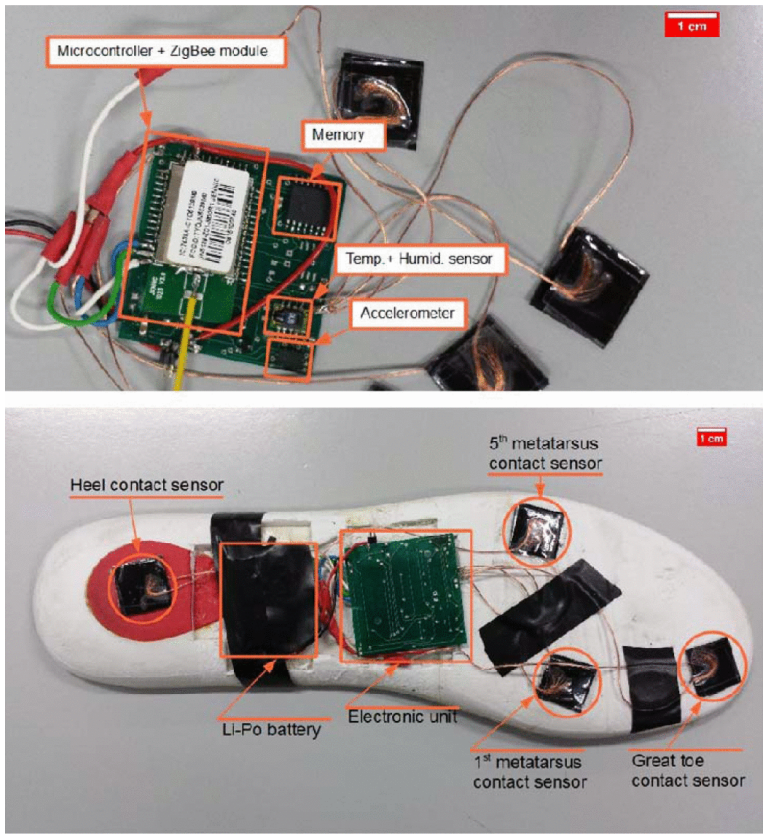

Figure 1.42: The sensorized insole prototype.[117].

1.8.3 Previous work by the research group

The research group where the candidate has been developing his Ph.D. thesis have some experience in the field of instrumented insoles to monitor timing parameters during gait, running and jumping exercises. Actually, this group own a patent in the Spanish Patents Office (Spanish Government)r, called "Sistema de medición de los parámetros temporales de la marcha, la carrera y el salto mediante fotodetectores"[7].

It includes instrumentation components (hardware), programming components (software), and a set of detection elements based on photodetectors located at the sole of a sport shoe. It working principled consists in a register of the changes in signal coming from photodetectors, using a common timing reference for all of them.

Software Module

Software module is basically a personal computer application, that integrates a graphic user interface and permits to access to a database where the subject data are registered. It also allows the user to program test to carry out, sensors to be used, measurements, etc.

Using this module, the user will be able to define the test to perform (gait, running, jumping) and the protocol to use, depending the parameters such as initial and final sensor by means of the photocell, using a metronome to stablish a gait or running rate, number of jumps to do, test duration, start and finish sounds, electronic noise filtering, test distance, event cancelling, etc.

Once the test is started is possible to show statistics in real time, as well as timing plot of active or inactive sensors configured at the beginning of the test.

Hardware Module

Measurement system of timing parameters of gait, running and jumping using photodetectors has a main hardware module placed on subject body's, and it is described next.

This module is a physical unit that admit as inputs the signal coming from photodetectors elements located at the sole and have as an output the connectivity to a computer not only wired (RS232, USB, etc.) but also wireless. It main components are:

1. Supply module that permit batteries and connection to the electrical network using conventional voltage adapters.

2. Wired and wireless communications modules.

3. Conditioning module for signals coming from photodetectors to be afterwards processed by digital systems.

4. Fast data and high capacity memory to be an intermission storage point until final computer communication (for example, RAM memory).

5. One or several secondary or slave process units (two in this case) that manage the acquisition of events which stablish support times of each sensor.

6. Main process unit with capacity for supervision of the rest of modules previously described.

An scheme of the proposed system is shown of figure 1.43.

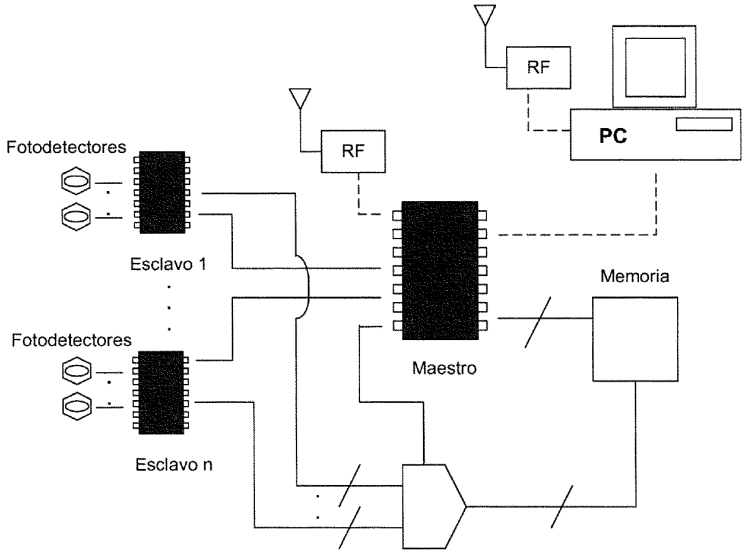

Figure 1.43: Schematic of presented patent[7].

Detection Module. Photodetectors located at the shoe's sole

It is composed by photodetectors elements (por example, photodiodes, phototransistors) that work both visible range and infrared range (including in this case infrared emitters) located at the shoe's sole. When sole support and lift, the light level coming from ground reflexion or due to direct effect changes on the photodetector, modifying its output. This modification is the change that is processed to highlight the dynamic of the foot. Figure 1.44a shows the proposed shoe with the photodetectors placed at sole, while in figure 1.44b the complete system is presented.

(a) Sole of the sport shoe including photodetectors.

(b) Instrumented shoe and datalogger designed

Figure 1.44: Previous work by the research group patented. Figure 1.44a shows the sole fo the sport shoe including photodetectors while 1.44b presents the instrumented shoe and datalogger designed[7].

Chapter 2

Instrumented insole prototypes

Contents

2.1 ECnsole v1.0 64
2.1.1 Instrumented Insoles 65
2.1.2 Datalogger Unit 71
2.1.3 Software Processing 89
2.2 ECnsole v1.2 92
2.2.1 Changes on Datalogger Unit 92
2.3 ECnsole v1.5 98
2.3.1 Changes on Instrumented Insole 98
2.3.2 Changes on Datalogger Unit 103
2.3.3 Changes on Software Processing 107
2.4 ECnsole v2.0 108
2.4.1 Changes on Instrumented Insoles 110
2.4.2 Changes on Datalogger Unit 116
2.4.3 Changes of Software Processing 123

In this chapter the description and evolution of the instrumented insoles will be explained. Only those prototypes that have taken part into experimental cases have been included, so the numeration of the different versions corresponds to the experimental test that are shown in chapters 3 to 6.

2.1 ECnsole version 1.0

The first version designed by the research group consisted of two instrumented insoles connected to two data-processing and logging modules[8, 9] (see figure 2.1). The sensors in the insole are powered and read-out by the respective data logger. One of the data-processing modules acts as master and the other as slave. Therefore, the master sends the measurement start and stop commands to the slave, and the data acquired by the slave are then sent to the master and stored on a Micro Secure Digital (μSD) memory card.

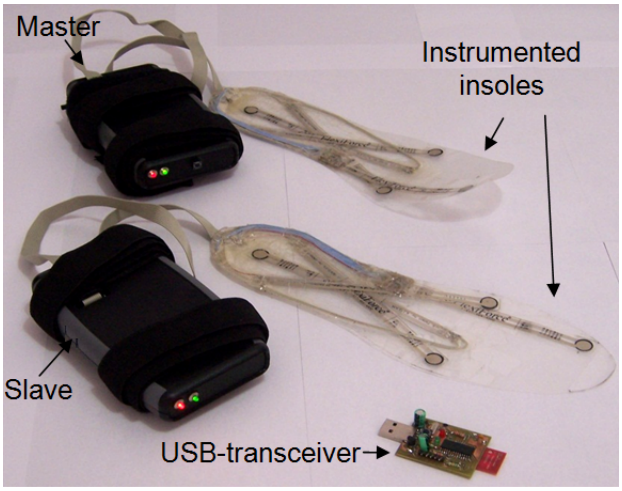

Figure 2.1: Measurement system ECnsole v1.0. Each insole is connected to a datalogger unit. Master unit, start and stop the measurement and store it into a μSD memory card or send it wiressly to a the usb-transceiver connected to a computer.

In addition, the results can be sent to a computer via radio depending on the operation mode. The system can operate in two different modes: in manual mode, in which measurements are started or stopped by a button located on the master module; or in remote mode, where the computer controls the experiment and the results are received and displayed in the real-time application. In both operation modes, the results can be stored on the μSD memory card or uploaded via radio or Universal Serial Bus (USB).

2.1.1 Instrumented Insoles

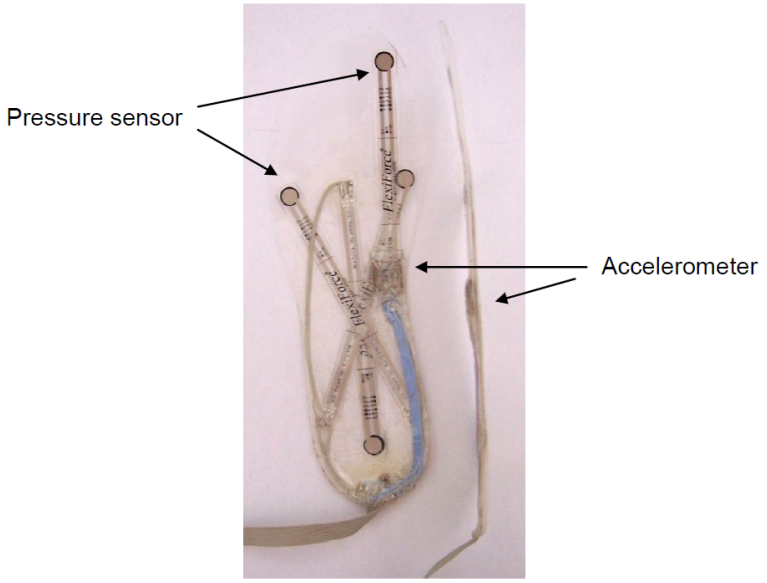

Figure 2.2: Top and side views of instrumented insoles v1.0. Pressure sensors are located at the head of the first and fifth metatarsals, big toe, and the heel. The accelerometer is located at the arc of foot.

Pressure/Force Sensors

In this first version of the ECnsole, the goal was to measure up to four pressure points as possible and to acquired data from a kinetic sensor, in this case an accelerometer. The thickness of the insole is a critical requirement in order to manufacture it as comfortable as possible. It is very important for the subject not to notice the attempt to prevent any modifications in gait, running or jumping due to insole itself. Another requirement was to make it onto a flexible substrate to permit to test it in exercises that requires a more complex foot movement.

The instrumented insoles are made of a flexible plastic substrate composed of polyethylene terephthalate (PET), where the sensors are affixed. In order to prevent shifting, a plastic adhesive layer covers the entire insole, anchoring the pressure sensors and the accelerometer in place. Each insole has a total of four pressure sensors located at the heads of the first and fifth metatarsals, big toe, and heel, respectively (see figure 2.2). Four sensors are considered the minimum needed for a basic plantar-pressure study in accordance with previous studies[75]. The sensors at the big toe and heel indicate the start and end of contact during locomotion. The sensors at the first and fifth metatarsals have been added to determine the lateral pressure distribution in the front part of the foot. Obviously, a greater number of sensors would report more information, but the cost of such a system would increase considerably[119]. Two different sizes of insoles were manufactured, UK size 7 and 8.5, to study participants with different foot size.

Figure 2.3: Flexiforce Force Sensor A201[120].

The main types of sensors to measure force or pressure were described in chapter 1. As literature described, most typical sensors for instrumented insoles are resistive (FSR) or piezoresistive. *Holliger and Wanderley* reported[121] that Flexiforce sensors provide better precision at long term test. Therefore, the sensor chosen was a piezoresistive type (Flexiforce). Specifically, the Flexiforce A201 (TekScan, USA[120]), specifications of his sensors are shown on table 2.1. It consist in a ultra thin and flexible piezoresistive sensor. It is manufactured by means of adhesive and two different substrate layers (polyester and polyamide). In each layer a conductive and force sensitive material is applied. The resistance of the sensor is very high (on the order of few $M\Omega$) when there is no load, and it reduces when some force is applied.

Flexiforce A201 Specifications	
Thickness	0.208 mm (0.008 in.)
Length	51 mm (2 in.) 102 mm (4 in.) 152 mm (6 in.) 197 mm (7.75 in.)
Width	14 mm (0.55 in.)
Sensing Area	9.53 mm (0.375 in.) ⊘
Connector	3-pin Male Square Pin (center pin is inactive)
Substrate	Polyester (ex: Mylar)
Pin Spacing	2.54 mm (0.1 in.)
Force Ranges	0 - 1 lb. (4.4 N) 0 - 25 lb. (110 N) 0 - 100 lb. (440 N)
Linearity (Error)	$< \pm 3\%$
Repeatability	$< \pm 2.5\%$ of full scale
Hysteresis	$< 4.5\%$ of full scale
Drift	$< 5\%$ per logarithmic time scale
Response Time	$< 5\mu sec$

Table 2.1: Specification of Flexiforce A201 sensors[120].

ECnsole v1.0 contains flexiforce sensor A201 of 25 lb (see figure 2.3). The manufacturer guarantees at least 10^6 impacts, so the instrumented insoles should last for 700 km, considering a minimum step length of about 70 cm. In fact, these insoles have been used for around 100 km in combined tests performed, without damage or appreciable aging in any of the eight sensors. Each sensor was individually calibrated in the range of interest (upto 400 kPa or 3 kg for the metatarsal pressure sensors and upto 1,000 kPa or 8 kg for the heel and toe sensors) with a press, obtaining a non-linearity and hysteresis total error of less than 5%. The response of a pair of sensors are shown in figure 2.4.

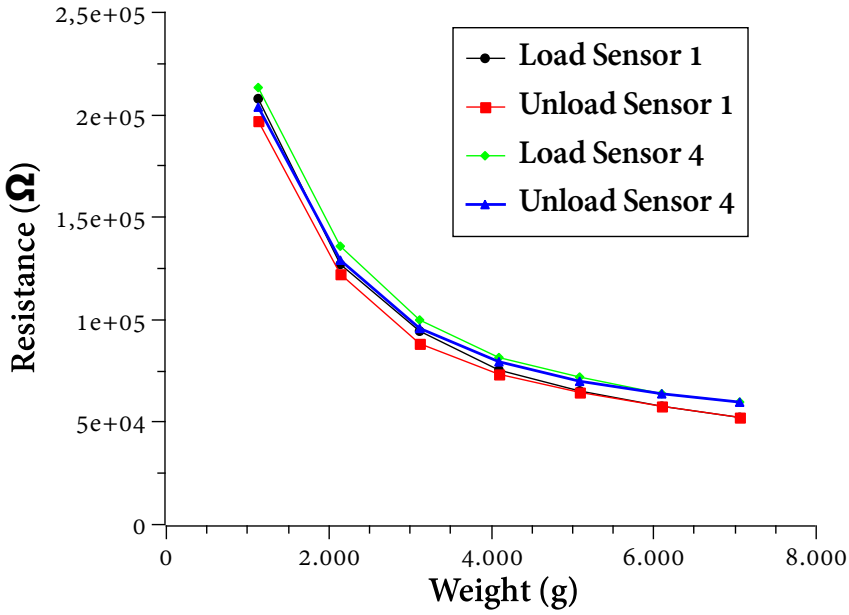

Figure 2.4: Flexiforce A201 Sensor characteristic. Many sensors were calibrated, these two are just an example of the response of these type of sensors.

An example of the response of the sensor placed at the head of the fifth metatarsal of the left foot is plotted in figure 2.5, showing its hysteresis cycle. The pressure and conductance of the sensors were fitted to a linear regression,

and the coefficients were used to calculate the pressure in our application.

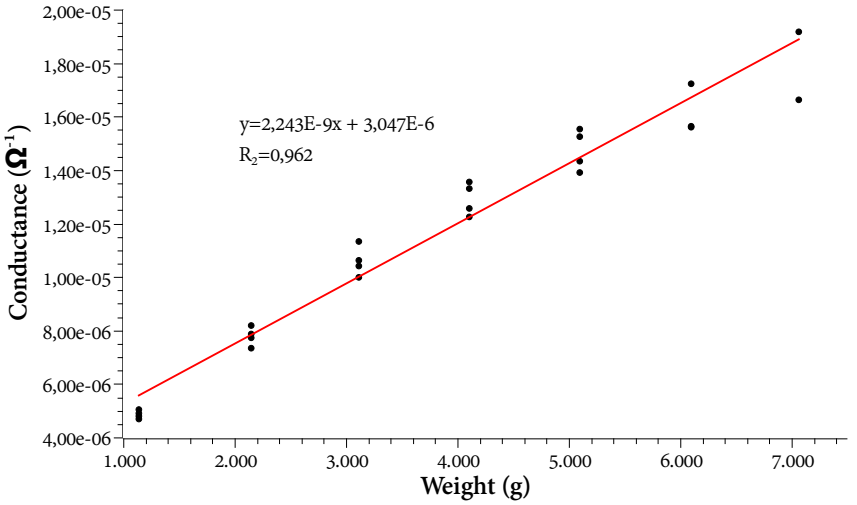

Figure 2.5: Response of the A201 sensor placed at the head of the fifth metatarsal of the left insole.

Accelerometer

In addition, a three-axis accelerometer has been included in the insole at the foot arch location to monitor movement during the foot flight time and the forces generated. Below, we will use the combined information of both kinds of sensors (pressure and acceleration) for the gait analysis with a very low number of sensors. It must be noted that, while the foot is in motion, vertical gravitational acceleration cannot be separated from acceleration due to linear motion, but relevant information can be extracted from the lateral acceleration components, X-Axis Acceleration (A_X) and Y-Axis Acceleration (A_Y).

The accelerometer need to accomplish some requirements to be chosen as the kinetic sensor of the system:

1. *Small size* to be able to embedded into the insole without modifying gait,

running or jumping practice. Most recommended area would be the foot arc.

2. *Reduced consumption* to increase the autonomy of the system powered by batteries.

3. *Supply at aproximately 3.3 Volts (V)* to avoid extra circuitry and to share supply with rest of elements of the system.

4. *Sensitivity* to obtain some accuracy in results measured.

5. *Bandwidth* adjustable to the application requirements. A too high bandwidth may include a high noise level.

6. *Good linearity* to facilitate calibration and sampling processing.

7. *Low cost.*

Finally, the accelerometer selected was the *ADXL330* (Analog Devices[89], USA) due to its small package, low power consumption, and sensitivity of $330^{mV}/_{g}$ in its three-axis measurements, where g is the gravity acceleration ($9.8^{m}/_{s^2}$). In table 2.2 some specifications of the accelerometer used are shown. The bandwidth of the output is adjustable by means of an external capacitor in each axis as figure 2.6 shows. Equation 2.1 stablish the 3 Decibels (dB) bandwidth. Fixing this value to 50 Hz, the capacitor obtained is approximately of 100 nF.

$$BW_{-3dB} = \frac{1}{2\pi \cdot (32k\Omega) \cdot C_{(X,Y,Z)}} = \frac{5\mu F}{C_{(X,Y,Z)}} \tag{2.1}$$

The calibrations provided by the accelerometer datasheet were considered valid, assuming that an error of 5% in acceleration would be acceptable for this application. Nonetheless, several independent tests of acceleration measurements were carried out. The instrumented insoles were orientated to the three spatial directions and acceleration was recorded by the three axes correctly. The low-pass filtered output of the *ADXL330* comprises the internal output resistance of the accelerometer of $32k\Omega$ and two external parallel capacitors. The filter and bypass capacitors are mounted over a thin printed circuit board in

order to disturb normal activity as little as possible (insole 5.6mm thick in this area). The rest of the instrumented insole is 1.0mm thick, allowing to it be included in normal shoes without modifications (see figure 2.2). The low-pass filter has a bandwidth of 30Hz.

ADXL330 Specifications	
Number of axis	3
Package	4 mm x 4 mm x 1.45 mm LFCSP
Supply Current	320μA at $V_s = 3V$
Operating Voltage Range	1.8 to 3.6 V
Sensitivity	300$^{mV}/_{g}$

Table 2.2: Specification of ADXL330 accelerometer[89].

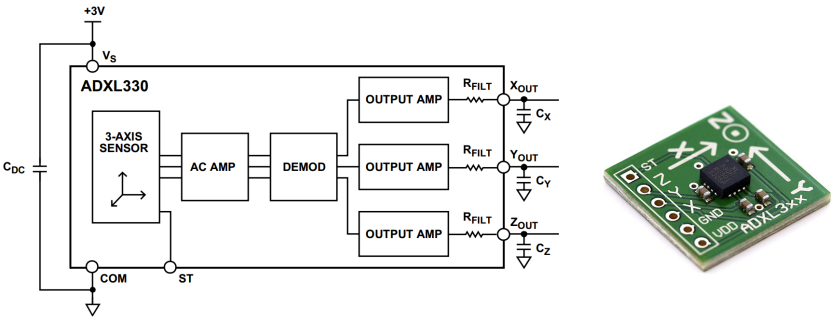

Figure 2.6: Functional block diagram of ADXL330 accelerometer.

2.1.2 Datalogger Unit

As it was described before, this system consists in two almost identical units: master/coordinator and slave. Hardware is practically the same in both units, however master contains the circuitry required to store the data into a μSD,

those to start and stop measurements manually, and a USB connector to download data from μSD card directly to a PC. Figure 2.7 represents the schematic of the datalogger units.

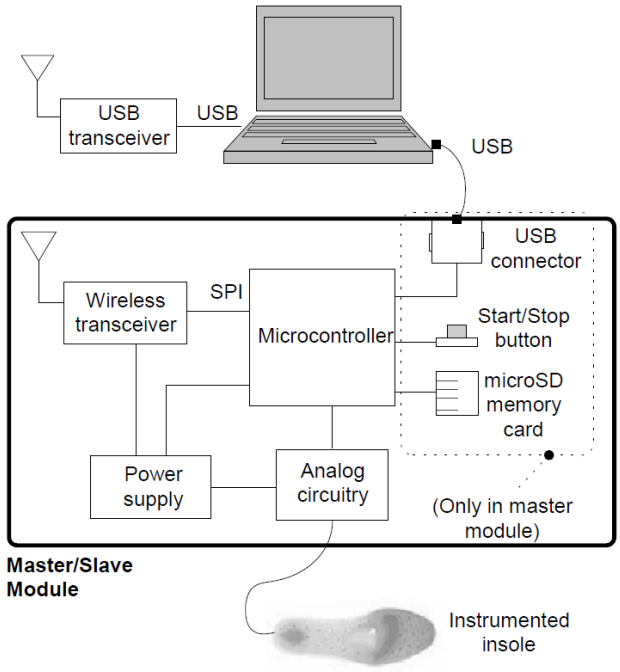

Figure 2.7: Schematic diagram of ECnsole v1.0, both master and slave modules.

Both units are controlled by a microcontrolled, which sampling data from insole's sensors and send it throught a wireless transceiver. The slave module, send it to the master, and this one is in charge of forward it together with the information for its own insole to the PC. Besides, master module owns all the configuration parameter for data acquisition and is the one who starts synchronization between insoles. A conditioning circuitry is the responsible to adapt signal from analogue sensors.

Power Supply

Related to the power supply of the system, it is important to highlight that operating voltage for datalogger units is 3.3 V. The strategy followed for the power supply stage was to convert the DC voltage from a battery using a DC-DC Converter, and then, a low drop-out regulator. It is critical to distinguish analogue and digital parts of the circuit, to avoid noise and interferences. Therefore, the power supply consists of two sources, one digital and another analogue. Both sources are designed using the same converter, the LM2623 from National Semiconductor(Adquired by Texas Instrument[100], Texas, USA), that was already used in some designs by the research group.

This DC-DC converter is a general purpose one, specially indicated for those systems powered by batteries or low input voltage. It accepts input voltages from 0.8 to 14 V and convert then to a regulated output between 1.24 and 14 V, with a efficiency up to 90%. In order to adapt its utility to a large number of applications, LM2623 allows to vary output voltage, switching frequency (from 300 kHz to 2 MHz), and the duty cicle (from 17% to 90%) to optimize its working principle.

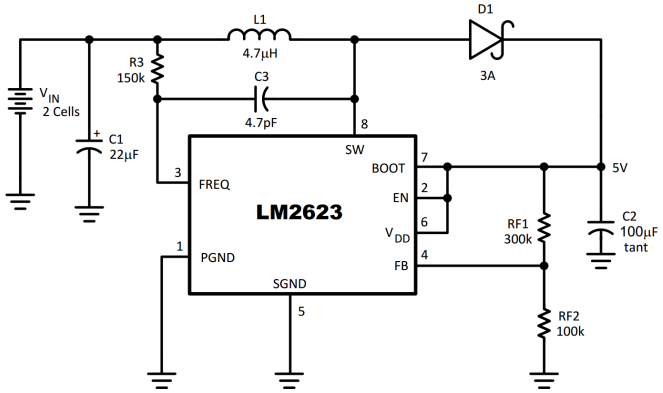

Figure 2.8: Typical Application circuit of LM2623 DC-DC converter.

The operating voltage of digital block must be 3.3 V, that is working voltage of digital integrated elements of our system: microcontroller, wireless mod-

ule and storage module (in the master unit). In LM2623, the output voltage is adjustable by means of feedback voltage divider formed by R_{F1} and R_{F2}, as the typical applications circuit of figure 2.8. According to analogue block, the design remains the same, because both sensors (pressure sensors and accelerometer) and operational amplifiers are able to work in the voltage range provided by the next design of the DC-DC converter. The resistive values are chosen using the equation:

$$R_{F1} = R_{F2} \cdot [(\frac{V_{OUT}}{1.24}) - 1] \tag{2.2}$$

Therefore, for the desired voltage $V_{OUT} = 3.3V$:

$$\frac{R_{F1}}{R_{F2}} \approx 1.66$$

with final values for resistors of $R_{F1} = 370k\Omega$ and $R_{F2} = 270k\Omega$.

Despite the fact that digital and analogue power supplied voltage were the same (3.3 V), a voltage regulator was included to reduce the switching noise typical in switching sources. Even though this ripple is usually pretty small (around 0.6% of V_{OUT}), working with analogue circuits is better to avoid this type of noise by filtering or regulating the voltage. Due to this new configuration, the DC-DC converter must supply a higher voltage to respect the drop-out of the regulator.

The regulator used in this design is the low drop-out L4931CZ33 manufactured by STMicroelectronics[109]. Its drop-out voltage is 0.4 V. It has a very low quiescent current (Typical $50\mu A$ in off mode and $600\mu A$ in on mode). Due to regulator needs a voltage higher than 3.3 V, the design of the DC-DC converter was modified to achieve a voltage of 4.2 V. This was obtained using $R_{F1} = 270k\Omega$ and $R_{F2} = 100k\Omega$.

Finally, since a step-up DC-DC converter is used, almost any battery with an output voltage higher than 1.1 V. This can be a advantage, but a consideration about the efficiency must be considered because efficient is higher if output and input voltages are similar. Figure 2.9 plots how the efficiency varies within the input voltage for a fixed output voltage of 5 V. In view of this possibility, a

pair of batteries AA type of 1.5 V were chosen to be the supply of the ECnsole v1.0 prototype.

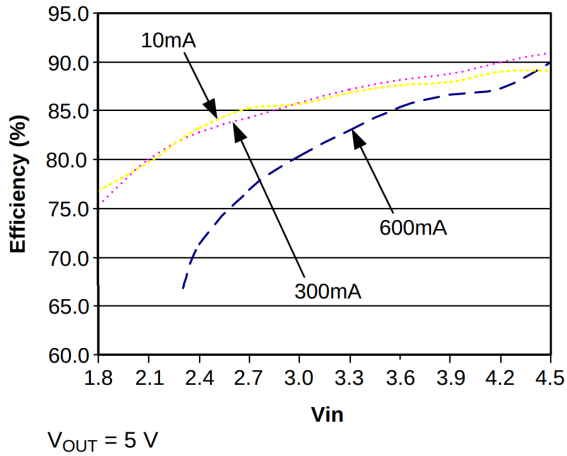

Figure 2.9: Efficiency versus input voltage for a fixed output voltage of 5 V, for output currents of $10mA$, $300mA$, and $600mA$.

Conditioning sensors circuitry

Next block to be explained is the conditioning circuitry for the pressure sensors and for the accelerometer. The Flexiforce A201 sensors, as it was explained before, are piezoresistive sensors, whose resitance varies depending on the applied force. The output of the conditioning circuitry is the input of Analog-digital converter (ADC) of the microcontroller, so these maximum input rates must be considered, that in case of ECnsole v1.0 are associated to supply voltages.

The most practical and the simplest solution for this stage is the one recommended by the manufacturer of the force sensors, that is an operational amplifier using an inverter configuration. Filtering after this stage is not really necessary because the low working sampling frequency so in this case the noise may be considered as negligible. Figure 2.10 shows the recommended circuit proposed by Flefiforce. This circuit requires a negative voltage source for the

non inverter input, while ECnsole v1.0 only provides a voltage of 3.3 V. Therefore, to avoid extra circuitry, this circuit had to be modified and use only the a positive power source already explained in this section.

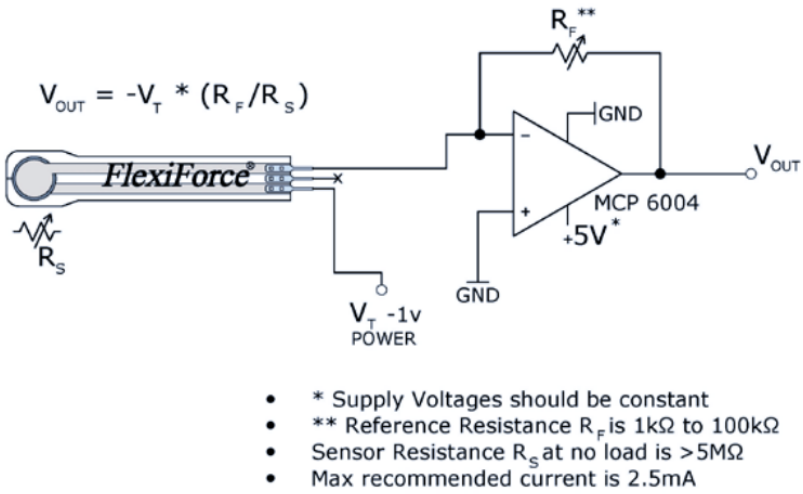

Figure 2.10: Recommended circuit for flexiforce sensor A201.

Due to this reason, the conditioning circuitry finally used was a non-inverter amplifier, like the configuration of figure 2.11. Then, according to the circuit of figure 2.11, the output voltage of operation amplifier, V_{ADC}, is defined by equation 2.3.

$$V_{ADC} = V_+ \cdot (\frac{R_F}{R_{Sensor\,A201}} + 1) \tag{2.3}$$

The operational amplifier used is the *MCP6044*[103] manufactured by Microchip. It is an integrated quadruple operational amplifier which operates with single supply, so it is enough for the insole designed, that is formed by four pressure sensors. Besides, its input supply range fulfil the power supply range of our design.

As the configuration of internal ADC of the microcontroller is configured to use as positive reference voltage the voltage supply fixed a 3.3 V and as negat-

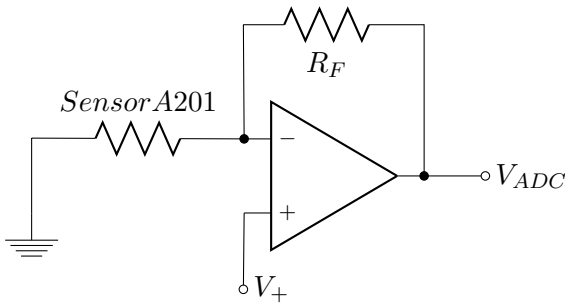

Figure 2.11: Conditioning circuitry based on the non-inverter operation amplifier used in ECnsole v1.0.

ive reference voltage the reference ground, V_{ADC} must be within those limits. When it is unloaded,R_{Sensor} can be tens of $M\Omega$, and when it is loaded at maximum pressure, around $100k\Omega$. It means, for a fixed value R_F a non inventer voltage must be found to fulfil the requirements of V_{ADC}. After many test with different weights and feedback resistors, the value of V_+ was fixed to $^{V_{CC}}/_2$ and R_F to $91k\Omega$. The main problem of this configuration, is that complete range of the ADC is not well used.

To obtain the $^{V_{CC}}/_2$, a voltage reference *REF3033* by Texas Instrument[100] together with a voltage divider was used. Main characteristics of *REF3033* are its low quiescent current, $50\mu A$ as maximum, its ouput current of $25mA$ and its low thermal drift, around $50^{ppm}/_{\circ}$, and a voltage input range of 3.3 to 5.5 V, so it accomplish perfectly the design requirements.

Since accelerometer has an output in the voltage range of the power supply(0 to 3.3 V), there is no need of extra circuitry to adapt signal for the ADC. It is important to avoid that signals from the outputs of the accelerometer get pulsed due to the cable length, for that purpose, it was decided to include some capacitors to filter the signals without modifying bandwidth. Therefore, it was added a capacitor of 10 nF to those of 100nF that were already included on the insole. This new capacitor does not modify in excess the value of BW_{-3dB} of equation 2.1 to 45 Hz, that is not a big difference comparing to 50 Hz obtained by means of 100 nF capacitor.

Wireless module

The protocol used in ECnsole v1.0 was MiWi™ P2P from Microchip[103] (Chandler, Arizona, USA), that is just a simpler alternative to the ZigBee® standard.

MiWi™ P2P[122, 123] is a wireless protocol, used in personal area networks based on IEEE 802.15.4 standard which includes Low-Rate Wireless Personal Area Network (LR-WPAN). This is head for low cost devices and networks, which do not need high transference rate (up to 250 kilo bits per second (kbps)), a low distance (up to 100 m), and reduced power consumption. It is developed by Microchip, based on a open source project, and compatible with all IEEE 802.15.4 and ZigBee® transceivers. It is free and does not required licenses to use it, whenever Microchip components are used. The main different in comparison with Zigbee® is that it does not have the same infrastructure capabilites, being the number of nodes reduced to 1024 in MiWi™ for 65536 of ZigBee® . It is quite simple, with a reduce protocol stack, oriented to low cost solutions that do not need interoperability with ZigBee® devices.

The protocol provide a direct and reliable wireless communication by means of a user friendly programming interface. It has some characteristics which can be compiled inside or outside from the stack to collect a wide range of user needs and to minimize the stack size. Some of the main characteristics of MiWi™ P2P are:

- It supplies 16 channels at 2.4 GHz band, using the *MRF24J40* transceiver from Microchip.
- It works over the majority of Microchip microcontroller families PIC18, PIC24, dsPIC33, and PIC32.
- It supports new Microchip compilers XC8, XC16, and XC32 as well as their older versions C18, C30, and C32.
- It works as a state machine (no RTOS-dependent).
- Supports a slept device at the end of communication.
- It makes possible to perform a detection energy scan to work over the lowest noise channel.

- It provides an active scanner to detect existence networks.
- It supports security modes defined in IEEE 802.15.4.
- It makes possible channel jumping.
- It supports star topology and point to point links.

The topology finally chosen was the star topology. Where Master module coordinates both slave insole and remote device at PC. In figure 2.12 the wireless module used, the *MRF24J40MA* is shown, it uses Serial Peripheral Interface (SPI) to communicate it with the microcontroller. Table 2.3 contains its specifications. Communication protocol will be described later in detail when the description of the firmware is presented.

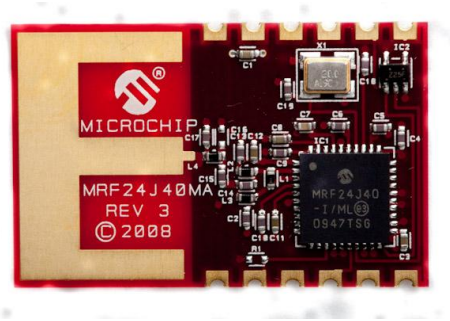

Figure 2.12: Wireless Module MRF24J40MA.

MRF24J40MA Specifications	
Protocols supported	ZigBee®, MiWi™, and MiWi™ P2P
Small Dimensions	17.8mm x 27.9mm. Surface mounting
Includes	Crystal, voltage regulator, and antenna
Certificates of regulation	United States (FCC), Canada (IC), and Europe (ETSI)
Range	400m in direct vision
Low power consumption	RX Mode: 19mA (typical), Tx Mode: 23mA (typical), Sleep Mode: 2μA (typical)
Frequency band	ISM 2.405 - 2.48 GHz
Data rate	250 kbps

Table 2.3: Main characteristics of MRF24J40MA wireless module.

Data Storage

As it was already explained, all electronics components related to data storage are contained in the master module. The requirements were quite simple: high capacity, possibility to save the results in text or Comma Separated Values (CSV) format files, and to keep a configuration file were many parameters related to sampling are stored.

The type of memory chosen was a μSD, that is a flash memory card smaller than typical SD. Although its speed rate is not too high, there are some versions that support reading rates of 10 Mega bits per second (Mbps).

Its working mode is not very complex. A μSD card socket and SPI bus is only needed, that almost any microcontroller has it. In addition, the supply needed for this type of memory cards is usually between 2.7 and 3.6 V, so it fulfil perfectly to the design proposed. Using a FAT file system, it is possible that any PC see the device as a USB memory. For that, it is only needed to store the FAT stack into the microcontroller, that is provided by Microchip[124]. In table 2.4 there are the estimations of memory usage required depending on the functionalities programmed and the compiler used.

Functions Included	**Program Memory (C30/X16)**	**Data Memory (C30/X16)**	**Program Memory (C18)**	**Data Memory (C18)**
Read-Only mode	+11934 bytes	+1454 bytes	+11099 bytes	+2121 bytes
File search enable	+1854 bytes	+0 bytes	+2098 bytes	+0 bytes
Write enable	+6810 bytes	+0 bytes	+7488 bytes	+0 bytes
Format enable	+2499 bytes	+0 bytes	+2314 bytes	+0 bytes
Directories enable	+6870 bytes	+70 bytes	+13796 bytes	+79 bytes

Table 2.4: Memory usage of the Microchip file I/O library. It is important to highlight that compilers C30 and C18 are no longer available, they are replaced by XC16 and XC8[103].

Microcontroller

PIC24FJ256GB106 Specifications	
Working Frequency	Up to 32 MHz (16 MIPS)
Program Memory	256 Kilo Bytes (KB)
RAM data memory	16 KB
Remappable Pins	29 (28 I/O, 1 Input only)
Timers	5
Capture/Compare/PWM Channels	9
UART	4
SPI	3
I2C	3
10 Bits ADC channels	16
USB On-The-Go (OTG)	Yes
Package	64-Pin Thin Quad Flat Package (TQFP)

Table 2.5: Specifications of PIC24FJ256GB106 microcontroller[103].

Once different elements have been described, a microcontroller that can support all these blocks must be selected. Due to the research group experi-

ence with Microchip microcontrollers, no other manufacturer was considered for this prototype. After many tests, and taking into account that the microcontroller needed to have enough memory to store the MiWi™stack, File I/O stack, and USB, and besides, it needs to have several ADC channels input and SPI dedicated pins. Finally, the microcontroller chosen was one from family PIC24 (16 bits), the *PIC24FJ256GB106*, that is able to perform up to 16 Millions of Instructions Per Second (MIPS) and provides lots of digital buses that includes Universal Asynchronous Receiver-Transmitter (UART), Inter-Integrated Circuit (I^2C), USB OTG, etc. This microcontroller contains 64-Pins in a surface package TQFP. Table 2.5 sums up some characteristic of this microcontroller.

Firmware

The complete microcontroller firmware have been programming using C30 Microchip compilers. The MiWi™P2P stack, the File I/O stack and the USB OTG stack have been programming from the libraries provided by the compiler. As both datalogger units contain the same microcontrolller, programming of the communication using MiWi™P2P stack is easier.

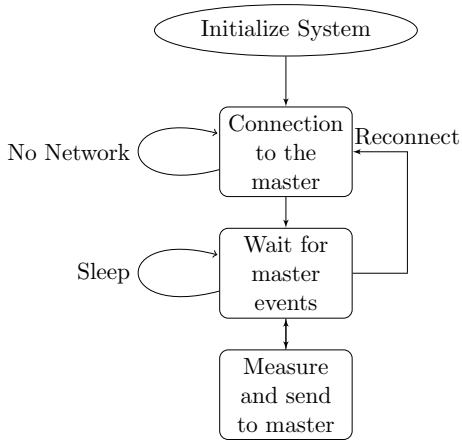

Figure 2.13: Flowchart of slave datalogger unit in ECnsole v1.0.

The slave firmware will be explained first because it is much simpler than the master one. Slave unit does not have any USB connector and uSD memory slot card, so the programming of this firmware will present less difficulty than in case of the master unit. As a reference point, it is good to check the flowchart of the slave datalogger unit (figure 2.13).

Firstly, the slave initialize the systems, managing the digital outputs that are connected to LEDs and to enable the analogue power source by means of the enable pin. After that, it starts the ADC. Finally, it communicates through SPI bus with the wireless module. After the initialization of internal systems (including timers) and peripheral modules, the slave tries to search the master module to establish a communication link with it.

Once the connection with the master is established, slave unit is just waiting for an event from master, to start the sampling of the sensors located in the insole, according to the sampling parameters that are previously received from the master. Once a sample is acquired by the slave, it is sent to the master. In case no more events from master are received, the slave remains sleep to reduce power consumption to provide a longer life to the batteries.

Next, the master module firmware will be explained. As well as in slave firmware, the master one is based on a state machine. Figure 2.14 represents the flowchart of the master unit, that will help to explain and understand the behaviour and the states of this device.

At first, and as slave does, master unit starts a initialization of the internal modules and peripheral devices. The second oscillator based on a 32 kHz crystal is enabled to use the Real Time Calendar/Clock (RTCC). Digital pins are configured as inputs or outputs depending on the operation mode, some are used as output LEDs or to enable the analogue power supply and input for the start/stop button. The ADC module is initialized, the seven inputs are configured as analogue input channels and the sampling and conversion parameters are set. Two SPI buses of the three available are configured for the wireless MiWi™module and for the communication with the μSD memory card. Finally, some variables needed for the state machine are also started.

Together with the configuration of the digital pin as input, an interrupt is enabled to start measurements once the button is pressed. It detect a rising up change in the pin value.

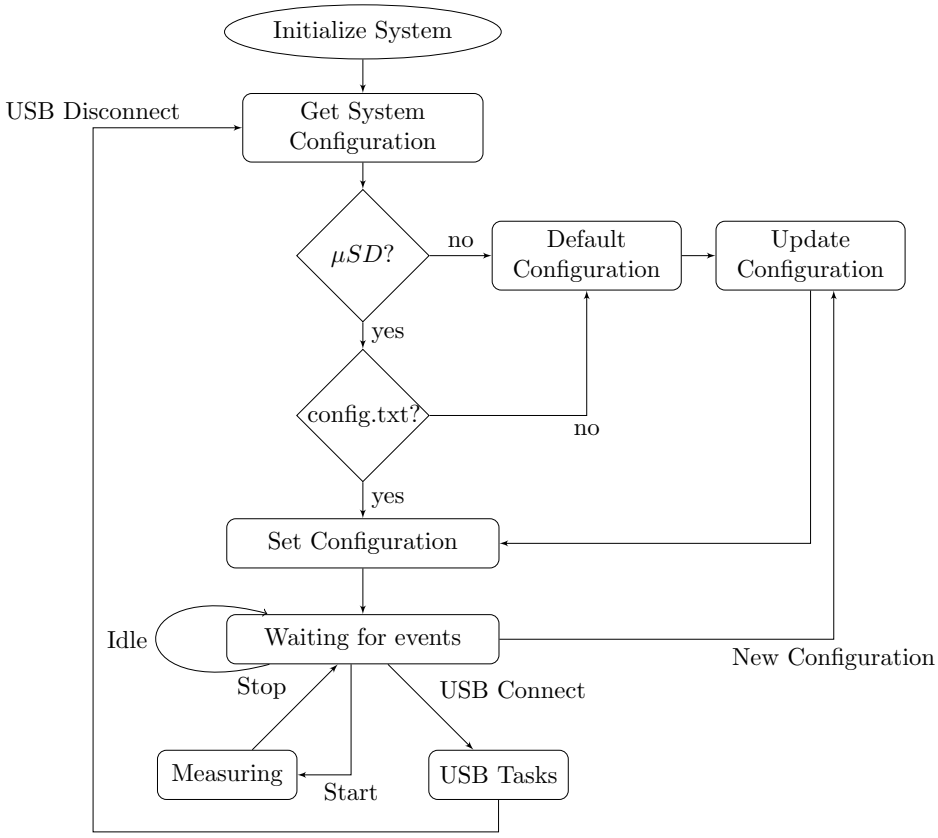

Figure 2.14: Flowchart of master datalogger unit in ECnsole v1.0.

Related to the SPI configuration, first, the remapable pins that are going to be used as pins for the SPI bus must be enabled (Serial Data In, Serial Data Out, and Serial Clock). After that, the different sets of parameters are done according to the peripheral module to be used, MiWi™module or ADC memory card.

After the initialization, next step is "Get System Configuration". During this step, configuration and calibration parameters are set. The options that are configurated are:

- Sampling and storing of data.
- Wireless communication.
- Sensors calibration.

For that purpose, first thing that the system does is checking if a μSD card is inserted, in case it is not, it set the default configuration, that is programmed in the default configuration of the firmware. If is was already inserted, it looks for a configuration file named "config.txt", if it does not exist that file, it created a new one with the default configuration, but in case it exists, it reads it content and set the configuration according the parameters that are specified on it. The content of the "config.txt" file defines several parameters and customization options that are shown next:

```
1 Ts=0050
2 DATE=01/01/10
3 TIME=00:00:00
4 WIRELESS\_CHANNEL=12
5 WRITE\_TO\_SD\_CARD=Y
6 DATA\_FILENAME=data
7 COORDINATOR\_CALIBRATION={(+000.215,-110.000),(+000.215
   ,-110.000),(+000.215,-110.000),(+000.215,-110.000),(
   +000.011,-005.500),(+000.011,-005.500),(+000.011,
   -005.500)}
8 SLAVE\_DEVICE\_CALIBRATION={(+000.215,-110.000),(+000
   .215,-110.000),(+000.215,-110.000),(+000.215,-110.000),
   (+000.011,-005.500),(+000.011,-005.500),(+000.011,
   -005.500)}
9 *** END OF THE FILE ***
```

Each parameter is specified on a new line, its meaning is:

Ts It represents the sampling period of the ECnsole system. It is specified in milliseconds.

DATE It represents the date stamp for the RTCC module.

TIME It represents the time stamp for the RTCC module.

WIRELESS_CHANNEL It determines the wireless channel through the MiWi™sends the information to the PC.

WRITE_TO_SD_CARD It is used to store or not the data into the μSD card. It is a boolean value.

DATA_FILENAME It sets the prefix name of the file that is stored into the μSD card. It adds a two a suffix of two numbers to indicate the order of the files already stored.

COORDINATOR_CALIBRATION It represents the seven calibration values for the insole connected to the master unit. It corresponds to four pressure sensors and three coordinates of the accelerometer.

SLAVE_DEVICE_CALIBRATION It represents the seven calibration values for the insole connected to the slave unit. It corresponds to four pressure sensors and three coordinates of the accelerometer.

Once the configuration is done, master unit starts the wireless network. At the beginning, it checks if there is any node already connected to him, in case it is, it sends a broadcast message to carry out a reconnection. This is done because in case that master creates a new channel and any node is connected to it using another channel, both ends would send data through different channels. After that, the application assures that all nodes will request a new connection again, so it can proceed to the network initialization. Next, the master unit remains in a “waiting state” which is waiting for user events, either by pressing the button or receiving a command from the PC, or even connecting the USB cable.

In order to reduce the power consumption, microcontroller enters into a idle mode, which stops Central Processing Unit (CPU) and code execution, keeping peripheral modules activated like RTCC. In case of event caused by the button, the transceiver or the USB, the CPU continues its operation and process those interruptions:

- If the button is pressed, it means that measuring must be started or stopped in case it was already initiated.
- If a message from transceiver is received, it is processed and then, microcontroller will act depending on the command received from PC. This message can start a new measurement or even modify any sampling parameter.
- If a USB connection is detected, it will start with the functions of the USB.

As it has been explained, there are two different ways to start measurement, by means of the button located in the master datalogger unit, or by receiving a message through the MiWi™ transceiver. Before starting the acquisition using the ADC, some task must be carried out by the microcontroller:

1. It enables the power supply of the analogue block.
2. If the μSD card is ready and storing is enabled, it creates a new CSV file; for that purpose, it first look for the last file created into the memory card, and then, creates the next according to numerical suffix added to the prefix name.
3. It enables the timers used for sampling

On other the hand, if the button is pressed once the measurement has been started, or a stop command is received from wireless module, both the power supply (using the enable pin of LM2623) and the timers are disabled. In figure 2.15 a sequence diagram is shown in case the communication is done directly using the wireless module.

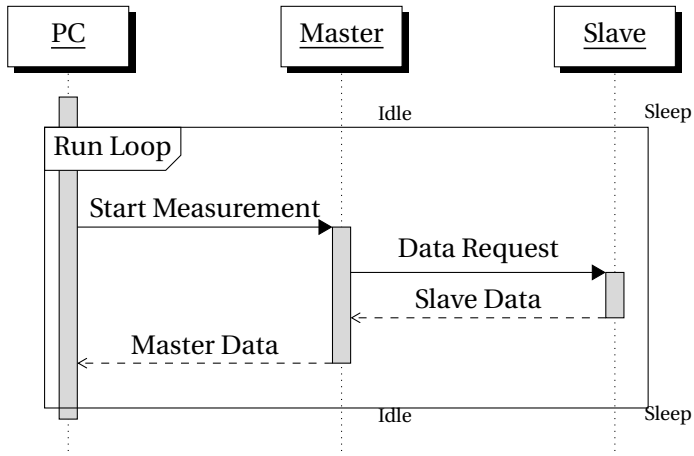

Figure 2.15: Sequence diagram of ECnsole v1.0.

If the option of storing data into the μSD is selected, the microcontroller stores the data from sensors in the next order: first, the value of the timer, in order to be able to know if any sample has been lost; after that, the pressure values of the sensors of right foot, next the values from the accelerometer, and repeat the same order for left foot, dividing each sensor value using commas. The resulting CSV file would contain a text like this:

```
1 Date=18:34:23,26/04/2010
2 Presion $->$ N/cm2, Aceleracion $->$ g
3 0000000000,1,0006.87,0006.60,0010.72,0017.60,+0.31,+0
   .03,-0.80,1,0006.32,0004.95,0007.15,0009.07,-0.20,+0.09
   ,-0.76;
4 0000000050,1,0006.60,0006.32,0007.42,0017.32,+0.30,+0
   .01,-0.80,1,0005.77,0004.95,0007.15,0008.25,-0.21,+0.08
   ,-0.76;
5 0000000100,1,0006.87,0006.87,0008.80,0017.60,+0.31,+0
   .03,-0.80,1,0006.32,0005.22,0006.87,0007.97,-0.20,+0.08
   ,-0.77;
```

First column of data corresponds to the time stamp in milliseconds, the next four columns are the pressure sensors of master unit, next there are three columns for the A_X, A_Y, and Z-Axis Acceleration (A_Z), and the subsequent columns corresponds to the same data but related to the slave insole.

The complete ECnsole v1.0 system is shown on figure 2.1. The insoles were placed inside the footwear while datalogger units were located on the legs or ankles of the subject, figure 2.1 shows the using example of ECnsole v1.0.

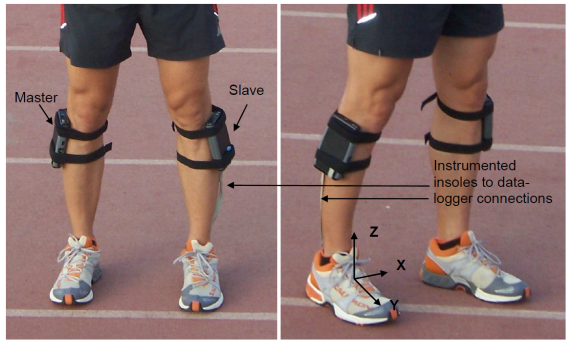

Figure 2.16: Case of use of ECnsole v1.0.

2.1.3 Software Processing

As it has been explained before, the data collected by the instrumented insoles can be stored into a μSD memory card or send it using a MiWi™ transceiver to a PC as it has been explained in this section. Next, a brief explanation about the software developed to received and plot the data from the instrumented insoles is done.

This software application is programmed using Java[125] programming language. It has two working modes: real time and animation modes. In real time mode, the data received from the master module are displayed on the screen(see figure 2.17) in real time. In animation mode, a previously downloaded file from the master module can be reproduced, simulating real time operation.

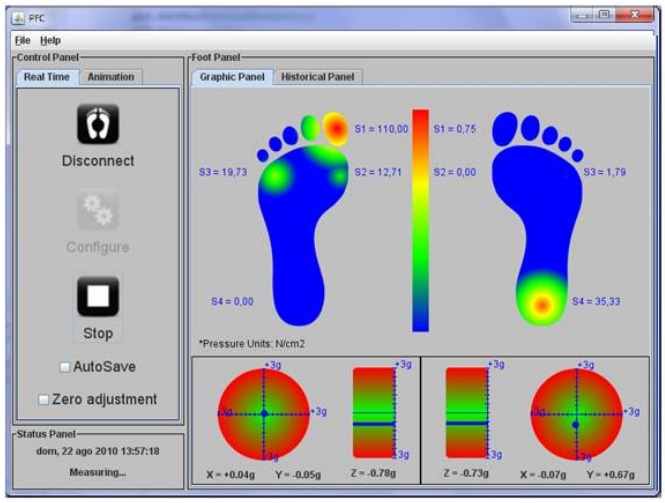

(a) Graphic Panel

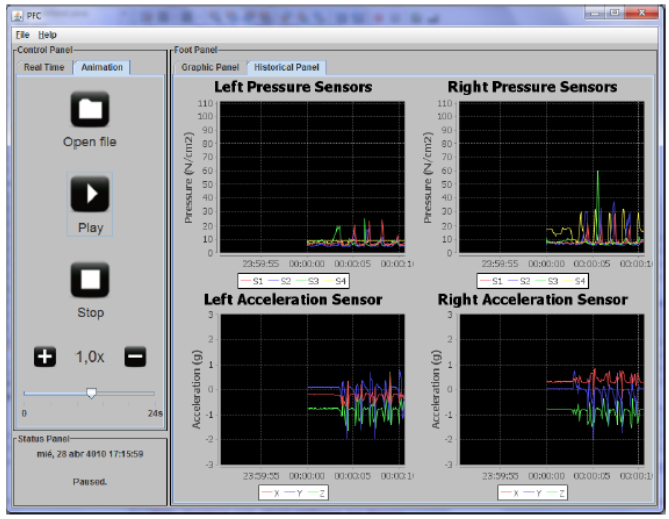

(b) Historical Panel

Figure 2.17: ECnsole v.1.0 Software Application.

As figure 2.17a shows, there are two footprints that represent both insoles. The colour scale means the level of pressure on the pressure sensors corresponding to the area specified during this chapter (big toe, head of first and fifth metatarsal, and heel) . In the bottom of the window, there are some other graphs, to represents the deviation of the acceleration due to changes in position of the accelerometer. It is important to remind that accelerometer is located on the foot arc. As the accelerometer used is owns three space coordinates (A_X,A_Y, and A_Z), A_X and A_Y are represented in a polar diagram while A_Z is evaluated in a vertical bar diagram. In the historical panel (figure 2.17b), there is a temporal plot of the values of each sensor. In fact, there are two types of plots, one for pressure sensors and another one for accelerometer. In addition, the data are grouped by foot (left and right foot).

ECnsole v1.0 Specifications	
Acceleration linear range (g)	±3.6
Acceleration resolution (g)	0.017
Acceleration errors (%)	±5
Pressure range (kPa)	1000
Pressure resolution (kPa)	2.5
Pressure error (%)	±5
Master/slave weight (with batteries) (grams)	219/213
Master/slave size (cm)	$14.5x7.5x2$
Insole weight (grams)	32
Thickness of arch insole (mm)	5.6
Thickness of rest of insole (mm)	1.0
Battery time (h)	3
Wireless transmission distance, in open air (m)	60
Sampling frequency (Hz)	62
Memory Capacity in a 2-GB uSD (h)	50

Table 2.6: Technical specifications of the measurement system ECnsole v1.0.

To sum up, table 2.6 shows the technical specifications of the first version of the instrumented insoles developed by the research group. It is important to highlight that sampling frequency of this version of the ECnsole is 62 Hz because it will one of the parameter whose improvement will be the biggest.

2.2 ECnsole version 1.2

MiWi™ is an interesting alternative to ZigBee®. It is a simple protocol with a reduced stack, oriented to low cost solutions. However, in real applications, it seems that the connectivity between nodes can be rather fragile. This problem happened some times in ECnsole v1.0. For that reason, together with the goals of improve its performance and reduce its cost, a new prototype was designed, the version 1.2.

Next, only the modifications on the different parts of the previous ECnsole version are explained. Therefore, as starting point, it is important to highlight that no modifications on insoles have been carried out.

2.2.1 Changes on Datalogger Unit

There is an important change in this version. There is only one datalogger unit, removing the slave unit. The placement of this unit will be also modified because now it is need to connect both insoles to the same datalogger unit. It is much more comfortable to place the device into the waist.

Power Supply

As the previous version, both analogue and digital blocks operates at 3.3 V. In the preceding prototype, switching voltage sources were used due to great efficiency compared to others configurations. They allow to work with smaller voltages, which can mean to reduce the number of batteries. Two switching sources were used for both analogue and digital blocks using the same integrated converter, the *LM2623* from National Semiconductor[100]. In analogue part, this converter was used together with a voltage regulator to reduce switch-

ing noise. They were supplied by two AA batteries of 1.5 V. However, after several experimental test, some problems were observed:

- Electronic noise over the main supply line can cause interferences. Despite this ripple is pretty small (around 0.6 %), by working with electrical circuits is preferred to avoid these kind of noises by filtering or voltage regulators.
- Switching sources need a hardware design much more complex than lineal sources.
- When working with high frequencies with switching sources, losses in PCB tracks by inductances or parasitic capacitances become very important.
- Currents generated may produce undesirable electromagnetic interferences, however, lineal sources do not produce these interferences.

Therefore, finally it was decided to replace power supply strategy of previous design by using only voltage regulators. Two voltage regulators have been used for analogue and for the digital block to avoid switching noise typical in digital stages.

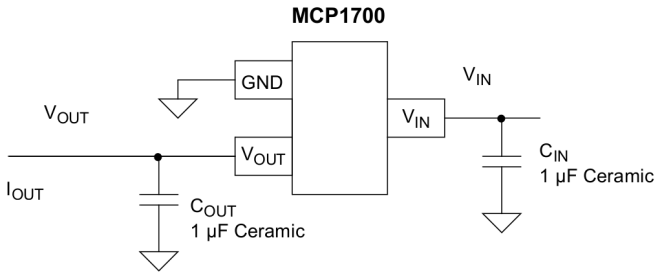

Figure 2.18: Configuration of MCP1700 recommended by the Manufacturer[103].

The objectives for the new voltage regulator were a low drop-out voltage and a straightforward soldering process to prototyping. Finally, the regulator

chosen was the *MCP1700* from Microchip. Figure 2.18 represents the typical configuration of this regulator. As input, three AAA rechargeable batteries of 1.2 V were used to provided a nominal voltage of 3.6 V.

Conditioning sensors circuitry

As this prototype consists only in one unit, conditioning circuitry from both insoles must be contained in one device. The main novelty in this part of the prototype is the use of two *MCP6044* for both insoles. Same circuit that figure 2.11 with feedback resistor $R_F = 91k\Omega$ is used.

Although microcontroller *PIC24FJ256GB106* supports up to 16 input channels in the ADC, and our design only needs 14 (4 channels for pressure sensors + 3 channels for accelerometer coordinates, which means 7 channels per insole), there is a conflict of interest between other channels and SPI buses.

This new problem forces a new strategy for data acquisition. The research group proposed to use a multiplexer system to control the acquisition of the signals. For this purpose a multiplexer with an architecture 8-to-1 for insole. A multiplexer that was previously used by the research group was selected for a rapid prototyping. It was the ADG608 from Analog Devices[89]. It is a single supply Integrated Circuit (IC) that can work at 3.3 V.

Just after the multiplexer and before the data acquisition a low pass filtering was used. The goal is to reduce the noise level, and to act as voltage buffer amplifier for the input of the ADC in order to remove the negative effects of the load and to uncouple impedances. The filter designed corresponds to a second order Sallen-Key, with a cut-off frequency of 300 Hz and unity gain. In figure 2.19 the typical Sallen-Key filter is shown.

Considering a cut-off frequency of 300 Hz and unity gain, and using the transfer function of the equation 2.4, the values of the resistor R, and the capacitances C_1 and C_2 can be calculated. Obtained as results: $R = 1k\Omega, C_1 = 680nF, C_2 = 330nF$.

$$T(s) = \frac{1}{R^2 C_1 C_2 s^2 + 2RC_2 s + 1} \tag{2.4}$$

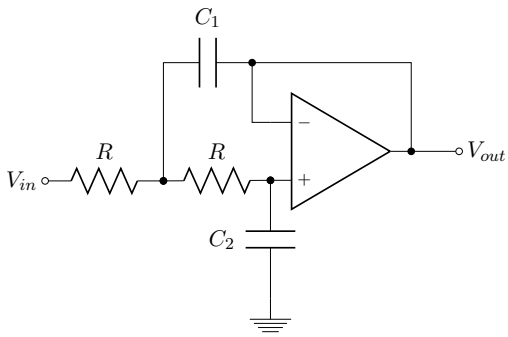

Figure 2.19: Second order low pass filter Sallen-Key.

The behaviour of this filter was simulated using the open source software for circuit simulation Qucs (Quite Universal Circuit Simulator), the frequency response is plot in figure 2.20.

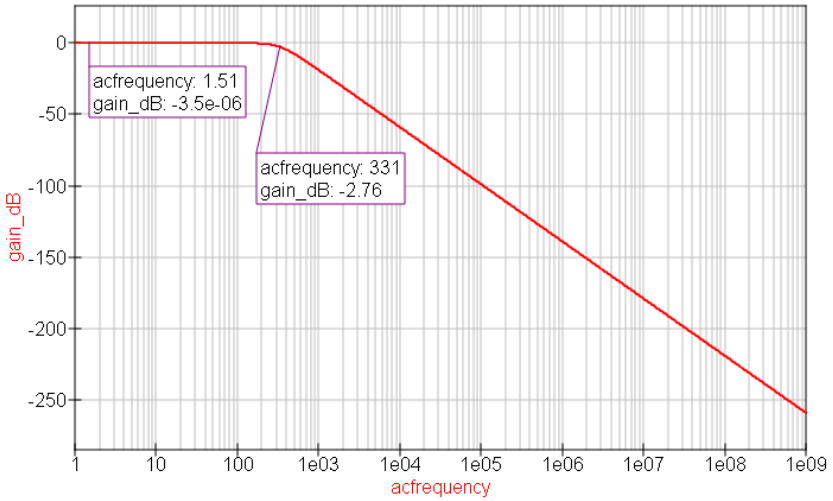

Figure 2.20: Frequency response of Sallen-Key filter.

This configuration was duplicated to be able to filter signals from both multiplexer's outputs.

Firmware

The are no significant changes in firmware for ECnsole v1.2. As it have been explained, most important change is the union in one unique device the hardware presented in ECnsole v1.0. That means any functions related to communication between master and slave are removed because they are not need any more.

Additional functions related to multiplexer controls are added in comparison to previous version. It corresponds to the control of digital outputs to be able to switch between inputs of multiplexers.

An improvement on the algorithm of acquisition was achieved to increase the frequency sample. Samples are store into a digital buffer while it is being sent to the computer or stored into μSD.

Table 2.7 presents the technical specifications of the ECnsole version 1.2. Some of them are the same presented in version 1.0. As it was explained, most remarkable changes are the union of both datalogger units into a unique device and the improvement in the frequency sample from 62 to 77 Hz.

ECnsole 1.2 Specifications	
Datalogger weight (with batteries) (grams)	220
Datalogger size (cm)	14.5 x 7.5 x 2
Sampling frequency (Hz)	77

Table 2.7: Technical specifications of the measurement system ECnsole v1.2. Only those parameters different from previous versions are shown.

Figure 2.21 shows the layout both top and bottom layers while figure 2.22 presents the final board once all components are solder. It is possible to distinguish the different blocks described in this thesis document. Final result of the prototype designed in ECnsole v1.2 is shown of figure 2.23.

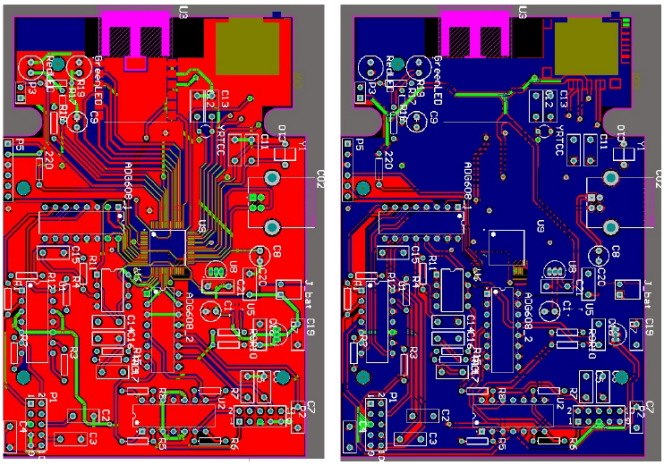

Figure 2.21: Layout of ECnsole version 1.2. Top (red) and bottom (blue) layers are shown.

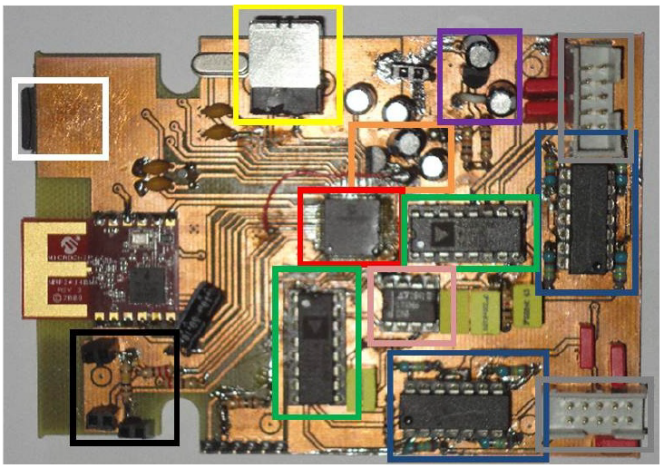

Figure 2.22: ECnsole v1.2 PCB with components: digital power supply (orange), analogue power supply (purple), microcontroller (red), conditioning circuitry (blue), multiplexer (green), filter (pink), μSD card (white), USB (yellow), LEDs (black), and insoles connectors (grey).

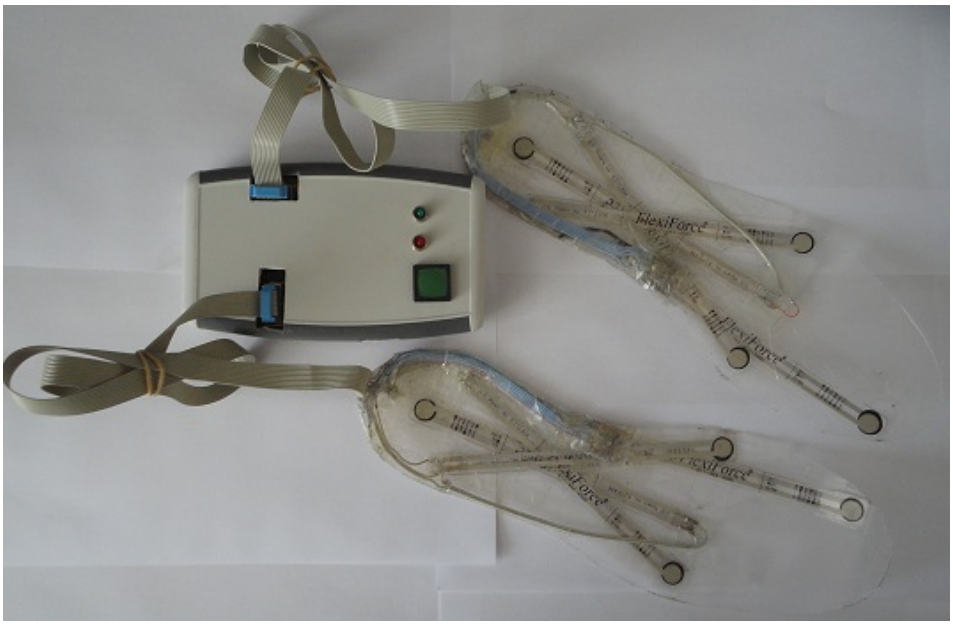

Figure 2.23: Instrumented insoles ECnsole version 1.2 showing both instrumented insoles, the datalogger unit and the interconnections.

2.3 ECnsole version 1.5

The design of this new prototype was a breakthrough compared to previous versions, specially regarding to the insole. As v1.2 raised, this device also works with one unique datalogger unit, a block diagram is shown in figure 2.24.

2.3.1 Changes on Instrumented Insole

In ECnsole v1.5, the same substrate was used for the insoles. Pressure sensors were located as well as in first version explained in this chapter, that are big toe, head of first and fifth metatarsals, and the heel.

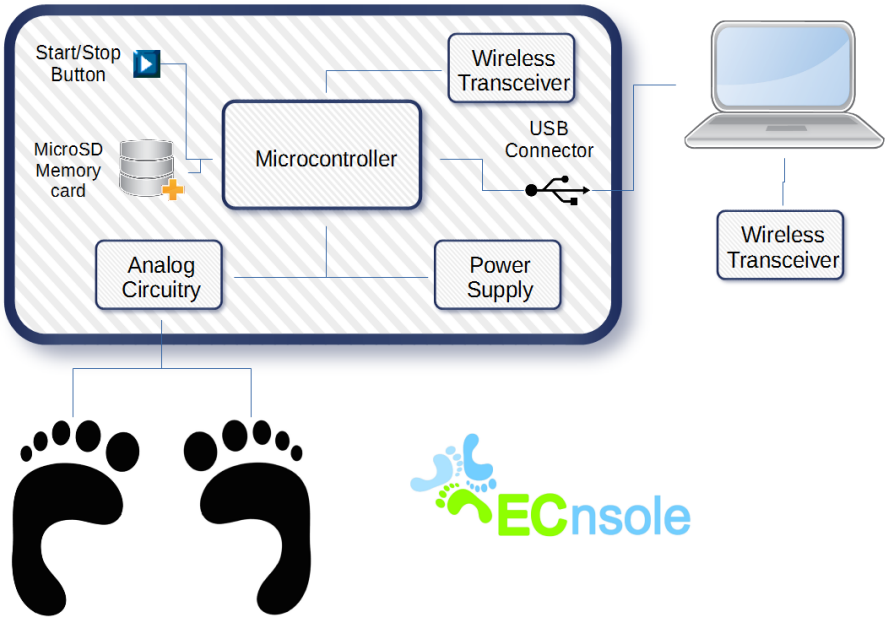

Figure 2.24: Schematic diagram of ECnsole v1.5.

IMU

The major novelty is the replacement of the accelerometer ADXL330 by an IMU integrating an gyroscope, accelerometer, and magnetometer.

Gyroscope used was the L3GD20 from STMicroelectronics[109], which is a three axis gyroscope. Table 2.8 presents the specifications of the gyroscope. It includes a sensing element and an IC interface capable of providing the measured angular rate to the external world through a digital interface (I^2C/SPI). Its scale is selectable (three scale values in Degree Per Second (dps)) and works with the supply range designed. It owns an embedded temperature sensor to compensate measurements. Figure 2.25 shows the top view of L3GD20 including the axis.

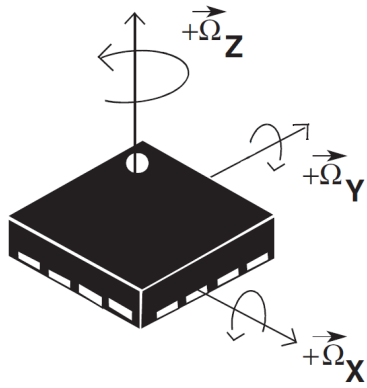

Figure 2.25: Top view and axis layout of L3GD20.

L3GD20 Specifications	
Selectable full scales (dps)	250/500/2000
Digital Output Interfaces	I^2C and SPI
Sensor data output	16 bits
Temperature data output	8 bits
Integrated filters	User selectable bandwidth
Supply range	2.4 to 3.6 V
Current consumption (typical)	6.1 mA

Table 2.8: Technical specifications of gyroscope L3GD20.

On the other hand, accelerometer and magnetometer are integrated in the same IC, the *LSM303DLHC* also manufactured by STMicroelectronics (see table 2.9). Both sensors are also triaxials as well as the gyroscope. *LSM303DLHC* includes an I2C serial bus interface that supports standard and fast mode 100 kHz and 400 kHz. The system can be configured to generate interrupt signals by inertial wakeup/free-fall events as well as by the position of the device itself. Thresholds and timing of interrupt generators are programmable by the end user on the fly. Magnetic and accelerometer parts can be enabled or put into

power-down mode separately. Access to data from accelerometer and magnetometer are done by accesing different I^2C address. Figure 2.26 shows the directions of the accelerometer axes and the axes of the magnetic field of *LSM303DLHC*. Figure 2.27 shows the board of the IMU used.

LSM303DLHC Specifications	
Magnetic field full scale(gauss)	±1.3/1.9/2.5/4.0/4.7/5.6/8.1
Selectable full scale	$\pm 2g/4g/8g/16g$
Sensor data output	16 bits
Digital interface	I^2C
Temperature data output	8 bits
Supply range	2.16 to 3.6 V
Current consumption (typical)	110 μA (normal mode), 1 μA (sleep mode)

Table 2.9: Technical specifications of accelerometer and compass *LSM303DLHC*.

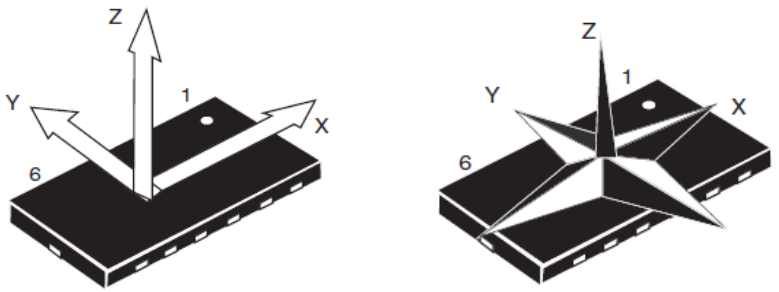

(a) Direction of detectable accelerations

(b) Direction of detectable magnetic fields

Figure 2.26: Top view of *LSM303DLHC* accelerometer and magnetometer.

The resulting insole of ECnsole version 1.5 with pressure sensors and the IMU board can be observed in figure 2.28.

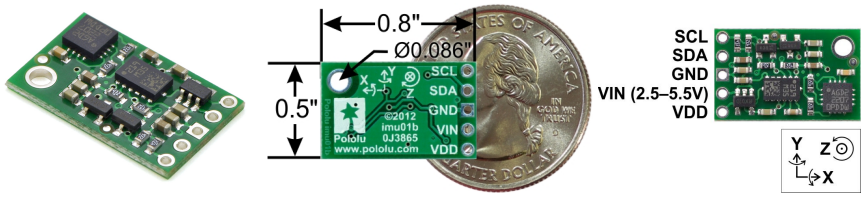

Figure 2.27: Instrumented insole ECnsole version 1.5 showing the four pressure sensors, the IMU (the small green board at the arch of the foot) and the interconnection wire.

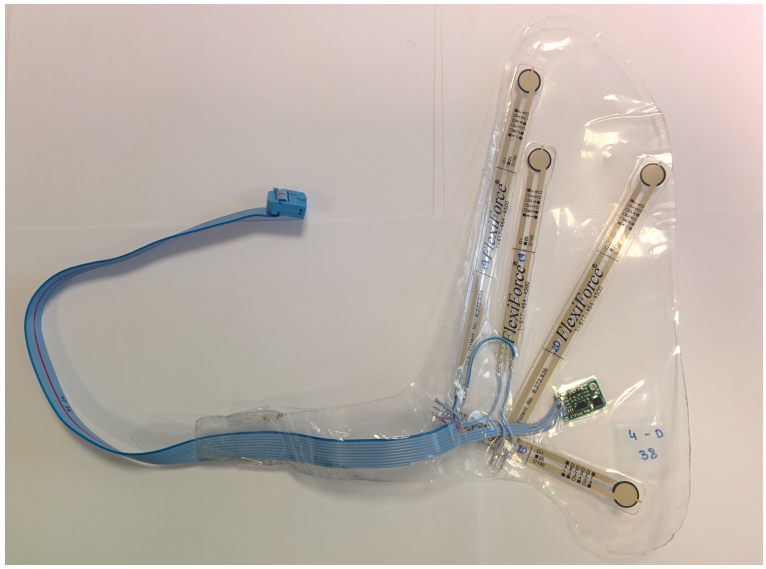

Figure 2.28: Instrumented insole ECnsole version 1.5 showing the four pressure sensors, the IMU (the small green board at the arch of the foot) and the interconnection wire.

2.3.2 Changes on Datalogger Unit

The same architecture that previous version is used in this prototype. Only a modification in the conditioning circuitry that acquires pressure sensors signals is done.

Conditioning sensors circuitry

As it was already explained, a non inverter configuration (see figure 2.11) was designed to adapt signal from pressure sensors. The main problem of the configuration selected is that dynamic range was halved due to non inverted input of operational amplifier was set at $V_{CC}/2$, that is 1.65 V.

In order to increase the dynamic range and improve performance of the pressure sensors, it was decided to use an inverter configuration, as figure 2.29 shows. Equation 2.5 presents the voltage output of the inverter configuration.

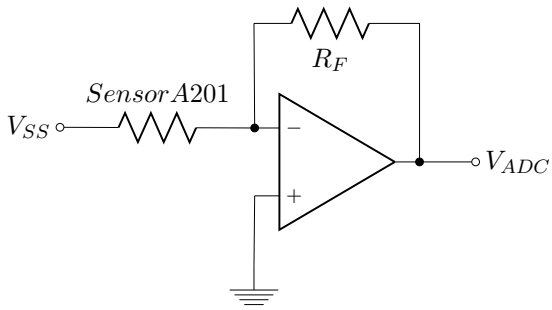

Figure 2.29: Conditioning circuitry based on inverter operation amplifier used in ECnsole v1.5.

$$V_{ADC} = -V_{SS} \cdot \frac{R_F}{R_{Sensor A201}} \tag{2.5}$$

Power supply of analogue components remains as in version 1.2. However, in order to achieve a voltage output between 0 and 3.3 V, which corresponds to the voltage supply by the regulator, we need to supply a negative voltage V_{SS} to the sensors.

For that purpose a charge pump DC-DC converter was included into the design. The integrated charge pump used was the *TC1044S*, from Microchip[103]. It is a 8 pin integrated circuit with a low power consumption ($80\mu A$ at $V_{IN} = 5V$) and efficiency conversion of the 99.9 %. The design used is shown on figure 2.30

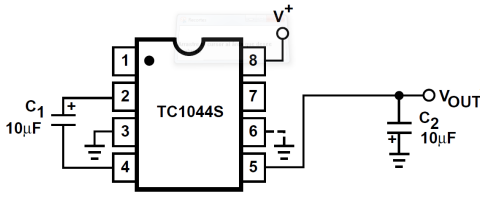

Figure 2.30: Charge pump DC-DC converter *TC1044S*. $V_{OUT} = -V^+$ for $1.5V \leq V^+ \leq 12V$

Firmware

Few modifications were done in firmware. However, during the initialization phase of the microcontroller's peripheral, I^2C buses were initialized to enable communication with the IMU. As it was explained during microcontroller description, there are three I^2C channels in PIC24FJ256GB106, in ECnsole v1.5, channels 2 and 3 are used for communication with the sensor's insoles. As well, during measuring state, there is an acquisition through I^2C protocol by Microchip XC16 compiler's libraries.

There was an improvement in the sampling frequency that ECnsole is able to sample data from sensors. It is important to highlight, that there is a great increment in data sensors. In previous versions (both v1.0 and v1.2), there were 8 pressure sensors (both feet) and 6 inertial sensors (3D accelerometer from both feet), that is a total of 14 variables. Now the system adds 12 new data from 3D gyroscope and 3D magnetometer (both feet also). Including all these new variables, the frequency sample reached was 333 Hz (sampling period of 3 ms).

Figure 2.31 shows the layout both top and bottom layers of the designed PCB as a datalogger unit. The solder PCB with the different blocks described is highlighted in figure 2.32.

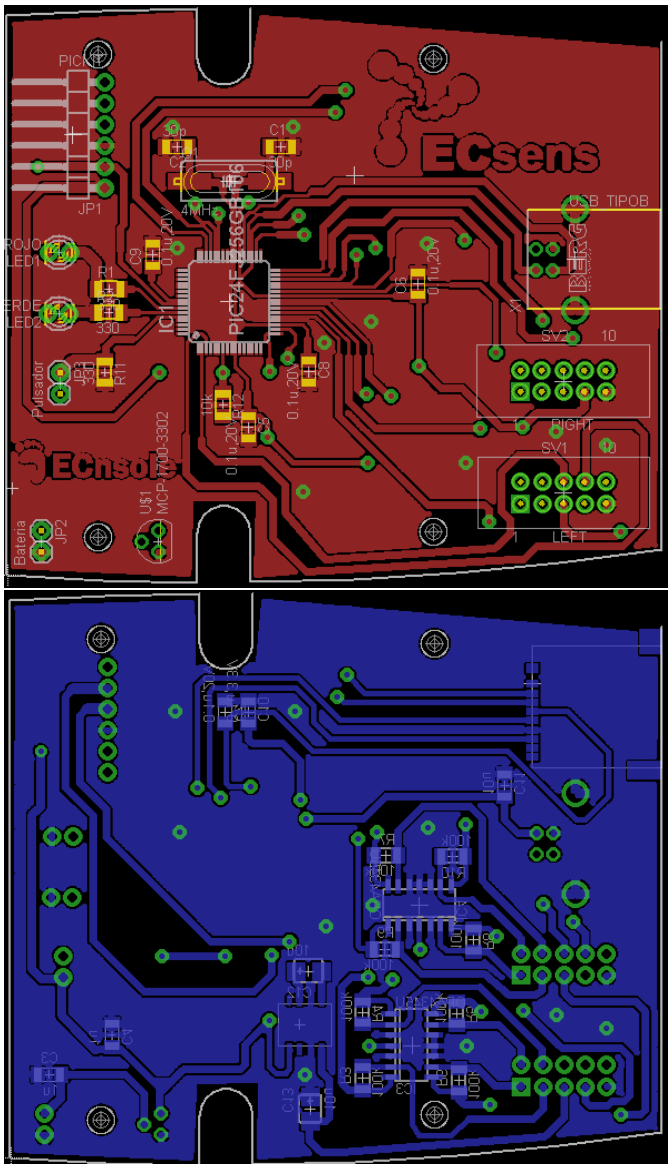

Figure 2.31: Layout of ECnsole version 1.5 Top (red) and bottom (blue) layers are shown.

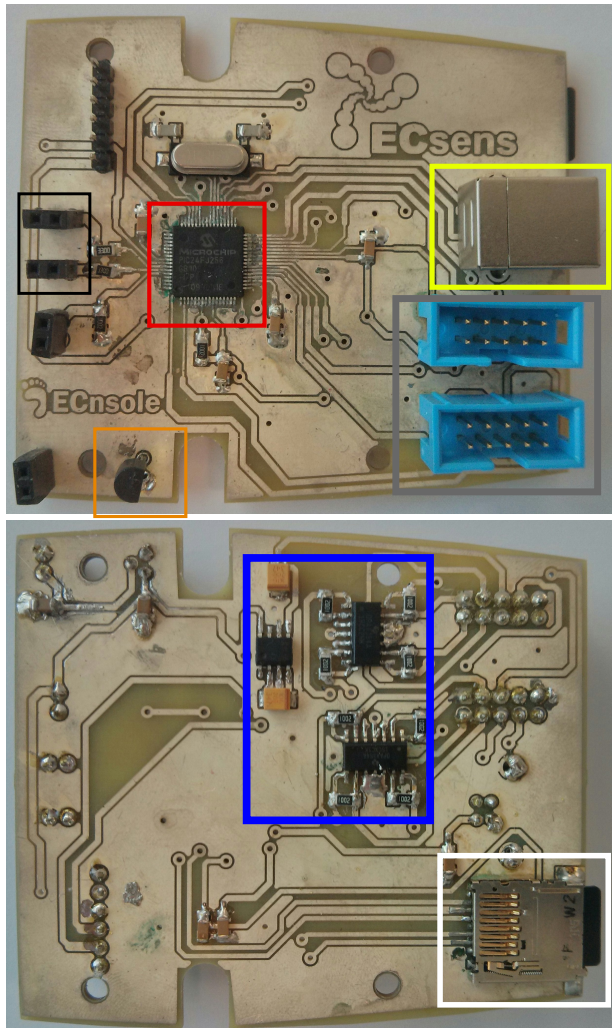

Figure 2.32: ECnsole version 1.5 PCB top (left) and bottom (right) with components: digital power supply (orange), microcontroller (red), conditioning circuitry (blue), μSD card (white), USB (yellow), LEDs (black), and insoles connectors (grey).

2.3.3 Changes on Software Processing

Software application designed on ECnsole version 1.0 provides a user friendly interface, but its capabilities to work with the data were limited. Since the application where the instrumented insoles are used can be decisive for the type of data required by researchers, specialist, doctors, or athletes, it was very important to have a new user interface were the data plotted were completely configurable, and a system that could be easy to improve or to add new functionalities not only by the research group but also for anyone who could use the ECnsole system.

Therefore, a new application in Matlab® was developed to plot the data from the sensors (see figure 2.33). It also works in 2 different modes: remote and post-measurement mode. In remote mode, the software application plots the data from the sensor previously selected in real time. While in post-measurement mode, any sensor the user desires can be plotted for analysis.

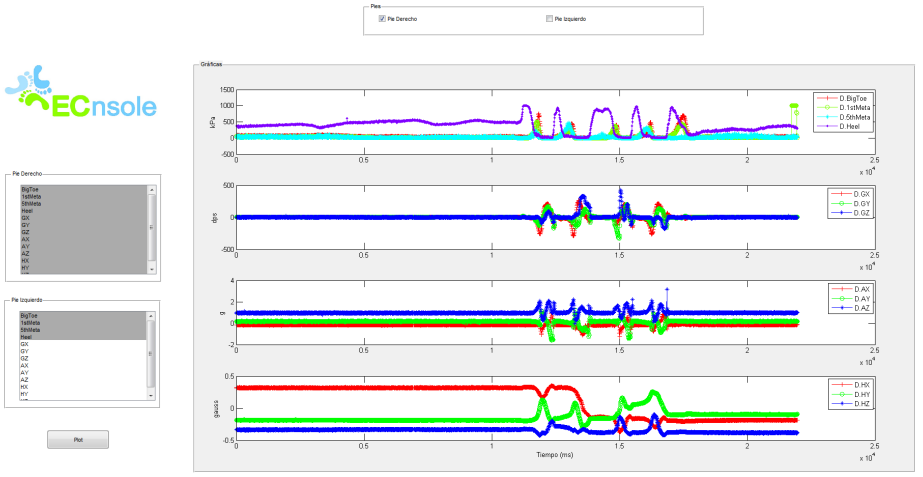

Figure 2.33: Matlab®application on the PC side. It allows the user to plot any variable from ECnsole from any foot.

The final prototype is shown in figure 2.34. Specifications are almost the same compared to the version 1.2 except for the sampling frequency, that was increased to a very adequate value of 333.33Hz, even for running and jumping monitoring.

Figure 2.34: Prototype ECnsole v1.5.

2.4 ECnsole version 2.0

These version of ECnsole means a huge advance compared to versions 1.x, mainly because it modifies completely the architecture of the system. As in version 1.0, the datalogger unit is divided into two new devices because, as the

major improvement that provides this new system, is that there are no cables since datalogger unit is embedded into the insole.

The new architecture proposed is presented in figure 2.35. As the objective is to embed all the electronics in the insole, it is necessary to divide again the datalogger unit into two independent devices. Besides, there are 2 new pressure sensors on the insole located in the head of the third metatarsal and in midfoot area, because it was an area where no information was obtained in previous versions.

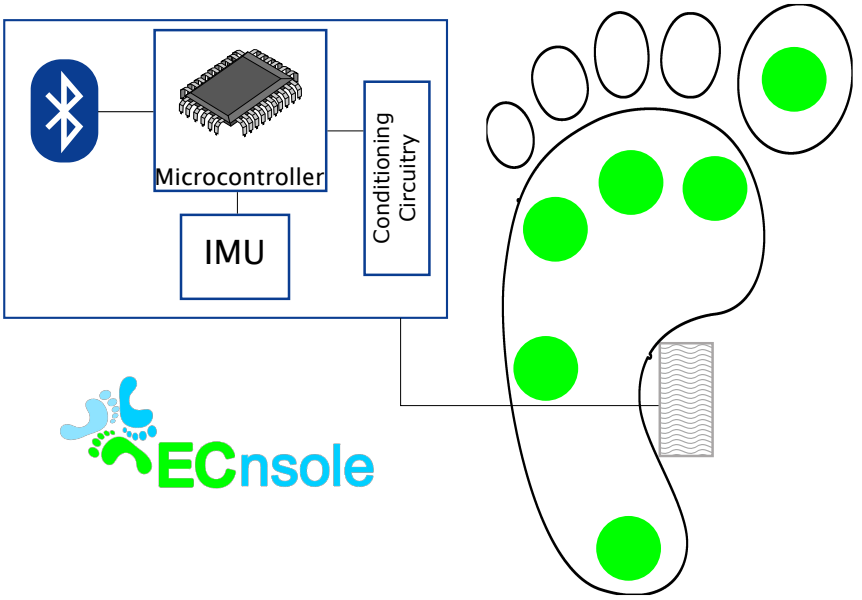

Figure 2.35: Architecture of ECnsole version 2.0. Major novelties are the increment in number of pressure sensors (green circles) from 4 to 6, and the replacement of MiWi™by Bluetooth for wireless communication. Everything is embedded in the insole.

2.4.1 Changes on Instrumented Insoles

In order to design an embedded instrumented insoles, it is necessary to include all electronics, communications, batteries, and sensors in the insole.

For that purpose, substrate used must be modified because a thicker one is required to not modify any exercise (gait, running, jumping, etc.) because of the size of electronics. Finally, the substrate chosen is a Ethylene-vinyl acetate (EVA) obtained from a commercial sport insole. To use ECnsole version 2.0 in a comfortable and correct way, it is recommended to remove the insoles usually included in any shoe.

Processing electronics, comunications modules, and batteries, which will be described later, were all included in the foot arch, that is the place that allows a thicker space due to the typical foot shape.

Pressure/Force sensors

In ECnsole v2.0, pressure sensors are replaced for Flexiforce A401 (figure 2.36), that have pretty similar properties that A201, but they have bigger area and shorter length. Specifications are presented in table 2.10.

Figure 2.36: Flexiforce Sensor A401 [120].

Flexiforce A401 Specifications	
Thickness	0.208 mm (0.008 in.)
Length	56.8 mm (2.24 in.)
Width	31.8 mm (1.25 in.)
Sensing Area	25.4 mm (1 in.) ⊘
Connector	2-pin Male Square Pin
Force Ranges	0 - 25 lb. (110 N)

Table 2.10: Specification of Flexiforce A401 sensors[120].

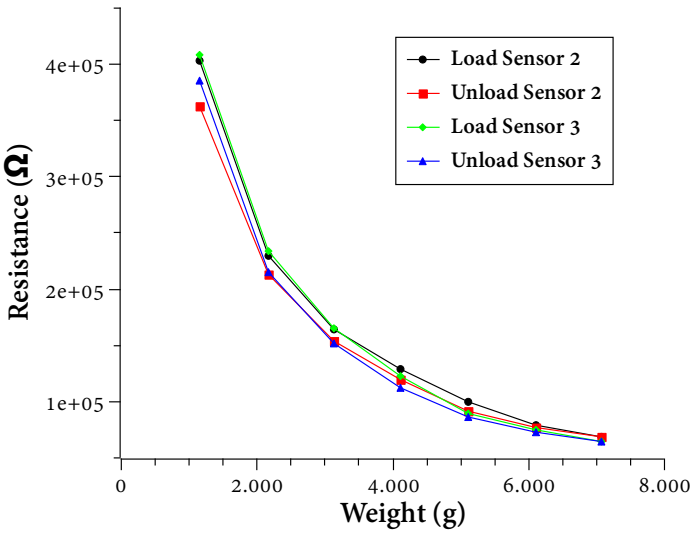

Figure 2.37: Flexiforce A401 Sensor Response. Many sensors were calibrated, these two are just an example of the response of these type of sensors.

This type of sensor has a similar response (see figure 2.37) than flexiforce A201. The main differences are related to the sensitive sensor area as it is explained in chapter 1. These sensor were also calibrated individually by means of the electronics system designed taking into account the digital counts of the integrated ADC. An example of the calibration curves obtained for right foot of one of the manufactured insoles are shown in figure 2.38.

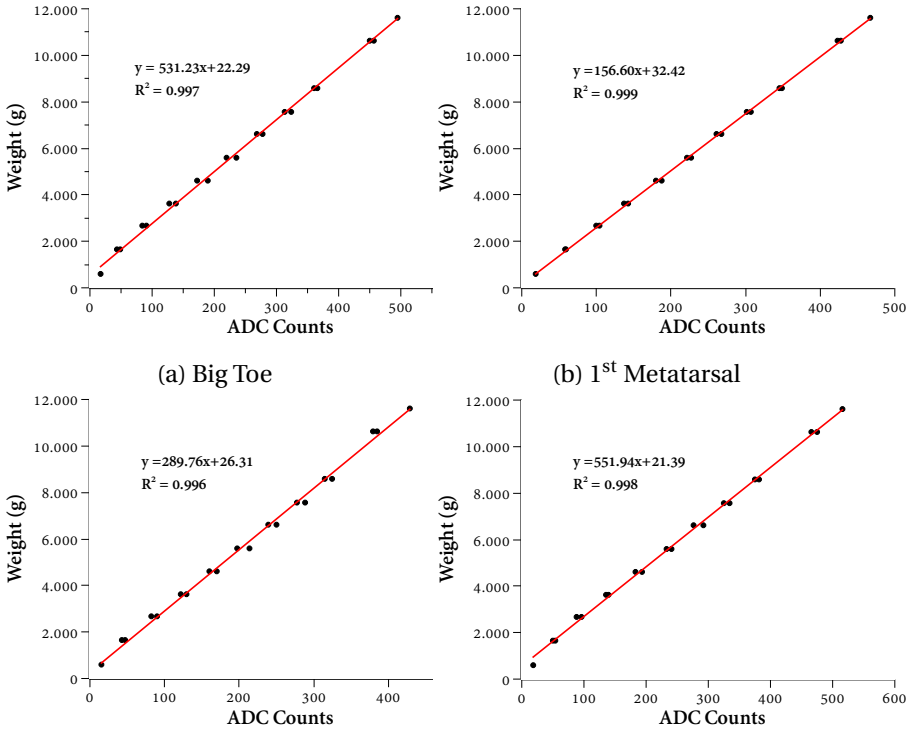

(a) Big Toe

(b) 1st Metatarsal

(c) 5th Metatarsal

(d) Heel

Figure 2.38: Calibration curves of A401 sensor of right foot ECnsole version 2.0.

IMU

On the other hand, the IMU used in version 1.5 is discontinued by the manufacturer. For that reason, the replacement was mandatory. The gyroscope is replaced by *L3GD20H* while accelerometer + magnetometer were substitute by *LSM303D*, both from STMicroelectronics[109]. The communication with those sensors is still digital using I^2C bus. The *L3GD20H* has a full scale of $\pm 245/\pm 500/\pm 2000$ dps and is capable of measuring rates with a user selectable bandwidth. Main specifications of *L3GD20H* are shown in table 2.11

L3GD20H Specifications	
Selectable full scales (dps)	2450/500/2000
Digital Output Interfaces	I^2C and SPI
Sensor data output	16 bits
Temperature data output	8 bits
Integrated filters	User selectable bandwidth
Supply range	2.4 to 3.6 V
Current consumption (typical)	5 mA

Table 2.11: Technical specifications of gyroscope L3GD20H.

LSM303D Specifications	
Magnetic field full scale(gauss)	$\pm 2/m4/m8/m12$
Selectable full scale	±2/4/8/16
Sensor data output	16 bits
Digital interface	I^2C
Temperature data output	8 bits
Supply range	2.16 to 3.6 V
Current consumption (typical)	300 μA (normal mode), 1 μA (sleep mode)

Table 2.12: Technical specifications of accelerometer and compass *LSM303D*.

The communication with *LSM303D* is slightly different because in previous version, magnetometer and accelerometer have different I^2C addresses, but in this IC, both have same address. The *LSM303D* has linear acceleration full-scales and a magnetic field full-scale fully selectable by the user (see table 2.12 for specifications). In the figure 2.39 is possible to observe the board of the new IMU used.

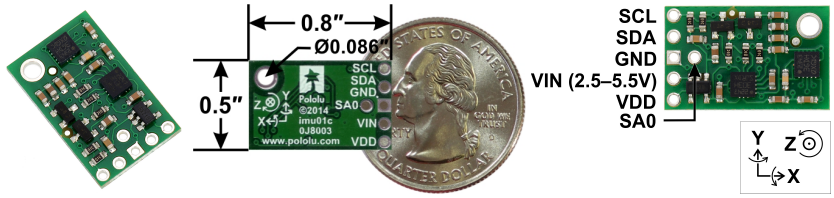

Figure 2.39: Instrumented insole ECnsole version 1.5 showing the four pressure sensors, the IMU (the small green board at the arch of the foot) and the interconnection wire.

Last version of ECnsole is shown on figure 2.40. Thickness of this new insole is 3.8 mm and 7.5 mm in the arch of the foot and weight is 45 grams. Specifications of this new prototype are described in table 2.13.

ECnsole 2.0 Specifications	
Datalogger weight (with batteries) (grams)	12
Datalogger size (cm)	6.8 x 2.7 x 0.8

Table 2.13: Technical specifications of the measurement system ECnsole v2.0. Only those parameters different from previous versions are shown.

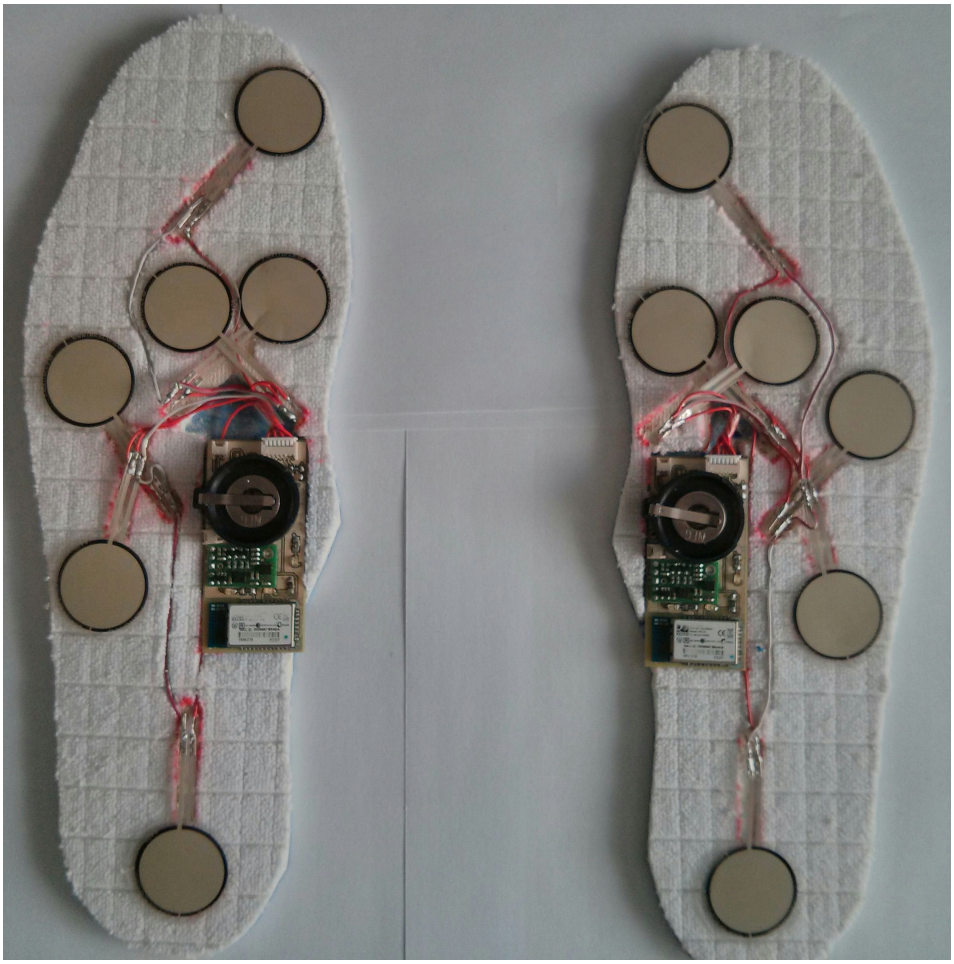

Figure 2.40: Instrumented insole ECnsole version 2.0. 6 pressure sensors are used located at big toe, 1st, 3rd, and 5th metatarsal heads, midfoot, and heel. The microcontroller unit, together with the IMU and Bluetooth transceiver, and battery is located at the arch of the foot.

2.4.2 Changes on Datalogger Unit

In order to reduce the dimensions of the datalogger unit and the power consumption, the μSD memory card module was removed. In addition, microcontroller is replaced by one of PIC18F family, and the communication is done using bluetooth instead of MiWi™. Finally, the supply of the device is done by using a rechargeable coin battery.

Power Supply

In previous versions of ECnsole, batteries of type AA or similar were used. They are very common and easy to find in any supermarket. Using several of these batteries in series allows to obtain a voltage high enough to supply all the system. The problem of these types of batteries is mainly the size. It occupies a lot of size, making it impossible to located them embedded in the insole.

Several alternatives were studied. At the beginning, a lithium flexible battery is the choice. However, using this type of battery implies the need of the design of a circuit battery charger, that could increase size of the final datalogger.

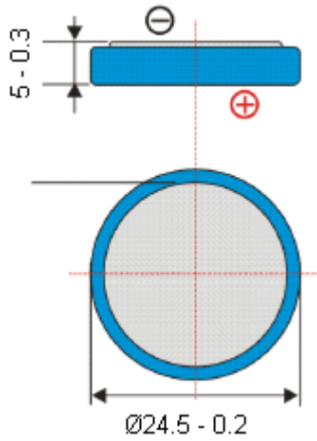

Figure 2.41: Dimensions of LIR2450 battery. Units are in millimetres.

For that reason, finally a rechargeable coin battery is selected. It is low cost and small dimension. In order to fulfil power consumption requirements and to reduce the size as much as possible, a battery type *LIR2450*. It provides 3.6 V and 120 mAh. This resulting voltage is again regulated to 3.3 V using a low drop-out voltage regulator.

Conditioning sensors circuitry

It is important to highlight that the maximum premise is to reduce the datalogger unit size as much as possible. On the other hand, as it is explained, the number of pressure sensors is increased from 4 to 6. Therefore, in order to increase the number of sensors without enlarging PCB size, new strategies of conditioning circuitry must be adapted. In versions 1.0 and 1.2, a non-inverter amplifier configuration was adapted. In order to increase dynamic range of ADC, in version 1.5 a inverter configuration replaced by the non-inverter configuration.

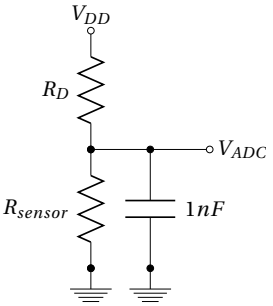

Figure 2.42: Conditioning circuitry based on voltage divider used in ECnsole v2.0.

In this new version, a voltage divider is chosen (see figure 2.42). It has several advantages for ECnsole design. First, it does not need any additional IC as operational amplifiers, filters, etc. And second, depending on the resistor R_D chosen, we can reduce power consumption without affecting significantly the performance of this type of circuit. R_D value was selected after experimental and individual calibration of each sensor. Final value obtained was $100k\Omega$.

Wireless module

The limitations of MiWi™ were explained in previous sections. Besides, it is more interesting to use wireless protocols that are more accessible to regular users. For that reason, MiWi™ was replaced by Bluetooth®. The Bluetooth module used in ECnsole v2.0 is the *RN-42* from Microchip[103] (see figure 2.43).

Figure 2.43: *RN-42* Bluetooth module. Antenna is integrated.

RN-42 Bluetooth module supports version 2.1 + Enhanced Data Rate (EDR). It is backwards compatible with Bluetooth version 2.0, 1.2, and 1.1. It provides several communications protocols, like UART Serial Port Profile (SPP) or UART Host Controller Interface (HCI), and USB HCI, and it is widely used. It is not the smallest one, but its dimensions and cost fulfil completely the requirements.

The most important features of *RN-42* modules are:

- Fully qualified Bluetooth®version 2.1 module, supports version 2.1 + EDR.
- Backwards compatible with Bluetooth version 2.0, 1.2, and 1.1.
- Postage stamp sized form factor 13.4 mm x 25.8 mm x 2 mm.
- Low power (26 μA sleep, 3 mA connected, 30mA transmit).
- UART (SPP or HCI) and USB (HCI only) data connection interfaces.
- Sustained SPP data rates: 240 kbps (slave), 300 kbps (master).

- HCI data rates: 1.5 Mbps sustained, 3.0 Mbps burst in HCI mode.
- Embedded Bluetooth stack profiles.

The main applications where *RN-42* is recommended to use it are in measurement and monitoring systems, industrial sensors and controls, medical devices, and computer accessories, which means that is perfect for ECnsole.

RN-42 supply voltage range from 3.0 to 3.6 V. Therefore, there is no need to add any additional components to supply this wireless module since our supply voltage is 3.3 V as it was explained during this chapter.

Microcontroller

In previous versions of ECnsole a microcontroller from PIC24F family was used. *PIC24FJ256GB106* meets all the ECnsole design requirements. However, this microcontroller has an excess of power, pins and peripheral that oversized the final design required for this system.

There are few requirements that microcontroller must fulfil. On the one hand, it must contains digital buses, specifically UART to communication with *RN-42* Bluetooth module and I^2C to acquires data from inertial digital sensors (gyroscope, accelerometer, and magnetometer). On the other hand, it must be able to operate at a working frequency high enough to sample data from sensors as fast as possible to obtain a high sampling frequency.

A microcontroller replacement is done by a PIC18F family, the *18LF26K22* in the package Shrink small outline package (SSOP) of 28 pins. This microcontroller is a 8-bit, so it means to modify the compiler used. Table 2.14 shows all the most significant specifications of the microcontroller used.

Firmware

The replacement of the microcontroller meant a change in the compiler used. In previous versions, a 16-bits compiler XC16 is used, while in this new prototype XC8 (for 8-bits microcontrollers) is the compiler selected, also provided by Microchip[103]. To describe this new firmware is necessary to present the flowchart diagram of figure 2.44.

PIC18LF26K22 Specifications	
Working Frequency	Up to 64 MHz (16 MIPS)
Program Memory	64 KB
RAM data memory	3896 Bytes
Input/Output Pins	25
Timers	4
Capture/Compare/PWM Channels	2
UART	2
SPI	2
I^2C	2
10 Bits ADC channels	19
Package	28-Pin SSOP

Table 2.14: Specifications of *PIC18LF26K22* microcontroller[103].

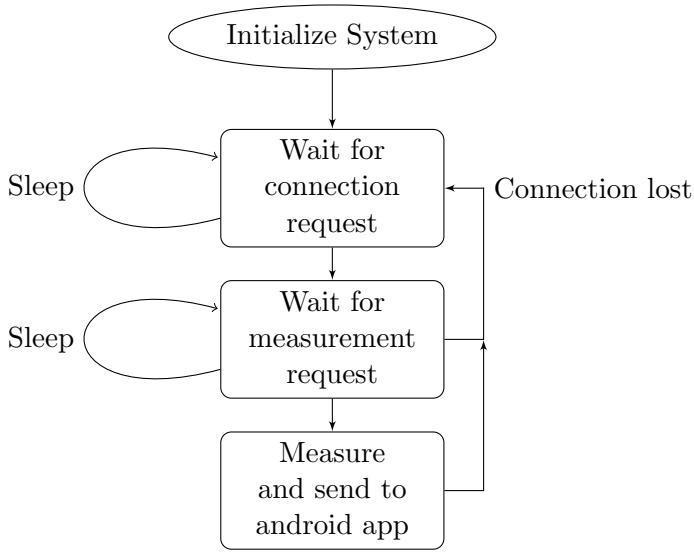

Figure 2.44: Flowchart of firmware datalogger unit in ECnsole v2.0.

At first, the microcontroller initializes all the systems and peripherals (ADC, UART, and I^2C). It enables digital sensors into a sleep mode. Once all the systems are activated, microcontroller gets into an sleep mode, waiting for the remote controller (Smartphone) a message to stablish the Bluetooth connection.

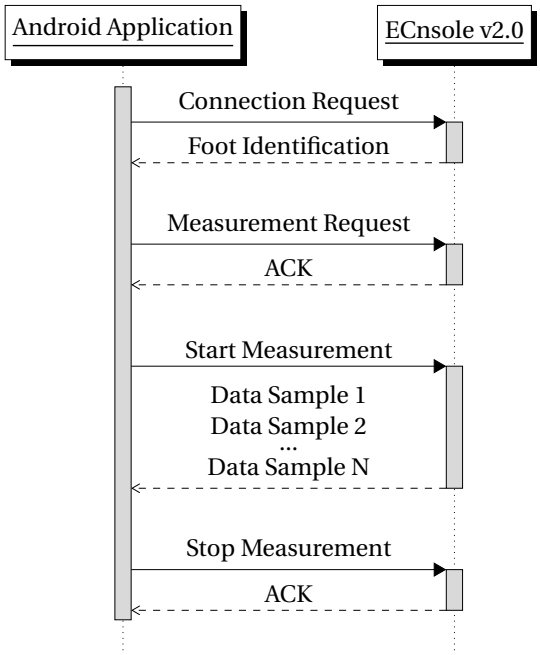

Figure 2.45: Sequence diagram connection and measurement protocol of ECnsole v2.0.

The mobile application, that will be explained in next section, searches for the instrumented insoles. It is important to highlight that both insoles must transmit during the connection protocol its foot identification. Figure 2.45 presents the message transmission during connection between the remote controller (Android tablet or smartphone) and the ECnsole v2.0 for one insole. At the beginning, both insoles are in sleep mode, when they received a connection request, they wake up a answer the mobile application with the foot identifica-

tion. It is very important for the android application to be able to plot logically the results from data sensors.

Once the connection is established, ECnsole goes again into sleep mode, waiting for a "Measurement Request" message. This state is necessary to be sure that both insoles are awake before measurement is started. Once both devices send an Acknowledgement (ACK). The application is ready to send a message to start measurement.

Then, both insoles send according to the sampling frequency established during the measurement request message the data from sensors until a "Stop Measurement" message is received. In that moment, microcontroller gets again into sleep mode waiting for a new measurement.

The layout of both the top and bottom layers of the PCB designed in this version is shown in figure 2.46. Figure 2.47 presents the solder PCB with the different blocks described is highlighted.

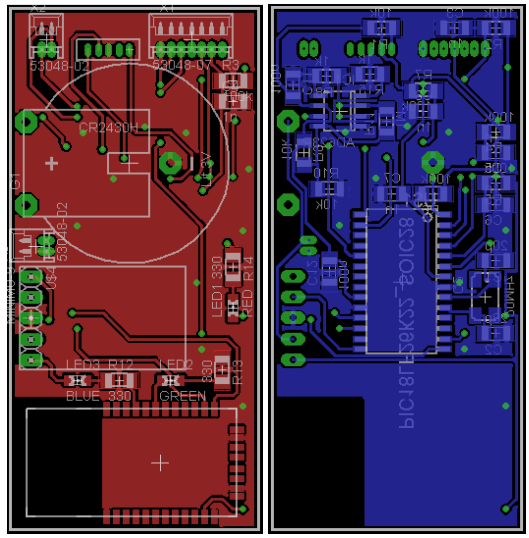

Figure 2.46: Layout of ECnsole version 1.5 Top (red) and bottom (blue) layers are shown.

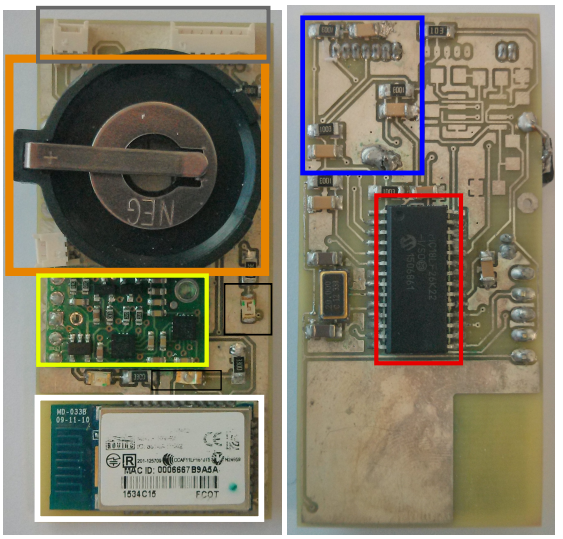

Figure 2.47: ECnsole version 2.0 PCB top (left) and bottom (right) with components: power supply (orange), microcontroller (red), conditioning circuitry (blue), Bluetooth module (white), IMU (yellow), LEDs (black), and insoles connectors (grey).

2.4.3 Changes of Software Processing

Software applications developed in previous versions were programmed using Java (version 1.0 and 1.2) or Matlab (version 2.0). In this last version bluetooth is the wireless technology selected for communications between insoles and the remote controller. For that reason, a mobile application is the first option that research group considered to develop.

The development of a mobile application depends on the operating system that the smartphone or table is working on. There are many operating systems available on the market, but only the three most important (see figure 2.48) of them will be described in this section.

(a) Android (b) iOS (c) Windows Mobile

Figure 2.48: Main mobile operating systems.

Windows Mobile is the operating system that has fewer users, however, in last years it is experiencing a significant increase. It is designed by Microsoft Corp.[126]. The applications developed for Windows Mobile can be programmed by using Visual Basic, .Net or C#. The second operating system in user numbers is the iOS developed by Apple Inc.[127]. Its main problem is that it runs only on Apple devices such as iPhone, iPad, and iPod. This system covers the 40% of the market. Their application can be programmed using Objective-C. Finally, the most common among smartphone and tablet users is Android. This operating system belongs to Google[128], who bought it on 2005. It covers a bit more of the 50% of the market. It is based on Linux. It has its own programming language, that is based on Java, with a huge community. All these reasons, make to the research group to choose Android as the operating system to program the mobile application that will control and plot the data from sensors of the insoles.

This android application will be in charge of managing bluetooth connections with both insoles, sending commands to start and stop measurements, and to plot data results from sensors. In addition, it will maintain a database of patients or users that are involve with any exercise or activity using ECnsole version 2.0. The icon of the application is presented in figure 2.50. First, the flowchart of the ECnsole android application will be presented. It will help to understand how the application works and to presents the different snapshots of real working situations. The flowchart is shown in figure 2.49.

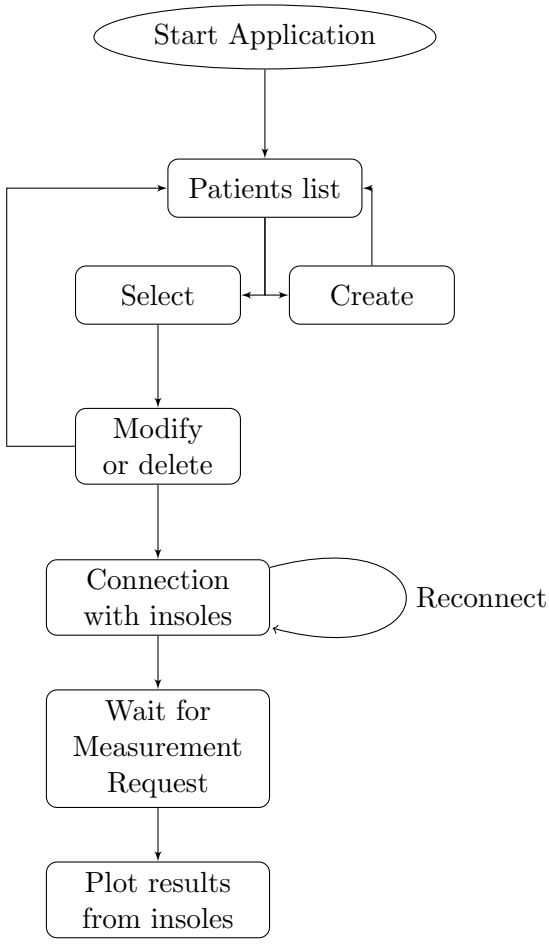

Figure 2.49: Flowchart of android application ECnsole v2.0.

Figure 2.50: Icon of the application developed for the instrumented insoles Ecnsole version 2.0.

Once the application is started, the splash screen of the ECnsole android app is shown (figure 2.51). During this stage, the application checks if bluetooth is activated, in case it is not, it asks to the user to activated. It is not possible to continue without activating bluetooth, even if the user just want to check latest recordings. After that, the patients list is shown (figure 2.52). In this window, the user can select a patient to modify its data or remove it, or even can create a new patient. The current data fields needed to create a new patient are: name and surname, age, sex, height, and weight. If a patient is selected, a new window will open. It allows to modify the patient data. Using the icon on the upper right corner, the user can establish the connection with the instrumented insoles by means of Bluetooth. This windows contains different buttons to access to the graphs that might be plotted (see figure 2.53).

Finally, if the user desires to see the pressure results in real time that sensors are measuring, it is enough to click on the graphs buttons to observe and analyse the data (figure 2.54). In the figure 2.54a there are two footprints that represents the user's feet. There are six blacks points that correspond to the sensors, and a colour scale bar, that means how hight is the pressure value measured on the piezoresistive sensor's insole. In case that the user prefers to analyse timing of the pressure values, it just necessary to click on the corresponding button to obtain that plot (figure 2.54b).

Figure 2.51: Splash screen of the application developed for the instrumented insoles Ecnsole version 2.0.

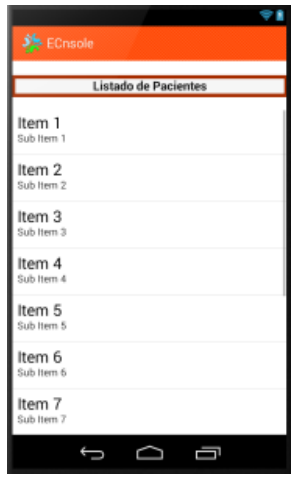

Figure 2.52: Patients list of the application developed for the instrumented insoles Ecnsole version 2.0.

Figure 2.53: Patient selected in the application developed for the instrumented insoles Ecnsole version 2.0. Buttons for plotting data sensors graphs are shown.

(a) Feet pressure (b) Timing pressure

Figure 2.54: Pressure graphs available in android application ECnsole v2.0 from a previous version of the instrumented insoles.

In case that user is interested in data from IMU, it is possible to print data of any of the sensors: gyroscope, accelerometer, and magnetometer, in any of the three axis. Figure 2.55 presents an snapshot of a measurement result of the three sensors available on IMU. The data presented both in figure 2.54 and 2.55 correspond to recorded data from previous version 1.5 of the prototype. Using all the information of the sensors provided by the mobile application, it is very easy to carry out an analysis of the exercises performed by any participant in any of the frameworks that will be explained in chapters from 4 to 7.

Version 2.0 of the ECnsole is still under validation by the candidate and the research team. Current works are related to improving synchronization between both insoles and the smartphone and increasing the sampling frequency.

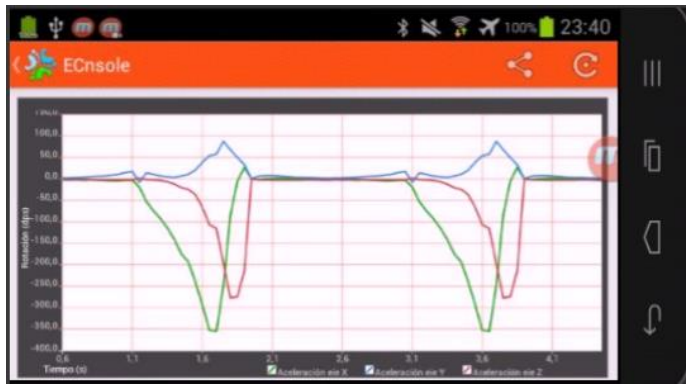

(a) Gyroscope

(b) Accelerometer

(c) Magnetometer

Figure 2.55: Graphs available ECnsole v2.0 for IMU data from a previous version of the instrumented insoles. Gyroscope 2.55a is in dps, accelerometer 2.55b in g, and magnetometer 2.55c in gauss.

Chapter 3

ECnsole validation and preliminary test

Contents

3.1 Validation of pressure sensor values 132
3.1.1 Test definition 132
3.1.2 Results 133
3.2 Validation of foot position by means of inertial sensor values 134
3.2.1 Test definition 135
3.2.2 Results 138
3.3 Preliminary test 139
3.4 Conclusions 147

3.1 Validation of pressure sensor values

3.1.1 Test definition

At first, in order to be able to consider the ECnsole as a valid tool the measure the plantar pressure distribution, a validation of the system using a commercial system was done. A total of 10 volunteers took part in this experiment.[129].

Participants

For this preliminary study, the ECnsole version 1.2 was used. Pressure and acceleration were recorded during 5 minutes walking for a total of ten subjects. The participants walked freely on a flat surface without any impositions concerning velocity or other parameters in order to study the participants' natural gait. The characteristics of the participants are summarized in table 3.1. By previous biomechanical and medical tests, four of the subjects were diagnosed as walkers who supinate slightly, one pronates, and the rest were considered neutral. In addition, participant 2 has a claw foot and number 9 has collapsed arches. These characteristics are evident in the results, as compared to a normal walker as shown below.

Participant	Sex	Mass (kg)	Height (m)	Age (years)	BMI	Foot Type
1	Male	76	1.82	30	22.9	Neutral
2	Male	80	1.81	33	24.4	Supinated, claw feet
3	Male	75	1.78	27	23.7	Supinated
4	Male	94	1.83	35	28.1	Neutral
5	Male	73	1.77	41	23.8	Supinated
6	Male	72	1.71	23	24.6	Neutral
7	Male	73	1.76	18	23.6	Over-Supinated
8	Male	79	1.85	38	23.1	Neutral
9	Female	61	1.60	17	23.8	Supinated, collapsed arches
10	Female	54	1.65	17	19.8	Pronated

Table 3.1: Participant characteristics of the preliminary study performed with ECnsole v1.2.

Hardware equipment

Plantar pressure during gait was measured, and compared data with those recorded using the F-scan system (Tekscan Inc., Boston, USA). To measure plantar pressure in equivalent regions of ECnsole v1.2 sensors, F-scan insoles were fixed (by using adhesive tape) to the instrumented insoles developed. Each FlexiForce sensor covered the area between four or six sensing points on the F-scan insoles. The average of the pressure values for all the F-scan sensing points was calculated and compared to the corresponding FlexiForce sensor value. The variations in the plantar pressure were measured simultaneously by our system and the F-scan system for three participants.

3.1.2 Results

Typical plantar pressure curves obtained from both devices are shown on the same graph in figure 3.1. The solid line is the result of our device and the dashed line is the F-scan result. The differences in peak pressure ranged from -1.8 kPa to 27.9 kPa, where the maximum difference was in big toe sensor. We can observe a very good agreement between both systems with an error below 8.1% pressure. Moreover, from the dynamic point of view, the average delay between the signal from our system and F-scan system was below 30 ms. Therefore, the developed system was confirmed to provide a quantitative estimation of plantar pressure.

After analysing these results and validate pressure sensors used in the instrumented insoles (see figure 3.1). It is possible to claim that in the status of ECnsole version 1.2, the working sampling frequency (77 Hz) obtained allowed the system to be used for walking analysis as other works in the literature presented[87, 130]. However, in case of running or jumping exercises, sampling frequency must be increased.

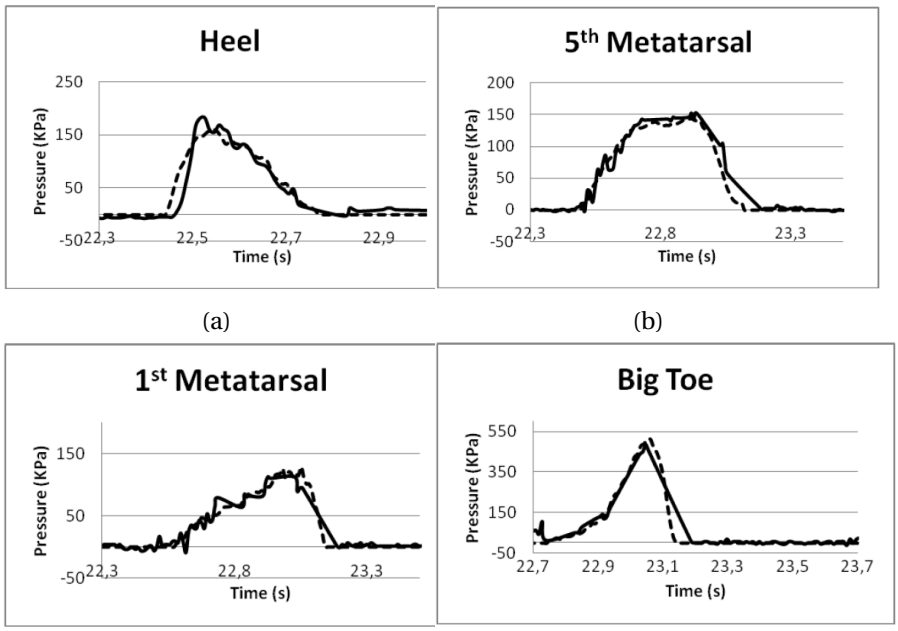

Figure 3.1: Pressure patterns obtained from ECnsole v1.2 system (solid line) and a F-scan system (dashed line) on the left foot. Heel sensor (3.1a), 5th Metatarsal sensor (3.1b), 1st Metatarsal sensor (3.1c) and Big Toe sensor (3.1d)

3.2 Validation of foot position by means of inertial sensor values

For this experimental validation, version 1.5 of ECnsole was used. Validation of the instrumented insoles was done at Instituto Mixto Universitario de Deporte y Salud (IMUDS), in Granada.

3.2.1 Test definition

Participants

A total of 5 participants (4 male and 1 female) volunteered for this study (age: 30.60 ± 2.19 years, height: 181.80 ± 5.22 cm, and weight: 82.50 ± 3.91 kg). The participants were member of the research group. All of them were physically active as they did more than 3 exercise sessions per week, but none of them performed sport at an elite level. Before the test started, participants were asked to warm up for 5 minutes doing running over the treadmill at a comfortable speed.

Hardware equipment

Participants use their regular sport running shoes. They put inside the ECnsole version 1.5, and then placed over the instrumented insole a common sport sole in order to assure that ECnsole is not going to displace from its position in a way that can alter the measurements.

The volunteers of this experiment will be walking and running at different speeds. To maintain an stable velocity, a treadmill was used. The model of treadmill used was the Woodway PRO XL (Woodway, USA). Main characteristics of the treadmill are summarised in table 3.2.

Specifications	
Running surface dimensions	70 x 224 cm
User weight capacity	Run: 400 lb. / Walk: 800 lb. (4 mph max)
Inclination range (standard)	0 - 25%
Speed range (standard)	0 - 15 mph
Reverse working mode	optional feature
Jump plate	optional feature
Hospital grade circuitry	optional feature

Table 3.2: Specification of Treadmill Woodway PRO XL. Both inclination and speed range can be increased.

In order to validate the position of the foot obtained by means of the IMU located at the ECnsole a set of 12 high speed infrared video cameras will be used. It consist of a motion capture 3D system. The video cameras are located in the different positions to be able to record the foot position in all the space. For that purpose four passive markers of 15.9 mm of diameter are placed on the foot at first and fifth metatarsal heads, and in upper and lower calcaneus, to track the angles and foot position during the complete exercise. The video cameras used are the model Prime 41 by Optitrack (Optitrack, USA). They are able to record up to 180 Frame Per Second (fps).

The analysis of the angle obtained by the video cameras is performed using the Kwon 3d XP software (Visol, South Korea). It calculates the angles using as starting point the reflectors located at the human body (in our case, legs and feet). It creates a 3D model of the leg and foot, and then the angle can be calculated during the complete exercise. In case of the ECnsole, the foot position is calculated the algorithm proposed by *Madgwick et al.*[131].

The goal of this work is not to validate the algorithm, which authors considered absolutely valid as it was publish in scientific journals of high impact factor. The objective is to validate the use of the IMU to obtain relative position of the foot in a in-shoe system, specially when IMU is located in the arc of the foot. Many previous systems designed by works presented in chapter 1 use also an IMU but placing externally to the insole or shoe. The information provided by these sensors can be interesting to know the position of the foot during swing phase and specially the impact angle of the foot during toe-off and heel-strike gait stages.

The procedure for this experiment was quite straight forward. After placing the instrumented insoles and the passive markers (see figure 3.2) the experiment can start. It consisted in a total of 4 test walking at two different speeds (2 and 4 $^{km}/_{h}$) and running at also two different speeds (8 and 10 $^{km}/_{h}$) during 2 minutes per test. First and last 15 seconds are discarded. As it was explained the speed was controlled using the treadmill.

Test started from a stand up position to ease the synchronization between data from both systems. Once the recording is done, it is need to map the passive markers placed into the shoe to a 3D model. This is necessary for the sofware to be able to consider the foot as a unique element in space. Once the

angles are calculated, they are extracted into an spreadsheet. Data collected by t
frar
the

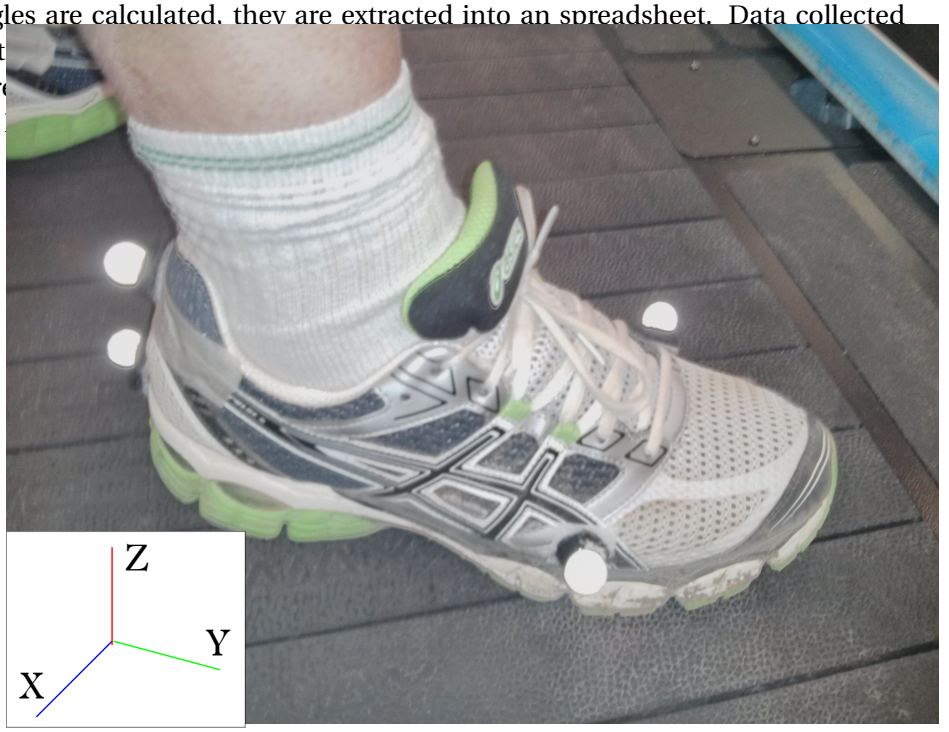

Figure 3.2: Passive markers placed on the shoe. The markers are located at 1st and 5th metatarsal heads, and in upper and lower calcaneus

It is very important to understand that to be able to compared the results obtained, it is necessary to map the angles of the video-cameras and ECnsole, due to the axis are not considered the same in both systems. To do this, the Z-axis both schemes is considered the same, however, the IMU is placed on the insole in such a way that the movement is in the same direction than Y-axis while in video cameras is in X-Axis, and vice versa. That means that the comparison between the roll angle of the insoles must be performed with the pitch angle of the video-cameras and the insoles's pitch with the roll in case of the video cameras. As Z-axis corresponds perfectly in both system, Yaw is just fine and it is possible to compared them directly.

3.2.2 Results

Euler angles are three angles to describe the orientation of a rigid body by using a combination of three rotations about different axes. For convenience,a multiple coordinate frames is used to describe the orientation of the sensor, figure 3.3 shows a normal reference frame and its Euler angles. Euler Angles are simple and intuitive and they lend themselves well to simple analysis and control. On the other hand, Euler Angles are limited by a phenomenon called "Gimbal Lock", that occurs when the orientation of the sensor cannot be uniquely represented using Euler Angles. The exact orientation at which gimbal lock occurs depends on the order of rotations used.

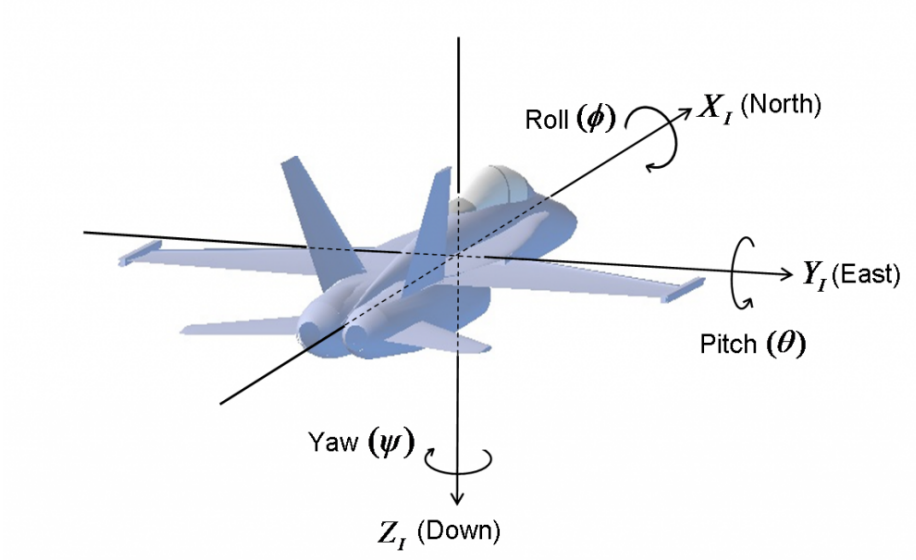

Figure 3.3: Inertial frame with the corresponding Euler angles[132].

Due to the complexity of the algorithm and filtering used to obtain the Euler angles, the algorithm requires of a while until the calculations reach an acceptable values. However, once it stabilises, results shown a very good agreement

with the data obtained by the video-camera. As it was explained, the Euler angle that corresponds to the natural movement of the foot during gait is the roll in case of the instrumented insoles, due that it is the rotation on the X-axis. Figure 3.4 shows the comparison between both systems for the different Euler angles measured in the test performed at $2^{km}/_{h}$, rest of velocities also produce a very accuracy agreements between the gold-standard and the ECnsole. Even in Yaw, that is supossed to be the angle with the least variation due to that in gait and running, rotations over the Z-axis are not as common as in X or Y-axis.

3.3 Preliminary test

After the validation of the pressure sensors and IMU of our instrumented insoles, tests were carried out in order to assess system comfort and usability. In trials, the instrumented insole was placed on top of and under the sports shoes' insole. It was concluded that the instrumented insole must be under the insole of the sports shoes for maximum comfort. It must be taken into account that the pressure was recorded under the shoe insole. Indeed, the measured pressure depends on the absorption of the sole of the shoes, however the accuracy and the time response of the system remained unchanged. The absorption coefficient of the used shoe insoles was 1.19, calculated as the ratio of the average pressure registered without and with shoe insole. This coefficient was also validated with the commercial system F-scan. Therefore, the pressure values have to be considered as dependent on the shoes used in the study. In addition, it was found that the foot slid less over the shoe insole than directly over the plastic cover of the instrumented insole. The instrumented insole does not significantly disturb locomotion patterns because the thickest area, the board with the accelerometer, is located under the foot arch; as a consequence, no modification of the shoes' insoles was required. For the case of participant with low or collapsed arches, the thickness of the shoe insole could be reduced in the arch to increase comfort. Nevertheless, one participant with collapsed arches did not feel any discomfort while using the instrumented insole under the shoe insoles.

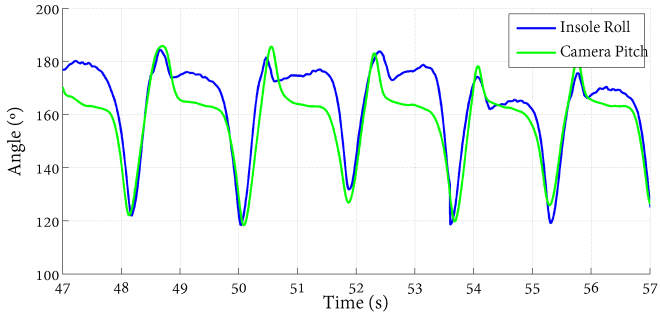

(a)

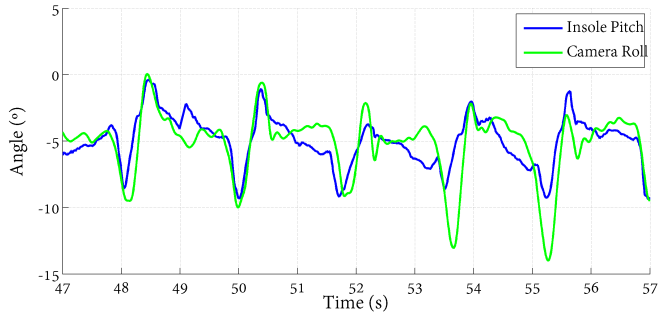

(b)

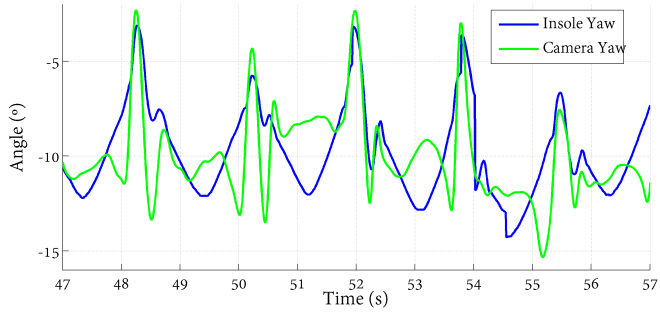

(c)

Figure 3.4: Comparison of Euler's angles between the ECnsole and the infrared video-camera.

The results from the experiment of participant 1 are plotted in figure 3.5a, where A_X, A_Y and A_Z represent the acceleration components. The major events in gait can be observed. The step starts with the heelstrike, during which acceleration in the direction of movement, A_Y, reduces to its minimum value, and pressure in the center of the heel starts to increase [4, 87, 130]. The maximum pressure value in the centre of the heel is recorded during the flat-foot stage, when the foot reaches horizontal and the fifth metatarsal touches the ground. At the beginning of the experiment, when the foot is totally resting on the ground, the acceleration components are constant, and the inclination of the accelerometer can be zeroed. Then, the mid-stage starts, and pressure decreases in the rear of the foot and increases in the front due to the mass centre movement of the subject. The mid stage phase ends when the foot acceleration changes, as the figure 3.5a shows. During the mid stage the pressure in the heel drops down to zero; and ends with the heel-off. The acceleration in Z-axis changes due to heel elevation movement, as figure 3.5a shows. During the heel-off the sensor at the fifth metatarsal reaches a maximum, and after falls to zero when the pressure in the big toe starts to increase. The contact of the foot with the ground, the stance phase, finishes with the big toe take off (toe-off). Finally, the foot advances through the air in the swing phase, or foot flight, until the next heel contact. During the swing phase, the foot inclination changes, and the point where A_Y is equal to zero can be considered the mid-swing.

The set of four pressure sensors could be enough to detect certain anomalous gait parameters. As an example, figure 3.5b shows the results of participant 2, who presented a slight claw foot. During the heel-off phase, the pressure increases in the first and fifth metatarsal, but when the first metatarsal makes contact with the ground, pressure in the big toe is reduced for a moment, and then increases once again at the end of contact with the ground. This fact is accentuated in subjects with a slight claw foot, such as participant 2. In addition, the maximum pressure in the heel is slightly reduced for a moment in participant 2, just when pressure increases at the fifth metatarsal, due to the claw foot. In both cases (figures 3.5a and 3.5b), the acceleration in the Y direction (direction of participant movement) is negative during landing due to the braking of the foot, and A_Y reaches values of up to -5 g, exceeding the linear range of the sensor ($\pm$3.6 g). This fact indicates that the accelerometer should

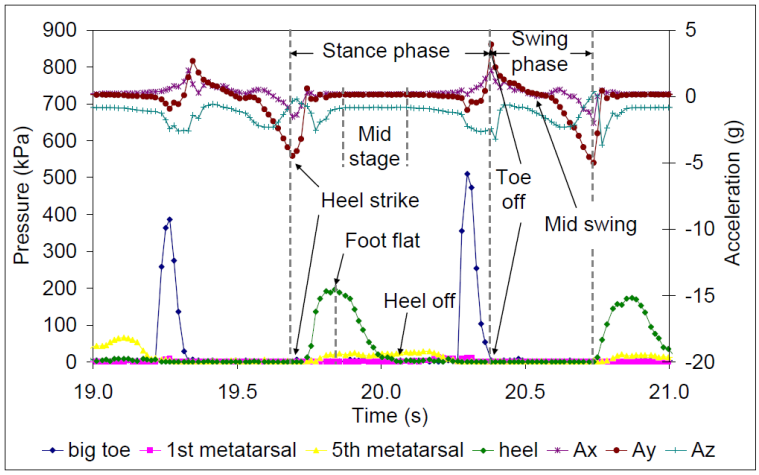

(a) Participant 1

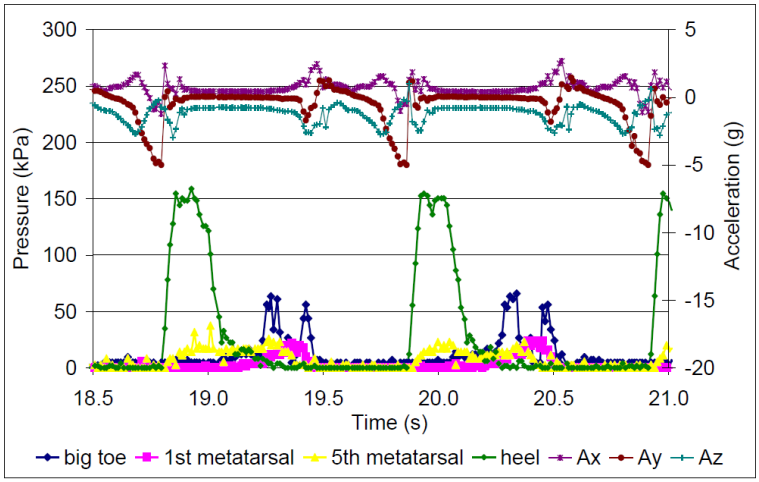

(b) Participant 2

Figure 3.5: Right plantar pressure and accelerations during walking: Participant 1 (figure 3.5a) Participant 2 (figure 3.5b).

be replaced by another with a higher range in this direction. Once the heel is on the ground, the time the Z acceleration component takes to reach a resting value will be longer in shoes with higher absorption. However, the minimum of A_Z component marks the exact moment when the heels impacts on the floor, as figure 3.5 shows. The maximum of pressure happens some milliseconds later than the minimum of A_Y due to the pressure sensor is placed in the center of the heel and not on the edge. Observing the X acceleration component at the moment of the impact (heel strike), the inclination of the foot can be estimated and then, we can know the orientation of the foot with respect to the rest position (when the foot is resting on the floor). If the A_X of participant 1 and 2 (figures 3.5a and 3.5b, respectively) is compared at the heel strike moment, we can see that the maximum for the participant 1 is higher than the participant 2. Finding the changes of A_X (ΔA_X) with respect to the rest positions, the figures 3.6a, 3.6b and 3.6c are obtained patient 1, 2 and 7. These patients were diagnosed as neutral, supinated and over-supinated foot, respectively, by previous biomechanical tests (see table 3.1). As it can be observed in figure 3.6, during the swing phase, the foot of over-supinator suffers more changes of ΔA_X than supinator or neutral foot.

The experimental data presented in figure 3.6, can be justified as follows: During the swing phase, the foot can move in the X direction (normal to advance direction) and this movement can be quantified by analysing the data provided by the accelerometer. The A_X increment can be found, zeroing the acceleration components in the rest time just before starting the test, when the participant is motionless. The temporal evolutions of the A_X increments are plotted in figure 3.6 for participants 1, 2 and 7, the latter diagnosed as a walker who supinates considerably (over-supinated foot, 3.1). The temporal average of the absolute value of A_X, $< |A_X(t)| >$, indicates how much the foot moves in the X direction, and this parameter was calculated over 60 seconds for each participant. In our study, supinator walkers show a higher value of $< |A_X| >$, as table 3.3 shows.

Once the participants are classified as pronator, supinator or neutral, the $< |\Delta A_X| >$ could provide the amount of pronation or supination. And in fact, the results of participant 7, who supinates his right foot considerably, exceed the rest of the participants. However, participant 6 moves his feet in the X-

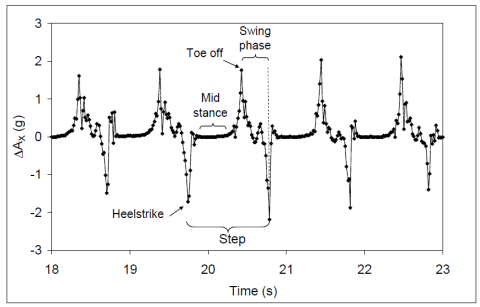

(a) Participant 1

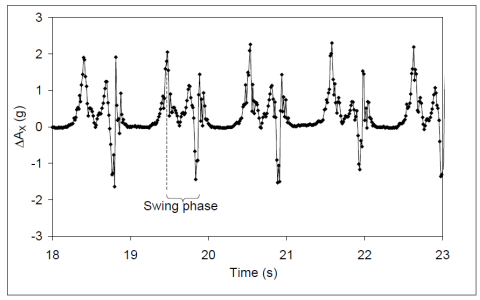

(b) Participant 2

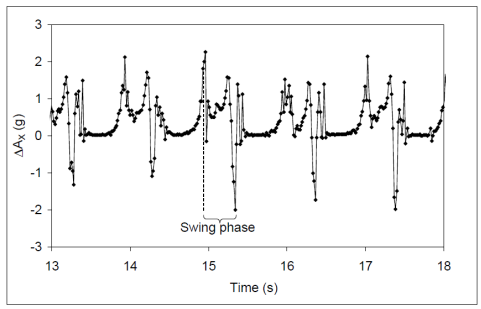

(c) Participant 7

Figure 3.6: ΔA_x of the right foot: Participant 1 (3.6a), Participant 2 (3.6b), and Participant 7 (3.6c).

Participant	$<\|\Delta A_X\|>$(g)			
	Right	Left	Average	Symmetry (%)
1	0.291	0.287	0.289	101
2	0.375	0.302	0.339	124
3	0.434	0.371	0.403	117
4	0.261	0.277	0.269	94
5	0.389	0.302	0.346	129
6	0.236	0.190	0.213	124
7	0.512	0.399	0.455	128
8	0.256	0.263	0.260	97
9	0.354	0.368	0.361	96
10	0.272	0.283	0.278	96

Table 3.3: $<|\Delta A_X|>$ of right and left feet of participants.

direction less than the other participants; therefore, this subject will lose less energy due to lateral movements during walking. The symmetry of the two feet has been calculated as the rate between the $<|\Delta A_X|>$ for the right and left feet. Significant asymmetries can be found in several participants due to muscular or bone imbalances.

The acceleration component in the direction of movement can also provide useful information for finding certain temporal gait parameters. As mentioned above (see figure 3.7), the gait cycle starts with the heelstrike, which involves a minimum in A_Y; and the cycle finishes with the toe-off with a maximum in A_Y. Therefore, the stance and swing times can be found from A_Y by finding the maxima and minima, as figure 3.7 shows. The stance time and time per step have been calculated over 60 seconds, and the average and the standard deviations are summarized in table 3.4.

The period of a step is practically equal for the different participants when they walked freely, and the averaged cadence is (0.92 ± 0.05) Hz, very similar for all the subjects. In addition, the ratio between the stance time and the

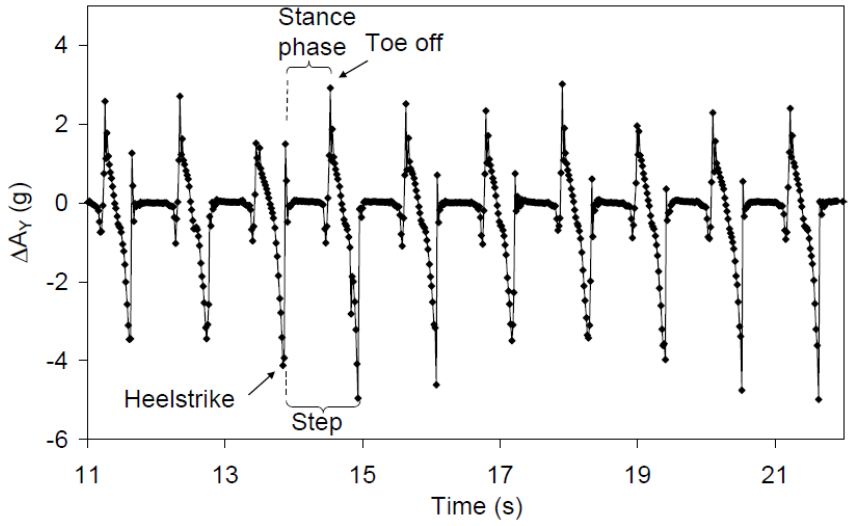

Figure 3.7: A_Y of the left foot of participant 4 over ten steps.

time per step (duty) has been calculated, resulting in around 2/3 for most of the participants walking freely without restrictions which is in agreement with the literature [133]. The mean stance time for the set of participants (global) is (0.727 ± 0.034) s.

	RIGHT FOOT							LEFT FOOT						
	Time per Step(s)		Stance Time(s)		Swing Time(s)		Duty(%)	Time per Step(s)		Stance Time(s)		Swing Time(s)		Duty(%)
	Mean	SD	Mean	SD	Mean	SD		Mean	SD	Mean	SD	Mean	SD	
1	1.030	0.009	0.685	0.017	0.346	0.011	66.4	1.030	0.011	0.675	0.016	0.356	0.015	65.5
2	1.058	0.028	0.712	0.017	0.346	0.022	67.3	1.056	0.023	0.706	0.016	0.350	0.014	66.8
3	1.048	0.027	0.717	0.018	0.331	0.020	68.4	1.050	0.013	0.716	0.016	0.334	0.008	68.2
4	1.097	0.015	0.745	0.014	0.352	0.006	67.9	1.114	0.040	0.716	0.029	0.397	0.025	64.3
5	1.086	0.010	0.712	0.012	0.373	0.014	65.6	1.085	0.022	0.701	0.019	0.385	0.015	64.5
6	1.117	0.017	0.758	0.015	0.359	0.016	67.8	1.112	0.018	0.742	0.008	0.369	0.019	66.8
7	1.023	0.013	0.686	0.014	0.337	0.011	67.1	1.025	0.012	0.679	0.019	0.347	0.014	66.2
8	1.201	0.020	0.791	0.019	0.410	0.017	65.9	1.201	0.030	0.835	0.020	0.366	0.015	69.5
9	1.052	0.016	0.713	0.013	0.339	0.013	67.8	1.053	0.016	0.723	0.011	0.330	0.008	68.7
10	1.113	0.021	0.754	0.012	0.359	0.019	67.7	1.097	0.022	0.710	0.014	0.387	0.013	64.7
Global	1.082	0.053	0.727	0.034	0.355	0.023	67.2	1.082	0.052	0.720	0.045	0.362	0.023	66.5

Table 3.4: Temporal parameters in gait test for the ten participants.

3.4 Conclusions

In this chapter, sensors included in our prototypes have been validated with gold standards. Pressure sensors have been compared with in-shoe commercial pressure sensor system while IMU has been compared to a infrared video camera system. Moreover, preliminary tests shown allow to conclude that the use of a instrumented insoles, in this case the ECnsole, with an IMU placed inside just in the arch of the foot, can provide a very useful information. A priori, it can help hugely from professionals to amateur runners, to adapt their running style or they shoes, according a diagnosis about supination or pronation during these activities. On the other hand, it can also help in medicine, to prevent injuries not only in the low trunk but also in the back, in those cases that the people have a gait disorder due to the supination or pronation.

The system presented in this work can simultaneously provide the pressure values for the big toe, first and fifth metatarsals, heel and the angular components in the three spatial axes including all the sensors in the instrumented insole. The data analysis can be carried out with a software program or with a standard spreadsheet. The software analysis shows the results in real time on the computer screen or in replay mode for experiment analysis. These display modes make immediate feedback possible, and therefore the subject gets immediate feedback on his or her pathology and can try to correct it at once. Moreover, the accelerometer readouts report additional information during both swing and stance time in walking tests. For instance, detection of anomalous pressure distribution, excess lateral movement, determination of stance time, and the detection of asymmetry could prevent future injuries or help a person choose the most suitable shoes. In this work, we have combined the analysis of the pressure and acceleration data to clearly distinguish among neutral, pronator or supinator participants, even estimating different amount of supination. This system could be very useful in studying walking patterns in people affected by illnesses such as Parkinsons, astronauts after a weightless period, rehabilitation from different injuries, or to choose the most appropriate shoes.

Part I

Sports and physical activity experiments

Chapter 4

Height measurements in vertical jumps

Contents

4.1 Introduction 152
4.2 Test Definition 154
4.2.1 Participants 154
4.2.2 Hardware equipment 154
4.2.3 Procedure 156
4.2.4 Experimental setup and data collection 158
4.2.5 Statistical Analysis 160
4.3 Results 160
4.4 Discussion 162
4.5 Limitations 166
4.6 Conclusions 166

4.1 Introduction

The vertical jump is an essential skill contributing to higher performance in many different sports such as basketball[134], volleyball[135], and football[136], and it is frequently used as an objective functional measurement[137]. As many studies have previously described, flight time and jump height provide useful information to estimate anaerobic power and capacity[138]. The height of a vertical jump, especially the countermovement jump (CMJ), is commonly used in performance evaluation to diagnose lower body power.

There are different types of laboratory tests that collect and analyse lower body power by means of kinematics and kinetics. In most kinetic studies, a force platform is used to calculate vertical ground reaction forces and flight time during a vertical jump[139]. Studying plantar forces or plantar pressure can also be useful in measuring vertical jump and flight times[71]. Nowadays, there are several in-shoe systems used mainly to monitor plantar pressure distribution while walking or running, both in research[140, 141] and as commercial devices such as the F-Scan measurement system (TekScan, Boston, USA), the Novel Pedar System (Novel, USA), and the Biofoot (Universidad Politécnica de Valencia, Spain)[71, 139]. Another way to measure flight time by using kinematic systems such as laser beams together with a contact mat[142, 143], photosensitive cells[144, 145, 143], high-speed camera systems[146], and optical timing[147]. Numerous researchers have used platform forces to estimate the height of the vertical jump, proving it to be a valid and reliable system; therefore, platform forces are a widely used gold standard to validate other measurement systems[137]. Although less common, kinematic methods have also been used to determine the concurrent validity of flight time and the double integration of vertical reaction force methods in the estimation of vertical jump height with the video method as a reference using sophisticated high-speed cameras and video analysis software[148, 149]. In accordance with other studies, using 2D-3D photogrammetry[71, 150, 146] and photocell mats[144], we considered the high-speed motion capture system (HSC) and a laser platform (SJS) to be the method of reference for the estimation of vertical jump height, despite the fact that force platforms are the most commonly used method. Furthermore, kinematic methods provide kinematic variables to assess whether the jump test

has been properly executed.

In the last few years, new systems based on accelerometers and inertial measurement units [151, 152, 149] have appeared. Other studies use the accelerometer on smartphones[153] to measure flight time and jump height. All these units are usually placed on the hip or back of the athlete, which makes it difficult to determine when the flight time starts in some types of jumps.

Currently, there are not many systems that can use data from force sensors together with data from kinetic systems such as accelerometers and inertial measurement units located in the foot. Previous kinetic studies have provided very useful information in gait analysis, especially in swing phases[154, 112]. Other authors have combined force sensors with an accelerometer[106] or an inertial measurement unit[72], which includes an accelerometer, gyroscope, and magnetometer. Additionally, a recent study has presented a plantar pressure insole based on 64 optical sensors, introducing the design and development of a pressure-sensitive foot insole for monitoring plantar pressure distribution during walking[114, 115]. The combination of force sensors and accelerometer or inertial measurement units makes it possible to obtain information during the entire jump. Unlike force sensors, which report information only during the landing and stance phases, inertial measurement units and accelerometers report data during the flight and swing phase. Providing this kind of information can also be very useful to improve jump technique.

As an alternative, our flight-time measurement system is based on instrumented insoles using the readout data from an accelerometer, as well as force pressure sensors specifically located to determine the flight time in vertical jumps wirelessly. This system, termed ECnsole[129], includes 4 pressure sensors (PreECnsole) and one accelerometer (AccECnsole) and sends the information from the sensors via radiofrequency to a transceiver for computer analysis. These in-shoe systems can provide a lot of useful information to the scientific, medical, and sports communities and allow patients or athletes to perform stress tests of vertical jumps outside the laboratory.

Therefore, the aim of this study has been to validate the ECnsole system by comparing the data registered by the ECnsole system with a high-speed motion capture system (HSC) and a sport jump system (SJS) as reference methods. We hypothesized that there would not be a significant difference between the

height of a vertical jump calculated by the ECnsole system vs. the HSC and SJS.

4.2 Test Definition

4.2.1 Participants

A total of 61 participants (44 male and 17 female) volunteered for this study (age: 20.4 ± 2.9 years, height: 173 ± 8.1 cm, and weight: 69.4 ± 11.1 kg). The participants were physical education students at the University of Cadiz (Spain). All of them were physically active as they did more than 3 exercise sessions per week, but none of them performed exercise at an elite level. Written informed consent was obtained from all participants before starting the study and the protocol was approved by the University Ethics Committee and met the requirements of the Declaration of Helsinki and the ethical standards in sports and exercise science research[155].

4.2.2 Hardware equipment

ECnsole

For this experimental, the version 1.5 of ECnsole was used(see figure 2.34). Sampling frequency of the insoles were fixed at 100 Hz. Figure 4.1 presents one of the participant carrying out the jumps during this test. It is possible to observe, that ECnsole datalogger unit is placed at the lower back. It is important to remember that this insole versions contains 4 force sensors and a IMU, located at the arch of the foot.

Laser Platform

The SportJump system (SJS) (DSD, Inc., León, Spain) is a photocell mat with a photoelectric circuit based on laser beams. It consists of 2 parallel bars, one laser transmitter module with 32 laser lights longitudinally placed 3 cm apart, and one photosensitive receiver module, with 32 laser receivers placed in front of the laser lights. It has a temporal resolution of 0.001 s. This hardware is

connected to a laptop where an adaptation of the SportJump-v1.0 software[142] was installed (SportJump-v2.0; DSD Inc).

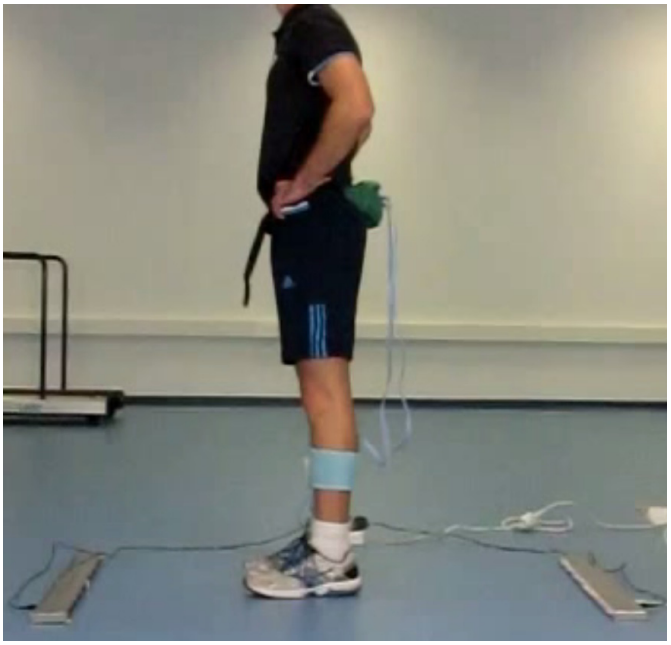

Figure 4.1: Participant in heigh jump measurement test.

High-speed motion capture system

The High-speed captured system (HSC) used was a Casio Exilim EX-ZR1000 camera (Casio Computer Co., Ltd., Tokyo, Japan), equipped with a 24-mm wide-angle lens and a 12.5x optical zoom. The digital camera was mounted on a rigid tripod (Velbon, Maidenhead, United Kingdom) 60 cm above the ground and 6 m away from the participant. The camera recordings were analysedusing the open license Kinovea software (Kinovea 0.8.15 for Windows). The movement space was calibrated with a 2 x 2 m^2 wooden frame placed along the midline of the jumping movement. The film was made from the sagittal plane in order to

more clearly see the moment of take-off and the test execution. A camera position focusing on the participant's foot would have allowed greater accuracy in measurements of flight time, but would not have allowed control of the proper execution of the test (SJ, CMJ, and ABK).

4.2.3 Procedure

The experiment consisted of 2 sessions separated by a week. In order to evaluate the validity of the ECnsole system, each participant performed 3 different jump tests: Squat Jump (SJ), CMJ, and ABK. The heights reached by the participants in each of the jumps were assessed simultaneously using the systems described above. These tests were performed according to the protocol proposed by Bosco et al. (1983)[156]. The test is composed of 3 different types of jumps. In the squat jump, the participant stands with the knees bent at an angle of approximately 90°, hands on the hips and the trunk erect(see figure). The participant then jumps vertically as high as possible, and lands with the knees still extended at an angle of 180°. In the countermovement jump, the participant stands erect with a knee angle of 180°with hands on the hips. A countermovement is performed until the knee angle reaches approximately 90 °and immediately he or she jumps vertically as high as possible, landing with the knees still extended at an angle of 180 °. In the Abalakov jump, the participant stands upright, as still as possible on the mat with his or her weight evenly distributed over both feet. When ready, the participant squats down until the knees are bent at 90°whilst swinging the arms back behind the body. Without pausing, the arms are swung forward and the participant jumps as high as possible, landing back on the mat on both feet at the same time[157].

During the first session, participants received comprehensive instructions and learned the proper technique for each jump test. In the second session, all participants completed 15 min of warm-up exercises, directed by one of the researchers, consisting of jogging and practising the jump tests. After the warm-up, one of the researchers placed the ECnsole into the participant's shoes and placed the data logger around the participant's waist using a belt. For the jump tests, the participants stood between the SJS bars in a test area of 95 x 93 cm. Measurements began when the participant left the ground and ended when the

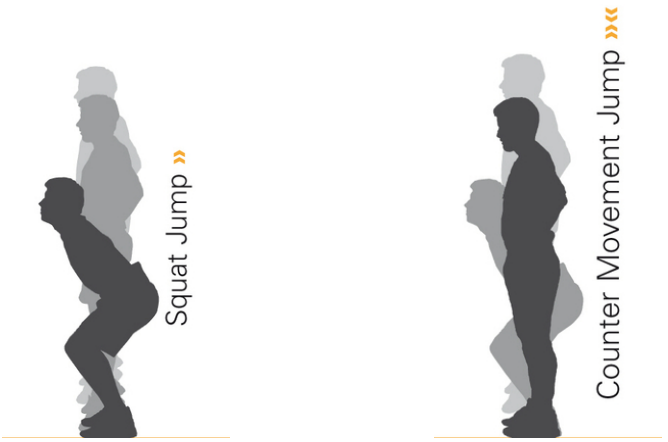

(a) Squat Jump (b) Countermovement Jump

Figure 4.2: Squat Jump and Countermovement Jump process(Front and sideway view). SJ start in a 90°bending position with both hands on the hips while CMJ starts in an standing up position to bend as in SJ just before jumping execution[158].

participant landed and made contact with the laser beam. At the same time, jumps were recorded using the HSC, operating at 240 Hz and 1.25 ms shutter speed. For measuring the height of a vertical jump through cinematic techniques, the take-off and landing positions must be equal. Since the angles of the ankles, knees, and hips during take-off may be more extended than in the landing[159, 160], the videos were viewed and then those whose positions at take-off and landing were not equal were discarded to respect the protocols.

All testing sessions for each participant were administered on the same day under the same environmental conditions. In order to ensure all participants were warmed up and to avoid risk of injury, participants were called in at different times in groups of 5, with an interval of 20 min between groups. All the participants performed the tests twice in the same order (SJ, CMJ, and ABK), and if the jump was not performed properly, it was repeated. Once all tests were performed, the jumps were viewed and analysed using HSC, with incor-

rect jumps being discarded together with the information provided by SJS and ECnsole (PreECnsole and AccECnsole). 66 participants took part in the experiment, but 5 were discarded after watching the videos, so in all 61 were analysed, with a total of 366 jumps.

4.2.4 Experimental setup and data collection

The following information was gathered from the jumps with the different systems:

- The SportJump System Pro software provides jump heights and flight times directly.
- Using kinematic techniques, the HSC and Kinovea video processing software can measure the flight time as well as the jump height[161]. Once all the jumps performed by each participant had finished, a reference frame was placed in order to accurately measure the jump height during video processing. The instant of take-off was defined as the first clear frame in which the participant's feet were observed to break contact with the ground, and the instant of landing was defined as the first clear frame in which the participant's feet were observed to contact the ground. Flight time was calculated by the number of frames in which the participant's feet were not touching the ground.
- The flight time can be obtained by ECnsoles in 2 different ways: using pressure data from force sensors and using z-axis acceleration data from the accelerometer sensor (Fig. 3). To measure the jump flight time with the force sensors, we quantified the time elapsed from the instant in which the last sensor of the insole detected a signal of zero, normally the sensor situated at the big toe, until the moment in which one of the pressure sensors begins providing a measurement again, normally the same sensor. The minimum value to establish whether the pressure sensor is active or not was fixed at 1.5 N or 20 kPa. In the case of z-axis acceleration, we consider the beginning of the jump as the first maximum and the lowest minimum after the peak as the end of the jump (when the participant is

in the air), as figure 4.3 shows. Once the flight time is obtained, the jump height can be found using the formula described in the literature[156]:

$$h = g \cdot \frac{t_f^2}{8} \tag{4.1}$$

where h is the height of the jump, g is the gravity acceleration $^{m}/_{s^2}$ (value g in Cadiz, Spain), and t_f is the flight time in seconds.

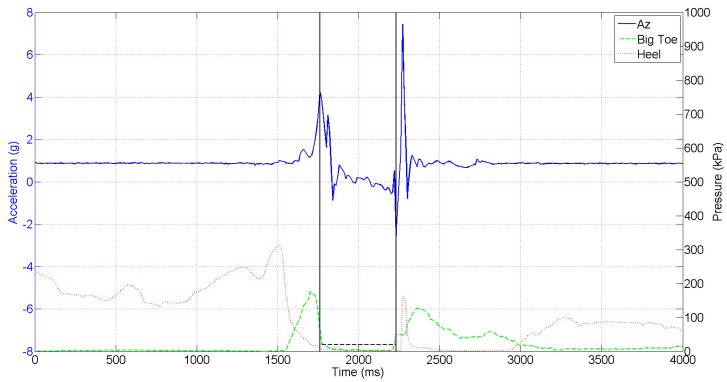

Figure 4.3: Vertical coordinate of the accelerometer response (top line) and big toe and heel pressure data (dashed line and dotted line, respectively) of our system vs. time for a squat jump. Note: The figure shows vertical acceleration and pressure data from our instrumented insole corresponding with the typical time transient of a squat jump[151, 149]. With the z-Axis coordinate of the accelerometer, we measure the time between the first maximum and the lowest minimum after the peak as the end of the jump. In this figure, we have marked with vertical solid lines the 2 coinciding flight stage limits, shown by the sign produced by the accelerometer as well as by the pressure sensor, providing a more robust and reliable method to measure this magnitude by double checking.

4.2.5 Statistical Analysis

Mean and Standard Deviation (SD) with 95% Confidence Interval (CI) were calculated for all variables. One-way analysis of variance (ANOVA) with the Bonferroni correction was used to compare the results among devices. Simple linear regression was used to examine the association between laser platform, pressure sensor, and accelerometer measurements with video analysis. In addition, systematic bias ± Random Error (re) was calculated using the Bland-Altman method[162]. Statistical power was calculated using $G*Power3$[163] and it was 1 for all the simple linear regression models (effect size ranged from 0.979 to 0.994). All the analyses were performed using the R software Statistical Package for Social Sciences[164]. For all analyses, the level of significance was set at $P < 0.05$.

4.3 Results

No significant systematic bias was observed between SJS, PreECnsole, or AccECnsole and HSC results (P > 0.05). Regardless of the jump test performed, all the systems show a systematic bias close to 0 and a low random error (see table 4.1). PreECnsole shows the lowest systematic bias when compared with HSC and SJS in the CMJ test (0.0 ± 2.3 cm and - 0.1 ± 2.3 cm respectively), whereas AccECnsole gives the lowest systematic bias with HSC in the ABK test (0.0 ± 3.2 cm) and with SJS in the SJ and ABK (0.1 ± 2.7 cm and 0.1 ± 2.8 respectively). Both PreECnsole and AccECnsole show similar random errors regardless of the criteria measured (range: 2.3-3.2 cm for PreECnsole and 2.7-3.4 cm for AccECnsole). PreECnsole and AccECnsole also show a similar high association with video analysis and the laser platform. PreECnsole has a slightly higher association with the criteria measured (R^2 = 0.967, 0.978 with HSC and SJS respectively; all P < 0.001) than the AccECnsole (R^2 = 0.958, 0.966 with HSC and SJS respectively; all P < 0.001) (see table 4.2 and figure 4.4).

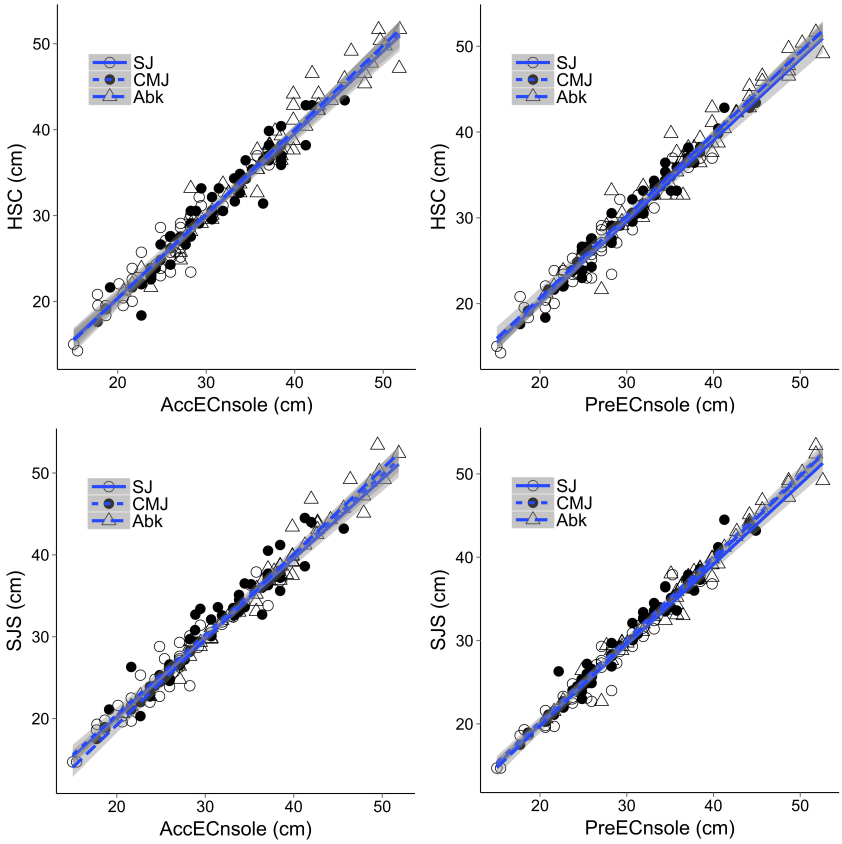

Figure 4.4: Scatter plots between HSC and SJS vs.PreECnsole and AccECnsole results. Data points represent individual jump height values for the squat jump (SJ), countermovement jump (CMJ), and Abalakov jump (ABK). 3 different regression lines have been added to fit the values of each type of jump.

	SJ (cm)	CMJ (cm)	ABK (cm)
HSC			
Mean ± SD	26.8 ± 5.9	31.0 ± 6.6	37.1 ± 8.0
(95% CI)	(25.3-28.3)	(29.2-32.8)	(34.9-39.3)
SJS			
Mean ± SD	26.6 ± 5.9	31.1 ± 6.7	37.0 ± 8.2
(95% CI)	(25.1-28.2)	(29.3-33.0)	(34.8-39.3)
Pressure sensor			
Mean ± SD	27.0 ± 6.0	31.0 ± 6.7	37.3 ± 8.1
(95% CI)	(25.4-28.6)	(29.2-32.9)	(35.1-39.5)
Bias ± re (vs. HSC)	0.2 ± 2.9	0.0 ± 2.3	0.2 ± 3.2
Bias ± re (vs. SJS)	0.4 ± 2.3	-0.1 ± 2.3	0.3 ± 2.5
Accelerometer			
Mean ± SD	26.7 ± 5.9	30.8 ± 6.6	37.1 ± 7.7
(95% CI)	(25.1-28.2)	(29.3-32.9)	(35.0-39.2)
Bias ± re (vs. HSC)	-0.1 ± 3.0	-0.2 ± 3.2	0.0 ± 3.2
Bias ± re (vs. SJS)	0.1 ± 2.7	-0.3 ± 3.4	0.1 ± 2.8

Table 4.1: Descriptive data from the variables of the study for every vertical jump type. Average jump height ± SD. Squat Jump (SJ), Countermovement Jump (CMJ), Abalakov Jump (ABK), High-speed captured system (HSC) and SportJump system (SJS)

4.4 Discussion

This study was designed to analyse the validity of the ECnsole system to calculate the height in a vertical jump with the HSC and SJS as reference methods. The results indicate a high association between the 2 systems, with the ECnsole system showing a systematic bias close to 0 regardless of the jump test performed. The main purpose for conducting this study was to determine whether the measurements of vertical jump height from different devices could be compared. The results indicate that PreECnsole and AccECnsole provide a

Devices	β	**SE**	R^2	**P**
Criterion Measure: HSC				
Pressure sensor	0.983	0.014	0.957	<0.001
Accelerometer	0.979	0.016	0.958	<0.001
Criterion Measure: SJS				
Pressure sensor	0.989	0.011	0.978	<0.001
Accelerometer	0.983	0.015	0.966	<0.001

Table 4.2: Standardized regression coefficients (β), standard error (SE) and coefficients of determination (R^2) examining the association between pressure sensor and accelerometer measures with video analysis (HSC) and the laser platform (SJS).

very high correlation with the HSC and SJS reference systems. PreECnsole and AccECnsole measure flight times and vertical jump heights, so it was expected that this study would find a high correlation between the measurements with each device.

Similar studies on the validity of alternative systems for measuring vertical jump heights used similar protocols, recording the 3 systems simultaneously for each jump[151, 146]. The study performed by Balsalobre-Fernandez[153] analyses the reliability of the HSC-Kinovea method for measuring the flight time and height of vertical jumps. That study shows a high correlation (ICC = 0.997, $p < 0.0001$) between the observers' measurements of flight time and jump height using the HSC-Kinovea method and those obtained using an infrared platform. As in this study, the HSC was recording at 240 Hz. In addition, in our experiment we also consider video analysis with a high-speed camera to be the reference method for the calculation of vertical jump height[165, 146, 166]. Other studies that have compared SJS with a force plate as a gold standard[144] have obtained a high correlation with the force plate ($R^2 = 0.994$).

In our research, PreECnsole shows a high degree of agreement with the HSC reference method (with a systematic bias between 0.2 cm (SJ), 0 cm (CMJ), and

0.2 cm (ABKJ)), differing systematically by a random error of ≤ 3.2. PreECnsole also shows a high degree of agreement with SJS (with a systematic bias between 0.4 cm (SJ), and 0.3 cm (ABK)), differing systematically by a random error of ≤ 2.5. The PreECnsole gives the lowest jump height bias values in the CMJ test, and this method shows a high degree of agreement with the reference method SJS, slightly underestimating the systematic bias by - 0.1 cm. With respect to the AccECnsole vs. HSC, we observe lower bias values in the 2 jumps (SJ/CMJ), slightly underestimating with a systematic bias of - 0.1 cm and - 0.2 cm respectively and the same value zero in ABK. However, the random error of ≤ 3.2 was higher than with the HSC. In the case of the AccECnsole vs. SJS, we observe higher bias values in the 2 jumps (SJ/ABK) with a systematic bias of 0.1 cm in both jumps and of - 0.3 cm in ABK. However, the random error of ≤ 3.4 is higher than with the SJS (4.1).

We note a high degree of association between the HSC and the SJS. The value obtained between the video analysis and AccECnsole is slightly lower (R^2 = 0.958) than with the SJS (R^2 = 0.966). In the case of the pressure sensor (PreECnsole), there is a higher degree of association (R^2 = 0.978) with SJS and slightly lower (R^2 = 0.967) with HSC. Similar values were also found by another author who compared video analysis vs. platform forces (R2 = 0.988) and video analysis vs. a contact mat (R^2 = 0.979)[148]. The study by Asdís, Baldur, and Brynjar (2014) compared video analysis vs. an accelerometer device (KineJump) and also found a high correlation (r = 0.85), although in that case the device was placed on the waist, not in the insole. Other studies found that the accelerometer is a reliable device at frequencies as low as 50 Hz, with the best results at 250 Hz; therefore, 250 Hz is considered an acceptable sampling frequency when testing with accelerometers. Additionally, the accelerometer overestimates some variables, perhaps due to the inclusion of bodyweight in the calculations[135]. In our study, no overestimation or underestimation of the result of the vertical jump occurred with any of the 3 measuring instruments vs. the video analysis. ECnsole is sampled with a frequency of 100 Hz. This frequency might seem low, but the correlation is high, as reflected in the scatter plot and regression lines between HSC and SJS vs. PreECnsole and AccECnsole (figure 4.4).

In all methods, based on flight time, the vertical displacement of the centre

of mass can be calculated using a uniform acceleration equation, but it is very important that the position of the centre of mass be the same at the beginning (take-off) and end (landing) of the jump (Moir 2008)[139].

The differences between the 4 measuring systems seem to be determined by the sensitivity of each of the systems used (HSC 4 ms, SJS 1 ms, ECnsole 10 ms) and the location of each of the sensors in the ECnsole, but not by the jumping technique of each participant, despite which the jumps performed incorrectly were eliminated. As well, Moir[139] and Kibele[160] suggest that differences in the high jump may be linked to changes in the participant's posture between take-off and landing. Consequently, the jumper's centre of mass at take-off should be the same as at landing[148]. Therefore, the flight time during the ascending phase must be equal to the flight time during the descent period[165]. Other methods to measure flight times and jump heights involve placing infrared beams parallel to the floor and connected to a timer[143] or using photogrammetry in 2D and 3D[150]. The main problems of this method concern the positions during take-off and landing in a jump, which are not usually the same because the angles of the ankles, knees, and hips may be more extended during take-off than in landing[159, 160]. However, Hatze (1998) recognizes the usefulness of these methods for the assessment of vertical jump height in most biomechanics laboratories[159].

In this work, 4 systems were used simultaneously, so it is irrelevant whether the participant had good or bad technique since the ultimate goal is to compare the variation in the extent of flight time, determined by each of the instruments, and not assess whether the measurement of jump height by flight time is a valid method to calculate the height of the centre of mass. However, to obtain different measurements of flight time and to use already standardized and validated protocols, we opted to do 3 different jump tests (SJ, CMJ, and ABK). Therefore, the variations in the range of the measured data is due to the different techniques required to perform each kind of jump. In SJ we only obtain the capability of the participants to produce concentric force in the lower body, in CMJ we add the capability to produce elastic energy, and finally, in ABK we combine concentric and elastic force by using the arms to obtain a higher jump. Therefore, we have obtained a great variability in jump height, providing excellent validation of ECnsole as a high jump measurement device, regardless

of the height obtained.

This study shows the validity of a new instrument, called ECnsole, as a measurement tool to quantify, among other variables, flight time during vertical jump performance. The advantages of ECnsole with respect to laser platform, video-based methods, and even force platforms are that it does not require a subsequent display of images to measure jump heights, it does not limit the jump of the athletes, it is easy to transport (especially compared to heavy platforms), and finally, it does not need electric power outlets nearby to function and does not require a fixed installation laboratory.

4.5 Limitations

Participant characteristics were a limitation to this study. Participants were university students, so the variability in vertical jump height might also have been limited, although they performed 3 different jump tests. Having participants with a greater variation in age would provide a wider range of vertical height measurements. Future research with a larger number of participants with a greater age range would provide a better comparison of ECnsole and the reference camera system to further determine the reliability of measurement results.

4.6 Conclusions

After analysing and comparing the data obtained with ECnsole, the HSC, and the SJS, we conclude that the PreECnsole data has a higher concurrent validity, although both systems (PreECnsole and AccECnsole) have a high validity for measuring the flight time of a vertical jump. However, considering that measuring the vertical jump height, in most cases, should be done in a practical and objective manner in the field of sports, in which the athlete does not perform the jump within the limitations of a platform, it would be more useful to use ECnsole, taking into account that both have high validity. Therefore, ECnsole may be the more viable option as it imposes fewer restrictions.

Chapter 5

Influence of fatigue on gymnasts in vertical jump performance

Contents

5.1 Introduction 168
5.2 Test Definition 169
5.2.1 Participants 169
5.2.2 Hardware equipment 169
5.2.3 Procedure 169
5.3 Results 171
5.4 Conclusions 174

5.1 Introduction

Most of the disciplines related to gymnastics perform training sessions in different surfaces. This change of surface during exercise practising may affect to the sport performance [167, 168] by increasing muscular fatigue. Basic types of jumps defined by Bosco protocol[156] imply several components of jumping technique, since muscular component, to elastic or coordinative component. The majority of studies related to muscular fatigue in jumping performance are based on plyometrics studies and trainings[169, 170, 171, 172].

Several experiments of how fatigue influences in training have been realised. *Burt et al.* carried out a study to prevent injuries in a group of pre-pubertal female artistic gymnastics by performing several exercises in different surfaces and using different loads[168]. Similar studies have been done but applying just to specifically jump techniques like DJ[173]. Other works claim that also rest length can also influence on the jump performance[174].

As far as it is reported in the literature, there are not too many works related to study of the ground reaction forces or about plantar pressure distribution changes after the training in some surfaces o after any sport fatigue. *Seegmiller et al.* studied the ground reaction forces in drop landing[175] while group of *Mills et al.* concluded that a reduction of the ground reaction forces might produced an increasing in internal loading[176]. On the other hand, there are not detailed studies that analyse how the plantar pressure distribution is modified after a general training or how the training in a concrete surface can alter the plantar pressure pattern.

Therefore, the aim of this study, is to analyse not only the plantar pressure distribution but also some standard parameters related to high jump performance before and after the practice of a stablish training protocol carried out in the surface of the gymnastics discipline of tumbling by using instrumented insoles.

5.2 Test Definition

5.2.1 Participants

A set of 12 volunteers participated in this study, all of them males (age: 20.75 ± 3.93 years, height: 169.70 ± 6.70 cm, weight: 65.14 ± 7.16 kg, and IMC: 22.41 ± 2.52 $^{kg}/_{m^2}$). All of them were acrobatic and sport gymnast of Acróbatos Gymnastic Club at different levels (from amateur to elite level). They are physically active due to their training sessions that are usually four times a week. Written informed consent was obtained from all participants before starting the study and the protocol was approved by the University Ethics Committee and met the requirements of the Declaration of Helsinki and the ethical standards in sports and exercise science research[155].

5.2.2 Hardware equipment

For this study, version 1.5 of ECnsole was used. In order to have redundant information also the laser platform described in chapter 4 was used. All the jumps performed during experimental session were done in a concrete surface, while for DJ typical gymnastic equipment was used to obtain proper high. However, the training protocol was performed into the tumbling surface. Tumbling is an acrobatic sporting discipline. Tumbling surface is a type of "floor", which is 25 metres long by 2 metre wide track consisting of fibreglass rods under two layers of foam mats (see figure 5.1). The instrumented insoles are already validated to measure vertical high jumps as it was explained in chapter 4.

5.2.3 Procedure

At the beginning of the experiment participants received comprehensive instructions and learned the proper technique for each jump test. In the second session, all participants completed 10 minutes of warm-up exercises, directed by one of the researchers, consisting of jogging and practising the jump tests. After completing the warm-up, the participants wear a sport shoes that included the ECnsole. The research group provided the sports shoes in order to avoid any modifications due to the footwear used.

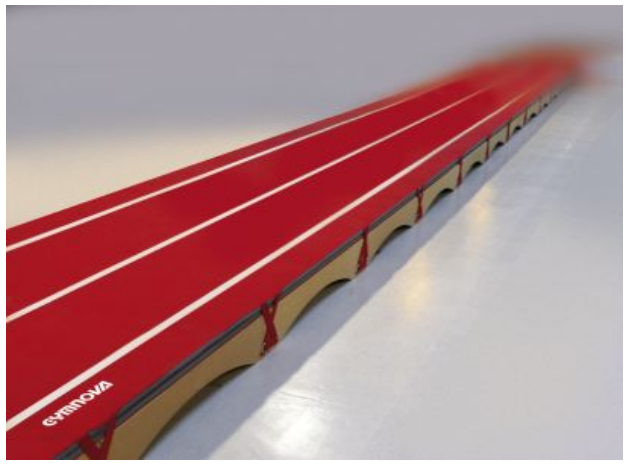

Figure 5.1: Novatrack One tumbling track[177].

The experiment consist in 3 experimental sessions per participant. In each session, gymnast must perform 5 types of jumps: SJ, CMJ, and ABK, which were described in chapter 4, and as a novelty, DJ and RJ. DJ consist in sinking from a platform elevated 60 cm from the floor, and once the floor is reached jump energetically and finally absorb the reception. Figure 5.2 shows the technique of this type of jump. RJ is basically same proceeding that CMJ but repeating as many jumps as possible during 15 seconds.

The different experimental sessions in which the whole study is divided are:

PreTest: After the warm-up, the participant starts doing the five jumps already described in this work. Every jump is repeated three times except the RJ. When this session is finished, a training protocol designed to produce fatigue in the low body trunk stars. The training consist in 12 series of 6 forward tucked somersault, with 10 seconds between somersaults and 2 minutes between series. This protocol is done in a tumbling surface.

PostTest: Immediately after the training protocol is done. The gymnasts repeat the same 5 types of jumps that in PreTest. Once they finish all the jumps, they rest for 15 minutes.

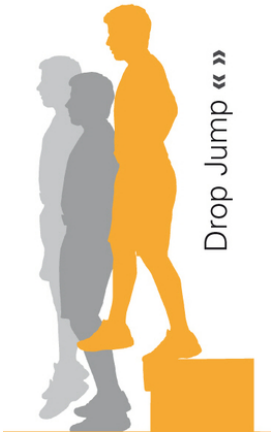

Figure 5.2: Drop Jump Process. The height of the elevated platform was 60 cm from the floor[158].

ReTest: This sessions corresponds to the last replay of the jumps after the resting time of 15 minutes.

5.3 Results

Several variables were analysed during this experiment. Using the ECnsole, calculations of the pressure at jumping, pressure at landing, accelerometer values also at jumping and landing, and the flight time (that is directly proportional to the height jump) are obtained.

Table 5.1 presents a multivariate analysis of the variables for every type of jump comparing the three sessions where the jumps were performed.
From the results obtained, only flight time in DJ, pressure at jumping instant in CMJ, ABK, and RJ, and the pressure at landing instant in DJ were taken into account. Next, a pairwise comparison is done by a Repeated Measures ANOVA. Some others are close to the significant limit of the P value like for instance, the flight time in the RJ, the pressure at landing of ABK, and the accelerometer

	SJ	**CMJ**	**ABK**	**DJ**	**RJ**
Flight time (ms)	0.151	0.101	0.709	**0.030**	0.099
Pressure at jumping (kPa)	0.203	**0.013**	**0.001**	0.264	**0.008**
Pressure at landing (kPa)	0.404	0.452	0.062	**0.019**	0.365
Accelerometer at jumping (g)	0.579	0.264	0.863	0.379	0.797
Accelerometer at landing (g)	0.166	0.290	0.375	0.165	0.074

Table 5.1: Multivariate analysis of the jumps performed. Significant P value at 95%.

value at landing in the case of RJ, considering in that case P value significant at 90%. Therefore, a pairwise comparison of those significant variable is studied.

Table 5.2 presents the data for the pressure at jumping for the CMJ. There is a difference between the value of the pressure at jumping instance between the PreTest and ReTest, being the first one higher than in Retest by 1.111. That can be understood as an influence of the fatigue in the elastic component of the low trunk. However there are no differences between PreTest and PostTest, neither between PostTest and ReTest.

	PreTest		**PostTest**		**ReTest**	
	Mean Diff.	P value	Mean Diff.	P value	Mean Diff.	P value
PreTest	-	-	0.418	1.000	1.111	**0.008**
PostTest	-0.418	1.000	-	-	0.693	0.637
ReTest	-1.111	**0.008**	-0.693	0.637	-	-

Table 5.2: Repeated Measures ANOVA of pressure at jumping instant in CMJ. Mean difference and P value. Mean difference value is in kPa. Significant P value is at 95%.

In the case of ABK variable, there is just a significant difference between the PreTest and ReTest (P value of 0.006) where the pressure at the jumping instant is slightly lower in ReTest than in PreTest. That means that there is an influence

of the fatigue in the coordinative component of the jump performance.

	PreTest		**PostTest**		**ReTest**	
	Mean Diff.	P value	Mean Diff.	P value	Mean Diff.	P value
PreTest	-	-	0.552	0.684	1.117	**0.006**
PostTest	-0.552	0.684	-	-	0.566	0.137
ReTest	-1.117	**0.006**	-0.566	0.137	-	-

Table 5.3: Repeated Measures ANOVA of pressure at jumping instant in ABK. Mean difference and P value. Mean difference value is in kPa. Significant P value is at 95%.

	Flight time					
	PreTest		**PostTest**		**ReTest**	
	Mean Diff.	P value	Mean Diff.	P value	Mean Diff.	P value
PreTest	-	-	-8.944	0.966	4.389	0.786
PostTest	8.944	0.966	-	-	13.333	0.162
ReTest	-4.389	0.786	-13.333	0.162	-	-
	Pressure at landing					
	PreTest		**PostTest**		**ReTest**	
	Mean Diff.	P value	Mean Diff.	P value	Mean Diff.	P value
PreTest	-	-	-0.408	1.000	1.085	0.267
PostTest	0.408	1.000	-	-	1.493	0.080
ReTest	-1.085	0.267	-1.493	0.080	-	-

Table 5.4: Repeated Measures ANOVA of significant variables in DJ. Mean difference and P value. Mean difference value is in ms for the flight time and in kPa for Pressure at landing. Significant P value is at 95%.

Table 5.4 summarised the pairwise comparison test of the significant variables detected in test performed for table 5.1. However, the P values obtained shows that the are no convincing results to claim that there are differences

between the sessions PreTest, PostTest, and ReTest.

The results of pressure at jumping instance of the RJ in the pairwise comparison is shown on table 5.5. In this case, there is only a significant difference between the PreTest and the PostTest (P value 0.006) with a mean difference value of 0.768.

	PreTest		**PostTest**		**ReTest**	
	Mean Diff.	P value	Mean Diff.	P value	Mean Diff.	P value
PreTest	-	-	0.768	**0.006**	0.375	0.390
PostTest	-0.768	**0.006**	-	-	-0.393	0.160
ReTest	-3.75	0.390	0.393	0.160	-	-

Table 5.5: Repeated Measures ANOVA of pressure at jumping instant in RJ. Mean difference and P value. Mean difference value is in kPa. Significant P value is at 95%.

5.4 Conclusions

12 gymnast were subjected to an evaluation of the fatigue gained before and after a specific training in tumbling surface. Data resulting from ECnsole instrumented insoles show that there is a modification in some variables related to the high jump performance. Statistical analysis shows that the there is an influence of the fatigue in elastic component of the low trunk in CMJ (P value 0.008) in pressure value at the instance of the jump between the PreTest and ReTest. An influence on the elastic component in ABK (P value 0.006) also for the pressure at the beginning of the jump. Finally also a modification on the high jump performance of the pressure at the jumping instance of the RJ between the PreTest and PostTest was found P value 0.006).

Part II

Medical experiments

Chapter 6

Plantar pressure alterations during pregnancy

Contents

6.1 Introduction 178
6.2 Test Definition 179
6.2.1 Participants 179
6.2.2 Test description 180
6.2.3 Materials and methods 181
6.3 Results 183
6.3.1 Clinical study 185
6.3.2 Plantar pressure study 192
6.4 Conclusions 198

6.1 Introduction

In last few years the study of plantar pressure distribution is becoming a very important tool to obtain information about any type of foot or gait disorders. The study of these foot or gait disorder is usually related to orthopaedic surgery [1], but it can be the consequence of many neurological disease that may manifest in many gait disorders[2, 3, 4, 5]. Therefore the study of both statics (posture) and dynamics (gait patterns) provides a very useful information for doctors from any speciality to perform better diagnosis, it is very important to have such a useful information about gait or posture to be able to make an early diagnosis or to observe the patient response to any treatment. Pregnancy is one of those cases that can provoke a gait or postural disorder due to increment of the weight in pregnant. These alterations may have as a consequence a deep or light pain, specially in the back, shoulders or hip. In this way, in can be very interesting to have a method to analyse all those variations during pregnancy evolution.

Traditionally, static studies have been carried out by using complex systems like force platforms, podoscopes, and pedobarograph; while dynamics have been performed using video recording, support detectors in conductive corridors or by means of instrumented insoles. This last example is expanding very much due to the benefits that provide to the patient in order to acquire the plantar pressure distribution without affecting too much in normal gait or posture[112, 111, 72, 141, 178, 179, 106].

There are many works that have studied a relationship between the pregnancy and the back pain and their associated pains[180, 181]. Lumbar pain is one of the most frequently pathologies in pregnant[182, 183], for that reason, the study of this type of pain is getting a lot of importance within last decades[184]. It is very common that lumbar pain starts around 18^{th} week of gestation and it intensifies as pregnancy increases, even after the birth[182, 185]. The pelvic pain is the second pain most frequent in pregnant, that usually appears in the back part of the pelvis[186]. Some studies have claimed that the best treatment possible to avoid back pain is the maintain a correct posture[187].

It is obvious that pregnant increase not only their weight as the pregnancy progresses, but also many others physical changes specially in lower extremit-

ies [188]. Some studies found that there is an increase in forefoot peak pressure, total plantar force and total contact area in class 1 obese subjects in static when only middle foot peak was higher in the dynamic study[189]. This increase on the body weight, that has as a consequence the obesity in some cases, is related to musculoskeletal problems like hyperuricemia, gout, immobilisation, low back pain, knee and hip osteoarthritis[190], and of course cause the deviation of the centre of gravity[191].

However, not many studies have compared what happen to the evolution of the plantar pressure distribution of pregnant during gestation and correlated it with the back pain. *Gaymer et al.* found using an in-shoe measurement system that there is a significantly increase on midfoot plantar pressure during late gestation[192] by comparing a control group of non-pregnant and a pregnant group at 38 weeks gestation. They also compared what happen at post-partum, finding that the increase on the midfoot pressure was solved. Others groups, like *Karadag-Saygi et al.*[193] carried out an study of 35 pregnants with foot pain and 35 non-pregnant looking for a relationship between the foot pain and plantar pressure but only in the last trimester of pregnancy. The research group of *Ribas & Guirro* [194] compared the plantar pressure distribution and posture during different phases of pregnancy, but they did analyse different groups of women in each phase. So, there is no an study, that performs a deep study on the plantar pressure distribution during pregnancy in the same group of pregnant and correlate it with back pain.

Therefore, the aim of this study has been to evaluate the plantar pressure distribution of pregnant in weeks 12^{th}, 20^{th} and 32^{nd} of pregnancy and correlated those data with the back pain.

6.2 Test Definition

6.2.1 Participants

This experiment was performed together with Clinical Management Unit of Obstetrics and Gynaecology at University Hospital San Cecilio, therefore all the documentation related to the approved ethics committee were signed at first. For the recruitment process, the research group attended to first check-up date

which is usually at week 12th of pregnancy. Exclusion criteria was women with some back, feet or legs injuries were discarded as well as women with twins pregnancy because this work wanted to be focused on the evolution in regular pregnancies. Therefore, recruitment process was quite simple: first the study was explained in detail, and after that, in case they agreed to take part in the experiment, they were asked to sign a informed consent, and then, the experiment starts. The informed consent document as well as the approved ethics committee are shown in appendix II. At first check-up, test were performed to a total of 76 pregnant, although, only 62 completed the study. The demographic characteristics of the study group are shown in table 6.1.

	Mean	SD	Minimum	Maximum
Age (years)	31.27	4.66	17.00	41.00
Height (cm)	163.21	7.37	150.00	183.00
Weight in week 12th (kg)	63.60	11.45	48.00	106.00
Weight in week 20th (kg)	69.34	11.46	53.00	111.00
Weight in week 32nd (kg)	76.01	12.75	56.00	123.00
Perimeter in week 20th (cm)	92.77	8.89	66.00	117.00
Perimeter in week 32nd (cm)	104.08	8.39	89.50	127.00
IMC in week 12th ($^{kg}/_{m^2}$)	23.91	4.22	18.17	44.89
IMC in week 20th ($^{kg}/_{m^2}$)	26.15	3.94	19.26	45.04
IMC in week 32nd ($^{kg}/_{m^2}$)	28.38	4.27	20.21	46.67

Table 6.1: Study group demographic characteristics (N=62).

6.2.2 Test description

Test were carried out just after their typical gynaecology check-ups, at weeks 12th, 20th and 32nd of pregnancy. First, pregnant women must fill a questionnaire which contains questions about their perception of their pain. This questionnaire was an add-hoc questionnaire designed based on the bibliography, it contains question not only about their evaluation of the pain but also about

their physical activities changes. The questionnaire both in English and Spanish are added in the appendix II. Once pregnant have filled the questionnaire, they are weighted and measured, both height and abdominal perimeter.

6.2.3 Materials and methods

In order to be sure that shoes were not conditioning the results, the same kind of shoes were used. An sport shoes were provided to all the participants by the research group. This sports shoes included the instrument insoles. The ECnsole version used for this experiment are the 1.5. Once the shoes are tied and the device placed on the waist, test can start. Experimental test consist on 2 laps walking in a 10 meters corridor at comfortable speed, where the 3 first and last steps were discarded.

During this experiment, not only the mean values of the pressure in any sensor is interesting in calculations, but also the CoP of both feet. For that purpose, a Cartesian coordinates system in each insole is defined, taking into account that zero value of both X and Y axis correspond to the upper left corner of each foot (forefoot left side). Then, it is necessary to obtain the coordinates of all sensors contained in the insoles. From now on, the centre of pressure will be referred as CoP^L for left foot and CoP^R for right foot.

Therefore, the CoP position in both axis (x_0^α and y_0^α, with $\alpha = L$ for left foot or $\alpha = R$ for right foot) can be obtained by:

$$x_0^\alpha = \frac{\sum_{i=1}^{4} F_i^\alpha \cdot x_i^\alpha}{\sum_{i=1}^{4} F_i^\alpha} \tag{6.1}$$

$$y_0^\alpha = \frac{\sum_{i=1}^{4} F_i^\alpha \cdot y_i^\alpha}{\sum_{i=1}^{4} F_i^\alpha} \tag{6.2}$$

where x_i^α, y_i^α are the coordinates of a single sensor and F_i^α is the force on that

sensor. As it was described before, the origin of coordinates is always located at the forefoot-left side.

Other variable of interest is the *distribution pressure point* (C_s). The distribution pressure point is the projection of the body's gravity centre of gravity on the Cartesian coordinate system. The location of this point depends on[195, 58]:

- The values of CoP^L and CoP^R.
- The value of $W^\alpha = \sum_{i=1}^{4} F_i^\alpha$

The idea of this measurement is to be dynamically calculated, so they are usually recorded against a discrete time point t. The dynamic Cartesian coordinates of the point $C_s(t)$ can be calculated as follows:

$$x(t) = \frac{W^L(t)x_0^L(t) + W^R(t)x_0^R(t)}{W^L(t) + W^R(t)} \tag{6.3}$$

$$y(t) = \frac{W^L(t)y_0^L(t) + W^R(t)y_0^R(t)}{W^L(t) + W^R(t)} \tag{6.4}$$

for $t = 1, 2, ..., n$, where n is a number of the recorded samples of the test being studied.

It is very important to highlight, that the calculation of the distribution pressure point has no sense in dynamics (during any gait or running test) and it only provided useful information in stance position. This is because when the subject is in movement, the positions of the pressure or force sensor are continuously changing. Calculations of the CoP are correct because the same frame is always considered, that is that $(0,0)$ corresponds to the upper left corner for both foot, that is the forefoot left side.

6.3 Results

Preliminary results

A preliminary study was perform using only 15 pregnant. These results were published into 37th Annual International Conference of the IEEE Engineering in Medicine and Biology Society (EMBC).

	Left Foot	Right Foot
Big Toe (kPa)	-6 ± 10	1 ± 7
1st Meta (kPa)	6 ± 6	2 ± 10
5th Meta (kPa)	7 ± 12	6 ± 6
Heel (kPa)	-8 ± 4	-9 ± 9
CoP Maximum X-Axis (cm)	-1.0 ± 0.3	-0.8 ± 0.4
CoP Mean X-Axis (cm)	-0.9 ± 0.4	-0.7 ± 0.3
CoP Minimum X-Axis (cm)	-0.7 ± 0.7	-0.7 ± 0.4
CoP Maximum Y-Axis (cm)	-4 ± 2	-4 ± 1
CoP Mean Y-Axis (cm)	-4.0 ± 0.8	-4 ± 1
CoP Minimum Y-Axis (cm)	-4 ± 1	-3 ± 1

Table 6.2: Evolution from week 12 to week 32 in all the parameters measured (CoP refers to Centre of Pressure).

Table 6.2 shows the results on the evolution of plantar pressure values in each sensor, as well as the deviation of the maximum and minimum value in both axis of the centre of pressure and its mean value.

Authors would like to emphasised that in the analysis of week 32nd the 70% of the pregnant women had back pain. As table 6.2 shows, the deviation of the centre of pressure in Y-axis seems to be related with the back pain.

Figure 6.1 shows the deviation of the mean value of centre pressure is shown. It can be observed that when pregnant women had back pain, the centre of pressure is deviated slightly towards the heel.

This preliminary results presents an study of the plantar-pressure evolution of pregnant women and its relationship with back pain in a group of 15 parti-

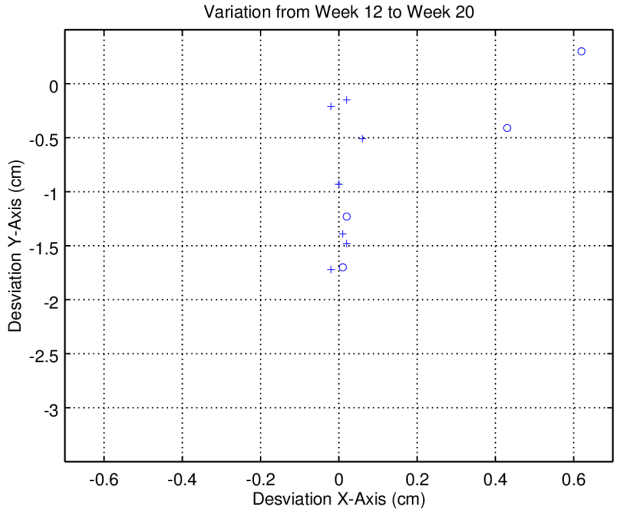

(a) Deviation from week 12th to nth20

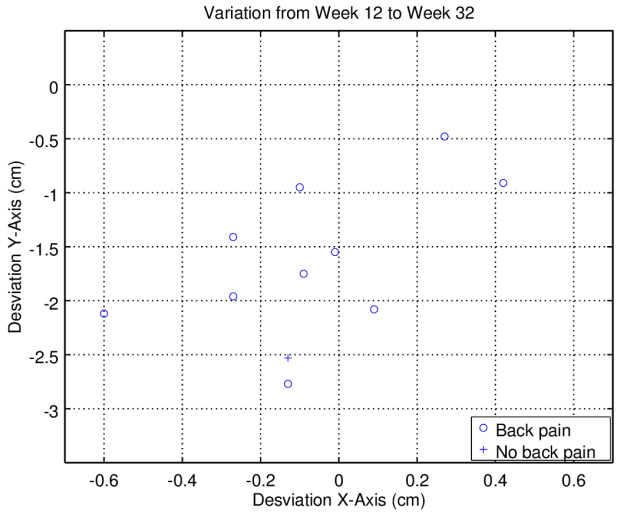

(b) Deviation from week 12th to nth32

Figure 6.1: Deviation of the mean value of Centre of Pressure in the left foot. Deviation since week 12 to week 20 (figure 6.1a) and deviation since week 12 to week 32 (figure 6.1b).

cipants. A gait study during the tree gynaecology checkout that took place on weeks 12^{th}, 20^{th} and 32^{nd} was carried out. The ECnsole version 1.5 was used in this study. Preliminary results show that a deviation in the centre of pressure in Y-axis is significant and could be related to the back pain suffered by pregnant women. Besides, the pressure values observed are slightly bigger in first and fifth metatarsals when big toe and heel decrease. This information could help to prevent incorrect postures that cause back pain in women.

6.3.1 Clinical study

At first, a clinical study of the participants were performed. The objective was to obtain some relationship between any variable related to pregnancy or related to the woman herself and lumbar, should, or pelvic pain. The variable were obtained from the questionnaire which were filled at the beginning of each experimental session (see appendix II).

Pain is a very subjective perception. It is very difficult to describe and quantify. Lumbar, shoulder, and pelvic (or inguinal) pain as well any other type of pain, is a perception that the patient or person that suffer it can adapt and get used to it. It means that the perception of the pain can be lower because the patient have been getting used to it after several week, modifying its real perception. It makes very hard to be able to quantify the pain even using a simple questionnaire as in this work has been done. Figure 6.2 shows how the percentage of pregnant that declared to suffer any of the pains described before (lumbar, shoulder, or inguinal pain). Total number of pregnant were 62.

As figure 6.2 presents, the percentage of woman that suffered lumbar pain in week 12^{th} was 24.19% while in week 20^{th} was 61.29%. It is possible to observe that in week 32^{nd} decreased to 58.06%, the reason of this fall could be that some of the pregnant get used to the pain therefore they declared not to suffer any pain. Something very similar happened to the inguinal pain while the shoulder pain was not modified in relative values.

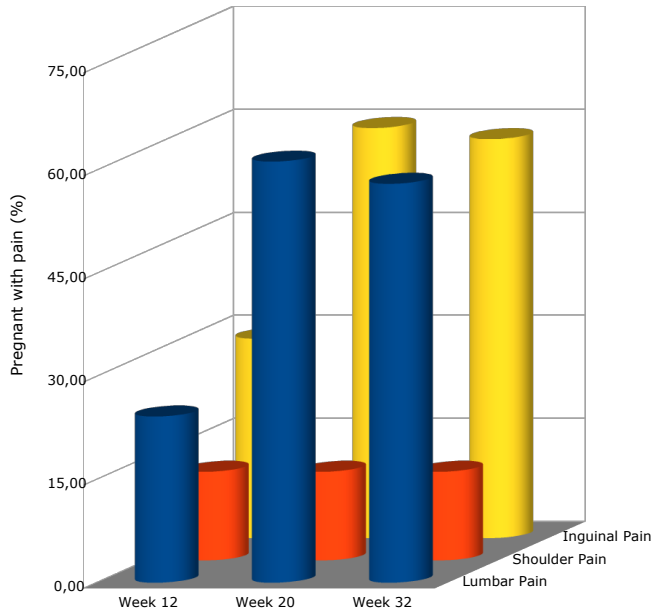

Figure 6.2: Distribution of women with pain over the weeks 12^{th},20^{th}, and 32^{nd}.

There is a significant information about the variables obtained from that questionnaire, they do not follow a normal or Gaussian distribution. For those variables the U-Mann-Whitney test was performed, for the results obtained the significant P-value < 0.05 (95%) was considered. Table 6.3 shows a summary of the results obtained by comparing pregnant that answered they suffered any type of pain with those who did not by means of a bivariate study. The results are organised depending on the type of pain they filled in the questionnaire. Any pregnant can declare that suffered from every types of pains to none of them.

Observing the table 6.3 it is possible to realise that younger women suffered more lumbar pain than older in week 12^{th}. Related to the shoulder pain, those pregnant whose Body Mass Index (BMI) was higher were more numerous. Finally, the inguinal pain was much more present in those women who have more

physical working load during the first twelve weeks of pregnancy.

LUMBAR PAIN	**Pain**	**No-Pain**	**P value**
Age	30.13	31.88	**0.044**
BMI	23.82	23.93	0.874
Physical working load	4	4.87	0.369
Hours of sleep	7.53	7.35	0.986
SHOULDER PAIN	**Pain**	**No Pain**	**P-value**
Age	32.13	31.31	0.307
BMI	25.72	23.63	**0.019**
Physical working load	4.63	4.67	0.975
Hours of sleep	6.75	7.48	0.248
INGUINAL PAIN	**Pain**	**No Pain**	**P-value**
Age	30.61	31.75	0.549
BMI	24.43	23.68	0.187
Physical working load	5.94	4.14	**0.086**
Hours of sleep	7.11	7.51	0.290

Table 6.3: Results of clinical study in week 12^{th}. U-Mann-Whitney test of non Gaussian variables. Significant P-value <0.05 (95%).

In the case of the rest of important variables obtained from the questionnaire, Chi-Square test was performed to obtain a similar relationship between those variables and the different pain asked in the questionnaire. The results are summarized in table 6.4.

In this case, those women that took hormonal contraceptives before pregnancy suffered more lumbar pain while those that were working at home, that have any history of previous back pain and were pregnant by the first time suffered more inguinal pain. None of these variables seems to be related with shoulder pain according to the questionnaire.

PAIN	LUMBAR	SHOULDER	INGUINAL
Work outside/at home	0.817	0.162	**0.087**
Houseworks	0.795	0.233	0.769
Physical activity	0.290	0.768	0.942
Hormonal contraceptives	**0.003**	0.400	0.773
Smokers	0.642	0.482	0.465
History of back pain	0.199	0.746	**0.012**
Any birth before	0.374	0.646	**0.093**
Epidural in the previous birth	0.698	0.627	0.411
Previous prolonged birth	No pain	0.438	0.400

Table 6.4: P-value of Chi-Square test of rest of variables in week 12^{th}. Fisher exact test in those cases which accepted this type of test.

Table 6.5 presents the results obtained from U-Mann-Whitney test in week 20^{th} of pregnancy. In case of the variables such as the weight gain and the abdominal perimeter T-Student test was used considering the equality in the variance by means of Levene test. Same questionnaire was used.

In this check-up, there is no significant results related to lumbar pain. However, there are more shoulder pain cases in those pregnant with less hours of sleep, and many more inguinal pain cases in those whose BMI was higher at the check-up of week 20^{th}, those with a higher physical working load and those with less hours of sleep.

As well as in week 12^{th}, table 6.6 presents the P-value resulting of a Chi-Square test concerning to rest of variables of interest. The table shows there is only significant result in inguinal pain for those pregnant that have not used hormonal contraceptives before the pregnancy. For pains like lumbar and shoulder pain, there are not significant P-value results that could stablish if there is any relationship between any variable and those types of pain.

LUMBAR PAIN	**Pain**	**No Pain**	**P-value**
Age	31.21	31.75	0.637
BMI	26.31	25.89	0.366
Weight gain	6.35	5.02	0.148
Abdominal perimeter	94.03	91.33	0.291
Physical working load	5.55	5.42	0.776
Hours of sleep	6.47	6.92	0.168
SHOULDER PAIN	**Pain**	**No Pain**	**P-value**
Age	33.88	31.06	0.177
BMI	26.65	26.05	0.356
Weight gain	6.50	5.75	0.571
Abdominal perimeter	96.75	92.42	0.186
Physical working load	4.5	5.65	0.391
Hours of sleep	5.62	6.81	**0.011**
INGUINAL PAIN	**Pain**	**No Pain**	**P-value**
Age	31.84	30.80	0.345
BMI	26.34	25.86	**0.080**
Weight gain	6.19	5.31	0.333
Abdominal perimeter	93.62	92.04	0.191
Physical working load	5.92	4.88	**0.049**
Hours of sleep	6.43	6.96	**0.08**

Table 6.5: Results of clínical study in week 20^{th}. U-Mann-Whitney test of non Gaussian variables. In case of the weight gain a T-Student test was used. Significant P-value <0.05 (95%).

PAIN	LUMBAR	SHOULDER	INGUINAL
Work outside/at home	0.587	0.788	0.473
Houseworks	0.352	0.652	0.710
Physical activity	0.933	0.530	0.880
Current physical activity[a]	0.841	0.233	0.849
Hormonal contraceptives	0.798	0.400	**0.011**
Smokers	0.630	0.482	0.340
History of back pain	0.925	0.206	0.411
Any birth before	0.297	0.128	0.437
Epidural in the previous birth	0.538	0.589	0.199
Previous prolonged birth	0.451	0.700	0.451

Table 6.6: P-value of Chi-Square test of rest of variables in week 20$^{\text{th}}$. Fisher exact test in those cases which accepted this type of test.

[a] They do not do any/reduces or continues/modify physical activity.

Finally, same studies were carrying out on week 32$^{\text{nd}}$. In table 6.7 the P-values of U-Mann-Whitney test for non Gaussian variables as well as T-Student test for those variables as weight gain and abdominal perimeter are shown. In the same way as in the case of week 20$^{\text{th}}$, there are no remarkable evidences of any relationship between lumbar pain and any of the variables studied. However, those women who sleep less hours and have a high physical working load suffer more shoulder and inguinal pain. In addition, pregnant with higher BMI also claim to suffer inguinal pain. There is no important changes respect data from table 6.5 because there is no variation in women who declared any kind of pain between week 20$^{\text{th}}$ and 32$^{\text{nd}}$(see figure 6.2).

In table 6.8 is possible to check the P-values of the Chi-Square test performed to the rest of variables of interest. It is important to highlight that again women who have taken hormonal contraceptives suffer more inguinal pain as well as those who were inject with the epidural during their previous birth. On other hand, those pregnant who have been already mothers declared to suffer both lumbar and inguinal pain.

LUMBAR PAIN	Pain	No Pain	P-value
Age	31.42	31.42	0.847
BMI	28.33	28.44	0.909
Weight gain[a]	11.65	11.95	0.797
Weight gain[b]	5.90	6.04	0.830
Abdominal perimeter	103.72	104.46	0.521
Physical working load	6.69	6.08	0.407
Hours of sleep	5.78	6.12	0.361
SHOULDER PAIN	**Pain**	**No Pain**	**P-value**
Age	33.75	31.07	0.214
BMI	28.69	28.34	0.450
Weight gain[a]	12.71	11.64	0.527
Weight gain[b]	5.84	5.98	0.880
Abdominal perimeter	107.06	103.58	0.308
Physical working load	4.38	6.74	**0.088**
Hours of sleep	4.63	6.11	**0.013**
INGUINAL PAIN	**Pain**	**No Pain**	**P-value**
Age	31.69	31.04	0.694
BMI	29.01	27.51	**0.051**
Weight gain[a]	12.11	11.31	0.494
Weight gain[b]	6.18	5.65	0.398
Abdominal perimeter	104.79	102.98	0.253
Physical working load	6.83	5.88	**0.043**
Hours of sleep	5.31	6.77	**0.001**

Table 6.7: Results of clínical study in week 32nd. U-Mann-Whitney test of non Gaussian variables. In case of the weight gain a T-Student test was used. Significant P-value <0.05 (95%).

[a] Respect week 12th
[b] Respect week 20th

PAIN	LUMBAR	SHOULDER	INGUINAL
Work outside/at home	0.756	0.270	0.380
Houseworks	0.564	0.652	0.986
Physical activity	0.701	0.470	0.701
Hormonal contraceptives	0.301	0.726	**0.002**
Smokers	0.329	0.482	0.671
History of back pain	0.765	0.206	0.411
Any birth before	**0.026**	0.303	**0.039**
Epidural in the previous birth	0.438	0.589	**0.06**
Previous prolonged birth	0.451	0.700	0.392

Table 6.8: P-value of Chi-Square test of rest of variables in week 32nd. Fisher exact test in those cases which accepted this type of test.

6.3.2 Plantar pressure study

At first, a descriptive statistical analysis of all variables is shown for all the experimental sessions that took place on weeks 12th, 20th, and 32nd. Table 6.9 presents the values of mean value of the peak pressure of every sensor located in the instrumented insoles. In addition, the coordinates of the CoP is presented in its mean, maximum, and minimum value, in this case it is interesting to emphasize that the minimum value of CoP corresponds to the closer value to forefoot while maximum is the closer to the hindfoot.

It is possible to observe that there are some alterations in plantar pressure distribution along of all sensors as well as a slightly displacement of the coordinates of the CoP, however it is not correct to conclude that those differences are significant. The variations of these values can be observed in table 6.10, which presents the difference between the experimental test sessions.

Making a brief analysis of the descriptive data obtained, despite it is not possible to claim that those differences are significant and related to the pain. Pressure distribution increase in the metatarsal heads while in big toe and heel decrease. It agrees with the literature that claimed that pressure in midfoot increases according to the increment of weight, since there is not sensor at mid-

	Week 12th		**Week 20th**		**Week 32nd**	
	Left	**Right**	**Left**	**Right**	**Left**	**Right**
Big Toe (kPa)	55.22 ± 35.66	45.42 ± 36.74	49.82 ± 31.43	46.98 ± 40.61	49.04 ± 33.90	41.60 ± 39.57
1st Meta (kPa)	48.10 ± 28.92	45.58 ± 30.12	52.81 ± 32.96	54.53 ± 35.27	70.61 ± 39.39	65.57 ± 34.39
5th Meta (kPa)	43.78 ± 28.33	74.05 ± 239.04	54.66 ± 35.76	52.56 ± 42.03	60.68 ± 38.74	62.12 ± 29.98
Heel (kPa)	145.31 ± 58.23	155.66 ± 72.13	164.80 ± 61.75	186.73 ± 75.76	135.83 ± 50.14	177.61 ± 73.15
CoP^{α}_{x} Mean (cm)	5.42 ± 0.39	5.53 ± 0.42	5.46 ± 0.35	5.39 ± 0.40	5.37 ± 0.35	5.37 ± 0.33
CoP^{α}_{x} Max (cm)	6.00 ± 0.37	5.91 ± 0.46	6.07 ± 0.39	5.72 ± 0.44	5.95 ± 0.37	5.66 ± 0.35
CoP^{α}_{x} Min (cm)	4.96 ± 0.53	4.81 ± 0.51	5.04 ± 0.48	4.73 ± 0.50	5.06 ± 0.44	4.65 ± 0.44
CoP^{α}_{y} Mean (cm)	19.44 ± 1.43	19.48 ± 1.68	19.51 ± 1.77	19.40 ± 1.43	18.60 ± 1.72	19.05 ± 1.20
CoP^{α}_{y} Max (cm)	25.10 ± 1.91	25.70 ± 1.61	25.25 ± 1.71	25.74 ± 1.37	24.57 ± 1.46	25.04 ± 1.37
CoP^{α}_{y} Min (cm)	12.46 ± 1.85	12.24 ± 2.23	11.78 ± 2.43	11.99 ± 1.77	11.17 ± 2.41	11.73 ± 1.44
Support (ms)	986.85 ± 357.83	998.56 ± 460.43	924.68 ± 307.80	869.02 ± 193.69	867.97 ± 165.24	888.08 ± 242.16

Table 6.9: Descriptive analysis of plantar pressure for each experimental session.

foot position.

	Δ_P[a]		Δ_T[b]	
	Left	**Right**	**Left**	**Right**
Big Toe (kPa)	-5.40 ± 33.37	1.56 ± 45.48	-6.18 ± 42.05	-3.82 ± 52.69
1st Meta (kPa)	4.71 ± 24.83	8.96 ± 28.81	22.51 ± 33.20	19.99 ± 30.23
5th Meta (kPa)	10.88 ± 28.61	-21.49 ± 209.89	16.89 ± 31.80	-11.92 ± 235.62
Heel (kPa)	145.31 ± 19.48	53.59 ± 31.07	-9.48 ± 54.17	174.81 ± 130.18
CoP_x^α Mean (cm)	0.04 ± 0.33	-0.14 ± 0.43	-0.05 ± 0.38	-0.16 ± 0.35
CoP_x^α Max (cm)	0.08 ± 0.42	-0.19 ± 0.40	-0.05 ± 0.40	-0.25 ± 0.42
CoP_x^α Min (cm)	0.08 ± 0.42	-0.08 ± 0.56	0.09 ± 0.53	-0.16 ± 0.48
CoP_y^α Mean (cm)	0.07 ± 1.65	-0.08 ± 1.68	-0.84 ± 1.75	-0.53 ± 2.12
CoP_y^α Max (cm)	0.16 ± 1.91	0.04 ± 1.62	-0.67 ± 1.60	-1.29 ± 2.68
CoP_y^α Min (cm)	-0.68 ± 2.88	-0.25 ± 2.63	-1.29 ± 2.68	-0.51 ± 2.45
Support (ms)	-62.18 ± 399.96	-129.55 ± 441.79	-118.89 ± 371.58	-110.48 ± 493.82

Table 6.10: Descriptive analysis of plantar pressure evolution. Data are calculated as the difference between week 20th and week 12th in case of Δ_P and between week 32nd and week 12th for Δ_T.

[a] Refers to the differences between session at week 20th and week 12th
[b] Refers to the differences between session at week 32nd and week 12th

Next, an study to evaluate if the centre of pressures have changed within the gestation is done, but just in the Y-axis, considering as the literature says, that the centre of pressure must displace to the midfoot area. The criteria is the same than in chapter 5. An Repeated Measures ANOVA test is performed. At first, it is necessary to check if any of the variables related to the CoP changes within the weeks. Therefore a multivariate test is done (see table 6.11).

From these results it might be concluded that there are significant differences between weeks 12th, 20th, and 32nd of pregnancy in the Y-axis of the centre of pressures of both foot, except in mean and minimum value of the right foot. To check those differences, a Repeated Measures ANOVA test is performed.

	P value
CoP_y^R Mean	0.083
CoP_y^R Max	**0.000**
CoP_y^R Min	0.206
CoP_y^L Mean	**0.000**
CoP_y^L Max	**0.026**
CoP_y^L Min	**0.001**

Table 6.11: Multivariate analysis of the jumps performed. Significant P value at 95%.

	Week 12th		**Week 20th**		**Week 32nd**	
	Mean Diff.	P value	Mean Diff.	P value	Mean Diff.	P value
Week 12th	-	-	-0.066	1.000	0.841	**0.001**
Week 20th	0.066	1.000	-	-	0.908	**0.000**
Week 32nd	-0.841	**0.001**	-0.908	**0.000**	-	-

Table 6.12: Pairwise comparison CoP_y^L Mean value. Mean difference and P value. Significant P value is at 95%.

According to the table 6.12 there is a significant changes (P value 0.001) between weeks 12th and 32nd with a mean displacement of this point 0.841 towards the forefoot. It happend the same between weeks weeks 20th and 32nd (P value 0.000) with a slightly higher displacement.

	Week 12th		**Week 20th**		**Week 32nd**	
	Mean Diff.	P value	Mean Diff.	P value	Mean Diff.	P value
Week 12th	-	-	-0.156	1.000	0.532	0.157
Week 20th	0.156	1.000	-	-	0.689	**0.023**
Week 32nd	-0.532	0.157	-0.689	**0.023**	-	-

Table 6.13: Pairwise comparison CoP_y^L Max value. Mean difference and P value. Significant P value is at 95%.

Similar results are obtained for the maximum value of the CoP_y^L (see table 6.13), that tends to displace to the midfoot/forefoot area (P value 0.023) a mean displacement of 0.689 from week 20th to week 32nd.

	Week 12th		**Week 20th**		**Week 32nd**	
	Mean Diff.	P value	Mean Diff.	P value	Mean Diff.	P value
Week 12th	-	-	0.677	0.208	1.288	**0.001**
Week 20th	-0.677	0.208	-	-	0.611	**0.033**
Week 32nd	-1.288	**0.001**	-0.689	**0.033**	-	-

Table 6.14: Pairwise comparison CoP_y^L Min value. Mean difference and P value. Significant P value is at 95%.

In case of the last variable related to left foot it is possible to observe a similar trend in which the minimum value of the centre of pressure of the left foot displaces towards to midfoot/forefoot with significant changes in the measurements of the second and third check-up (see table 6.14).

Only one of the variables of the centre of pressure on the right foot was compared, those results are presented in table 6.15. As well as in left foot, the maximum vale of the centre of pressure of right foot moves towards the midfoot/forefoot presenting a mean difference between week 12th and 32nd of 1.288 (P value 0.001). Therefore, the CoP of both feet has a displacement in the Y axis towards the forefoot.

	Week 12th		**Week 20th**		**Week 32nd**	
	Mean Diff.	P value	Mean Diff.	P value	Mean Diff.	P value
Week 12th	-	-	0.677	0.208	1.288	**0.001**
Week 20th	-0.677	0.208	-	-	0.611	**0.033**
Week 32nd	-1.288	**0.001**	-0.689	**0.033**	-	-

Table 6.15: Pairwise comparison CoP_y^R Max value. Mean difference and P value. Significant P value is at 95%.

Last analysis is an ANOVA test considering two main groups of pregnant: those with no pain (level of pain under 5) and those with pain (level of pain above 5).

	Week 12th		**Week 20th**		**Week 32nd**	
	Left	**Right**	**Left**	**Right**	**Left**	**Right**
Big Toe	0.995	0.889	0.239	0.811	0.607	**0.029**
1st Meta	0.880	0.679	0.560	0.725	0.848	0.528
5th Meta	0.298	0.738	0.598	0.789	0.320	0.765
Heel	0.682	0.626	0.237	0.856	0.342	0.094
CoP_x^α Mean	0.531	0.592	0.782	0.545	0.744	0.657
CoP_x^α Max	0.862	0.453	0.707	0.944	0.481	0.801
CoP_x^α Min	0.398	0.705	0.797	0.829	0.476	0.426
CoP_y^α Mean	0.591	0.457	0.504	0.938	0.403	0.383
CoP_y^α Max	0.875	0.799	0.094	0.194	0.913	0.117
CoP_y^α Min	0.653	0.713	0.925	0.572	0.333	0.091
Support	0.444	0.297	0.098	0.440	0.417	0.094

Table 6.16: ANOVA test considering pain as a factor. Week 12th: 55 no pain, 7 pain. Week 20th: 51 no pain, 11 pain. Week 32nd: 41 no pain, 21 pain

From table 6.16, the null hypothesis of there is no changes between the back pain group and no back pain can only be rejected in one case by means of this

test: in the big toe of the right foot during the week 32nd. The rest of the resulting data do not provided significant information to claim that there is any kind of relationship between the lumbar or any type of pain and the changes in the plantar pressure distribution.

6.4 Conclusions

This experiment have carried out a tracking to a group of 62 pregnant to evaluate if there is any relationship between plantar pressure distribution and pregnancy. On the one hand, a clinical study has been performed, concluding:

1. In week 12th, younger women and those who consumed hormonal contraceptives suffer more lumbar pain. Pregnant with high BMI have more shoulder pain. And women who have high physical working load, those who work outside, who have some history of back pain, or those who have been mother before, have more inguinal pain.

2. In week 20th, pregnant who have less hours of sleeping suffer more shoulder pain and inguinal pain, while those with high BMI, high physical working load, and consumed hormonal contraceptives have more inguinal pain.

3. Finally, in week 32nd, the trend remains like in other weeks, but in this case those pregnant who were mother before also declare lumbar pain.

Related to the plantar pressure distribution. It was performed a descriptive analysis of the plantar pressure distribution, and a Repeated Measures ANOVA test, to determine the variation and its influence on the CoP in the Y-Axis, concluding that the centre of pressure of both feet displace towards the forefoot as continuing the pregnancy. Also an ANOVA test was carried out to evaluate the differences between a painful group and a non painful, obtaining only significant differences in the pressure on the big toe of the right foot in week 32nd. However, due to the complexity of the data, and considering the difficulty that the pain as a subjective opinion provides, both the candidate and the research

group are still analysing this huge amount of data to achieve a more complete study.

Chapter 7

Gait analysis in neurological diseases

Contents

7.1 Introduction 202
7.2 Test Definition 203
7.3 Results 204
7.3.1 Initial contact 204
7.3.2 Heel-off 206
7.3.3 Terminal contact 206
7.3.4 Impact of velocity 206
7.4 Discussion 208

7.1 Introduction

Recording of human gait is important in medicine, rehabilitation and sport. With the introduction of small lightweight inertial sensors (accelerometers and gyroscopes) it became possible to record human gait outside of the limited space of a gait laboratory. Because the data obtained by inertial sensors are not related to an external reference system (other than gravity), events such as the initial and terminal contact of the foot (IC, TC) must be defined in these data on the basis of a pattern recognition approach. These values constitute the cornerstones of gait analysis because they are needed for the calculation of stance time and swing time. Accelerometers can be used to determine these events[196] but most researchers define TC and IC in the trace of gyroscopes mounted at the shank which show a characteristic peak during the swing phase of the foot and two troughs at the beginning and at the end which are taken as IC and TC[197, 198, 199, 200]. Whereas most researchers agree upon taking the trough following the gyroscope peak as the moment of heel strike, the determination of the toe-off moment from these curves is under discussion: One study[197] reported 'toe-off' to be 10 ms earlier than the trough of the gyroscope curve. Others[200] reported that toe-off coincides with the gyroscope trough. A third study reported large variations between a signal from a switch mounted at the toe and the trough[198]. A fourth study found an error of 43.4 ms between the assumed TC in the gyroscope curve and data from a force plate[201]. To clarify these issues, we set out to study the exact timing of gait events with a motion capture system as well a pressure sensitive soles and correlated these date with shank mounted gyroscope data to allow for a definition of gait cycle events in the gyroscope traces. Second, we sought to determine whether gait velocity may influence the relative timing of these events as defined in the gyroscope traces, which has to our knowledge not been investigated up to now.

7.2 Test Definition

Fourteen healthy young men (age 25-40), who were recruited from the hospital staff, walked on a treadmill (Woodway Inc., Waukesha, WI, USA) for 1.4 minutes at three different velocities (2, 4, and 6 $^{km}/_{h}$) in different trials. Data obtained during the acceleration and deceleration phases of the treadmill were discarded. About 20-30 steps were evaluated for each subject at each velocity. Gait was measured with inertial sensors and a motion capture system in all subjects and with additional pressure-sensitive soles in 8 subjects. The approval of the local ethics committee had been obtained. Inertial measurement system: for the recording of shank movements we used one analog gyroscope (IDG500, Invensense, Sunnyvale, CA, USA) and two analog accelerometers (ADXL335, Analog devices, Norwood, MA, U.S.A) on each shank. Data from these sensors were collected at 200 Hz/sensor by a microprocessor with 16 analog-digital converters with 12-bit resolution (ATXMEGA 128, Atmel, San Jose, CA, USA) and stored on an SD-card for offline evaluation. The sensitivity was 6 bits/deg/s for gyroscopes and 2095 bits/g for accelerometers. Data were sampled with 16 times the sampling frequency to enhance the resolution of the system to 14 bits (oversampling). Sensors were connected with the processor by dedicated shielded sensor cables. Sensors were mounted so that the axis of the gyroscope aligned with the mediolateral body axis and the accelerometers signaled acceleration in the direction of the vertical and anterior body segment axis. Sensors were tightly secured with bandages.

The Motion capture system we used the Oqus camera system (Qualisys AB, Gothenburg Sweden). Three infrared reflecting spheres were attached to each shank (2 on the shin, one on the calf muscle) and their position was recorded with 200 Hz by 8 cameras. The special resolution of this system is below 1 mm. Related to the pressure-sensitive soles: the version of the ECnsole used is the 1.5.

About the evaluation of the data obtained, they were evaluated with MATLAB R2014b (Natick, MA, USA). The data from the inertial sensors, soles and Qualisys system were synchronized after re-sampling to 200Hz (only soles). Synchronization between soles and inertial sensors was done by correlating the z-accelerometer traces of soles and inertial sensors (Matlab routine xcorr

was used for computing lag/lead of the data). For synchronization of motion-capture and shank-mounted gyroscope and accelerometer data we computed the pitch angle of the shank (Kalman-filter, using accelerometer and gyroscope data) and aligned this with the pitch of the motion capture data, also by computing the cross-correlation. This resulted in one data set containing data from gyroscopes, accelerometers, motion capture system and soles pressure on one single time axis.

Six events had to be detected in the data of each step: first, the peak of the shank gyroscope was defined (Matlab routine 'findpeak' after low-pass filtering of the gyroscope trace: 20 Hz, 3rd order Butterworth with zero phase-shift, Matlab routine filtfilt). Then, the troughs before and after the peak were reliably detected by Matlab (zero-crossing of first derivative of 20 Hz-filtered gyroscope curves). The trough after the peak was taken as the 'initial contact' (see results). The 'toe-off' moment was manually defined in the curves of the pressure sensors of the soles. Finally, the 'heeloff' moment was manually marked in the Qualisys curves (steep increase of the shank marker in an upward direction). Finally, to complete the step cycle, the 'initial contact' before the stance phase was noted. The time of the occurrence of these events was recorded for each step for statistical evaluation as well as for averaging of the data using these events as triggers.

7.3 Results

7.3.1 Initial contact

The initial contact of the foot (heel strike) caused sharp transients in the curves of both shank accelerometers as well as a clearly recognizable trough in the gyroscope curve. The automatic Matlab routine identified the trough in the gyroscope curve reliably after spurious noise in these data had been removed by a 20-Hz low-pass zero-phase-lag filter (7.1). This trough clearly represents the initial contact as this is confirmed in the trace of the pressure-sensitive element mounted underneath the heel (7.1). It is noteworthy that during the stance phase the pressure sensors signal a continuous weight shift from heel to toe (7.1, lower left), even at low velocities.

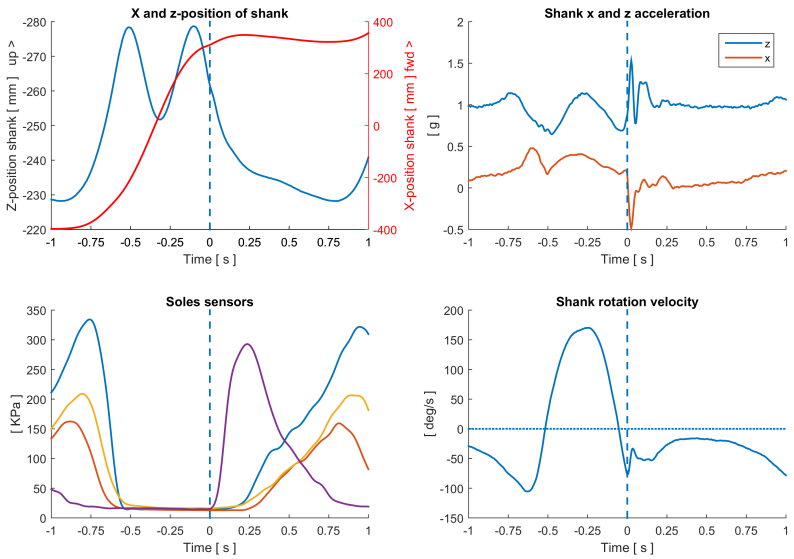

Figure 7.1: Initial contact, right leg: Data from 12 steps of a representative subject walking at 2 km/h were averaged. Lower right: the peak of the gyroscope trace denotes the peak rotation velocity during the swing phase. The trough after the gyroscope peak was detected by software (see text) and was seen in all subjects in this presentation and indicates the moment of heel strike. This is confirmed in the curves of the pressure-sensitive soles (lower left). The four traces represent four pressure-sensitive elements. Here, the purple trace (heel sensor) is the first to signal the heel contact. At the same time the accelerometers mounted at the shank show sharp transients (upper right). Upper left: shank position of one of three shank markers (Qualisys motion capture camera).

7.3.2 Heel-off

While the heel was lifted off the ground, the z-values of the Qualisys shank markers showed a characteristic increase after which two peaks were seen (figure 7.2). The beginning of this increase was taken as the 'heel-off' time and was manually marked. The averaged data of the pressure sensors confirmed that the heel was free of pressure at this moment. The 'heel-off' moment has no characteristic pattern in the gyroscope curve. However, in individual data traces it corresponds to a steep increase in 'backward' rotational velocity (figure 7.3).

7.3.3 Terminal contact

The terminal contact was manually marked according to the traces of the pressure-sensitive soles when all sensor values were below a threshold of 15 kPa (figure 7.4). This moment was between the initial trough of the gyroscope trace and the moment when the gyroscope trace crossed the midline, i.e. when the direction of rotation changed. TC was thus during shank 'backward' rotation, i.e. when the shank rotated in the opposite direction to that during the following swing phase. It is noteworthy that the 'toe-off' moment was clearly after the initial trough of the gyroscope trace in all subjects. Because no characteristic pattern of the gyroscope trace indicated this instant, we determined the 'toe-off' moment as a fraction of the distance (in deg/s) between the trough and peak (A) and second, as a fraction of the distance (in deg/s) between the trough and zero-crossing of the gyroscope traces (B) in each individual step for the right and left leg. This is illustrated in figure 7.5. These values were velocity-dependent (Table 7.1).

7.3.4 Impact of velocity

The timing of the different events during the step cycle was averaged for each subject, velocity and foot. Data were normalized to the step cycle (IC set to 0%, following IC: 100%). Average step cycles lasted 1804 ms (s.d. 247), 1260 ms (s.d. 128) and 1024 ms (s.d. 61) for the three different velocities (2,4, and 6 km/h). The heel-off event was at 51% (median) of the step cycle for all velocities (figure

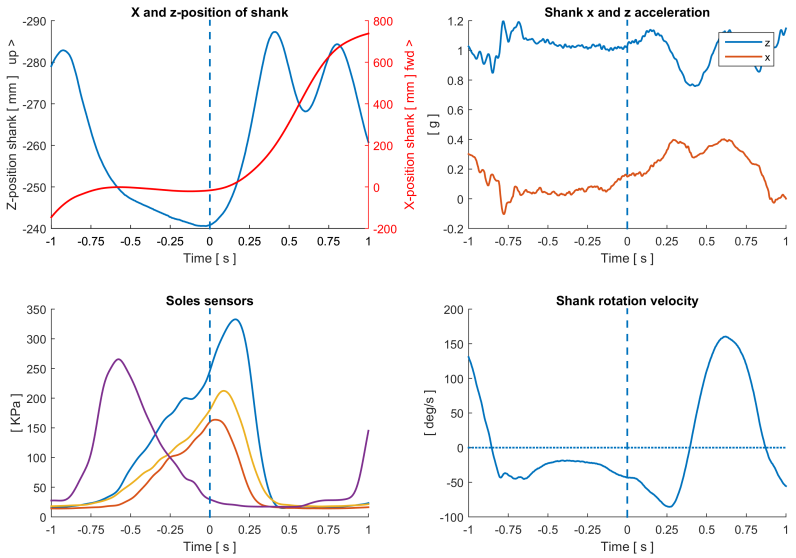

Figure 7.2: Heel-off, right leg. Data from 12 steps of a representative subject walking at 2 km/h were averaged. The beginning of the upward shank movement (upper left, blue curve) had been manually marked in all curves and was taken as the “heel-off” moment. This served as synchronization event for the averaged data presented here. The averaged data of the pressure sensors (lower left) confirm that the heel marker (purple) is released at this moment. Note that neither in the gyroscope trace nor in the accelerometer trace a characteristic patterns for “heel-off” can be seen.

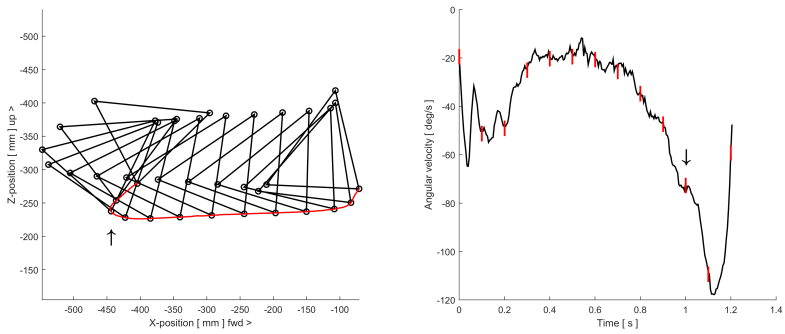

Figure 7.3: Correspondence between "heel-off" and gyroscope trace. Right: gyroscope trace during the stance phase, beginning immediately before IC. Gait velocity: $2^{km}/_{h}$. Vertical red bars at 100 ms intervals denote time at which marker triangles are plotted on the left. Left: two shank markers (Qualisys motion capture system) fixed at the shin and one at the calf are depicted as triangles every 100 ms. The lowest marker is connected with a red line. Triangles move leftwards during the stance phase as the treadmill moves leftwards. The upward arrow indicates the moment at which the shank is lifted (heel-off). At this moment, the gyroscope trace shows an increasing 'backward' rotation velocity (downward arrow, right panel).

7.6). The toe-off moment (TC) was less constant at 69%, 65% and 63% for the three velocities (2; 4; 6 km/h). Inter-individual variation was small, except for one subject who showed a very early heel-off. These data were checked twice. Lifting the heel so early is possibly a peculiarity of this individual subject.

7.4 Discussion

Precise determination of events within the gait cycle is crucial for the calculation of temporal gait parameters like duration of stance or swing phase, but also for more complex algorithms which attempt to determine the spatial parameters of gait. These models need to know the exact timing not only of TC

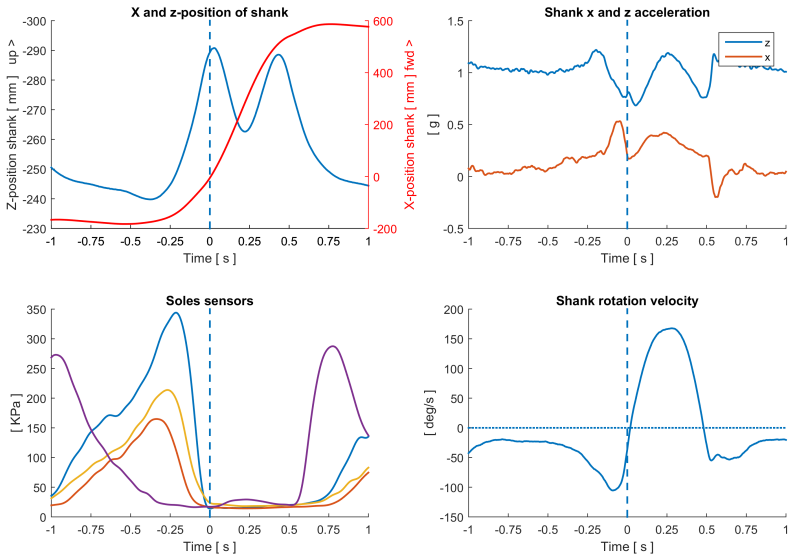

Figure 7.4: Terminal contact, right leg. Data are average of 14 steps of one representative subject. Gait velocity: 2 km/h. The vertical dashed line indicates the moment of the terminal contact which was manually set for all individual steps according to the data of the pressure sensors (lower left). Note that this moment does not coincide with the trough of the gyroscope trace (lower right) before the peak rotation velocity. With respect to the gyroscope trace, TC is approximately midway between the trough and the zero-crossing of the gyroscope trace. Upper left: Position of Qualisys shank marker, blue: z; red: x. Note that z increases (leg begins to lift off) about 300 ms before TC. TC is just before the peak of the z-trace is reached. The peak indicates that the foot is not lifted further, i.e. the foot is cleared off the ground at the time of the peak. Upper right: As the leg is bent forward before TC, and the gravity vector rotates relatively to the accelerometers, x increases and z decreases.

Velocity ($^{km}/_{h}$)	Shank rotation velocity ($^{deg}/_{s}$)	SD	A	SD	B	SD
2	296.29	49.72	0.14	0.09	0.36	0.24
4	490.09	91.09	0.20	0.06	0.49	0.16
6	642.21	81.05	0.28	0.16	0.60	0.23

Table 7.1: Computation of the terminal contact in gyroscope curves: Shank rot. velocity: Mean values and standard deviations for the peak-to-peak velocity of the gyroscope trace during the swing-phase. A: height of the 'toe-off' moment as fraction of the peak shank rotation velocity (measured against preceding trough) . B: height of the 'toe-off' moment as a fraction of the distance between trough and zero crossing of the gyroscope curve. The values for B show that the height of the gyroscope trace at toe-off is approximately half the height of the zero-crossing (as measured from the bottom of the trough, see figure 7.5 for a graphical representation of these measures)

and IC but also of the 'foot-flat' phase, since the stance foot must be seen as a pivotal point from which the chain of segments can be calculated[202]. When gait parameters are to be calculated from the inertial sensors, the shank gyroscope trace is mostly taken for the determination of these events. There is general agreement that IC coincides with a local trough of the gyroscope trace that occurs after the peak rotational velocity during the swing phase[197]. This trough has one or more sharp transients which are the sensor's representation of the jerk during heel-strike. This can also clearly be seen in the accelerometer traces (figure 7.1). In our data, it was easy to automatically detect this trough by software after applying a 20 Hz low-pass filter. Advanced algorithms to detect such troughs[203] do not seem to be necessary when analyzing gait data from a group of healthy volunteers as in our study. It is crucial to obtain data with minimum noise to reduce the need for filtering, which may blur the sharp transients associated with this event. Others have used low-pass filters of 3 or 5 Hz which we consider problematic in this regard.

Contrary to previous reports we found that the 'toe-off' moment (TC) does not coincide with the first trough of the gyroscope curve but is later. This is

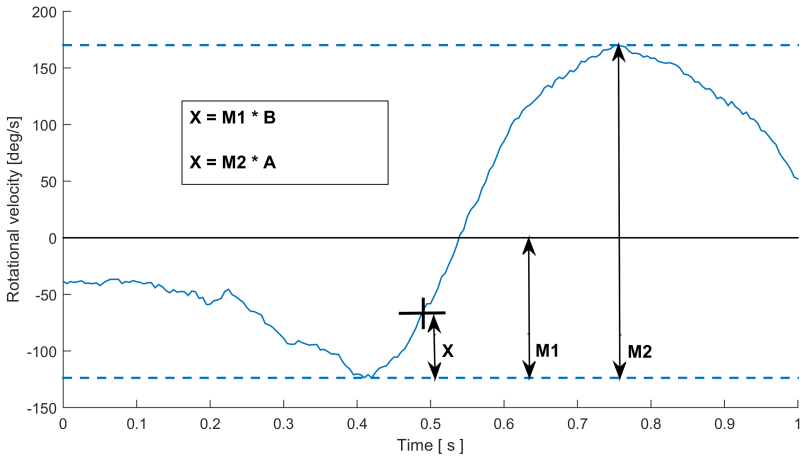

Figure 7.5: Computation of TC (toe-off) in shank mounted gyroscope. The blue curve shows the gyroscope trace with peak velocity at M2 (mid-swing phase). The cross denotes the moment in which the foot is cleared off the ground. This moment was found by analyzing the traces of the soles pressure sensors (figure 7.4). When only gyroscope data are available, this instance may be found by applying either of the two formulas. The values of A and B were empirically determined and are found in the table.

in contrast to four studies in which gyroscope signals as well as signals from pressure sensors under the foot were recorded and compared: in the paper by *Aminian et al.*[197] the authors noted that their pressure sensors at the toe signaled 'toe-off' 10 ms earlier than the algorithm which detected the trough of the gyroscope curve. Their algorithm to detect the trough (wavelet decomposition) may possibly play a role here. Also, low-pass filtering may have a crucial impact and can shift the trough forward by up to 100 ms (Lee and Park, 2011). In our study, the soles indicated 'toe-off' 84/67/52 ms after the trough (velocity: 2/4/6 km/h). In the study reported by Tong and Granat[200], one healthy subject was assessed and the authors report that toe-off coincides with the gyroscope trough. A third study reported large variations between a signal

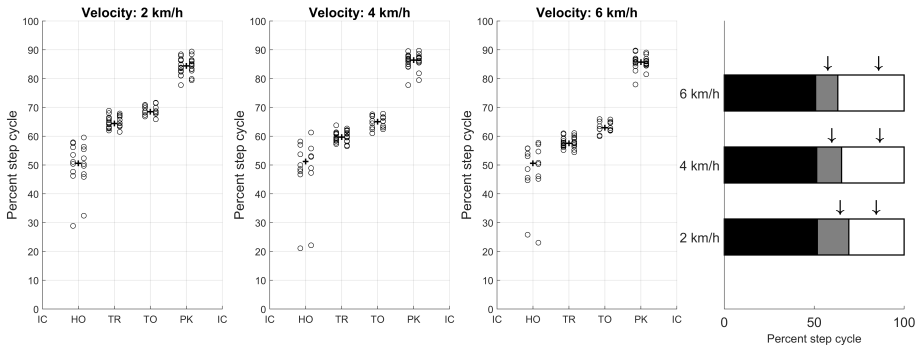

Figure 7.6: Timing of events in fractions of step cycle for different gait velocities. A step cycle begins at IC (set to 0%) and ends at the following IC (100%). A circle denotes the mean value of timing (percent of step cycle) of one subject for right or left foot. The cross indicates the median of the values of all subjects. HO: heel-off; TR: trough before gyroscope peak; TO: toe-off; PK: peak of gyroscope trace. Right: bar chart showing relative timing of events. Black: stance phase after IC; grey: stance phase after heeloff; white: swing phase. Arrows indicate trough of gyroscope curve before peak and peak of gyroscope curve during swing phase. Data are median of mean values of all subjects. Note that heeloff is constant at 51% of gait cycle whereas toe-off is varying with gait velocity. One subject showed diverging values for heel-off in all velocities.

from a switch mounted at the toe and the trough, but on average the trough was 8 ms before the signal of the switch[198]. A fourth study compared force plate data with gyroscope data and found an error of 43.4 ms between the assumed TC in the gyroscope curve (minimum before peak) and the data from the force plate[201]. The authors discuss a systematic error and state that 'the point in the angular velocity signal thought to represent TC may in fact represent a slightly different point in the gait cycle...'.

When gyroscopes are mounted on the foot, curves similar to those from shank-mounted gyroscopes can be registered[204]. Corresponding to our data, these authors found that 'toe-off' occurs after the trough of the gyroscope and

concluded that taking the trough as 'toe-off' was an 'important limitation of previous methods for HS and TO detection'.

From a physiological point of view it seems plausible that the trough assumed to be TC does not in fact represent this event: the trough of the gyroscope signal represents the maximum rotational velocity of the shank in opposite direction to that during the swing phase. This rotation is necessary to lift the foot from the ground and it would only be plausible that the toe is not cleared off the ground during maximum rotational velocity but rather at the end of this rotation because the opposite would create an unnecessary distance between toe and ground. In our data the toe was lifted at the end of this rotation phase, i.e. close to the moment of the change of rotational direction. It is noteworthy that the inversion of rotational direction can be reliably determined only on traces which are not high-pass filtered.

Because no distinct pattern in the gyroscope traces indicates TC, we suggested two ways of computing a surrogate event for TC from gyroscope traces (table 7.1; figure 7.5). A pragmatic way to determine TC may be to take a point midway between trough and zero-crossing. This corresponds roughly to an average of the three values in the table listed under 'B' (0.36, 0.49, 0.60) which would be adequate considering rather high standard deviations of the A and B values (table 7.1).

Sensors from the soles and the data of a motion capture system allowed us to determine the 'heeloff' moment, which was very constant at 51% of the gait cycle irrespective of gait velocity. This is the end of the 'foot-flat' phase. We made no attempt to determine the exact onset of the 'foot-flat' phase because of the very gradual increase of the signals from the forefoot pressure sensors which made a clear identification of the beginning of this phase difficult (figure 7.2). However, from the figures it becomes clear the 'foot-flat' phase begins at approximately 30% of the step cycle. This contrasts with the data obtained by Tong and Granat[200] who reported the heel-off event to be at 20% of the gait cycle. We cannot explain these differences but it must be mentioned that in the above-mentioned study data were obtained from one subject only.

Concerning the relative timing of events during the step cycle we found that the stance phase covered 69%/65%/63% (velocity 2/4/6 km/h) which is roughly in accordance with several reports in the literature using different methods:

when gait cycles of 105 healthy adults were studied with foot switches, the authors found that the stance phase was 61%[205], whereas for men over 70 years a stance phase of 64% was observed[206]. In 12 adults (mean age: 27 years) a stance phase of 60% was reported[207]. To the best of our knowledge there are no normative data available for heel-off and foot-flat from larger cohorts.

Some shortcomings of our study should be mentioned. TC and heel-off were determined manually on the curves of each individual step. Whereas this includes some inaccuracy, this should be overcome by the high number of steps analyzed and by averaging the results later. Manual marking was chosen because the sensors of the soles were not completely free of pressure even when the foot was off the ground. Second, the sampling rate of the soles was less than for the motion capture system and the shank mounted gyroscopes and had to be re-sampled to 200 Hz. This reduces the precision of the toe-off-measurements to roughly 12 ms. However this would not disapprove our main finding that the moment of toe-off is not coincident with a trough in the gyroscope curve.

In the future, small lightweight sensors will rapidly gain more importance for the measurement of gait in medicine, rehabilitation and sport. The data presented here may contribute to robust and precise software solutions in this field.

Part III

Conclusions

Chapter 8

Conclusions and Future Work

Contents

8.1 Development of instrumented insoles 218
8.2 Applications in sport framework 221
8.3 Applications in medical framework 222
8.4 Future Work 223

The analysis of plantar pressure distribution, gait and running patterns, and posture has gained a lot of importance in last few years, not only in medicine fields, but also in sports and physical education. The integration of several sensors in an in-shoe instrumented system can provide a very useful information for preventing or correcting certain bad habits or postures to improve the quality of life. On the other hand, the information provided by such instrumented insoles in other research fields such as sports training can enhance the sport performance or reduce the chances of injury.

The work here carried out has consisted in the development of several instrumented insoles and their application in different research studies, specifically, in sports and medicine framework. Main conclusions of the work developed during this thesis are summarised in this chapter.

8.1 Development of instrumented insoles

In this thesis a searching task of pressure and inertial sensors liable to be embedded into an instrumentation insole has been performed. As a result, next sensors have been selected, tested, and validated:

- Pressure/Force sensors:
  - Flexiforce A201: in ECnsole version 1.0, 1.2, and 1.5.
  - Flexiforce A401: in ECnsole version 1.5, and 2.0.
- Inertial sensors:
  - Accelerometer ADXL330: in ECnsole version 1.0 and 1.2.
  - Accelerometer and magnetometer LSM303DLHC: in ECnsole version 1.5.
  - Gyroscope L3GD20: in ECnsole version 1.5.
  - Accelerometer and magnetometer LSM303D: in ECnsole version 2.0.
  - Gyroscope L3GD20H: in ECnsole version 2.0.

A first prototype of the instrumented insoles name ECnsole version 1.0 was designed. It consists of two devices (master and slave) placed on the ankles or legs of the subject. Main characteristics of this version are:

- 4 pressure sensors located at big toe, 1^{st} and 5^{th} metatarsal heads, and heel.
- Analogue accelerometer placed in the arch of the foot.
- Wireless communication between datalogger units master ad slave using MiWi™ protocol.
- Wireless communication between master and PC using MiWi™ protocol.
- Recording of data into a μSD memory card.
- Sampling frequency of 62 Hz.
- Software application on PC side for data plotting.

The major weakness of this version are the fragility in the node connections and the limited sampling frequency. These reason together with the desire of reducing costs made that the new prototype design was necessary. ECnsole v1.2 remains using the same pressure sensors and accelerometer. In version 1.2 of the instrumented insoles the master and slave datalogger are joined together into a unique device responsible of sensor acquisition. Firmware is upgraded to sampling at frequency of 77 Hz.

In order to increase functionalities of the ECnsole, new sensors were added to the instrumented insoles in version 1.5. In addition, electronics of this device was improved for the acquisition of sensors. The greatest upgrades of this new prototype were:

- Replacement of the accelerometer by a digital IMU composed of triaxial gyroscope, triaxial accelerometer, and triaxial magnetometer.
- Improvement of the performance of the firmware reaching a sampling frequency up to 333 Hz (sampling period of 3 ms).

- New Matlab® software application for data processing.

The information provided by the new sensors added in version 1.5 can be very interesting to obtain important parameters related to the foot position and its movement during the swing phase. Main inconveniences of this version are mainly the wires. The possibility of achieve a new version that could be absolutely wireless was the biggest challenge of this thesis. ECnsole version 2.0, that is still under validation process, has supossed a huge change compared to rest of version. The datalogger unit is divided into two independent devices that sends the data from sensors to an android smartphone or table PC that acts as a datalogger. Main characteristics:

- Two pressure sensors are added in the 3rd metatarsal head and midfoot area.
- Everything is embedded inside in the insole.
- A coin rechargeable battery is used to supply the devices.
- Electronics for sensors acquisition is modified to reduced the size of the electronics system.
- MiWi™ is replaced by Bluetooth technology.
- Firmware is modified to reduce microcontroller working load and to improve sampling frequency.
- New android application is developed to plot and store data from sensors.

Sensors included in our prototypes have been validated with gold standards. Pressure sensors have been compared with in-shoe commercial pressure sensor system while IMU has been compared to an infrared video camera system. Moreover, preliminary tests shown allow to conclude that the use of a instrumented insoles, in this case the ECnsole, with an IMU placed inside just in the arch of the foot, can provide a very useful information. A priori, it can help hugely from professionals to amateur runners, to adapt their running style or

they shoes, according a diagnosis about supination or pronation during these activities. On the other hand, it can also help in medicine, to prevent injuries not only in the low trunk but also in the back, in those cases that the people have a gait disorder due to the supination or pronation.

The system presented in this work can simultaneously provide the pressure values for the big toe, first and fifth metatarsals, heel and the angular components in the three spatial axes including all the sensors in the instrumented insole. The data analysis can be carried out with a software program or with a standard spreadsheet. The software analysis shows the results in real time on the computer screen or in replay mode for experiment analysis. These display modes make immediate feedback possible, and therefore the subject gets immediate feedback on his or her pathology and can try to correct it at once. Moreover, the accelerometer readouts report additional information during the swing and stance time in walking tests. For instance, detection of anomalous pressure distribution, excess lateral movement, determination of stance time, and the detection of asymmetry could prevent future injuries or help a person choose the most suitable shoes. In this work, we have combined the analysis of the pressure and acceleration data to clearly distinguish among neutral, pronator or supinator participants, even estimating different amount of supination. This system could be very useful in studying walking patterns in people affected by illnesses such as Parkinsons, astronauts after a weightless period, rehabilitation from different injuries, or to choose the most appropriate shoes.

8.2 Applications in sport framework

After analysing and comparing the data obtained with ECnsole, the HSC, and the SJS, we conclude that both systems (PreECnsole and AccECnsole) have a high validity for measuring the flight time of a vertical jump. However, considering that measuring the vertical jump height, in most cases, should be done in a practical and objective manner in the field of sports, in which the athlete does not perform the jump within the limitations of a platform, it would be more useful to use ECnsole. Therefore, ECnsole may be the more viable option as it imposes fewer restrictions.

12 gymnast were subjected to an evaluation of the fatigue gained before and after a specific training in tumbling surface. Data resulting from ECnsole instrumented insoles show that there is a modification in some variables related to the high jump performance. Statistical analysis shows that the there is an influence of the fatigue in elastic component of the low trunk in CMJ (P value 0.008) in pressure value at the instance of the jump between the PreTest and ReTest. An influence on the coordinative component in ABK (P value 0.006) also for the pressure at the beginning of the jump. Finally also a modification on the high jump performance of the pressure at the jumping instance of the RJ between the PreTest and PostTest was found (P value 0.006).

8.3 Applications in medical framework

An experiment have carried out a tracking to a group of 62 pregnant to evaluate if there is any relationship between plantar pressure distribution and back pain. On the one hand, a clinical study has been performed, concluding:

1. In week 12^{th}, younger women and those who consumed hormonal contraceptives suffer more lumbar pain. Pregnant with high BMI have more shoulder pain. And women who have high physical working load, those who work outside, who have some history of back pain, or those who have been mother before, have more inguinal pain.

2. In week 20^{th}, pregnant who have less hours of sleeping suffer more shoulder pain and inguinal pain, while those with high BMI, high physical working load, and consumed hormonal contraceptives have more inguinal pain.

3. Finally, in week 32^{nd}, the trend remains like in other weeks, but in this case those pregnant who were mother before also declare lumbar pain.

Related to the plantar pressure distribution. It was performed a descriptive analysis of the plantar pressure distribution, and a Repeated Measures ANOVA test, to determine the variation and its influence on the CoP in the Y-Axis, concluding that the centre of pressure of both feet displace towards the forefoot as

continuing the pregnancy. Also an ANOVA test was carried out to evaluate the differences between a painful group and a non painful, obtaining only significant differences in the pressure on the big toe of the right foot in week 32nd. However, due to the complexity of the data, and considering the difficulty that the pain as a subjective opinion provides, both the candidate and the research group are still analysing this huge amount of data to achieve a more complete study.

On the other hand, a study to correlate the data from shank-mounted gyroscopes and three reference systems was done. 14 young healthy men participated voluntary in this study. Participants were member of the hospital staff of Klinikum Großhadern, in Munich (Germany). The three reference systems were accelerometers,pressure-sensitive soles and a motion capture system. The test performed were normal gait at three different velocities (2, 4, and 6 $^{km}/_{h}$). Data obtained during the acceleration and deceleration phases of the treadmill were discarded. As the literature presented in this document shows, the heel strike corresponds to a trough in the gyroscope curve. However, a new finding was done related to the 'toe-off' moment, that do not coincide with the first trough of the gyroscope of the shank but is later.

8.4 Future Work

Next, the future work and research lines that will be undertaken are detailed:

Pregnant study: The analysis of the data obtained in the experiment described in this thesis work will be continued in order to obtain a relationship between the plantar pressure modifications or any possible gait disorder and the lumbar, shoulder, or inguinal pain.

Validation of ECnsole version 2.0: Same tests that were carried out for previous versions will be performed on this prototype. Trying to make the firmware as efficiency as possible.

To Improve sampling frequency of ECnsole version 2.0: A new deep improvement of the firmware will be try to accomplish with the objective to increase the sampling frequency to be to compete with most of commercial systems.

Inclusion of a new biochemical sensor: It would be very interesting to monitor the pH of the sweat using a biochemical sensor. A new microfluidic throwaway pH sensor will be also embedded in the insole.

Longitudinal study of the influence of a deep training process on gymnasts: A new study will be carried out that consist of analysing and comparing the performance in vertical jump test with two groups of gymnast. Those who will do a special training for three months and those who will do a regular one.

Metatarsalgia study using instrumented insoles: This new research work will be carried out Hospital Virgen de las Nieves in Granada. Metatarsalgia is used to refer to any painful foot condition affecting the metatarsal region of the foot. The objective of this work is to make a plantar pressure distribution study of metatarsalgia's patients.

Chapter 9

Conclusiones y trabajo futuro

Contents

9.1 Desarrollo de unas plantillas instrumentadas 226
9.2 Aplicaciones en el ámbito deportivo 230
9.3 Aplicaciones en el ámbito médico 230
9.4 Trabajo Futuro 232

El análisis de la distribución plantar, los patrones de marcha y carrera, y la postura ha ganado una gran importancia en los últimos años, no sólo en los campos relacionados con la medicina, si no también en deporte y la educación física. La integración de varios sensores en un sistema instrumentado dentro del calzado puede proveer una información muy útil para prevenir o corregir ciertos malos hábitos o posturas para mejorar la calidad de vida. Por otro lado, la información obtenida por dichas plantillas instrumentadas en otros campos de investigación como el entrenamiento deportiva puede mejorar el rendimiento deportivo o reducir las posibilidades de lesión. El trabajo que se ha llevado a cabo ha consistido en el desarrollo de varias plantillas instrumentadas y su aplicación en diferentes estudios de investigación, concretamente, en los marcos de trabajo deportivo y médico. Las principales conclusiones de este trabajo se resumen en este capítulo.

9.1 Desarrollo de unas plantillas instrumentadas

En esta tesis se ha llevado a cabo una tarea de búsqueda de sensores de presión e inerciales susceptibles de ser embebidos en una plantilla instrumentada. Como resultado, se han encontrado, testado y validado los siguientes sensores:

- Sensores de presión/fuerza:
  - Flexiforce A201: en ECnsole versión 1.0, 1.2, y 1.5.
  - Flexiforce A401: en ECnsole versión 1.5, y 2.0.
- Sensores inerciales:
  - Acelerómetro ADXL330: en ECnsole versión 1.0 y 1.2.
  - Acelerómetro and magnetómetro LSM303DLHC: en ECnsole versión 1.5.
  - Giroscopio L3GD20: en ECnsole versión 1.5.
  - Acelerómetro and magnetómetro LSM303D: en ECnsole versión 2.0.
  - Giroscopio L3GD20H: en ECnsole versión 2.0.

Se diseñó un primer prototipo de plantillas instrumentadas denominado ECnsole versión 1.0. Este consiste en dos dispositivos (maestro y esclavo) localizados en el tobillo o parte baja de la pierna del sujeto. Las principales características de esta versión son:

- 4 sensores de presión localizados en el dedo gordo, primera y quinta cabeza metatarsiana y en el talón.
- Acelerómetro analógico situado en el arco del pie.
- Comunicación inalámbrica entre las unidades maestro y esclavo utilizando el protocolo MiWi™ .
- Comunicación inalámbrica entre el maestro y el PC utilizando el protocolo MiWi™ .
- Grabación de la información de los sensores en una tarjeta de memoria μSD.
- Frecuencia de muestreo de 62 Hz.
- Aplicación software en el lado del PC para representación gráfica de los datos.

Las mayores debilidades de esta versión son la fragilidad en la conexión entre nodos y la limitada frecuencia de muestreo. Estas razones junto con el deseo de reducir costes hicieron necesario el diseño de un nuevo prototipo. La versión 1.2 de ECnsole continua utilizando los mismos sensores de presión y acelerómetro. En la versión 1.2 de las plantillas instrumentadas, el maestro y el esclavo se fusionan en un único dispositivo responsable de la adquisición de los sensores. El firmware es actualizado y optimizado alcanzando una frecuencia de muestreo de 77 Hz. Para conseguir mejorar las funcionalidades de ECnsole, se añadieron nuevos sensores a la plantilla instrumentada en la versión 1.5. Además, la electrónica de este dispositivo ha sido mejorada para la adquisición y el acondicionamiento de los sensores. Las principales mejoras de este nuevo prototipo son:

- Sustitución del acelerómetro por una Unidad de Medida Inercial (IMU) compuesta por un giroscopio triaxial, un acelerómetro triaxial, y un magnetómetro triaxial.
- Mejora del rendimiento del firmware alcanzando una frecuencia de muestreo de 333 Hz (periodo de muestre cada 3 milisegundos).
- Nueva aplicación software basada en Matlab® para el procesamiento de los datos.

La información proporcionada por los nuevos sensores añadidos en la versión 1.5 puede ser muy interesante para obtener parámetros importantes relacionados con la posición del pie y su movimiento durante la fase de vuelo. Los principales inconvenientes de esta versión son principalmente el cableado de conexionado. La posibilidad de conseguir una nueva versión que pudiera ser absolutamente inalámbrica ha sido un gran reto en esta tesis. La versión 2.0, que actualmente está en proceso de validación, ha supuesto un gran avance en comparación con el resto de versiones. La unidad de procesamiento se divide en dos dispositivos independientes que envían la información de los sensores a un smartphone o tableta android que actúan como unidades de procesamiento. Las principales características son:

- Se han añadido dos sensores de presión en la tercera cabeza metatarsiana y en la zona media del pie.
- Todo está embebido en la plantilla.
- Se utiliza una pila de botón recargable para alimentar los dispositivos.
- La electrónica para la adquisición de los sensores ha sido modificada para reducir el tamaño del sistema electrónico.
- Se ha reemplazado MiWi™ por la tecnología Bluetooth.
- El firmware ha sido modificado para reducir la carga de trabajo del microcontrolador y mejorar la frecuencia de muestreo.

- Se ha desarrollado una nueva aplicación android para la representación y almacenamiento de la información de los sensores.

Los sensores incluidos en nuestro prototipos han sido validados con sistemas estándares. Los sensores de presión han sido comparados con un sistema de medida de presión comercial mientras que la IMU se ha comparado con un sistema de cámaras infrarrojas. Además, las pruebas preliminares mostradas permiten concluir que el uso de nuestras plantillas instrumentadas, ECnsole, puede proporcionar información muy útil. A priori, puede ayudar enormemente tanto a corredores profesionales como aficionados, para adaptar su estilo de carrera o su calzado, de acuerdo a un diagnostico acerca de su grado de supinación o pronación durante dicha actividad. Por otro lado, puede ayudar, en el caso de la medicina, a prevenir lesiones no sólo de la parte inferior del tronco si no también de la espalda, en aquellos casos que las personas tiene un desorden de la marcha debido a la pronación o supinación.

El sistema presentado en este trabajo proporciona simultáneamente información de valores de presión en el dedo gordo, primer y quinto metatarso, y el talón, así como componentes angulares en los tres ejes del espacio incluyendo todos los sensores en la plantilla instrumentada. Los análisis puede llevarse a cabo con una aplicación software o mediante hojas de cálculo. El software de análisis presenta en la pantalla del ordenador los datos en tiempo real o simulación temporal para el análisis del experimento. Estos modos de representación permiten la realimentación de forma inmediata, y por lo tanto los sujetos tienen conocimiento instantáneo de su patología con el fin de corregirla. Además, las lecturas del acelerómetro proporcionan información adicional durante la fase de vuelo y la fase de apoyo en los test realizados. Por ejemplo, la detección de distribuciones de presión plantar anómalas, el movimiento lateral excesivo, la determinación del tiempo de apoyo, y la detección de asimetrías podría prevenir lesiones en el futuro y ayudar a las personas a elegir el calzado más adecuado. En este trabajo, se ha combinado el análisis de los datos de presión y aceleración para distinguir claramente entre neutral, pronador y supinador, incluso estimando diferentes grados de supinación. Este sistema es muy útil en estudios de patrones de marcha en los que las personas están afectadas por enfermedades tales como el Parkinson, astronautas después de los periodos de

gravedad cero, rehabilitación de diferentes lesiones, o simplemente para elegir el calzado más apropiado.

9.2 Aplicaciones en el ámbito deportivo

Después del análisis y comparación de los datos obtenidos con el sistema ECnsole, HSC, y el SJS, podemos concluir que ambos sistemas (PreECnsole y AccECnsole) tienen una alta validez para medir el tiempo de vuelo de un salto vertical. Sin embargo, considerando que la medida de la altura del salto vertical, en la mayoría de casos, se debe de hacer de forma práctica y objetiva en deportes, en los cuales el atleta no tenga ninguna la limitación de hacerlo sobre una plataforma, sería más útil utilizar ECnsole. Por lo tanto, ECnsole es una opción más viable ya que impone menos restricciones.

Se ha evaluado la fatiga conseguida antes y después de un entrenamiento especifico para 12 gimnastas sobre una superficie de tumbling. Los datos obtenidos por ECnsole muestran que hay una modificación en algunas variables relaciones con el rendimiento en el salto vertical. El análisis estadístico muestra que hay una influencia de la fatiga en la componente elástica de la zona baja del tronco en CMJ (P valor 0.008) para el valor de la presión en el instante de inicio del salto entre el PreTest y el ReTest. Se ha hallado influencia de la componente de coordinación en ABK (P valor 0.006) también en la presión al inicio del salto. Finalmente se ha detectado una modificación en el rendimiento del salto vertical para la presión al inicio del salto entre el PreTest y el PostTest en RJ (P valor 0.006).

9.3 Aplicaciones en el ámbito médico

Se ha llevado a cabo un experimento con 62 mujeres embarazadas para evaluar si existe alguna relación entre la distribución de la presión plantar y el dolor de espalda. Por un lado, se ha realizado un estudio clínico, concluyendo:

1. En la semana 12, las mujeres más jóvenes y aquellas que han consumido anticonceptivos hormonales sufren más dolor de espalda. Las embara-

zadas con un alto índice de masa corporal (IMC) tienen más dolor de hombros. Y aquellas mujeres que tienen una alta carga de trabajo físico, aquellas que trabajan fuera, que tienen historiales de dolor de espalda, o aquellas que han sido madres anteriormente, sufren más dolor pélvico.

2. En la semana 20, las embarazadas que duermen menos horas sufren más dolor de hombros y pélvico, mientras que aquellas con altos IMC, alta carga de trabajo físico, y que han consumido anticonceptivos hormonales tienen un mayor dolor pélvico.

3. Finalmente, en la semana 32, la tendencia se mantiene como en las anteriores semanas, aunque en este caso, aquellas mujeres que han sido madres anteriormente declaran también tener dolor de espalda.

En lo que concierne a la distribución de la presión plantar, se realizó un análisis descriptivo y un test ANOVA para medidas repetidas, con el fin de determinar la variación y la influencia del centro de presiones (CoP) del eje Y. Se concluye que el centro de presiones de ambos pies se desplaza hacia la zona posterior del pie a medida que progresa el embarazo. Además un test ANOVA se ha llevado a cabo para evaluar las diferencias entre los grupos de mujeres que les afectaba el dolor de espalda y aquellas que no, obteniendo diferencias significativas en la presión del dedo gordo del pie derecho en la semana 32 de embarazo. Sin embargo, debido a la complejidad de los datos, y considerando la dificultad que la opinión subjetiva del dolor supone, tanto el candidato como el grupo de investigación están todavía analizando está enorme cantidad de datos para conseguir un estudio más completo.

Por otro lado, se ha realizado un estudio para correlacionar los datos de un giroscopio montado en la pierna con tres sistemas de referencia. 14 hombres jóvenes participaron en este estudio. Los participantes era miembros de la plantilla del hospital Klinikum Großhadern, en Munich (Alemania). Los tres sistemas de referencia eran acelerómetros, nuestras plantillas ECnsole, y un sistema de captura de movimiento. Los test se llevaron a cabo a tres velocidades diferentes (2, 4 y 6 $^{km}/_{h}$). Los datos obtenidos durante las fases de aceleración y desaceleración de la cinta de correr se descartaron. Como se presenta en la literatura, el instante de inicio de apoyo (Heel-Strike) corresponde con un mínimo

de la curva del giroscopio. Sin embargo, hemos hallado que el instante de fin de apoyo (Toe-off), no se corresponde con el primer mínimo del giroscopio de la pierna sino después, como se había asumido hasta ahora. Estos descubrimientos son cruciales para los sistemas de grabación de la marcha los cuales tienen como objetivo evaluar los descriptores tanto temporales como espaciales de la marcha humana.

9.4 Trabajo Futuro

A continuación se detallan el trabajo futuro y las lineas de investigación que se acometerán próximamente:

Estudio de embarazadas: Se continuará el analisis de los datos obtenidos en el experimento descrito en esta tesis con el objetivo the obtener una relación entre las modificaciones en la presión plantar o cualquier desorden de la marcha y el dolor lumbar, de hombros o pélvico.

Validación de la versión 2.0 de ECnsole: Se llevaran a cabo los mismos test que se hicieron en versiones previas de este prototipo. Buscando siempre optimizar al máximo la eficiencia del firmware.

Mejora de la frecuencia de muestreo de la version 2.0: Se tratará de conseguir una nueva mejora del firmware con el objetivo de aumentar la frecuencia de muestreo para ser capaces de competer con la mayoria de sistemas comerciales.

Inclusión de un sensor bioquímico: Sería muy interesante monitar el pH del usor utilizando un sensor bioquímico. Por lo tanto, se añadirá también de forma embebida un sensor de pH bioquímico microfluidico de un sólo uso.

Estudio longitudinal de la influencia de entrenamientos en gimnastas: se llevará a cabo un nuevo estudio que consistirá en analizar y comparar el rendimiento de pruebas en saltos verticales con dos grupos de gimnastas. Un grupo que hará un entrenamiento especial durante tres meses y otro grupo que hará un entrenamiento normal.

Estudio de la metatarsalgia utilizando plantillas instrumentadas: Este nuevo trabajo de investigación se llevará a cabo en el Hospital Virgen de las Nieves en Granada. Metatarsalgia se define como cualquier dolor en el pie que afecta a la región de los metatarsos. EL objetivo de este trabajo es hacer un estudio de la distribución de la presión plantar en pacientes con metatarsalgia.

Scientific Contributions

Journal Papers

- **Validation of Instrumented Insoles for Measuring Height in Vertical Jump**
  F Martínez-Martí, J.L. González-Montesinos, D.P. Morales, J.R.F. Santos, J. Castro-Piñero, M.A. Carvajal, A.J. Palma
  International Journal of Sports Medicine **2016**, In press.

- **Gait recording with inertial sensors-how to determine initial and terminal contact**
  Kai B′otzel, **Fernando Martínez-Martí**, Miguel Ángel Carvajal Rodríguez, Annika Plate, Alberto Olivares Vicente
  Journal of Biomechanics **2016**, In press.

- **Passive UHF RFID Tag with Multiple Sensing Capabilities**
  José Fernández-Salmerón, Almudena Rivadeneyra, **Fernando Martínez-Martí**, Luis Fermín Capitán-Vallvey, Alberto J Palma, Miguel A Carvajal
  Sensors **2015**, *Volumen 15*, Number 10, 26769-26782.

- **Noise suppression in ECG signals through efficient one-step wavelet processing techniques**
  Encarnación Castillo, Diego P Morales, Antonio García, **F Martínez-Martí**, Luis Parrilla, Alberto J Palma
  Journal of Applied Mathematics **2013**, *Volumen 2013*, 13 pages.

- **Embedded sensor insole for wireless measurement of gait parameters**
  Fernando Martínez-Martí, María Sofía Martínez-García, Santiago G García-Díaz, Javier García-Jiménez, Alberto J Palma, Miguel A Carvajal
  Australasian Physical & Engineering Sciences in Medicine **2013**, *Volumen 37*, Issue 1, 25-35.

International Conferences

- **A preliminary study of the relation between back-pain and plantar pressure evolution during pregnancy**
  Fernando Martínez-Martí, Maria Sofia Martínez-García, Miguel A Carvajal, Alberto J Palma, Alejandro Molina-Molina, Victor M Soto Hermoso, Olga Ocón Hernández, Jesus Florido Navío
  37th Annual International Conference of the IEEE Engineering in Medicine and Biology Society (EMBC) **2015**, 1235-1238.

- **A dosimetry system for real time dose measurements using a commercial MOS transistor**
  Carvajal M.A., Martínez-García M.S., Torres del Río J., Guirado D., **Martínez-Martí F.**, Palma A.J.,
  Third Int. Conf. on Radiation and Dosimetry in various fields of research (RAD2015) **2015**.

- **Self-Powered System for Environmental Monitoring using Thermogenerators**
  F. Martínez-Martí, B. Molina-Farrugia, M.A. Carvajal, A.J. Palma, R. Muñoz-Bernardo, J. Banqueri
  European Congress and Exhibition on Advanced Materials and Processes (EUROMAT) **2013**.

- **Instrumented Insoles with Pressure and Acceleration Sensors**
  F Martínez-Martí, SG García-Díaz, J García-Jiménez, MS Martínez-García, A Martínez-Olmos, MA Carvajal
  International Work-Conference on Bioinformatics and Biomedical Engineering (IWBBIO) **2013**, 657 - 665.

- **Geometrical analysis of a MEMS microphone**
  A Rivadeneyra, **F Martínez-Martí**, AJ Palma, J Banqueri, RM Bernardo
  International Conference on Synthesis, Modeling, Analysis and Simulation Methods and Applications to Circuit Design (SMACD) **2012**, 169-172.

- **An imaging method for electrical capacitance tomography based on projections multiplication**
  A Martínez Olmos, E Castillo, **F Martínez-Martí**, DP Morales, A García, J Banqueri
  Journal of Physics: Conference Series **2011**, Volumen *Volumen 307*, Number 1, 1-6.

Part IV

Appendix

Apendix I

Pressure Calibration System

During instrumented insoles fabrication, a pressure calibration system was developed in order to improve calibration process both in speed and accuracy. ECsens research group have a Prusa I3 3D printer that was used to build different pieces of the calibration system.

I.a Design

For this purpose, the system proposed consist in an inverted cone with an stick cylinder where common weightlifting disc can be inserted. The cone tip was the same diameter than A201 and A401 pressure sensors. Also, a weightlifting disc filled with rice was designed to be able to monitor smaller weight changes. The pieces were designed using FreeCad open source software. Figures are shown in figure I.1. The dimensions of the pieces are shown in table I.1.

For A201 sensors	
Stick Length (mm)	150
Cone Length (mm)	35
Cone Base (mm)	90
Cone tip (mm)	9.53
For A401 sensors	
Stick Length (mm)	150
Cone Length (mm)	44
Cone Base (mm)	100
Cone tip (mm)	25.4

Table I.1: Dimensions of calibration systems designed.

As the printer has some printing error, once the pieces were printed, the real dimensions obtained are detailed in table I.2.

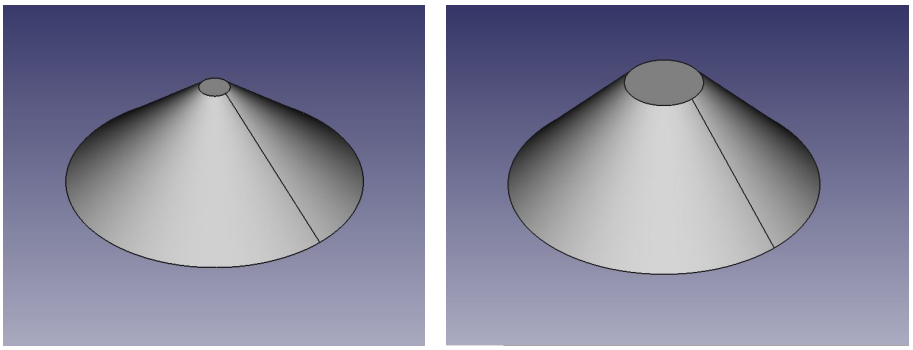

(a) A201 Cone.

(b) A401 Cone.

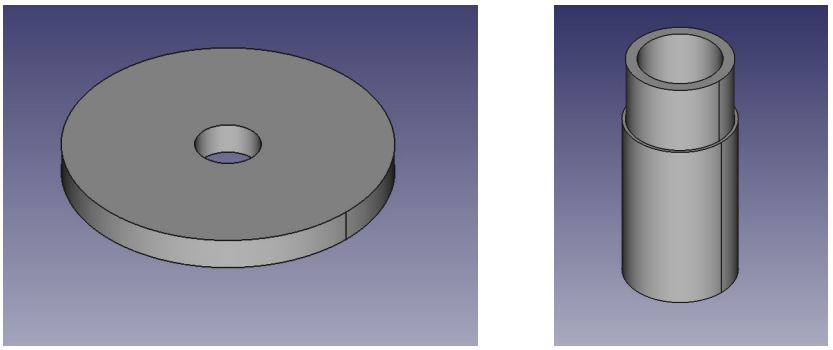

(c) Weightlifting disc.

(d) Stick cylinder.

Figure I.1: Pressure Calibration System designed using FreeCAD.

I.b Fabrication process

As it was explained, for the fabrication of the pieces, a 3D printer was used. Specifically, the model Prusa I3, that is a 3D printer with GPL license with a resolution of 80 micron and print volume of 20 x 20 x 20 cm.

The configuration parameters set on the printer are shown in table I.3

For A201 sensors	
Stick Length (mm)	150.10
Cone Length (mm)	35.2
Cone Base (mm)	88.52
Cone tip (mm)	9.60
For A401 sensors	
Stick Length (mm)	150.10
Cone Length (mm)	44.64
Cone Base (mm)	99.60
Cone tip (mm)	26.15

Table I.2: Real dimensions of calibration systems manufactured.

Quality	
Layer Height (mm)	0.3
Shell Thickness (mm)	3
Retraction	Enable
Fill	
Bottom/Top Thickness (mm)	0.9
Printing Temperature (°C)	228
Bed Temperature (°C)	105
Support	
Support Type	Everywhere
Platform Adhesion Type	Brim
Filament	
Diameter (mm)	2.85
Flow (%)	100.0

Table I.3: Configuration parameters of the 3D printer.

I.c Calibration System

The resulting calibration system is presented in figure I.2. The system is pretty straightforward to use. Once the type of sensor to calibrated is decided, the user only needs to insert the stick cylinder in the corresponding cone. After that, the calibration system is ready to use and the user only has to insert weightlifting disc (like the ones manufactured in figure I.2c) from a normal gym. An example of real use is shown on figure I.3.

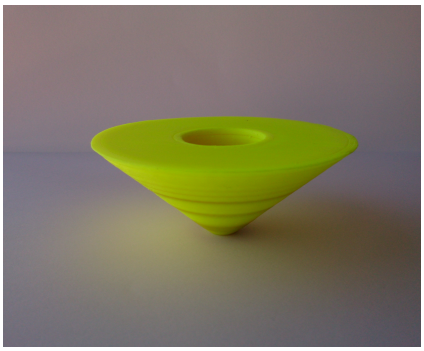

(a) A201 Cone.

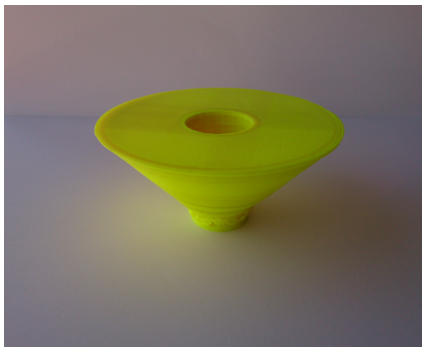

(b) A401 Cone.

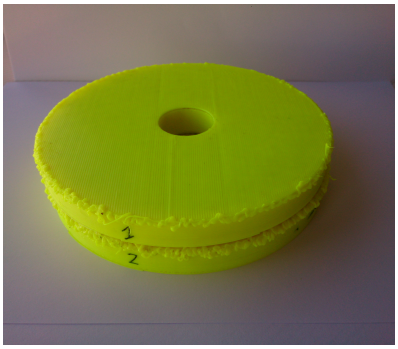

(c) Weightlifting disc.

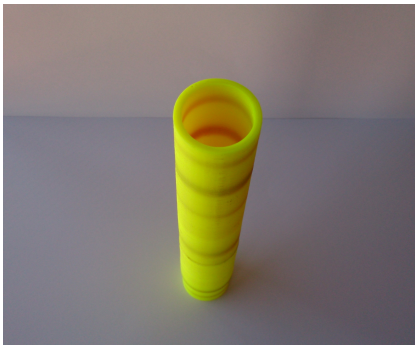

(d) Stick cylinder.

Figure I.2: Pieces of the pressure calibration system manufactured using 3D Printer Prusa I3.

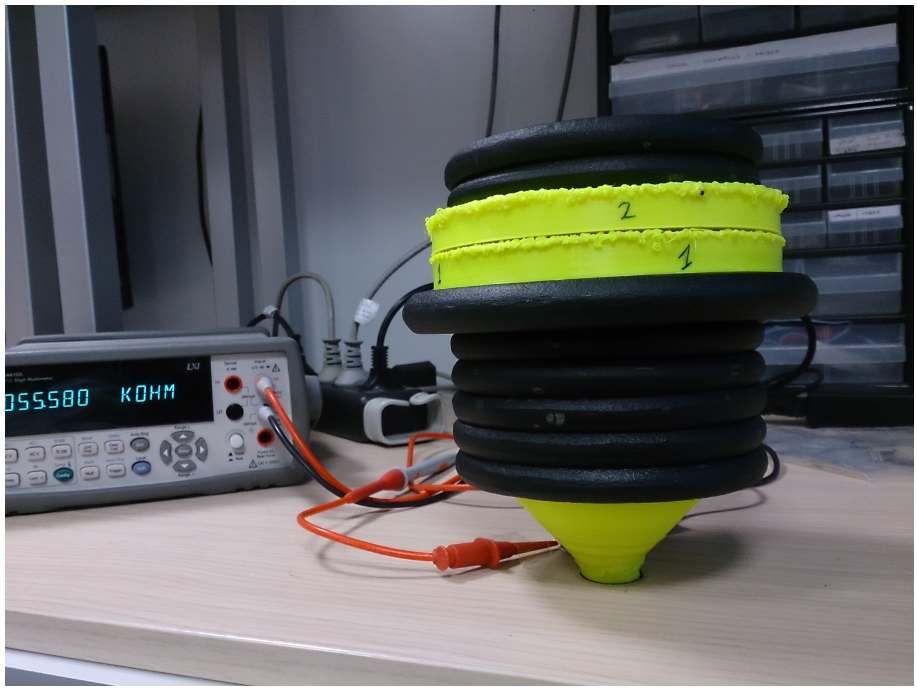

Figure I.3: Real use of the pressure calibration system manufactured.

Apendix II

Documentation related to pregnancy study

Contents

I.a Design 242
I.b Fabrication process 243
I.c Calibration System 245

II.a Hospital Ethics Committee

Servicio Andaluz de Salud
CONSEJERÍA DE SALUD

DON JUAN MORALES ARCAS, EN CALIDAD DE SECRETARIO DE LA COMISIÓN DE ÉTICA E INVESTIGACIÓN BIOMÉDICA DEL HOSPITAL UNIVERSITARIO SAN CECILIO DE GRANADA,

CERTIFICA

Que la Comisión ha informado favorablemente el proyecto presentado por la ***I.P.*** María Soledad Quezada Rojas Residente del Servicio de Obstetricia y Ginecología del Hospital Universitario San Cecilio, ***titulado: "relación entre los cambios de la presión plantar a lo largo de la gestación y el dolor lumbar"*** **Directores** Prof. Dr. Jesús Florido Navío Profesor Titular de Obstetricia y Ginecología de la Universidad de Granada Prof.Dr. Luis Navarrete López-Cózar Catedrático Departamento Obstetricia y Ginecología Dra. Carmen Padilla Vinuesa FEA Ginecología y Obstetricia H.U. San Cecilio

Que se cumplen los requisitos necesarios de idoneidad del protocolo en relación con los objetivos del estudio y están justificados los riesgos y molestias previsibles para el sujeto.

La capacidad del investigador y los medios disponibles son apropiados para llevar a cabo el mencionado estudio.

Es adecuado el procedimiento para obtener el consentimiento informado.

Y que este Comité acepta que dicho proyecto sea realizado en este Centro.

Lo que firmo en Granada, a siete de enero de dos mil diez.

HOSPITAL UNIVERSITARIO "San Cecilio"
Avda. Dr. Oloriz, 16. 18012 - GRANADA
Tfno.: 958 02 30 00

II.b Informed Consent

UGC de Ginecología y Obstetricia (HUSC-Granada) Departamento de Ginecología y Obstetricia

CONSENTIMIENTO INFORMADO – CONSENTIMIENTO POR ESCRITO DEL PACIENTE

Yo (Nombre y Apellidos):.....

- He leído el documento informativo que acompaña a este consentimiento (Información al Paciente)
- He podido hacer preguntas sobre el **Cambios de la presión plantar a lo largo de la gestiación.**
- He recibido suficiente información sobre el **Cambios de la presión plantar a lo largo de la gestiación..**
  He hablado con el investigador informador: .....
- Comprendo que mi participación es voluntaria y soy libre de participar o no en el estudio.
- Se me ha informado que todos los datos obtenidos en este estudio serán confidenciales y se tratarán conforme establece la Ley Orgánica de Protección de Datos de Carácter Personal 15/99.
- Se me ha informado de que la información obtenida sólo se utilizará para los fines específicos del estudio.

Comprendo que puedo retirarme del estudio:

- Cuando quiera
- Sin tener que dar explicaciones
- Sin que esto repercuta en mis cuidados médicos

Presto libremente mi conformidad para participar en el *proyecto:* **Cambios de la presión plantar a lo largo de la gestiación.**

Firma del paciente
(o representante legal en su caso)

Nombre y apellidos:.....
Fecha: .....

Firma del investigador informador

Nombre y apellidos: .....
Fecha: .....

Ejemplar para el investigador 2

II.c Questionnaire Spanish

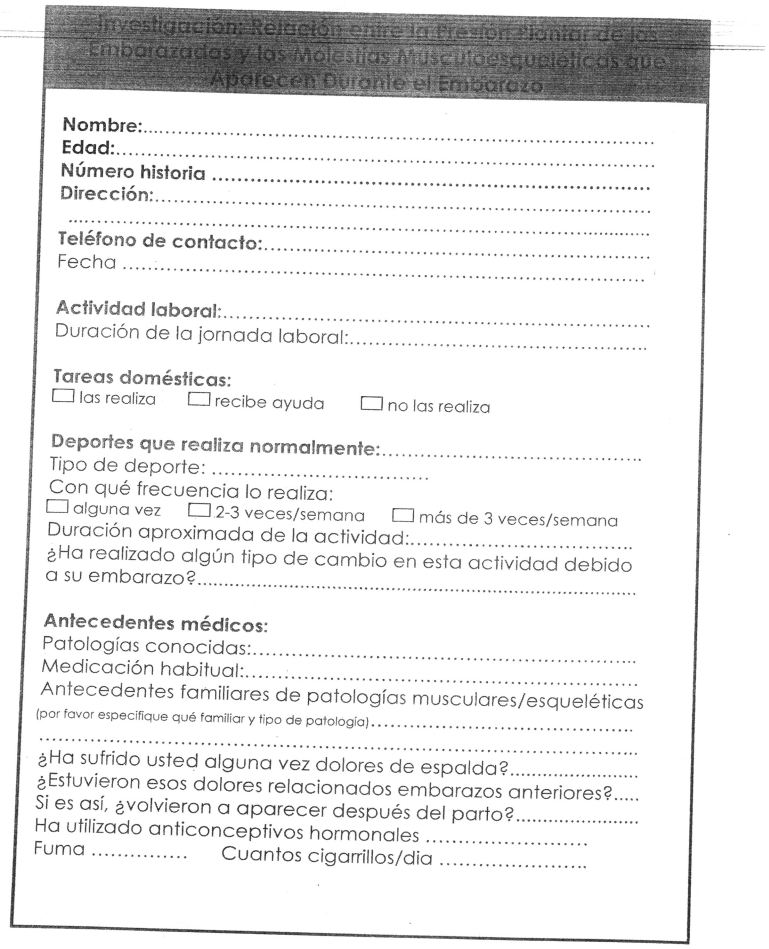

Investigación: Relación entre la Presión Plantar de las Embarazadas y las Molestias Musculoesqueléticas que Aparecen Durante el Embarazo

Nombre:.....
Edad:.....
Número historia .....
Dirección:.....
.....
Teléfono de contacto:.....
Fecha .....

Actividad laboral:.....
Duración de la jornada laboral:.....

Tareas domésticas:
☐ las realiza ☐ recibe ayuda ☐ no las realiza

Deportes que realiza normalmente:.....
Tipo de deporte: .....
Con qué frecuencia lo realiza:
☐ alguna vez ☐ 2-3 veces/semana ☐ más de 3 veces/semana
Duración aproximada de la actividad:.....
¿Ha realizado algún tipo de cambio en esta actividad debido a su embarazo?.....

Antecedentes médicos:
Patologías conocidas:.....
Medicación habitual:.....
Antecedentes familiares de patologías musculares/esqueléticas
(por favor especifique qué familiar y tipo de patología).....
.....
¿Ha sufrido usted alguna vez dolores de espalda?.....
¿Estuvieron esos dolores relacionados embarazos anteriores?.....
Si es así, ¿volvieron a aparecer después del parto?.....
Ha utilizado anticonceptivos hormonales .....
Fuma ..... Cuantos cigarrillos/dia .....

Datos físicos:
Talla:.....
Peso (anterior al embarazo):.....

Antecedentes obstétricos:
Número de embarazos(contando el actual).....
Abortos .....
Número de partos:
- vía vaginal:.....
- por cesárea:.....

Incidencias en embarazos anteriores:.....
Epidural .....
Trabajo de parto prolongado .....

Embarazo actual:
Semana de embarazo:.....
Incidencia durante embarazo .....
Peso fetal .....

1. ¿Le duele la espalda en este momento?..... ☐ si ☐ no

2. ¿Siente dolor entre sus hombros en este momento?..... ☐ si ☐ no

3. ¿Siente dolor en la zona púbica o en sus ingles?..... ☐ si ☐ no

4. ¿Tuvo dolores de espalda antes de su primer embarazo?..... ☐ si ☐ no

5. ¿Le ha dolido la espalda en sus embarazos anteriores?..... ☐ es mi primer embarazo ☐ si ☐ no

6. Por favor, cuantifique la carga física que supone su trabajo:
(ninguna carga) **0 1 2 3 4 5 6 7 8 9 10** (carga física importante)

7. Por favor, valore su dolor de la última semana:
(ninguno) **0 1 2 3 4 5 6 7 8 9 10** (incapacitante)

8. Valore su dolor en este momento:
(ninguno) **0 1 2 3 4 5 6 7 8 9 10** (incapacitante)

9. ¿Cuándo empezó el episodio actual de dolor?
- ☐ Hace menos de 1 semana
- ☐ Hace menos de 2 semanas
- ☐ Hace de 2 a 8 semanas
- ☐ Hace entre 8 semanas y 3 meses
- ☐ Hace entre 3 y 6 meses
- ☐ Hace 6 meses o más

10. Durante la última semana, ¿con qué frecuencia ha necesitado tomar analgésicos? (por ejemplo aspirina, ibuprofeno, paracetamol...)
☐ Nunca ☐ 1 vez ☐ 2 veces ☐ 3 veces ☐ 4 o más veces

11. ¿Cuántas horas duerme por la noche?

No puedo dormir 1 2 3 4 5 6 7 8 9 10 toda la noche

12. Ha tenido alguna vez tratamiento para el dolor de:

- ☐ espalda
- ☐ piernas
- ☐ cuello
- ☐ brazo
- ☐ pubis/ingles
- ☐ ninguno de los anteriores

13. Si ha tenido tratamiento, ¿Cómo de satisfactorio le ha parecido?

(nada satisfactorio) 0 1 2 3 4 5 6 7 8 9 10 (completamente satisfactorio)

A contestar a partir de la 2ª visita:

¿Ha realizado cambios en su actividad física desde su última visita? Por favor, si lo ha hecho, coméntelos:.....
.....
.....
.....
.....

¿Ha habido alguna incidencia en su embarazo desde la última? (por ejemplo, caídas, sangrados...) Por favor, si las ha habido, coméntelas:.....
.....
.....
.....
.....

Datos exploración física (a rellenara partir segunda visita)

Talla:.....
Peso actual:.....Ganancia:.....
Perímetro abdominal:.....
Peso Fetal .....

II.d Questionnaire English

Research: Relationship between plantar pressure of pregnant women and muscle-skeletal pain which appears during pregnancy.

Name: .....

Age: .....

Medical record: .....

Address:.....

Phone: .....

Date: .....

Work activity: .....

Duration of working time: .....

Housework:

.....

____ I do ____I have help ____I do not do

Sports you usually do: .....

Kind of sport: .....

How often:

____ sometimes ____twice/three times /week ____More than three times/week

Approximaty activity length: .....

Have you done any kind of change in this activity due to your pregnancy? .....

Mecical history: .....

Pathologies known: .....

Regular medication: .....

Family history of muscular/skeletal pathologies (please give the family member and type of pathology).....

Have you ever suffered lumbar pain?.....

Have those pains been related with previous pregnancies? .....

In that case, have they appeared after labour?.....

Have you ever used hormonal contraceptives?.....

Do you smoke? ..... How many cigarettes per day?.....

Physical data:

Size:

Weight (before pregnancy):

Obstetric history

Number of pregnancies (with the current pregnancy)

Miscarriage

Number of birth:

- Normal birth:
- Caesarian section:

Incidents in previous pregnancies:

Epidural:

Work of long birth:

Currently pregnancy:

Week of pregnancy:

Incident during pregnancy:

Fetal weight:

1. Do you have back pain right now? __Yes __No
2. Do you have shoulder pain right now? __Yes __No
3. Do you have inguinal or pubic pain? __Yes __No
4. Did you have back pain before your first pregnancy? __Yes __No
5. Did you have back pain in your previous pregnancies?
   __It is my first pregnancy __Yes __No
6. Please quantify the physical charge of your work:
   (None) 0 1 2 3 4 5 6 7 8 9 10 (Important physical charge)
7. Please, give a value to your pain during the last week:
   (None) 0 1 2 3 4 5 6 7 8 9 10 (Incapacitating)
8. Give a value to your pain right now:
   (None) 0 1 2 3 4 5 6 7 8 9 10 (Incapacitating)
9. When did it start the currently pain phase?
   __Less than 1 week
   __Less than 2 weeks

11. How many hours do you sleep during the night?

(I cannot sleep) 0 1 2 3 4 5 6 7 8 9 10 (During the entire night)

12. Did you have sometime treatment for the pain in?

__Back

__Legs

__Neck

__Arm

__Inguinal/pubic

__neither

13. If you had have treatment, how satisfied were you?

(No satisfactory) 0 1 2 3 4 5 6 7 8 9 10 (Completely satisfactory)

Answer from 2nd visit in advance:

Have you done changes in your physical activity from your last visit? Please, if you have done, explain them:

Have been there any incident during your pregnancy from last visit? (i.e. falls, bleeding…) Please, if there has been, explain them:

Physical examination data (answer from 2nd visit in advance :)

Size:

Actual weight: Increasing:

Abdominal perimeter:

Fetal weight:

Bibliography

[1] A. Martínez Assucena, J. Pradas Silvestre, M. Sánchez Ruiz, and M. Peydro de Moya, "Plantillas instrumentadas. Utilidad clínica," *Rehabilitación*, vol. 39, no. 6, pp. 324–330, jan 2005. [Online]. Available: http://www.sciencedirect.com/science/article/pii/S0048712005743668

[2] P. Esser, H. Dawes, J. Collett, and K. Howells, "Insights into gait disorders: Walking variability using phase plot analysis, Parkinson's disease," *Gait and Posture*, vol. 38, no. 4, pp. 648–652, 2013. [Online]. Available: http://dx.doi.org/10.1016/j.gaitpost.2013.02.016

[3] R. Okuno, S. Fujimoto, J. Akazawa, M. Yokoe, S. Sakoda, and K. Akazawa, "Analysis of spatial temporal plantar pressure pattern during gait in Parkinson's disease," in *Engineering in Medicine and Biology Society, 2008. EMBS 2008. 30th Annual International Conference of the IEEE*, 2008, pp. 1765–1768.

[4] A. D. Groot, R. Decker, and K. B. Reed, "Gait enhancing mobile shoe (GEMS) for rehabilitation," in *3rd Joint EuroHaptics Conference and Symposium on Haptic Interfaces for Virtual Environment and Teleoperator Systems, World Haptics 2009*, 2009, pp. 190–195.

[5] R. Schniepp, M. Wuehr, S. Huth, C. Pradhan, T. Brandt, and K. Jahn, "Gait characteristics of patients with phobic postural vertigo: Effects of fear of falling, attention, and visual input," *Journal of Neurology*, vol. 261, no. 4, pp. 738–746, 2014.

[6] A. Martínez Assucena, M. Sánchez Ruiz, M. Barrés Carsí, C. Pérez Lahuerta, A. Guerrero Alonso, and C. Soler Gracia, "Un nuevo método de evaluación diagnóstica y terapéutica de las patologías del pie basado en las plantillas instrumentadas Biofoot/IBV," *Rehabilitación*, vol. 37, no. 5, pp. 240–251, jan 2003. [Online]. Available: http://www.sciencedirect.com/science/article/pii/S0048712003733842

[7] J. Mora Vicente, P. Ruiz Gallardo, A. Martínez Olmos, A. J. Palma López, J. L. González Montesinos, and M. Á. Carvajal Rodríguez, "Sistema de medición de los parámetros temporales de la marcha, la carrera y el salto mediante fotodetectores," feb 2011. [Online]. Available: http://digibug.ugr.es/handle/10481/24575

[8] J. García-Jiménez, "Desarrollo de un sistema de monitorización de la marcha, carrera y salto," Master Thesis, University of Granada, 2010.

[9] S. G. García-Díaz, "Desarrollo del programa de control y análisis de un sistema de monitorización de la marcha, carrera y salto," Master Thesis, University of Granada, 2010.

[10] M. S. Martínez-García, "Desarrollo de un Sistema de Monitorización de Motricidad para Rehabilitación," Masther Thesis, Polytechnical University of Madrid, 2011.

[11] Blausen.com Staff, "Bones in lower leg and foot," 2014.

[12] E. N. Marieb and K. Hoehn, *Human Anatomy & Physiology*. Pearson Benjamin Cummings, 2007. [Online]. Available: https://books.google.com/books?id=x1uEB68iitwC{&}pgis=1

[13] M. R. Hawes and D. Sovak, "Quantitative morphology of the human foot in a North American population." *Ergonomics*, vol. 37, no. 7, pp. 1213–26, jul 1994. [Online]. Available: http://www.tandfonline.com/doi/abs/10.1080/00140139408964899

[14] L. Shu, T. Hua, Y. Wang, Q. Qiao Li, D. D. Feng, and X. Tao, "In-shoe plantar pressure measurement and analysis system based on fabric

pressure sensing array," *IEEE transactions on information technology in biomedicine : a publication of the IEEE Engineering in Medicine and Biology Society*, vol. 14, no. 3, pp. 767–75, may 2010. [Online]. Available: http://ieeexplore.ieee.org/articleDetails.jsp?arnumber=5378500

[15] P. Bennetti and L. Duplock, "Pressure distribution beneath the human foot," *Journal of the American Podiatric Medical Association*, vol. 83, no. 12, pp. 674–678, 1993. [Online]. Available: http://www.japmaonline.org/doi/abs/10.7547/87507315-83-12-674

[16] M. Nyska, C. McCabe, K. Linge, P. Laing, and L. Klenerman, "Effect of the shoe on plantar foot pressures," *Acta Orthopaedica Scandinavica*, jul 2009. [Online]. Available: http://www.tandfonline.com/doi/abs/10.3109/17453679508994640{#}.VgLnvdXtmko

[17] E. M. Hennig, A. Staats, and D. Rosenbaum, "Plantar Pressure Distribution Patterns of Young School Children in Comparison to Adults," *Foot & Ankle International*, vol. 15, no. 1, pp. 35–40, jan 1994. [Online]. Available: http://fai.sagepub.com/content/15/1/35.full

[18] D. L. Damiano, M. F. Abel, J. Fontaine, G. Juhl, and D. Carmines, "Age related changes in plantar pressure during gait in normally developing children," *Gait & Posture*, vol. 7, no. 2, pp. 175–176, mar 1998. [Online]. Available: https://www.infona.pl//resource/bwmeta1.element.elsevier-34b7ef30-175a-3ad2-a5dd-2b3851168873

[19] M. P. Murray, R. C. Kory, and B. H. Clarkson, "Walking patterns in healthy old men." *Journal of gerontology*, vol. 24, no. 2, pp. 169–78, apr 1969. [Online]. Available: http://www.ncbi.nlm.nih.gov/pubmed/5789252

[20] P. M.M. and J. F.W., "The Foot/Shoe Interface," in *Running Injuries*. WB Saunders, 1997, ch. The Foot/S, pp. 20–29.

[21] M. W. Whittle, *Gait analysis: an introduction*, Edinburgh, Ed. Butterworth-Heinemann, 2003.

[22] W. J. Crosbie and A. C. Nicol, "Reciprocal aided gait in paraplegia." *Paraplegia*, vol. 28, no. 6, pp. 353–63, jul 1990. [Online]. Available: http://dx.doi.org/10.1038/sc.1990.48

[23] K. Mueller, M. Cornwall, T. McPoil, D. Mueller, and J. Barnwell, "Effect of a Tone-Inhibiting Dynamic Ankle-Foot Orthosis on the Foot-Loading Pattern of a Hemiplegie Adult: A Preliminary Study." *Journal of Prosthetics and Orthotics*, vol. 4, no. 2, pp. 86–92, 1992. [Online]. Available: http://journals.lww.com/jpojournal/Abstract/1992/00420/Effect{_}of{_}a{_}Tone{_}Inhibiting{_}Dynamic{_}Ankle{_}Foot.3.aspx

[24] C. Soler Gracia, J. Sánchez Lacuesta, J. Prat, R. Lafuente, J. Belda, R. Poveda, and P. Vera, "Valoración de Ortesis de Descarga mediante Plantillas Instrumentadas. Ortesis de Inmovilización. Equalizer Air Walker," *Técnica Ortopédica Internacional*, vol. 37, no. 8, pp. 5–19, 1997.

[25] IWGDF, "The International Working Group of Diabetic Foot," 2003.

[26] T. J. Salpavaara, J. A. Verho, J. O. Lekkala, and J. E. Halttunen, "Embedded capacitive sensor system for hip surgery rehabilitation: Online measurements and long-term stability," in *2008 30th Annual International Conference of the IEEE Engineering in Medicine and Biology Society*, vol. 2008. IEEE, aug 2008, pp. 935–938. [Online]. Available: http://www.ncbi.nlm.nih.gov/pubmed/19162811

[27] K. E. Gordon, M. Wu, J. H. Kahn, Y. Y. Dhaher, and B. D. Schmit, "Ankle load modulates hip kinetics and EMG during human locomotion." *Journal of neurophysiology*, vol. 101, no. 4, pp. 2062–76, apr 2009. [Online]. Available: http://jn.physiology.org/content/101/4/2062.abstract

[28] E. Morag and P. Cavanagh, "Structural and functional predictors of regional peak pressures under the foot during walking," *Journal of Biomechanics*, vol. 32, no. 4, pp. 359–370, apr 1999. [Online]. Available: http://www.jbiomech.com/article/S0021929098001882/fulltext

[29] J. Bieber, J. Coates, K. Lohnmann, and J. Danoff, "The Effects of Pronation-Controlling Orthotic Devices on Pressure and Force under the

Foot during Dynamic Stance," *Physical Therapy*, vol. 68, no. 5, pp. 805–805, 1988.

[30] A. J. M. Boulton, C. A. Hardisty, R. P. Betts, C. I. Franks, R. C. Worth, J. D. Ward, and T. Duckworth, "Dynamic Foot Pressure and Other Studies as Diagnostic and Management Aids in Diabetic Neuropathy," *Diabetes Care*, vol. 6, no. 1, pp. 26–33, jan 1983. [Online]. Available: http://care.diabetesjournals.org/content/6/1/26.abstract

[31] E. Eils, S. Nolte, M. Tewes, L. Thorwesten, K. Völker, and D. Rosenbaum, "Modified pressure distribution patterns in walking following reduction of plantar sensation," *Journal of Biomechanics*, vol. 35, no. 10, pp. 1307–1313, oct 2002. [Online]. Available: http://www.jbiomech.com/article/S0021929002001689/fulltext

[32] A. J. Taylor, H. B. Menz, and A.-M. Keenan, "Effects of experimentally induced plantar insensitivity on forces and pressures under the foot during normal walking." *Gait & posture*, vol. 20, no. 3, pp. 232–7, dec 2004. [Online]. Available: http://www.gaitposture.com/article/S096663620400027X/fulltext

[33] E. Morag, S. Pammer, A. Boulton, M. Young, K. Deffner, and P. Cavanagh, "Structural and functional aspects of the diabetic foot," *E Morag, SE Pammer, AJM Boulton, MJ Young, KT Deffner, PR Cavanagh. 1997. Structural and functional aspects of the diabetic foot. Clinical Biomechanics 12 (3): S9-S10.*, vol. 3, no. 12, pp. S9–S10, 1997. [Online]. Available: https://www.infona.pl//resource/bwmeta1.element.elsevier-c851cd35-b9e1-33af-ae05-958456923c4f

[34] M. Zequera, S. Stephan, and J. Paul, "The "PAROTEC" foot pressure measurement system and its calibration procedures (2005)." *Conference proceedings : ... Annual International Conference of the IEEE Engineering in Medicine and Biology Society. IEEE Engineering in Medicine and Biology Society. Annual Conference*, vol. 1, pp. 4135–9, jan 2006. [Online]. Available: http://ieeexplore.ieee.org/articleDetails.jsp?arnumber=4462711

[35] T. M. Owings, J. Apelqvist, A. Stenström, M. Becker, S. A. Bus, A. Kalpen, J. S. Ulbrecht, and P. R. Cavanagh, "Plantar pressures in diabetic patients with foot ulcers which have remained healed." *Diabetic medicine : a journal of the British Diabetic Association*, vol. 26, no. 11, pp. 1141–6, nov 2009. [Online]. Available: http://www.ncbi.nlm.nih.gov/pubmed/19929993

[36] H. Pham, D. G. Armstrong, C. Harvey, L. B. Harkless, J. M. Giurini, and A. Veves, "Screening techniques to identify people at high risk for diabetic foot ulceration: a prospective multicenter trial," *Diabetes Care*, vol. 23, no. 5, pp. 606–611, may 2000. [Online]. Available: http://care.diabetesjournals.org/content/23/5/606.abstract

[37] M. J. Mueller, D. J. Lott, M. K. Hastings, P. K. Commean, K. E. Smith, and T. K. Pilgram, "Efficacy and mechanism of orthotic devices to unload metatarsal heads in people with diabetes and a history of plantar ulcers." *Physical therapy*, vol. 86, no. 6, pp. 833–42, jun 2006. [Online]. Available: http://ptjournal.apta.org/content/86/6/833.abstract

[38] H. C. Ostgaard and G. B. Andersson, "Postpartum low-back pain." *Spine*, vol. 17, no. 1, pp. 53–5, jan 1992. [Online]. Available: http://www.ncbi.nlm.nih.gov/pubmed/1531555

[39] C. D. Skaggs, H. Prather, G. Gross, J. W. George, P. A. Thompson, and D. M. Nelson, "Back and pelvic pain in an underserved United States pregnant population: a preliminary descriptive survey." *Journal of manipulative and physiological therapeutics*, vol. 30, no. 2, pp. 130–4, feb 2007. [Online]. Available: http://www.jmptonline.org/article/S0161475406003320/fulltext

[40] R. Alvarez, I. A. Stokes, D. E. Asprinio, S. Trevino, and T. Braun, "Dimensional changes of the feet in pregnancy." *The Journal of bone and joint surgery. American volume*, vol. 70, no. 2, pp. 271–4, feb 1988. [Online]. Available: http://jbjs.org/content/70/2/271.abstract

[41] M. N. Orlin and T. G. McPoil, "Plantar pressure assessment." *Physical therapy*, vol. 80, no. 4, pp. 399–409, apr 2000. [Online]. Available: http://ptjournal.apta.org/content/80/4/399.short

[42] M. Nyska, D. Sofer, A. Porat, C. B. Howard, A. Levi, and I. Meizner, "Planter foot pressures in pregnant women." *Israel journal of medical sciences*, vol. 33, no. 2, pp. 139–46, feb 1997. [Online]. Available: http://europepmc.org/abstract/med/9254877

[43] R. Margaria, P. Aghemo, and E. Rovelli, "Measurement of muscular power (anaerobic) in man." *Journal of applied physiology*, vol. 21, no. 5, pp. 1662–4, sep 1966. [Online]. Available: http://jap.physiology.org/content/21/5/1662.abstract

[44] A. Belli and C. Bosco, "Influence of stretch-shortening cycle on mechanical behaviour of triceps surae during hopping." *Acta physiologica Scandinavica*, vol. 144, no. 4, pp. 401–8, apr 1992. [Online]. Available: http://www.ncbi.nlm.nih.gov/pubmed/1605042

[45] J. L. Gonzalez-Montesinos, "Alternativa instrumental al test de repeat jump de Bosco: el pulsador plantar perfeccionado," *Inef Castilla-Leon. Tesina licenciatura (sin publicar*, 1996.

[46] K. K. J. Chia, S. Suresh, A. Kuah, J. L. J. Ong, J. M. T. Phua, and A. L. Seah, "Comparative trial of the foot pressure patterns between corrective orthotics,formthotics, bone spur pads and flat insoles in patients with chronic plantar fasciitis." *Annals of the Academy of Medicine, Singapore*, vol. 38, no. 10, pp. 869–75, oct 2009. [Online]. Available: http://www.ncbi.nlm.nih.gov/pubmed/19890578

[47] P.-l. Wong, K. Chamari, A. Chaouachi, D. W. Mao, U. Wisloff, and Y. Hong, "Difference in plantar pressure between the preferred and non-preferred feet in four soccer-related movements," *British Journal of Sports Medicine*, vol. 41, no. 2, pp. 84–92, feb 2007. [Online]. Available: http://bjsm.bmj.com/content/41/2/84.abstract

[48] P.-l. Wong, K. Chamari, D. W. Mao, U. Wisløff, and Y. Hong, "Higher plantar pressure on the medial side in four soccer-related movements." *British journal of sports medicine*, vol. 41, no. 2, pp. 93–100, feb 2007. [Online]. Available: http://bjsm.bmj.com/content/41/2/93.abstract

[49] O. Girard, F. Eicher, F. Fourchet, J. P. Micallef, and G. P. Millet, "Effects of the playing surface on plantar pressures and potential injuries in tennis," *British Journal of Sports Medicine*, vol. 41, no. 11, pp. 733–738, nov 2007. [Online]. Available: http://bjsm.bmj.com/content/41/11/733.abstract

[50] R. T. Cheung and G. Y. Ng, "Influence of Different Footwear on Force of Landing During Running," *Physical Therapy*, vol. 88, no. 5, pp. 620–628, feb 2008. [Online]. Available: http://ptjournal.apta.org/content/88/5/620.abstract

[51] Desarrollo de Software Deportivo S.L., "SportJump System Pro." [Online]. Available: http://dsd.es/jumpsysp.htm

[52] C. I. R. systems Inc, "GaitRide." [Online]. Available: http://www.gaitrite.com/about.htm

[53] A. Muro-de-la Herran, B. Garcia-Zapirain, and A. Mendez-Zorrilla, "Gait analysis methods: an overview of wearable and non-wearable systems, highlighting clinical applications." *Sensors (Basel, Switzerland)*, vol. 14, no. 2, pp. 3362–94, jan 2014. [Online]. Available: http://www.mdpi.com/1424-8220/14/2/3362/htm

[54] BTS Bioengineering, "BTS GaitLab." [Online]. Available: http://www.btsbioengineering.com/products/integrated-solutions/bts-gaitlab/

[55] I. d. B. de Valencia, "Biofoo/IBV. Sistema de plantillas instrumentadas para el análisis de las presiones plantares." [Online]. Available: http://www.ibv.org/

[56] A. Martínez-Nova, J. C. Cuevas-García, J. Pascual-Huerta, and R. Sánchez-Rodríguez, "BioFoot® in-shoe system: Normal values

and assessment of the reliability and repeatability," *Foot*, vol. 17, no. 4, pp. 190–196, 2007.

[57] Paromed, "Parotec." [Online]. Available: http://www.paromed.com.au/Foot-Pressure-Meas-.html

[58] P. Porwik, J. Zygula, R. Doroz, and R. Proksa, "Biometric Recognition System Based on the Motion of the Human Body Gravity Centre Analysis," *Journal of Medical Informatics & Technologies*, vol. 15, pp. 61–70, 2010.

[59] Tekscan, "F-Scan In-Shoe Plantar Pressure Analysis," http://www.tekscan.com/medical/system-fscan1.html.

[60] P. Catalfamo, D. Moser, S. Ghoussayni, and D. Edwins, "Detections of Gait Events Using and F-Scan In-Shoe Pressure MEasurement System," *Gait & Posture*, vol. 3, pp. 420–426, 2008.

[61] P. W. Kong and H. D. Heer, "Wearing the F-Scan mobile in-shoe pressure measurement system alters gait characteristics during running," *Gait & Posture*, vol. 29, pp. 143–145, 2009.

[62] M. Takano, H. Noguchi, M. Oe, H. Sanada, and T. Mori, "Development and evaluation of a system to assess the effect of footwear on the in shoe plantar pressure and shear during gait," *ROBOMECH Journal*, vol. 1, no. 1, p. 4, 2014. [Online]. Available: http://www.robomechjournal.com/content/1/1/4

[63] H. B. Menz and M. E. Morris, "Clinical determinants of plantar forces and pressures during walking in older people," *Gait & Posture*, vol. 24, no. 2, pp. 229–236, 2006. [Online]. Available: http://www.sciencedirect.com/science/article/pii/S096663620500175X

[64] R. Liu, Y. L. Kwok, Y. Li, T. T. Lao, and X. Zhang, "Skin pressure profiles and variations with body postural changes beneath medical elastic compression stockings." *International journal of dermatology*, vol. 46, no. 5, pp. 514–23, may 2007. [Online]. Available: http://www.ncbi.nlm.nih.gov/pubmed/17472687

[65] G. Vidmar and P. Novak, "Reliability of in-shoe plantar pressure measurements in rheumatoid arthritis patients," *International Journal of Rehabilitation Research*, vol. 32, no. 1, pp. 36–40, 2009. [Online]. Available: http://journals.lww.com/intjrehabilres/Abstract/2009/03000/Reliability{_}of{_}in{_}shoe{_}plantar{_}pressure.4.aspx

[66] N. Gmbd, "Pedar-X." [Online]. Available: http://novel.de/novelcontent/pedar

[67] a. Forner Cordero, H. J. F. M. Koopman, and F. C. T. Van Der Helm, "Use of pressure insoles to calculate the complete ground reaction forces," *Journal of Biomechanics*, vol. 37, no. 9, pp. 1427–1432, 2004.

[68] S. J. Ellis, H. Hillstrom, R. Cheng, J. Lipman, G. Garrison, and J. T. Deland, "The development of an intraoperative plantar pressure assessment device." *Foot & ankle international*, vol. 30, no. 4, pp. 333–40, apr 2009. [Online]. Available: http://fai.sagepub.com/content/30/4/333.full

[69] Moticon, "OpenGo." [Online]. Available: http://www.moticon.de/

[70] B. J. Braun, N. T. Veith, R. Hell, S. Döbele, M. Roland, M. Rollmann, J. Holstein, and T. Pohlemann, "Validation and reliability testing of a new, fully integrated gait analysis insole." *Journal of foot and ankle research*, vol. 8, p. 54, jan 2015. [Online]. Available: http://www.pubmedcentral.nih.gov/articlerender.fcgi?artid=4578601{&}tool=pmcentrez{&}rendertype=abstract

[71] A. H. Abdul Razak, A. Zayegh, R. K. Begg, and Y. Wahab, "Foot plantar pressure measurement system: A review," pp. 9884–9912, 2012.

[72] S. J. M. Bamberg, A. Y. Benbasat, D. M. Scarborough, D. E. Krebs, and J. a. Paradiso, "Gait analysis using a shoe-integrated wireless sensor system." *IEEE transactions on information technology in biomedicine : a publication of the IEEE Engineering in Medicine and Biology Society*, vol. 12, no. 4, pp. 413–423, 2008.

[73] H. Tanwar, L. Nguyen, and N. Stergiou, "Force sensitive resistor (FSR)-based wireless gait analysis device," in *Telehealth '07 The Third IASTED International Conference on Telehealth*. ACTA Press, may 2007, pp. 1–6. [Online]. Available: http://dl.acm.org/citation.cfm?id=1672136.1672138

[74] N. K. S. Lee, R. S. Goonetilleke, Y. S. Cheung, and G. M. Y. So, "A flexible encapsulated MEMS pressure sensor system for biomechanical applications," *Microsystem Technologies*, vol. 7, no. 2, pp. 55–62, may 2001. [Online]. Available: http://link.springer.com/10.1007/s005420100092

[75] S. Urry, "Plantar pressure-measurement sensors," *Measurement Science and Technology*, vol. 10, no. 1, p. R16, 1999. [Online]. Available: http://stacks.iop.org/0957-0233/10/i=1/a=017

[76] S. Beeby, *MEMS Mechanical Sensors*, 2004. [Online]. Available: https://books.google.com/books?hl=es{&}lr={&}id=6wg5oXzks9UC{&}pgis=1

[77] M. J. Madou, "MEMS Fabrication," in *The MEMS Handbook*, 2001. [Online]. Available: https://books.google.com/books?hl=es{&}lr={&}id=g0v3r6WNaBkC{&}pgis=1

[78] W. Putnam and R. B. Knapp, "Input/Data Acquisition System Design for Human Computer Interfacing," in *Online Course Notes. Stanford University*, Stanford, CA, USA, 1996, pp. 1–29.

[79] Tekscan, "Tekscan Website." [Online]. Available: https://www.tekscan.com/

[80] I. Electronics, "Interlink Electronics Website." [Online]. Available: http://interlinkelectronics.com/

[81] L.-y. Qin, H. Ma, and W.-H. Liao, "Insole plantar pressure systems in the gait analysis of post-stroke rehabilitation," in *2015 IEEE International Conference on Information and Automation*. IEEE, aug 2015, pp. 1784–1789. [Online]. Available: http://ieeexplore.ieee.org/lpdocs/epic03/wrapper.htm?arnumber=7279576

[82] A. Gefen, "Pressure-sensing devices for assessment of soft tissue loading under bony prominences: technological concepts and clinical utilization." *Wounds : a compendium of clinical research and practice*, vol. 19, no. 12, pp. 350–62, dec 2007. [Online]. Available: http://europepmc.org/abstract/med/25942685

[83] Measurement Specialties, "Measurement Specialties Website." [Online]. Available: http://www.meas-spec.com/

[84] PCB Piezotronics, "PCB Piezotronics Website." [Online]. Available: http://www.pcb.com/

[85] H. S. Zhu, N. Maalej, J. G. Webster, W. J. Tompkins, P. Bach-y Rita, and J. J. Wertsch, "An umbilical data-acquisition system for measuring pressures between the foot and shoe." *IEEE transactions on bio-medical engineering*, vol. 37, no. 9, pp. 908–11, sep 1990. [Online]. Available: http://www.ncbi.nlm.nih.gov/pubmed/2227977

[86] H. S. Zhu, J. J. Wertsch, G. F. Harris, J. D. Loftsgaarden, and M. B. Price, "Foot pressure distribution during walking and shuffling." *Archives of physical medicine and rehabilitation*, vol. 72, no. 6, pp. 390–7, may 1991. [Online]. Available: http://europepmc.org/abstract/med/2059106

[87] J. M. Hausdorff, Z. Ladin, and J. Y. Wei, "Footswitch system for measurement of the temporal parameters of gait," *Journal of Biomechanics*, vol. 28, no. 3, pp. 347–351, mar 1995. [Online]. Available: http://www.sciencedirect.com/science/article/pii/002192909400074E

[88] D. Gafurov, K. Helkala, and T. Søndrol, "Biometric gait authentication using accelerometer sensor," *Journal of Computers*, vol. 1, no. 7, pp. 51–59, 2006.

[89] Analog Devices, "Analog Devices," 2015.

[90] Y. Cong and M. Zhang, "Measurement of in-shoe plantar triaxial stresses in high-heeled shoes," in *2010 3rd International Conference on Biomedical Engineering and Informatics*, vol. 4. IEEE, oct 2010,

pp. 1760–1763. [Online]. Available: http://ieeexplore.ieee.org/lpdocs/epic03/wrapper.htm?arnumber=5639873

[91] Y. Feng, Y. Ge, and Q. Song, "A human identification method based on dynamic plantar pressure distribution," in *2011 IEEE International Conference on Information and Automation*. IEEE, jun 2011, pp. 329–332. [Online]. Available: http://ieeexplore.ieee.org/lpdocs/epic03/wrapper.htm?arnumber=5949011

[92] A. Healy, P. Burgess-Walker, R. Naemi, and N. Chockalingam, "Repeatability of WalkinSense® in shoe pressure measurement system: A preliminary study." *Foot (Edinburgh, Scotland)*, vol. 22, no. 1, pp. 35–9, mar 2012. [Online]. Available: http://www.sciencedirect.com/science/article/pii/S0958259211001088

[93] O. Tirosh, R. Begg, E. Passmore, and N. Knopp-Steinberg, "Wearable textile sensor sock for gait analysis," in *Sensing Technology (ICST), 2013 Seventh International Conference on*, 2013, pp. 618–622.

[94] T. Lawrence and R. Schmidt, "Wireless in-shoe force system [for motor prosthesis]," in *Proceedings of the 19th Annual International Conference of the IEEE Engineering in Medicine and Biology Society. 'Magnificent Milestones and Emerging Opportunities in Medical Engineering' (Cat. No.97CH36136)*, vol. 5. IEEE, 1997, pp. 2238–2241. [Online]. Available: http://ieeexplore.ieee.org/lpdocs/epic03/wrapper.htm?arnumber=758805

[95] S. J. Morris and J. A. Paradiso, "Shoe-integrated sensor system for wireless gait analysis and real-time feedback," in *Proc. Second Joint Engineering in Medicine and Biology 24th Annual Conf. and the Annual Fall Meeting of the Biomedical Engineering Society EMBS/BMES Conf*, vol. 3, 2002, pp. 2468–2469.

[96] S. J. Morris, "A Shoe-Integrated Sensor System for Wireless Gait Analysis and Real-Time Therapeutic Feedback," Ph.D. dissertation, 2004.

[97] M. Chen, B. Huang, and Y. Xu, "Intelligent shoes for abnormal gait detection," in *Proceedings - IEEE International Conference on Robotics and Automation*, 2008, pp. 2019–2024.

[98] Images Scientific Instruments, "Images Scientific Instruments Website." [Online]. Available: http://www.imagesco.com/

[99] M. Benocci, L. Rocchi, E. Farella, L. Chiari, and L. Benini, "A wireless system for gait and posture analysis based on pressure insoles and Inertial Measurement Units," in *Proceedings of the 3d International ICST Conference on Pervasive Computing Technologies for Healthcare*. ICST, 2009, pp. 1–6. [Online]. Available: http://eudl.eu/doi/10.4108/ICST.PERVASIVEHEALTH2009.6032

[100] Texas Instrument, "Texas Instrument Website." [Online]. Available: http://www.ti.com/

[101] C.-M. Yang, C.-M. Chou, J.-S. Hu, S.-H. Hung, C.-H. Yang, C.-C. Wu, M.-Y. Hsu, and T.-L. Yang, "A wireless gait analysis system by digital textile sensors." *Conference proceedings : ... Annual International Conference of the IEEE Engineering in Medicine and Biology Society. IEEE Engineering in Medicine and Biology Society. Annual Conference*, vol. 2009, pp. 7256–60, jan 2009. [Online]. Available: http://www.ncbi.nlm.nih.gov/pubmed/19965098

[102] T. Holleczek, A. Ru, H. Harms, and G. Tro, "Textile pressure sensors for sports applications," in *2010 IEEE Sensors*. IEEE, nov 2010, pp. 732–737. [Online]. Available: http://ieeexplore.ieee.org/lpdocs/epic03/wrapper.htm?arnumber=5690041

[103] Microchip, "Microchip Website." [Online]. Available: http://www.microchip.com/

[104] E. S. Sazonov, G. Fulk, J. Hill, Y. Schutz, and R. Browning, "Monitoring of Posture Allocations and Activities by a Shoe-Based Wearable Sensor," *IEEE Transactions on Biomedical Engineering*, vol. 58, no. 4, pp. 983–990,

apr 2011. [Online]. Available: http://ieeexplore.ieee.org/lpdocs/epic03/wrapper.htm?arnumber=5447796

[105] F. Neaga, D. Moga, D. Petreus, M. Munteanu, and N. Stroia, "A Wireless System for Monitoring the Progressive Loading of Lower Limb in Post-Traumatic Rehabilitation," in *International Conference on Advancements of Medicine and Health Care through Technology*, ser. IFMBE Proceedings, S. Vlad and R. V. Ciupa, Eds., vol. 36. Berlin, Heidelberg: Springer Berlin Heidelberg, 2011, pp. 54–59. [Online]. Available: http://www.springerlink.com/index/10.1007/978-3-642-22586-4

[106] N. A. Sazonova, R. Browning, and E. S. Sazonov, "Prediction of bodyweight and energy expenditure using point pressure and foot acceleration measurements." *The open biomedical engineering journal*, vol. 5, pp. 110–5, jan 2011. [Online]. Available: /pmc/articles/PMC3257550/?report=abstract

[107] N. Sazonova, R. Browning, E. Melanson, and E. Sazonov, "Posture and activity recognition and energy expenditure prediction in a wearable platform," in *Engineering in Medicine and Biology Society (EMBC), 2014 36th Annual International Conference of the IEEE*, vol. 35487, no. 205, 2014, pp. 4163–4167.

[108] S. Edgar, T. Swyka, G. Fulk, and E. S. Sazonov, "Wearable shoe-based device for rehabilitation of stroke patients." *Conference proceedings : ... Annual International Conference of the IEEE Engineering in Medicine and Biology Society. IEEE Engineering in Medicine and Biology Society. Annual Conference*, vol. 2010, pp. 3772–5, jan 2010. [Online]. Available: http://www.ncbi.nlm.nih.gov/pubmed/21097053

[109] STMicroelectronics, "STMicroelectronics Website." [Online]. Available: http://www.st.com/web/en/home.html

[110] C. Wada, Y. Sugimura, T. Ienaga, Y. Kimuro, F. Wada, K. Hachisuka, and T. Tsuji, "Development of a rehabilitation support system with a shoe-type measurement device for walking," pp. 2534–2537, 2010.

[111] M. Saito, K. Nakajima, C. Takano, Y. Ohta, C. Sugimoto, R. Ezoe, K. Sasaki, H. Hosaka, T. Ifukube, S. Ino, and K. Yamashita, "An in-shoe device to measure plantar pressure during daily human activity," *Medical Engineering and Physics*, vol. 33, no. 5, pp. 638–645, 2011. [Online]. Available: http://dx.doi.org/10.1016/j.medengphy.2011.01.001

[112] P. Paulick, H. Djalilian, and M. Bachman, "StabilitySole: Embedded sensor insole for balance and gait monitoring," *Lecture Notes in Computer Science (including subseries Lecture Notes in Artificial Intelligence and Lecture Notes in Bioinformatics)*, vol. 6777 LNCS, pp. 171–177, 2011.

[113] Freescale, "Freescale Website." [Online]. Available: http://www.freescale.com/

[114] S. M. M. De Rossi, T. Lenzi, N. Vitiello, M. Donati, A. Persichetti, F. Giovacchini, F. Vecchi, and M. C. Carrozza, "Development of an in-shoe pressure-sensitive device for gait analysis," in *2011 Annual International Conference of the IEEE Engineering in Medicine and Biology Society*. IEEE, aug 2011, pp. 5637–5640. [Online]. Available: http://ieeexplore.ieee.org/lpdocs/epic03/wrapper.htm?arnumber=6091364

[115] S. Crea, M. Donati, S. M. M. De Rossi, C. M. Oddo, and N. Vitiello, "A wireless flexible sensorized insole for gait analysis." *Sensors (Basel, Switzerland)*, vol. 14, no. 1, pp. 1073–1093, 2014.

[116] W. Xu, M.-C. Huang, N. Amini, J. J. Liu, L. He, and M. Sarrafzadeh, "Smart insole: A Wearable System for Gait Analysis," in *Proceedings of the 5th International Conference on PErvasive Technologies Related to Assistive Environments - PETRA '12*. New York, New York, USA: ACM Press, jun 2012, p. 1. [Online]. Available: http://dl.acm.org/citation.cfm?id=2413097.2413120

[117] A. M. Cristiani, G. M. Bertolotti, E. Marenzi, and S. Ramat, "An instrumented insole for long term monitoring movement, comfort, and ergonomics," *IEEE Sensors Journal*, vol. 14, no. 5, pp. 1564–1572, 2014.

[118] Sensirion, "Sensirion Website." [Online]. Available: http://www.sensirion.com/en/home/

[119] K. Kanitthika and K. S. Chan, "Pressure sensor positions on insole used for walking analysis," in *The 18th IEEE International Symposium on Consumer Electronics (ISCE 2014)*, 2014, pp. 1–2. [Online]. Available: http://ieeexplore.ieee.org/lpdocs/epic03/wrapper.htm?arnumber=6884394

[120] Flexiforce, "F-Scan." [Online]. Available: https://www.tekscan.com/products-solutions/systems/f-scan-system

[121] A. Hollinger and M. M. Wanderley, "Evaluation of Commercial Force-Sensing Resistors," *In Proceedings of International Conference on New Interfaces for Musical Expression*, pp. 1–4, 2006.

[122] Microchip, *Application Note AN1284, Microchip Wireless (MiWi) Application Programming Interface - MiApp*.

[123] ——, *Application Note AN1283, Microchip Wireless (MiWi) Media Access Controller-MiMAC*.

[124] ——, "Application Note AN1045, File I/O Functions Using Microchip's Memory Disk Drive File System Library."

[125] Oracle, "Java." [Online]. Available: https://www.java.com/es/

[126] Microsoft, "Microsoft Website." [Online]. Available: https://www.microsoft.com/es-es/

[127] Apple, "Apple Website." [Online]. Available: http://www.apple.com/es/

[128] Android and Google, "Android Website." [Online]. Available: https://www.android.com/intl/es{_}es/

[129] F. Martínez-Martí, M. S. Martínez-García, S. G. García-Díaz, J. García-Jiménez, A. J. Palma, and M. A. Carvajal, "Embedded sensor insole for wireless measurement of gait parameters," *Australasian Physical and Engineering Sciences in Medicine*, vol. 37, no. 1, pp. 25–35, 2014.

[130] T. Karčnik and A. Kralj, "Simple gait assessment system," *Gait & Posture*, vol. 6, pp. 193–199, 1997.

[131] S. O. H. Madgwick, A. J. L. Harrison, and R. Vaidyanathan, "Estimation of IMU and MARG orientation using a gradient descent algorithm," *IEEE International Conference on Rehabilitation Robotics*, 2011.

[132] CHRobotics, "Understanding Euler Angles." [Online]. Available: http://www.chrobotics.com/library/understanding-euler-angles

[133] S. Ounpuu, "The biomechanics of walking and running." *Clinics in Sports Medicine*, vol. 13, no. 0278-5919 (Linking), pp. 843–863, 1994.

[134] G. Ziv and R. Lidor, "Vertical jump in female and male basketball players-A review of observational and experimental studies," pp. 332–339, 2010.

[135] J. M. Sheppard, A. A. Dingley, I. Janssen, W. Spratford, D. W. Chapman, and R. U. Newton, "The effect of assisted jumping on vertical jump height in high-performance volleyball players," *Journal of Science and Medicine in Sport*, vol. 14, pp. 85–89, 2011.

[136] D. Baker, "Improving Vertical Jump Performance Through General, Special, and Specific Strength Training: A Brief Review," p. 131, 1996.

[137] M. Buckthorpe, J. Morris, and J. P. Folland, "Validity of vertical jump measurement devices," pp. 63–69, 2012.

[138] A. Kasabalis, H. Douda, and S. P. Tokmakidis, "Relationship between anaerobic power and jumping of selected male volleyball players of different ages." *Perceptual and motor skills*, vol. 100, pp. 607–614, 2005.

[139] G. L. Moir, "Three Different Methods of Calculating Vertical Jump Height from Force Platform Data in Men and Women," *Measurement in Physical Education and Exercise Science*, vol. 12, no. 4, pp. 207–218, 2008.

[140] E. M. Hennig and T. L. Milani, "Pressure distribution measurements for evaluation of running shoe properties." *Sportverletzung Sportschaden*

: Organ der Gesellschaft fur Orthopadisch-Traumatologische Sportmedizin, vol. 14, pp. 90–97, 2000.

[141] E. D. Lemaire, A. Biswas, and J. Kofman, "Plantar pressure parameters for dynamic gait stability analysis," in *Annual International Conference of the IEEE Engineering in Medicine and Biology - Proceedings*, 2006, pp. 4465–4468.

[142] J. García-López, J. Peleteiro, J. A. Rodgríguez-Marroyo, J. C. Morante, J. A. Herrero, and J. G. Villa, "The validation of a new method that measures contact and flight times during vertical jump," *International Journal of Sports Medicine*, vol. 26, pp. 294–302, 2005.

[143] J. T. Viitasalo, P. Luhtanen, H. V. Mononen, K. Norvapalo, L. Paavolainen, and M. Salonen, "Photocell contact mat: A new instrument to measure contact and flight times in running," *Journal of Applied Biomechanics*, vol. 13, pp. 254–266, 1997.

[144] J. García-López, J. C. Morante, A. Ogueta-Alday, and J. A. Rodríguez-Marroyo, "The type of mat (contact vs. photocell) affects vertical jump height estimated from flight time," p. 1, 2012.

[145] J. F. Glatthorn, S. Gouge, S. Nussbaumer, S. Stauffacher, F. M. Impellizzeri, and N. A. Maffiuletti, "Validity and reliability of Optojump photoelectric cells for estimating vertical jump height." *Journal of strength and conditioning research / National Strength & Conditioning Association*, vol. 25, pp. 556–560, 2011.

[146] J. S. Leard, M. A. Cirillo, E. Katsnelson, D. A. Kimiatek, T. W. Miller, K. Trebincevic, and J. C. Garbalosa, "Validity of two alternative systems for measuring vertical jump height." *Journal of strength and conditioning research / National Strength & Conditioning Association*, vol. 21, pp. 1296–1299, 2007.

[147] L. Bosquet, N. Berryman, and O. Dupuy, "A comparison of 2 optical timing systems designed to measure flight time and contact time during jumping and hopping." *Journal of strength and conditioning research*

/ *National Strength & Conditioning Association*, vol. 23, pp. 2660–2665, 2009.

[148] J. A. Dias, J. Dal Pupo, D. C. Reis, L. Borges, S. G. Santos, A. R. P. Moro, and N. G. Borges, "Validity of two methods for estimation of vertical jump height." *Journal of strength and conditioning research / National Strength & Conditioning Association*, vol. 25, no. 7, pp. 2034–2039, 2011.

[149] B. Requena, F. Requena, I. García, E. S. S. de Villarreal, and M. Pääsuke, "Reliability and validity of a wireless microelectromechanicals based system (Keimove\texttrademark) for measuring vertical jumping performance," *Journal of Sports Science and Medicine*, vol. 11, no. 1, pp. 115–122, 2012.

[150] A. Baca, "A comparison of methods for analyzing drop jump performance," *Medicine & Science in Sports & Exercise*, vol. 31, no. 3, pp. 437–442, mar 1999. [Online]. Available: http://europepmc.org/abstract/med/10188749

[151] M. Asdís, O. Baldur, and K. Brynjar, "Comparing Three Devices for Jump Height Measurement in a Heterogeneous Group of Subjects." *Journal of strength and conditioning research / National Strength & Conditioning Association*, 2014.

[152] P. Picerno, V. Camomilla, and L. Capranica, "Countermovement jump performance assessment using a wearable 3D inertial measurement unit." *Journal of sports sciences*, vol. 29, no. 2, pp. 139–146, 2011.

[153] C. Balsalobre-Fernández, M. Glaister, and R. A. Lockey, "The validity and reliability of an iPhone app for measuring vertical jump performance," *Journal of Sports Sciences*, no. February 2015, pp. 1–6, 2015.

[154] C. Kirtley, "An Instrumented Insole for Kinematic and Kinetic Gait Measurements," in *Proc. of the 5th Symp. on Footwear Biomechanics*, 2001, pp. 52–53.

[155] D. J. Harriss and G. Atkinson, "Ethical standards in sport and exercise science research: 2014 update·," *International Journal of Sports Medicine*, vol. 34, no. 12, pp. 1025–1028, 2013.

[156] C. Bosco, P. Luhtanen, and P. V. Komi, "A simple method for measurement of mechanical power in jumping," *European Journal of Applied Physiology and Occupational Physiology*, vol. 50, no. 2, pp. 273–282, jan 1983. [Online]. Available: http://link.springer.com/10.1007/BF00422166

[157] C. Lago-Peñas, L. Casais, A. Dellal, E. Rey, and E. Domínguez, "Anthropometric and Physiological Characteristics of Young Soccer Players According to Their Playing Positions: Relevance for Competition Success," pp. 3358–3367, 2011.

[158] Humotion, "Professional Training Support." [Online]. Available: http://www.humotion.net/?page{_}id=92

[159] H. Hatze, "Validity and reliability of methods for testing vertical jumping performance," *Journal of Applied Biomechanics*, vol. 14, no. 2, pp. 127–140, 1998.

[160] A. Kibele, "Possibilities and limitations in the biomechanical analysis of countermovement jumps: A methodological study," *Journal of Applied Biomechanics*, vol. 14, pp. 105–117, 1998.

[161] B. Fernandez, T. Gonzalez, V. Campo, and B. Nicolas, "The concurrent validity and reliability of a low-cost , high-speed camera-based method for measuring the flight time of vertical jumps (Article)," *Journal of Strength and Conditioning Research Volume*, vol. 28, no. 2, p. 2014, 2014.

[162] J. M. Bland and D. G. Altman, "Statistical methods for assessing agreement between two methods of clinical measurement., Tech. Rep. 8476, 1986.

[163] F. Faul, E. Erdfelder, A.-G. Lang, and A. Buchner, "G*Power 3: a flexible statistical power analysis program for the social, behavioral, and bio-

medical sciences." *Behavior research methods*, vol. 39, no. 2, pp. 175–191, 2007.

[164] R Development Core Team, "R: A language and environment for statistical computing. R Foundation for Statistical Computing, Vienna, Austria. URL http://www.R-project.org/." 2013.

[165] L. F. Aragón, "Evaluation of Four Vertical Jump Tests: Methodology, Reliability, Validity, and Accuracy," pp. 215–228, 2000.

[166] G. O. M. Markovic, D. R. D. Izdar, and I. G. O. R. J. Ukic, "Realiability and Factorial Validity of Squat and Countermovement Jump Tests," *Journal of Strength And Conditioning Research*, vol. 18, no. 3, pp. 551–555, 2004.

[167] P. Pérez, S. Llana, and E. Alcántara, "Standard tests ability to measure impact forces reduction on mats," *International Journal of Sports Science and Engineering*, vol. 2, no. 3, pp. 162–168, 2008.

[168] L. A. Burt, G. A. Naughton, D. G. Higham, and R. Landeo, "Training load in Pre-Pubertal female artistic gymnastics," *Science of Gymnastics Journal*, vol. 2, no. 3, pp. 5–14, 2010.

[169] B. A. Johnson, C. L. Salzberg, and D. A. Stevenson, "A Systematic Review: Plyometric Training Programs for Young Children," pp. 2623–2633, 2011. [Online]. Available: http://dialnet.unirioja.es/servlet/articulo?codigo=4720679{&}info=resumen{&}idioma=ENG

[170] K. A. Witzke and C. M. Snow, "Effects of plyometric jump training on bone mass in adolescent girls," *Medicine & Science in Sports & Exercise*, vol. 32, no. 6, pp. 1051–1057, jun 2000. [Online]. Available: http://europepmc.org/abstract/med/10862529

[171] J. C. Redondo, C. J. Alonso, S. Sedano, and A. M. de Benito, "Effects of a 12-week strength training program on experimented fencers' movement time." *Journal of strength and conditioning research / National Strength & Conditioning Association*, vol. 28, no. 12, pp. 3375–84, dec 2014. [Online]. Available: http://www.ncbi.nlm.nih.gov/pubmed/24942170

[172] H. Makaruk and T. Sacewicz, "Effects of Plyometric Training on Maximal Power Output and Jumping Ability," *Human Movement*, vol. 11, no. 1, pp. 17–22, jan 2010. [Online]. Available: http://www.degruyter.com/view/j/humo.2010.11.issue-1/v10038-010-0007-1/v10038-010-0007-1.xml

[173] H. Makaruk, T. Sacewicz, A. Czaplicki, and J. Sadowski, "Effect of Additional Load on Power Output during Drop Jump Training," *Journal of Human Kinetics*, vol. 26, no. -1, pp. 31–37, jan 2010. [Online]. Available: http://www.degruyter.com/view/j/hukin.2010.26.issue--1/v10078-010-0045-y/v10078-010-0045-y.xml

[174] M. M. Read and C. Cisar, "The influence of varied rest interval lengths on depth jump performance." *Journal of strength and conditioning research / National Strength & Conditioning Association*, vol. 15, no. 3, pp. 279–83, aug 2001. [Online]. Available: http://europepmc.org/abstract/med/11710651

[175] J. G. Seegmiller and S. T. McCaw, "Ground Reaction Forces Among Gymnasts and Recreational Athletes in Drop Landings." *Journal of athletic training*, vol. 38, no. 4, pp. 311–314, dec 2003. [Online]. Available: http://www.pubmedcentral.nih.gov/articlerender.fcgi?artid=314389{&}tool=pmcentrez{&}rendertype=abstract

[176] C. Mills, M. T. G. Pain, and M. R. Yeadon, "Reducing ground reaction forces in gymnastics' landings may increase internal loading." *Journal of biomechanics*, vol. 42, no. 6, pp. 671–8, apr 2009. [Online]. Available: http://www.sciencedirect.com/science/article/pii/S0021929009000244

[177] Gymnova, "Novatrack ONE." [Online]. Available: http://www.gymnova.com/

[178] R. M. Stess, S. R. Jensen, and R. Mirmiran, "The Role of Dynamic Plantar Pressures in Diabetic Foot Ulcers," *Diabetes Care*, vol. 20, no. 5, pp. 855–858, 1997. [Online]. Available: http://care.diabetesjournals.org/content/20/5/855.abstract

[179] T. G. McPoil, W. Yamada, W. Smith, and M. Cornwall, "The Distribution of Plantar Pressures in American Indians with Diabetes Mellitus," *Journal of the American Podiatric Medical Association*, vol. 91, no. 6, pp. 280–287, 2001. [Online]. Available: http://www.japmaonline.org/content/91/6/280.abstract

[180] E. Vermani, R. Mittal, and A. Weeks, "Pelvic girdle pain and low back pain in pregnancy: a review." *Pain practice : the official journal of World Institute of Pain*, vol. 10, no. 1, pp. 60–71, jan 2009. [Online]. Available: http://www.ncbi.nlm.nih.gov/pubmed/19863747

[181] S. D. Liddle and V. Pennick, "Interventions for preventing and treating low-back and pelvic pain during pregnancy." *The Cochrane database of systematic reviews*, vol. 9, p. CD001139, jan 2015. [Online]. Available: http://www.ncbi.nlm.nih.gov/pubmed/26422811

[182] M. Pullig Schatz, *El cuidado de la espalda: Dolor de espalda musculoesquelético crónico, tensión cervical, artritis espinal, osteoporosis, síndrome premenstrual, embarazo y escoliosis*, 1st ed. Paidotribo, 2009.

[183] F. M. Kovacs, E. Garcia, A. Royuela, L. González, and V. Abraira, "Prevalence and factors associated with low back pain and pelvic girdle pain during pregnancy: a multicenter study conducted in the Spanish National Health Service." *Spine*, vol. 37, no. 17, pp. 1516–33, aug 2012. [Online]. Available: http://europepmc.org/abstract/med/22333958

[184] P. Katonis, A. Kampouroglou, A. Aggelopoulos, K. Kakavelakis, S. Lykoudis, A. Makrigiannakis, and K. Alpantaki, "Pregnancy-related low back pain." *Hippokratia*, vol. 15, no. 3, pp. 205–10, jul 2011. [Online]. Available: http://www.pubmedcentral.nih.gov/articlerender.fcgi?artid=3306025{&}tool=pmcentrez{&}rendertype=abstract

[185] J. Sabino and J. N. Grauer, "Pregnancy and low back pain." *Current reviews in musculoskeletal medicine*, vol. 1, no. 2, pp. 137–41, jun 2008. [Online]. Available: http://www.pubmedcentral.nih.gov/articlerender.fcgi?artid=2684210{&}tool=pmcentrez{&}rendertype=abstract

[186] H. B. Albert, M. Godskesen, L. Korsholm, and J. G. Westergaard, "Risk factors in developing pregnancy-related pelvic girdle pain." *Acta obstetricia et gynecologica Scandinavica*, vol. 85, no. 5, pp. 539–44, jan 2006. [Online]. Available: http://www.ncbi.nlm.nih.gov/pubmed/16752231

[187] D. Gallo-Padilla, C. Gallo-Padilla, F. J. Gallo-Vallejo, and J. L. Gallo-Vallejo, "[Low back pain during pregnancy. Multidisciplinary approach]." *Semergen : Sociedad Espanola de Medicina Rural y Generalista*, jul 2015. [Online]. Available: http://www.sciencedirect.com/science/article/pii/S1138359315002476

[188] P. Ponnapula and J. S. Boberg, "Lower extremity changes experienced during pregnancy." *The Journal of foot and ankle surgery : official publication of the American College of Foot and Ankle Surgeons*, vol. 49, no. 5, pp. 452–8, jan 2010. [Online]. Available: http://www.sciencedirect.com/science/article/pii/S1067251610002735

[189] M. Birtane and H. Tuna, "The evaluation of plantar pressure distribution in obese and non-obese adults," *Clinical Biomechanics*, vol. 19, no. 10, pp. 1055–1059, 2004. [Online]. Available: http://www.sciencedirect.com/science/article/pii/S0268003304001627

[190] R. F. Kushner and J. L. Roth, "Assessment of the obese patient," *Endocrinology and Metabolism Clinics of North America*, vol. 32, no. 4, pp. 915–933, dec 2003. [Online]. Available: http://www.endo.theclinics.com/article/S0889852903000689/fulltext

[191] N. Ochsenbein-Kölble, M. Roos, T. Gasser, and R. Zimmermann, "Cross-sectional study of weight gain and increase in BMI throughout pregnancy." *European journal of obstetrics, gynecology, and reproductive biology*, vol. 130, no. 2, pp. 180–6, feb 2007. [Online]. Available: http://www.sciencedirect.com/science/article/pii/S0301211506001989

[192] C. Gaymer, H. Whalley, J. Achten, M. Vatish, and M. L. Costa, "Midfoot plantar pressure significantly increases during late gestation."

Foot (Edinburgh, Scotland), vol. 19, no. 2, pp. 114–6, jun 2009. [Online]. Available: http://www.sciencedirect.com/science/article/pii/S095825920900011X

[193] E. Karadag-Saygi, F. Unlu-Ozkan, and A. Basgul, "Plantar pressure and foot pain in the last trimester of pregnancy." *Foot & ankle international / American Orthopaedic Foot and Ankle Society*, vol. 31, no. 2, pp. 153–157, 2010.

[194] S. Ribas and E. Guirro, "Analysis of Plantar Pressure and Postural Balance During DIfferent Phases of Pregnancy," *Brazilian Journal of Physical Therapy*, vol. 11, pp. 391–396, 2007. [Online]. Available: http://www.scielo.br/scielo.php?script=sci{_}arttext{&}pid=S1413-35552007000500010{&}nrm=iso

[195] S. Chandzlik and J. Piecha, "A patient walk-data-record modelling using a spline interpolation method," *Journal of Medical Informatics & Technologies*, vol. 3, pp. MI–153, 2002. [Online]. Available: https://www.infona.pl//resource/bwmeta1.element.baztech-article-PWA4-0023-0022

[196] M. S. H. Aung, S. B. Thies, L. P. J. Kenney, D. Howard, R. W. Selles, A. H. Findlow, and J. Y. Goulermas, "Automated detection of instantaneous gait events using time frequency analysis and manifold embedding." *IEEE transactions on neural systems and rehabilitation engineering : a publication of the IEEE Engineering in Medicine and Biology Society*, vol. 21, no. 6, pp. 908–16, nov 2013. [Online]. Available: http://www.ncbi.nlm.nih.gov/pubmed/23322764

[197] K. Aminian, B. Najafi, C. Büla, P.-F. Leyvraz, and P. Robert, "Spatio-temporal parameters of gait measured by an ambulatory system using miniature gyroscopes," *Journal of Biomechanics*, vol. 35, no. 5, pp. 689–699, may 2002. [Online]. Available: http://www.sciencedirect.com/science/article/pii/S0021929002000088

[198] J. K. Lee and E. J. Park, "Quasi real-time gait event detection using shank-attached gyroscopes." *Medical & biological engineering &*

computing, vol. 49, no. 6, pp. 707–12, jun 2011. [Online]. Available: http://www.ncbi.nlm.nih.gov/pubmed/21267666

[199] A. Salarian, H. Russmann, F. J. G. Vingerhoets, C. Dehollain, Y. Blanc, P. R. Burkhard, and K. Aminian, "Gait assessment in Parkinson's disease: toward an ambulatory system for long-term monitoring." *IEEE transactions on bio-medical engineering*, vol. 51, no. 8, pp. 1434–43, aug 2004. [Online]. Available: http://www.ncbi.nlm.nih.gov/pubmed/15311830

[200] K. Tong and M. H. Granat, "A practical gait analysis system using gyroscopes," *Medical Engineering & Physics*, vol. 21, no. 2, pp. 87–94, mar 1999. [Online]. Available: http://www.sciencedirect.com/science/article/pii/S1350453399000302

[201] B. R. Greene, D. McGrath, R. O'Neill, K. J. O'Donovan, A. Burns, and B. Caulfield, "An adaptive gyroscope-based algorithm for temporal gait analysis." *Medical & biological engineering & computing*, vol. 48, no. 12, pp. 1251–60, dec 2010. [Online]. Available: http://www.ncbi.nlm.nih.gov/pubmed/21042951

[202] R. Takeda, S. Tadano, A. Natorigawa, M. Todoh, and S. Yoshinari, "Gait posture estimation using wearable acceleration and gyro sensors." *Journal of biomechanics*, vol. 42, no. 15, pp. 2486–94, nov 2009. [Online]. Available: http://www.sciencedirect.com/science/article/pii/S0021929009004205

[203] M. R. Patterson and B. Caulfield, "Comparing adaptive algorithms to measure temporal gait parameters using lower body mounted inertial sensors." *Conference proceedings : ... Annual International Conference of the IEEE Engineering in Medicine and Biology Society. IEEE Engineering in Medicine and Biology Society. Annual Conference*, vol. 2012, pp. 4509–12, jan 2012. [Online]. Available: http://www.ncbi.nlm.nih.gov/pubmed/23366930

[204] B. Mariani, H. Rouhani, X. Crevoisier, and K. Aminian, "Quantitative estimation of foot-flat and stance phase of gait using foot-worn inertial sensors." *Gait & posture*, vol. 37, no. 2, pp. 229–34, feb 2013. [Online]. Available: http://www.sciencedirect.com/science/article/pii/S0966636212002822

[205] Y. Blanc, C. Balmer, T. Landis, and F. Vingerhoets, "Temporal parameters and patterns of the foot roll over during walking: normative data for healthy adults," *Gait & Posture*, vol. 10, no. 2, pp. 97–108, oct 1999. [Online]. Available: http://www.sciencedirect.com/science/article/pii/S0966636299000193

[206] J. H. Hollman, E. M. McDade, and R. C. Petersen, "Normative spatiotemporal gait parameters in older adults." *Gait & posture*, vol. 34, no. 1, pp. 111–8, may 2011. [Online]. Available: http://www.sciencedirect.com/science/article/pii/S0966636211001019

[207] H. Stolze, J. Kuhtz-Buschbeck, C. Mondwurf, K. Jöhnk, and L. Friege, "Retest reliability of spatiotemporal gait parameters in children and adults," *Gait & Posture*, vol. 7, no. 2, pp. 125–130, mar 1998. [Online]. Available: http://www.sciencedirect.com/science/article/pii/S096663629700043X